Algorithms for Induction Motor Efficiency Determination

Maher Al-Badri

A Thesis
In the Department
of
Electrical and Computer Engineering

Presented in Partial Fulfillment of the Requirements
For the Degree of
Doctor of Philosophy (Electrical and Computer Engineering) at
Concordia University
Montréal, Québec, Canada

July 2015

CONCORDIA UNIVERSITY

School of Graduate Studies

This is to certify that the thesis prepared

By: Maher Al-Badri

Entitled: Algorithms for Induction Motor Efficiency Determination

and submitted in partial fulfillment of the requirements for the degree of

Doctor of Philosophy (Electrical & Computer Engineering)

complies with the regulations of the University and meets the accepted standards with respect to originality and quality.

Signed by the final examining committee:

_____Chair
Dr. Deborah Dysart-Gale

_____External Examiner
Dr. Emmanuel B. Agamloh

_____External to Program
Dr. Ashutosh Bagchi

_____Examiner
Dr. Shahin Hashtrudi Zad

_____Examiner
Dr. Luiz A.C. Lopes

_____Thesis Supervisor
Dr. Pragasen Pillay

Approved by

_____
Chair of Department or Graduate Program Director

_____ 2015 _____
Dean of Faculty

ABSTRACT

Algorithms for Induction Motor Efficiency Determination

Maher Al-Badri, Ph.D.

Concordia University, 2015

Induction motors are the most predominant motors used in the industry. They use two-thirds of the total electrical energy generated in the industrialized countries. Motors fail due to many reasons and many are rewound two or more times during their lifetimes. It is generally assumed that a rewound motor is not as efficient as the original motor. Precise estimation of efficiency of a refurbished motor or any existing motor is crucial in industries for energy savings, auditing and management. Full-load and partial load efficiency can be determined by using the dynamometer procedure which is a highly expensive way and available only in well-equipped laboratories. An inexpensive and easily applied procedure for efficiency estimation is therefore a target of researchers and engineers in the field. In this Ph.D. work, two novel methods for estimating repaired, refurbished, or any existing induction motors' efficiency are proposed. The two methods (named Method A and Method B) require only a DC test (including temperature measurement), nameplate details, and RMS readings of no-load input power, input voltage, and input current. Experimental and field results of testing a total of 196 induction motors by using Method A are presented and the degree of accuracy is shown by comparing the estimated efficiencies to the measured values. Method B was validated by testing 8 induction motors with acceptable accuracy. To provide the necessary credits to the proposed techniques, an error analysis study is conducted to investigate the level of uncertainty through testing three induction motors, and the results of uncertainty of the direct measurements and no-load measurements using the proposed technique are declared.

Derating is a necessary procedure to protect induction motors from overheating which is the main reason of motor failures. The overheating is caused by operating induction motors with unbalanced voltages, over or undervoltage, or harmonics rich power supplies. To derate a machine, its full-load efficiency with balanced undistorted voltages and with unbalanced or

distorted voltages must be measured.

In many situations in industry and due to critical processes, it is not allowed to interrupt induction machines operation. Hence, an in situ efficiency estimation technique is most required.

In this thesis, three novel in situ efficiency estimation algorithms are proposed. The first algorithm is to estimate the full-load and partial loads efficiency of induction motors operating with balanced undistorted voltages. The algorithm is validated by testing 30 induction motors with acceptable accuracy.

The second proposed algorithm is for full-load efficiency estimation of induction motors operating with unbalanced voltages. The technique is evaluated by testing 2 induction motors with different levels of voltage unbalance. The results showed an acceptable accuracy.

The third proposed algorithm is for full-load efficiency estimation of induction motors operating with distorted unbalanced voltages where the harmonics effect is added. The technique is evaluated by testing 2 induction motors with different levels of voltage unbalance. The results showed an acceptable accuracy.

The three novel algorithms are designed by using Genetic Algorithm, pre-tested data, and IEEE Method F1 calculations.

ACKNOWLEDGEMENTS

I would like to express my special appreciation, gratefulness, and many thanks to my advisor *Professor Pragasen Pillay*. He has been a tremendous mentor for me. I would like to thank him on his kind support and professional guidance throughout these years which finally crowned with a lot of knowledge and experience. His advice on my research has been priceless. I have learned a lot from his scientific knowledge, critical thinking, and punctuality, which are key factors of any success. Those persistent weekly meetings have developed my skills as a researcher and improved my capability to handle different tasks in a proper manner.

I would also like to thank my committee members, *Professor Luiz A.C. Lopes*, *Professor Shahin Hashtrudi Zad*, *Professor Ashutosh Bagchi,* and *Dr. Emmanuel B. Agamloh* for serving as my committee members even at hardship. I also want to thank all of them on their brilliant comments and suggestions and their valuable time.

I would like to extend my many thanks to *Mr. Pierre Angers* of Hydro-Québec on his generous contribution to this research work by providing a priceless data that significantly improved the outcome of this research. I would like to thank him on his valuable professional feedback and suggestions and his participation in the technical papers written out of this work.

My many thanks to *Dr. Constantin Pitis* and *Mr. Markus Zeller* of BC hydro on providing a valuable data that been utilized successfully in this research work and also on their professional feedback and suggestions.

I would also like to thank the technical monitor team of Hydro-Québec, BC hydro, Manitoba Hydro, SaksPower, and CEATI International Inc. on their support and valuable feedback and suggestions.

A special thanks to my family members. Words cannot express how grateful I am to my father *Mr. Mosa Issa Al-Badri* and my mother *Mrs. Suad Issa* for all of the sacrifices that they have made on my behalf. Your prayer for me was what sustained me thus far.

I would also like to thank all of my brothers and sisters on their moral support that incented me to strive towards my goal.

My big thank you and sincere appreciation to my beloved wife *Lisa Yap* who morally supported this scientific trip of mine and who was there for me in the moments when there was no one to answer my queries.

Many thanks to my colleagues and friends in the Power Electronics and Energy Research (PEER) group of Concordia University for the wonderful research environment I have experienced during the years I spent with them.

I would like to thank and acknowledge the support of the Natural Sciences & Engineering Research Council of Canada and Hydro-Québec for this work.

This work was supported in part by the R&D program of the NSERC Chair entitled "*Design and Performance of Special Electrical Machines*" established in Concordia University.

TABLE OF CONTENTS

LIST OF FIGURES

LIST OF TABLES

LIST OF SYMBOLS

B_2 per phase rotor susceptance;

B per phase rotor & magnetic circuit susceptance;

B_m per phase magnetizing susceptance;

f_r rated frequency (nameplate value);

G per phase rotor and magnetic conductance;

G_2 per phase rotor conductance;

G_{fe} per phase magnetizing branch conductance;

$G_{fe,i}$ per phase magnetizing branch conductance at operating point (i);

$I_{fl,\,m}$ measured full-load current;

$I_{fl,\,r}$ nameplate full-load current;

I_a phase (a) dc current;

I_b phase (b) dc current;

I_c phase (c) dc current;

I_1 per phase stator current;

$I_{2,i}$ per phase rotor current at operating point (i);

I_2 per phase rotor current;

$I_{fe,i}$ per phase magnetizing branch current through r_{fe} at operating point (i);

I_{fl} full-load current (nameplate value);

I_{in} no-load total input current;

$I_{m,i}$ per phase magnetizing branch current through x_m at operating point (i);

$I_{nl,i}$ no-load current at the operating point (i);

I_{nl} no-load input current at t_{cold};

I_φ per phase (no-load) input current;

K_1 constant; 234.5 for copper and 224.6 for aluminum;

N_s synchronous speed;

N_m motor measured speed;

N_r motor rated speed;

n_r full-load speed (nameplate value);

$n_{r,i}$ rotor speed at operating point (i);

n_s synchronous speed;

P_i input power;

P_o measured mechanical output power;

$P_{o,r}$ rated mechanical output power;

p number of poles (nameplate value);

P_{ag} full-load air-gap power;

P_{cov} the converted power;

PF_i power factor at operating point (i);

PF power factor;

P_{fw} friction and windage loss;

$P_{h,i}$ total core loss at operating point (i);

P_h the total core loss;

$P_{in,fl}$ full-load input power.;

P_{in} no-load total input power;

P_{nl} no-load input power;

P_{out} full-load output power (nameplate value);

$P_{out,ca}$ estimated full-load output power;

P_r the total rotor power;

$P_{rcl,fl}$ full-load rotor copper losses;

P_{rcl} the total rotor copper loss;

P_{rl} rotational losses that is assumed to be the same at t_{cold} and t_{fl};

P_s the total stator power;

$P_{scl,a}$ stator copper loss at temperature t_{cold};

$P_{scl,fl}$ full load stator copper loss;

$P_{scl,i}$ no-load stator copper loss at operating point (i);

P_{scl} the total stator copper loss;

P_{sll} full-load stray load loss;

P_t the total loss;

R_a phase (a) dc resistance;

R_b phase (b) dc resistance;

R_c phase (c) dc resistance;

$R_{1,cold}$ per phase stator winding resistance at t_{cold};

R_1 per phase stator resistance corrected to full-load temperature;

$R_{2,cold}$ per phase estimated rotor resistance at t_{cold};

R_2 per phase rotor resistance corrected to full-load temperature;

$R_{a,i}$ equivalent circuit total apparent resistance per phase at the operating point (i);

R_{ab} stator winding dc resistance value measured between terminals (a) and (b) at t_{cold};

R_{bc} stator winding dc resistance value measured between terminal (b) and (c) at t_{cold};

R_{ca} stator winding dc resistance value measured between terminal (c) and (a) at t_{cold};

$R_{dc,corr}$ stator winding average dc resistance corrected to the full-load temperature;

R_{dc} stator winding average dc resistance at t_{cold};

$R_{fe,i}$ per phase magnetizing branch resistance at operating point (i);

R_g per phase rotor & magnetizing circuit resistance;

R_t per phase total resistance of the equivalent circuit;

s full-load slip;

T_{cold} temperature during which the dc test conduct;

T_{fl} full-load temperature;

V_{ab} dc voltage between terminals (a) and (b);

V_{bc} dc voltage between terminals (b) and (c);

V_{ca} dc voltage between terminals (c) and (a);

$V_{2,i}$ per phase rotor input voltage at operating point (i);

$V_{1,i}$ no-load voltage at the operating point (i);

V_{in} no-load input voltage;

V_{φ} per phase (no-load) input voltage;

X_1 per phase estimated stator reactance;

$X_{1,\ new}$ per phase new estimated stator reactance;

X_2 per phase estimated rotor reactance;

$X_{2,\ new}$ per phase new estimated rotor reactance;

X_m per phase estimated magnetizing reactance;

X_{max} maximum per phase input reactance;

X_{min}	minimum per phase input reactance;
$X_{min,\ new}$	new value for minimum per phase input reactance;
$(X_1+X_m)_i$	no-load total input reactance per phase at the operating point (i);
$X_{a,i}$	equivalent circuit total apparent reactance per phase at the operating point (i);
X_g	per phase rotor and magnetizing circuit reactance;
X_t	per phase total reactance of the equivalent circuit;
Y_2	per phase rotor and magnetizing circuit admittance;
$Z_{2,i}$	per phase rotor impedance at operating point (i);
Z_2	per phase rotor impedance;
$Z_{a,i}$	equivalent circuit total impedance per phase at the operating point (i);
Z_{in}	motor input impedance;
Z_t	per phase total impedance of the equivalent circuit;
η_{fl}	full-load efficiency (nameplate value);
$\theta_{1,i}$	phase angle of the input current $i_{nl,\ i}$;
$\theta_{2,i}$	phase angle of the rotor current at operating point (i);
η	estimated efficiency (full-load or partial load);
P_o	measured mechanical output power;
$P_{o,r}$	rated mechanical output power;
$I_{fl,\ m}$	measured full-load current;
$I_{fl,\ r}$	nameplate full-load current;
η	estimated efficiency;
P_h	core loss;
P_{SLL}	stray load loss;
P_i	input power;
V_1	positive sequence voltage;
V_2	negative sequence voltage;
R_{fe}	per phase iron loss resistance;
k	harmonic order;
V_k	phase voltage of k^{th} harmonic order ;
s_1	slip associated to fundamental frequency ;

s_k	slip associated to k^{th} harmonic order;
I_{s_1}	per phase stator current at fundamental frequency;
I_{r_1}	per phase rotor current at fundamental frequency;
I_{s_k}	per phase stator current associated to k^{th} harmonic order;
I_{r_k}	per phase rotor current associated to k^{th} harmonic order;
$P_{sll,75}$	stray load loss at 75% load;
$P_{sll,50}$	stray load loss at 50% load;
$P_{sll,25}$	stray load loss at 25% load;
$P_{scl,75}$	stator copper loss at 75% load;
$P_{scl,50}$	stator copper loss at 50% load;
$P_{scl,25}$	stator copper loss at 25% load;
p	number of poles;
$P_{rcl,75}$	rotor copper loss at 75% load;
$P_{rcl,50}$	rotor copper loss at 50% load;
$P_{rcl,25}$	rotor copper loss at 25% load;
ζ	measurement error;
ζ_m	instrument error;
ζ_p	personnel error;
I_{x_i}	influence coefficient;
x_i	input variable;
W_{z_j}	influence coefficient of the additive noise;
z_j	additive noise;
Z	per phase total impedance;
V_{ph}	phase voltage;
I_s	per phase stator current;
I_r	per phase rotor current;
I_m	per phase total magnetizing current;
V_m	per phase magnetizing voltage;
$R_{1,corr}$	the stator resistance corrected to the full-load temperature;

$R_{2,corr}$ the rotor resistance corrected to the full-load temperature;

P_a the measured input power of phase a;

V_a the calculated voltage of phase a;

I_a the measured input current of phase a;

P_b the measured input power of phase b;

V_b the calculated voltage of phase b;

I_b the measured input current of phase b;

P_c the measured input power of phase c;

V_c the calculated voltage of phase c;

I_c the measured input current of phase c;

Y_m per phase admittance of the magnetizing branch;

Y_r per phase admittance of the rotor;

Z_r per phase impedance of both the rotor and the magnetizing branches;

Z_l per phase stator impedance;

Z per phase total impedance;

V_{ph_1} the positive sequence phase voltage;

I_{m_1} the positive per phase estimated total magnetizing current;

V_{m_1} the positive per phase estimated magnetizing voltage;

Z_m the positive sequence per phase impedance calculated based on measured +ve sequence current;

I_{s1m} the measured positive sequence current;

$P_{in,\ calc1}$ the calculated input power from measured current;

I^*_{s1m} the conjugate of the positive sequence measured stator current;

$P_{in,\ calc2}$ the calculated input power from calculated current;

I^*_{s1} the conjugate of the positive sequence estimated stator current in (6.30);

θ_{Z_m} the angle of the measured input impedance z_m;

θ_Z the angle of the calculated input impedance z;

P nameplate power;

Z_2 the rotor impedance;

G_2 the rotor conductance;

G the rotor and magnetic conductance;

B_2 the rotor susceptance;

B_m the magnetizing susceptance;

B the rotor & magnetic circuit susceptance;

Y_2 the rotor and magnetizing circuit admittance;

R_g the rotor & magnetizing circuit resistance;

R the total resistance of the equivalent circuit;

X_g the rotor and magnetizing circuit reactance;

X the total reactance of the equivalent circuit;

P_s the stator power;

P_r the rotor power;

P_{scl} the stator copper loss;

P_h the core loss;

P_{rcl} the rotor copper loss;

P_t the total loss;

P_{cov1} the positive sequence converted power;

P_{cov2} the negative sequence converted power;

s_1 the positive sequence slip;

s_2 the negative sequence slip;

η the estimated efficiency;

s_k^+ the positive sequence harmonic slip;

s_k^- the negative sequence harmonic slip;

P_{cov}^+ the positive sequence converted power;

P_{cov}^- the negative sequence converted power;

LIST OF ABBREVIATIONS

DOE	: U.S. Department of Energy's
EERE	: Office of Energy Efficiency and Renewable Energy
SE	: Standard efficient motors
EE	: Energy efficient motors
NEMA	: National Electrical Manufacturers Association
IEEE	: Institute of Electrical and Electronics Engineers
IEC	: International Electrotechnical Commission
FW	: Friction & Windage Loss
FL	: Full-Load
EASA	: Electrical Apparatus Service Association
EPRI	: Electric Power Research Institute
OP	: Operating Point
IM	: Induction Motor
GA	: Genetic Algorithm
CIGRÉ	: International Council on Large Electrical Systems
BFA	: Bacterial Forging Algorithm
WIN. CONF	: Winding Configuration

CHAPTER ONE

1. Introduction

In the industrialized countries, electric motors utilize nearly two-thirds of the electricity generated [1], and hence, contribute to the global environmental problem which is represented by the emission of greenhouse gases [2]. Several Canadian and U.S. utilities took serious steps in implementing demand side management programs [3] to reduce both greenhouse gas effects and the cost of power that feeds the tremendous population of electric motors.

Almost the same situation can be encountered in the developing countries, where a significant portion of the generated power is utilized by those motors. Taking South Africa as an example, motorized systems account for up to 60% of the total electricity utilization [4].

The advantages of the induction motor, namely, ruggedness, easy maintenance, and low cost, have made it the workhorse of industry [5]. In industry, only motors above 500 hp are usually monitored because of their high costs. However, motors below 500 hp make up 99.7% of the motors in service. These motors operate at approximately 60% of their rated load because of oversized installations or under-load conditions, and hence, they work at reduced efficiency which results in wasted energy [6]. Motor losses can represent a considerable cost over a long period due to high load factor [7].

Power costs are constantly rising at a rate that is even faster than both material and producer goods prices [8], many companies have hired energy managers whose sole purpose is to find practical ways to reduce power costs. These managers noticed that motors and other process components have been ignored, and they can present a major potential for cost reduction [9]. As an example, and according to the U.S. Department of Energy's (DOE) Office of Energy Efficiency and Renewable Energy (EERE), a large size paper mill could save an average of $659,000 a year through motor system efficiency [10]. In today's economy, it is more important than ever to optimize motor losses and keep the operating cost under control [8]. Efficient operation of electric motors can provide significant energy savings with benefits for both consumers and power utilities [11].

One approach to efficiently reduce wasted energy in the industrial sector and control the cost of utilized power is by retrofitting standard efficient (SE) motors with energy efficient (EE) motors [3]. The Energy Act of 1992 mandates that most types of commonly used electric motors manufactured as of October 1997 or later must be energy efficient designs [12].

If a replacement decision of a low efficient motor is taken as a result of the calculation of energy savings and payback periods that are based on nameplate motor efficiency or manufacturer's data only, this could lead to large errors [1], as will be explained later. To make a correct decision and select the optimal retrofit scenario, an engineering staff should be able to estimate the efficiency values of the motors under test with the least possible error. This demand from industry, drives practical work and research on the development and enhancement of methods for induction motors efficiency estimation [1].

A significant amount of research work have been conducted on the subject of induction motor efficiency estimation. The major research works are introduced in sections that follow this research objectives section.

1.1. Objectives

This Ph.D. work is initiated based on practical objectives proposed by the advisor, Professor P. Pillay.

The first goal of this work is to design a useful and reliable industrial tools that can help North America’s electric motor service centers to have their repaired, rewound, or any existing induction motor tested for efficiency before delivering them back to the customer as the efficiency of electric motors is a serious concern of customers especially after a rewind or repair process and as the cost of power is continuously increasing. It was found that there were many trials from the engineers and researchers to design such a tool, but they ended up with proposed algorithms that are only applicable in well-equipped laboratories and not in those electric motor centers due to the complexity of the algorithms and their requirements of sophisticated measuring devices and software.

In this Ph.D. work, it is decided that technical visits to electric motor workshops is the first necessary step to be taken. Hence, technical visits have been made to some of electric motor

service centers in Canada (Montréal area) to investigate the technical environment in such workshops (Figure 1-1).

To turn any proposed algorithm into a practical tool, a user-friendly and affordable software should be designed and developed. Hence, the second goal of this Ph.D. work is to develop a software based on spreadsheets that can be applicable in any electric motor workshop.

The third goal of this Ph.D. work is to design an in-situ algorithm that has the potential to replace the expensive dynamometer procedure for the efficiency determination and can be used on site without the need to move the machine to a testing site.

The fourth goal is to design algorithms that can be used in derating induction machines operating under unbalanced and distorted voltages as both voltage unbalance and harmonic have severe ill effect on the performance of induction motors.

In the following sections, the major induction motors efficiency estimation research works are reviewed.

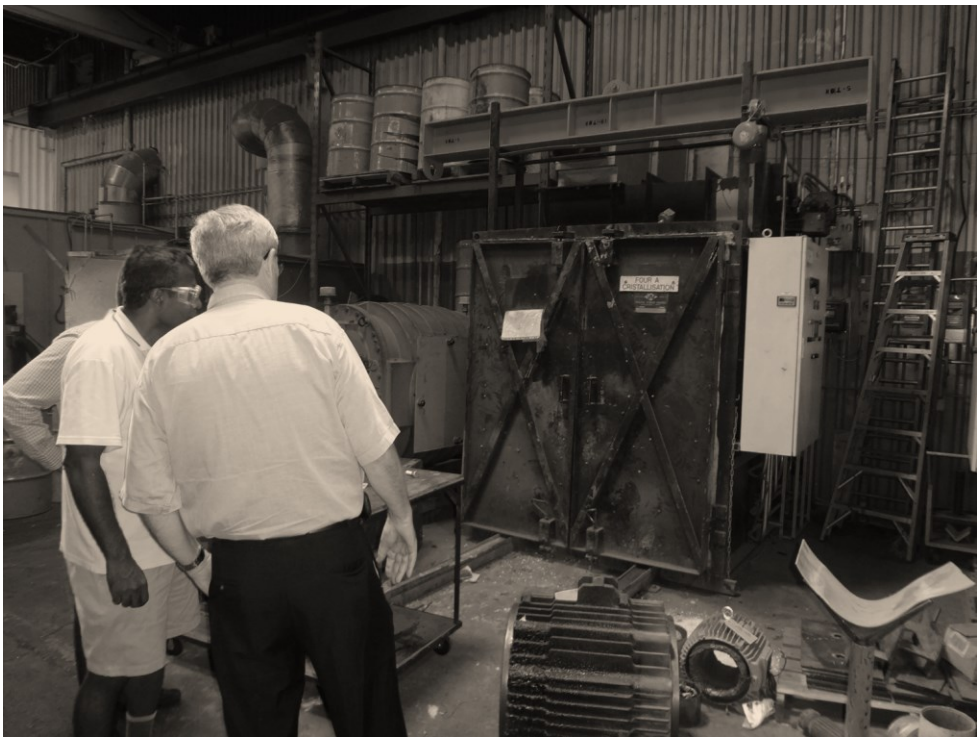

Figure 1-1. Professor P. Pillay of Concordia University with his team in one of the technical visits to an electric motor service center in Montréal area.
Photo is with permission of Moteurs Électriques Laval Ltée.

1.2. Nameplate Method

This method requires obtaining the information by only reading the nameplate details. In the nameplate method, it is assumed that the efficiency of the motor is constant and always equal to the value which appears on the nameplate [13]. This method is inaccurate and could lead to large errors since the nameplate data is approximated [14], for example, the nameplate rated speed is allowed a deviation of as much as 20% by standard NEMA MG1 [15] and IEC 34-2-1, which could lead to a significant errors on the estimation technique [16]. The real efficiency of a motor is usually different from the number mentioned on its nameplate, as efficiency may decrease significantly due to aging or rewinding [17], or it might not be given according to IEEE Std 112^{TM} Method B [18].

1.3. Slip Method

Other researchers have proposed the slip method as an approach to determine the efficiency of a motor. This method is based on the assumption that the percentage of load is linearly proportional to the percentage of the ratio of measured slip to full-load slip [13]. The formula to approximate the mechanical output power is:

$$P_o = \frac{N_s - N_m}{N_s - N_r} . P_{o,r} \qquad (1.1)$$

where, N_s is synchronous speed; N_m is motor measured speed; N_r is motor rated speed; P_o is measured mechanical output power; $P_{o,r}$ is rated mechanical output power;

The slip method can be considered as an improvement over the nameplate method, but it has been proven that it is not very accurate or useful due to the variations in motor nameplate data, line voltage unbalance, and temperature variation of the rotor [19].

1.4. Current Method

This method is based on the assumption that the percentage of load is proportional to the percentage of the ratio of measured current to full-load current. The mechanical shaft output power might be approximated as in (1.2).

$$P_o = \frac{I_{fl,\,m}}{I_{fl,\,r}} . P_{o,\,r} \qquad (1.2)$$

where, $I_{fl,\,m}$ is measured current; $I_{fl,\,r}$ is rated full-load current.

This method was proven impractical and inaccurate in [18], [13], and [20] due to the nonlinear relationship between the load and current which contradicts the assumption that the method based on.

1.5. Segregated Loss Method

In this method, each loss component is segregated (estimated). The IEEE StdTM-112 method E1 is the standard segregated loss method [21]. It assumes value for the stray load loss at rated load for different rated motors as shown in Table 1-I.

The procedure of this method is straightforward, the magnitudes of the five losses of induction motor, namely, stator copper loss, rotor copper loss, core loss, stray load loss, and friction and windage loss are estimated and then summed up and subtracted from the input power to determine the output power and hence the efficiency [20]. This method is modified by Ontario Hydro through assuming the combined FW and core loss to be 3.5 to 4.2% of rated input power [22]. The accuracy of the modified method is within ±2% to 3% error [18].

Table 1-I. Assumed Values for Stray Load Loss [21]

Machine Rating (kW)	**Stray Load Loss Percent of Rated Load**
1 - 90	1.8%
91 - 375	1.5%
376 - 1850	1.2%

1.6. Equivalent Circuit Method

In the IEEE Std 112^{TM}-2004, the equivalent circuit methods F/F1 are presented [21]. In these methods, the test procedure is as follows:

- Measure cold resistance.

- Perform the no-load test.
- Conduct the impedance test.
- Determine the friction and windage losses.
- Determine the core loss.
- Extract the six parameters of the motor.
- Measure or assume the stray load loss.
- Estimate the efficiency.

The degree of the accuracy of this approach depends on how close the assumed hot temperature and stray load loss are to the real values. The wider the difference, the larger the error obtained in estimating the efficiency.

Ontario Hydro proposed a modified version of the IEEE Std 112TM Method F1 [22]. A no-load test and a full-load test, both at rated voltage have to be conducted. This method eliminates the need for a variable-voltage required by IEEE Std 112TM Method F1 [20].

1.7. The Air gap Torque Method

The well-known air-gap equations are utilized for determining motor efficiency by a procedure called the air-gap torque method. In this method, the negative rotating torque caused by unbalance voltages and harmonics is considered. Once the air gap torque is obtained, the efficiency can be estimated according to (1.3):

$$\eta = \frac{(\text{Air gap torque}).2\pi\left(\frac{\text{rpm}}{60}\right) - P_{FW} - P_h - P_{SLL}}{P_i} \qquad (1.3)$$

where, η is efficiency; P_{FW} is friction & windage losses; P_h is core loss; P_{SLL} is stray load loss; P_i is input power.

The major disadvantage of this method is that current and voltage waveforms are required as input data, besides software is required to analyze the field measurements [20].

Most, if not all, of those methods in the literature have been designed to work properly in

only well-equipped laboratories environment, where the required instrumentation and software are available to handle the tests. The authors of those works did not pay close attention to make their proposed methods applicable in the electric motor service centers where there is a need to have the repaired and rewound motors tested for efficiency before delivering them back in service. In [11], although the author intended to make his procedure applicable to motor repair workshops, but the required instrumentation and the need for sophisticated software to analyze the measured values made the procedure not applicable in those workshops.

1.8. Motor Repair Industry's Market in North America

Most motor failures are due to mechanical reasons, and it is found that the largest percentage are associated with bearing failures [23], but typically, there are four interacting factors that contribute to motor failure; these factors are: mechanical fatigue; thermal fatigue; power supply pollution; and electrical stress. Any of these factors alone or in combination can bring a motor to a standstill [24].

When a motor fails, the basic decision of whether to rewind or replace, the owner might take, depends on many factors. Those factors are: the availability; the costs related to the size of the motor; the type of design; some special mechanical features; the operating costs; and the availability of funds are all factors that affect the replace/rewind decision [8]. Some utility surveys show that, in a given region, the total horsepower repaired is approximately equivalent to the total of new motors installed [25], but in general, more motor horsepower is repaired than sold each year [26]. In a study conducted by the U.S. Department of Energy's (DOE) Office of Energy Efficiency and Renewable Energy (EERE) in December 1998, it is found that there are roughly 12.4 million electric motors of more than 1 horsepower in service in the U.S. manufacturing plants [10]. Thousands of those motors fail and sent for rewind workshops for repair.

To shed some light on the size of this industry in North America, a study showed that a size of a typical "rewind shop" or electric motor service center, employs from 2-200 persons in the U.S. [25], where there are approximately 4,100 motor shops, repairing between 1.8 and 2.9 million motors per year. In 1993, these shops had annual revenue of $2 billion in gross, which is approximately two-thirds of the shops revenues from all sources [27]. Twenty-two hundreds of

motor repair shops in the U.S. are members of the Electrical Apparatus Service Association (EASA), the repair industry's largest and non-profit trade association founded in 1933. Most shop managers in the U.S. would say that most motors of 5 hp and below are thrown away, while in Canada, thousands of such motors are still being repaired. The Electric Power Research Institute (EPRI) and the U.S. Department of Energy's Bonneville Power Administration have contracted with the Washington State Energy (DOE) Office to conduct a Rewind Industry Assessment Project to determine the number of electric motors repaired, sorted by their power rating, in the U.S.

1.9. Electric Motor Rewind Issues

The cost of operating electric motors has become more expensive because of the rapid increase in the electrical power cost. This situation makes the question of how rewinding affects a motor's efficiency more important [9]. Because of power cost issue, many customers would ask what happens to efficiency when a motor is rewound which can occur two to more times during a motor's lifetime. The most probable answer would be "a rewound motor is never as efficient as the original", but yet, a customer may hear that "a high quality rewound motor can have a higher efficiency than the original". These two opposite answers to the same question is a clear indication that this is a complicated subject [8]. Many studies have been performed to measure the effect of rewinding on motor efficiency [10]. In a study conducted by General Electric, it has been shown that an average rewind increases motor losses by 40% [28]. Interesting finding have been published through significant studies conducted by Hydro-Québec, Ontario Hydro, and BC Hydro, to show the impact of rewound motors on the efficiency. The results are discussed thoroughly in [29].

Rewinding a motor improperly will definitely change the amount of the five motor losses associated with the motor's efficiency and defined in NEMA standard MG 1-2011 [15]. Those losses are: stator copper loss, rotor copper loss, core loss, stray load loss, and friction and windage loss [30]. The stator and rotor copper loss which are almost 50 percent of total losses can be dramatically changed in using different wire size or a different number of turns. Core loss can be increased in case of insulation damage. Friction and windage losses can be affected as well by a change in bearings or different grade of grease. Any damage to the frame, stator or

rotor cores, or endshields can increase stray load losses [8]. The efficiency of a motor can be decreased significantly if it is improperly repaired [26].

A 1 percent decrease in the efficiency may not have tangible consequences in some situations, but when taking into account the motor operating hours, the potential wasted energy could be significant. The operating efficiency of any motor is determined by its original design, the quality of the construction or rewind, how heavily it is loaded and the quality of the power supply [8]. However, efficiency decreases are not unavoidable or unexplainable consequences of repair or rewinding [26]. Research continues to try re-designing motors under repair and enhancing the efficiency and the performance. In [31], it has been shown that careful control of the stator winding design while maintaining the same number of turns can reduce stator copper loss and this reduction will offset the increase in core, friction and windage losses.

Several organizations like IEEE (Institute of Electrical and Electronics Engineers), NEMA (National Electrical Manufacturers Association), and EASA (Electrical Apparatus Service Association) put a lot of effort to enhance and influence the motor repair practice. By working with the motor repair industry, these organizations can provide information and services critical to helping industrial and commercial customers manage their energy use and improve productivity [26]. Providing these types of services and education is essential for both energy savings and green house emission reduction.

1.10. Impact of Unbalanced Power Supply

Unbalance in a power supply is an important index in evaluating power system quality. A balanced three-phase voltage source is when the voltages are identical in magnitude, and shifted between each other by 120^{o} [32]. Any power supply is never perfectly balanced. Sometimes, even a small voltage unbalance can dramatically increase rotor losses which result in stator and rotor temperature rises. On the other hand, the level of unbalanced must be accounted for when it reaches certain level [33] that can cause serious ill effects on the three-phase induction motors, such as, reduction in output torque [34], vibration and overheating that leads to a reduction on insulation life of the machine [35]. The level of unbalance is considerably large in power systems which supply large single-phase loads [36]. According to ANSI/NEMA MG 1-2011, it is not recommended to operate induction motors with voltage unbalance above 5% [15]. IEEE in [37]

attributes the excessive temperatures in parts of the rotor of induction motors to the excessive unbalanced (negative-sequence) currents. The fact that there are only sporadic reports of motor failures due to voltage unbalance is because that many motors operating in industry are less than fully loaded, and this can provide the needed thermal margin which will allow those motors to operate with a voltage unbalance condition without failure [38].

The unbalance voltage can be caused by unsymmetrical transformer windings or transmission impedances, unbalanced loads, large single-phase loads [39], incomplete transposition of transmission lines, open delta transformer connections [40], blown fuses on three-phase capacitor bank, operation of single-phase loads at different times, or defective transformers in power systems [41].

The induction motor positive and negative sequence equivalent circuit that are used to analyze the performance of the machine operated under unbalanced voltages are as shown in Figure 1-2 and Figure 1-3 respectively.

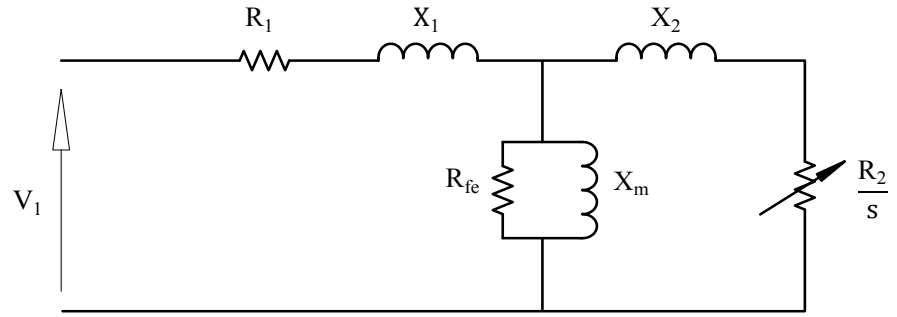

Figure 1-2. Positive sequence equivalent circuit.

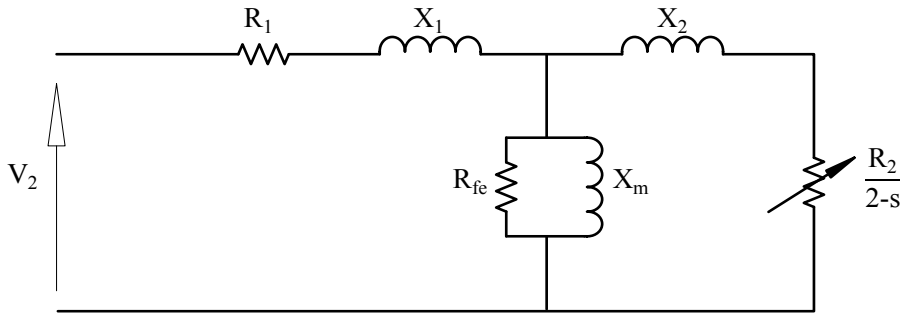

Figure 1-3. Negative sequence equivalent circuit.

where, V_1 is per phase positive sequence voltage; V_2 is per phase negative sequence voltage; R_1 is per phase stator winding resistance; R_2 is per phase rotor resistance; X_1 is per phase stator leakage reactance; X_2 is per phase rotor leakage reactance; X_m is per phase magnetizing reactance ; R_{fe} is per phase core loss resistance.

The behavior of the machine towards the positive sequence voltage is the same as for the balanced voltages, while it behaves in a different manner with the negative sequence voltage as illustrated in Figure 1-4. For a slip of value (s) with respect to positive sequence field, it will be (2-s) with the negative sequence field. The negative sequence torque will make the net shaft torque of the machine to be less than that produced under balanced voltages [33].

From Figure 1-4, it can be seen that the negative torque will affect: (1) the starting torque, which will be less than normal; (2) the maximum torque (breakdown torque), which will also be reduced; and (3) the full-load torque will be reduced to a level that if the same full-load is still applied on the machine, the motor will be forced to operate at lower speed (higher slip) which will definitely lead to higher machine's copper losses and overheat problems.

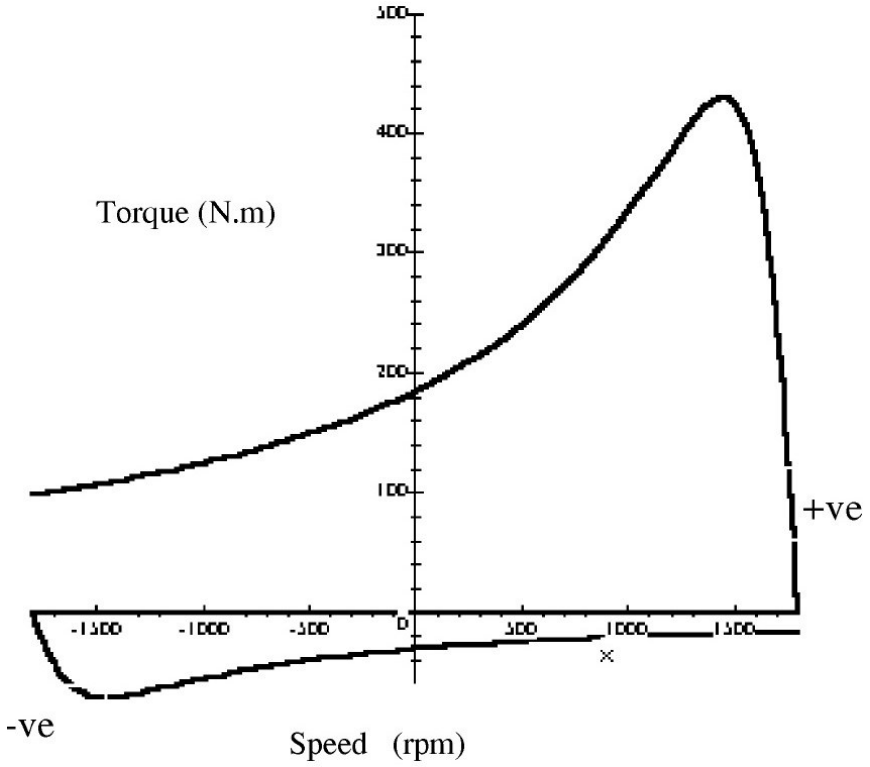

Figure 1-4. Positive and negative sequence torques of the IM [33].

1.11. Impact of Over or Undervoltage

The majority of industrial motors in the US are designed for 460 V operating voltage. Those motors are run with 480 V as this level of voltage is the rated value of the utility distribution system. The idea here is to avoid operating the motors with undervoltage when the system is heavily loaded in weak commercial or industrial systems [33].

According to ANSI/NEMA MG 1-2011 [15], induction motors that work with voltage supply of 10% or less of their rated voltage will operate with reduced pull-up and breakdown torque of approximately 20-30%. Loading such motors with their rated loads will definitely cause serious overheating problems which results in serious permanent damages.

In [42], it was claimed that undervoltage is the most frequent case in industry, whereas overvoltage is considered a much rarer phenomenon. While in [43], it was shown that overvoltage cases often occur during the off-peak period in many countries. For example, in Taiwan, the national power company has to add reactors and to trip one HV circuits to reduce the charging in power system during off-peak or national holidays.

It has been found that where utilization voltage exceeds 635 V, the safety factor of the insulation of motors rated to 575 V has been reduced to a level inconsistent with good engineering procedure [15].

1.12. Unbalanced and Fluctuated Voltages in the Literature

Perfect balanced voltages can never be maintained, because the loads are continually changing, causing the phase-voltage unbalance to vary continually [44]. Unbalanced voltages can cause serious problems that can bring any induction motor to a premature failure. The severe effect of voltage unbalance on the performance of the induction motors was the area of interest of many researchers since 1930's of the last century [45] when Reed and Koopman tried to analyze the performance of three-phase induction motors operating under unbalanced voltages by using the equivalent circuit and symmetrical components. In the 1950's, few researchers presented other useful approaches to the same issue [46] [47] [48] [49].

In [50], Gafford et al. concluded that the temperature rise above balanced operating temperature is due to increased copper loss. It was demonstrated that the negative sequence

current has a significant effect in terms of heating the motor, rather than an equal value of positive sequence, and that is due to the high negative sequence rotor resistance. It was also proven that core losses and friction and windage losses remain essentially independent of unbalance of negative sequence voltage that is less than 15%. It was also observed that negative sequence components cause vibration that may be injurious to bearings, to insulation, and to interconnecting mechanical parts of the machine.

The study in [51] by Berndt and Schmitz examined three 5 hp, 220 volts, 1800 rpm, NEMA design type B motors, from different manufacturers which were tested for temperature rise. To derate the machines, they were run under fixed unbalance and different loads. Two different methods were used to measure the winding temperature: (a) Change in winding resistance; and (b) thermocouples. The exact temperature at shut-off was extrapolated by having many resistance measurements for different elapsed time readings. 14 thermocouples were used to determine the hot spots. The negative sequence voltage was the main parameter that was used to derate the three motors. This study concluded that there is a need for a severe reduction in the rating of induction motors when operated with unbalanced line voltages.

In [34], Woll presented an important curve which shows the relationship between the percentage of voltage unbalance and the percentage of increase of motor losses and motor heating as shown in Figure 1-5. The motor heating curve in Figure 1-5 was drawn according to (1.4).

$$\%\Delta T \sim (\%\Delta V_U)^2 \quad \text{I}$$

where $\%\Delta T$ is the percentage increase of temperature, and $\%\Delta V_U$ is the percentage increase in voltage unbalance.

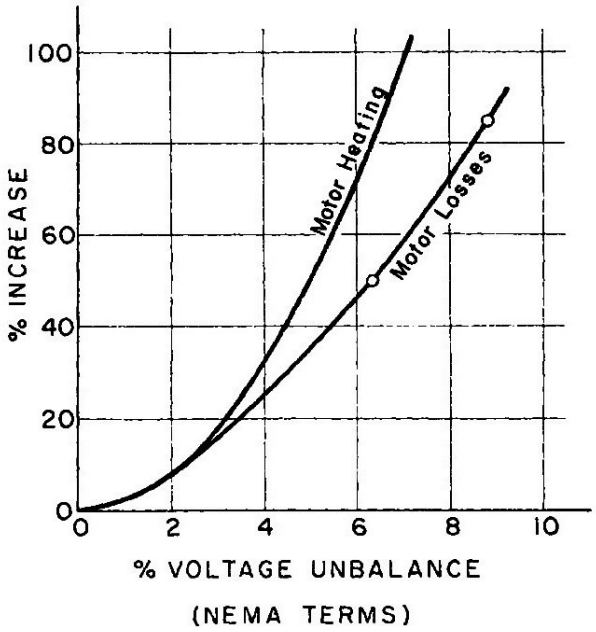

Figure 1-5. Increase in motor losses & heating due to voltage unbalance.

Kersting and Phillips in [52] conducted a practical study which showed that "It is not sufficient to merely know the percent voltage unbalance, but it is equally important to know how they are unbalanced". In this study, a detailed mathematical technique to analyze the performance of an induction motor under unbalanced voltages. The proposed technique shortened the conventional mathematical equations needed to achieve the same performance analysis on the machine. The study concluded that, beside what mentioned above of the importance of knowing the manner of the unbalanced voltages and its marked effect on the increase in losses, the rotor losses increase at a faster rate than the stator losses as the voltages become more unbalanced. The analysis included only the magnitude of the positive and negative sequence voltages without considering the effect of the angle on the performance of the machines.

The National Electrical Manufacturers Association has set a derating curve in ANSI/NEMA MG 1-2011 (shown in Figure 1-6) for medium polyphase induction motors working under unbalanced voltage up to 5% is established.

According to the amount of unbalance, the motor's rated output power should be multiplied by the derating factor, obtained from the curve, to have a new reduced full-load value that makes the motor running safely without the risk of overheating that is caused by the effect of unbalanced voltage if the motor kept running with its rated output power.

Lee claimed in [43] that the derating factor given by NEMA in Figure 1-6 is set in accordance only with voltage unbalance factor (VUF), without considering the many voltage unbalance cases which have the same VUF. The study conducted in [43] investigated 8 voltage unbalanced cases, which are as follows:

(a) Single phase undervoltage unbalance.
(b) Two-phase undervoltage unbalance.
(c) Three-phase undervoltage unbalance.
(d) Single phase overvoltage unbalance.
(e) Two-phase overvoltage unbalance.
(f) Three-phase overvoltage unbalance.
(g) Unequal single phase angle displacement.
(h) Unequal two-phase angle displacement.

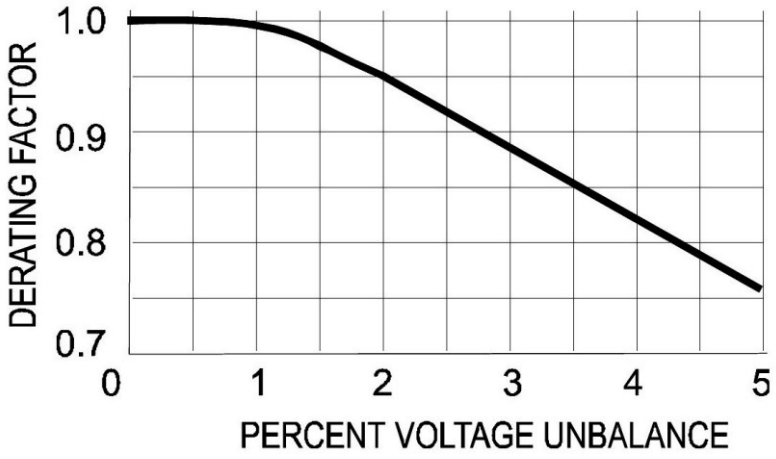

Figure 1-6. Medium motor derating factor due to unbalanced voltage [15].

The study is conducted on 2 different classes of induction motors (2 hp and 3 hp)[(1)]. The study showed that the worst case of temperature rise due to 4% and 6% VUF was with three-phase undervoltage unbalance.

An important study on the derating of induction motors operating with a combination of unbalanced voltages and over or undervoltages was conducted by Pillay and Hofmann in 2002 [33]. In this study, it was found that for a given percentage of voltage unbalance, based on the NEMA definition, there was a range of percentage unbalance, based on the true definition of

[(1)] The author did not mention the classes of the two machines.

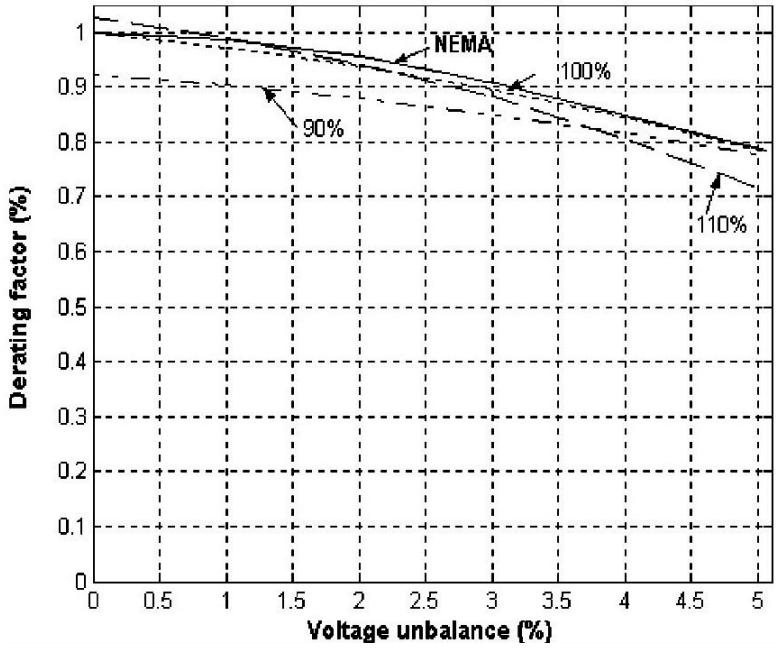

Figure 1-7. Inclusion of overvoltages and undervoltages on the derating curve [33].

unbalance which is the ratio of negative sequence voltage to positive sequence voltage. The derating factor was determined according to (1.5).

$$\text{Derating Factor} = \frac{P_{\text{out, calculated}}}{P_{\text{rated}}} \tag{1.5}$$

The study outcome was a practical extended NEMA derating curve as shown in Figure 1-7. The three curves were obtained from the following three cases:

(a) Case 1: a motor was supplied with unbalanced voltages at rated average voltage.

(b) Case 2: a motor was supplied with 10% overvoltage in combination with unbalanced voltages up to 5%.

(c) Case 3: a motor was supplied with 10% undervoltage in combination with unbalanced voltages up to 5%.

A comparison between graphical and mathematical methods of analyzing the performance of induction motors operated with unbalanced voltages was presented by Huang et al. in [32].

The complex voltage unbalance factor (CVUF) was used by Wang in [53]. This study showed the importance of the angle of the CVUF in analyzing the effect of unbalance on the performance of the induction motors. A method was proposed for determining the value of the

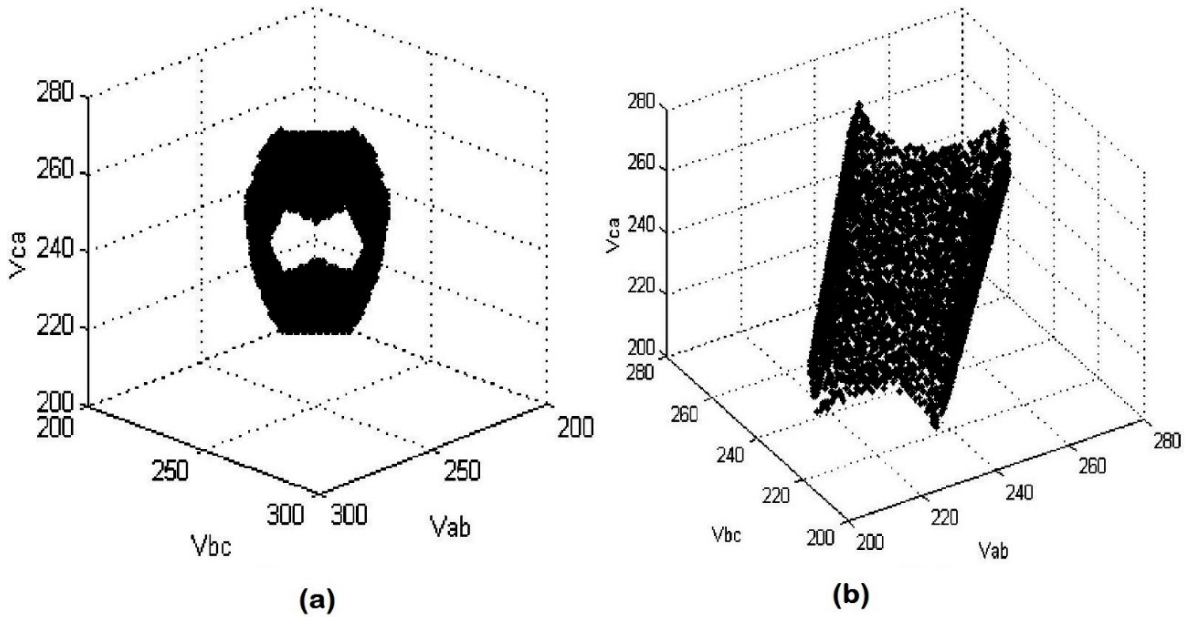

Figure 1-8. Terminal voltage variation of motor for VUF=6%. (a) NEMA definition, (b) True definition. [54].

angle for the worst cases that could cause a motor to be overheated.

An interesting study conducted by Faiz et al. in [54] suggested that the available definitions of unbalanced voltages are not comprehensive and complete. For example, in an unbalanced voltage case, the phase voltages can have any phase angel, however, in NEMA and IEEE definitions, only the voltage amplitudes have been included. The study also mentioned that in many studies, only general qualitative results were presented and no precise numerical values and characteristics have been provided, and it also claimed that the definition of unbalanced voltage and the resulting motor characteristics have not received attention and that what the study was about to prove. The study showed that an infinite number of line voltages can give the same voltage unbalance as illustrated in Figure 1-8. This figure shows that a 6% voltage unbalance, based on NEMA definition or True definition, will not lead to a unique terminal voltage of the motor. Each of those infinite number of line voltages that belongs to the same value of %VUF has different influence on the performance of the motor.

Two methods were suggested in [54] to reduce the range of input voltage variation for a given VUF. The first method was by specifying the positive sequence voltage component (V_1), and the second method was by using the complex voltage unbalance factor (CVUF) which has similar definition of VUF and it is calculated by using (1.6).

$$\%CVUF = 100 \times \frac{V_2}{V_1} \tag{1.6}$$

where V_1 and V_2 are the positive and negative vector components of the voltage, respectively.

By using the two methods, the infinite numbers shown in Figure *1-8* were reduced to the highlighted areas in Figure 1-10. A comparison between the results using NEMA and True definitions and the proposed method was carried out and showed that the variation in pull-out torque, starting torque, full-load torque, and efficiency of a motor under test were very large comparing to the results obtained by using the proposed first method of specifying a value for the positive sequence voltage.

The same author presented a practical example in [36] of induction machine's derating showing that the value of derating factor was 90% at 2.42% unbalance by using the CUVF, while its value for the same degree of unbalance was 94% using the NEMA derating curve.

A loss of life estimation technique due to operating induction motors on unbalanced voltages with a combination of over or undervoltage were proposed by Pillay and Marubini in [55]. The motor life is predicted by estimating the stator winding insulation life by using Arrhenius' equations. Five cases were tested and they were as follows:

(a) Case 1: a motor was run at full-load with unbalanced voltages.

(b) Case 2: the motor was derated to 95%.

(c) Case 3: the motor was derated to 85%.

(d) Case 4: a motor was run at full-load with 10% overvoltage in combination with 0% to 5% unbalanced voltages.

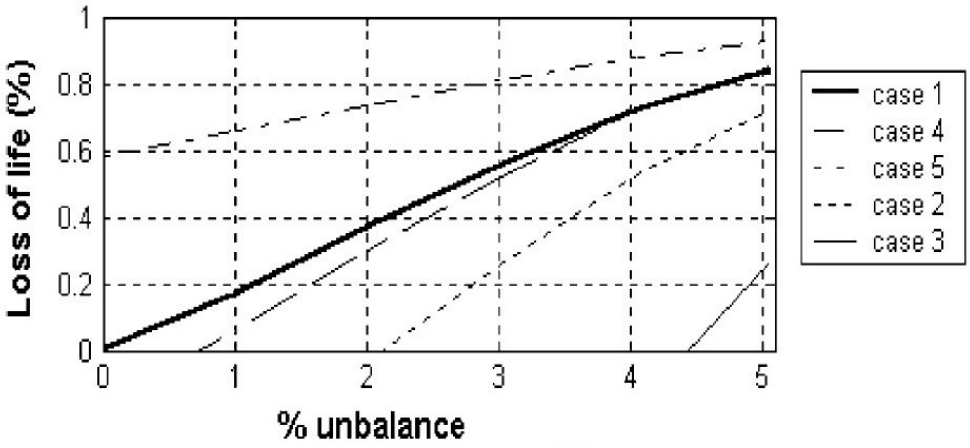

Figure 1-9. Loss of life under unbalanced voltages [55].

(e) Case 5: the motor run at full-load with 10% undervoltage in combination with 0% to 5% unbalanced voltages.

The loss of life curve produced by the study is illustrated in Figure 1-9. It can be clearly seen that Case 5 is the worst condition that can shorten the life of an induction motor.

In [56] and [42], a research for Gnacinski was published in 2008 and 2009 respectively,

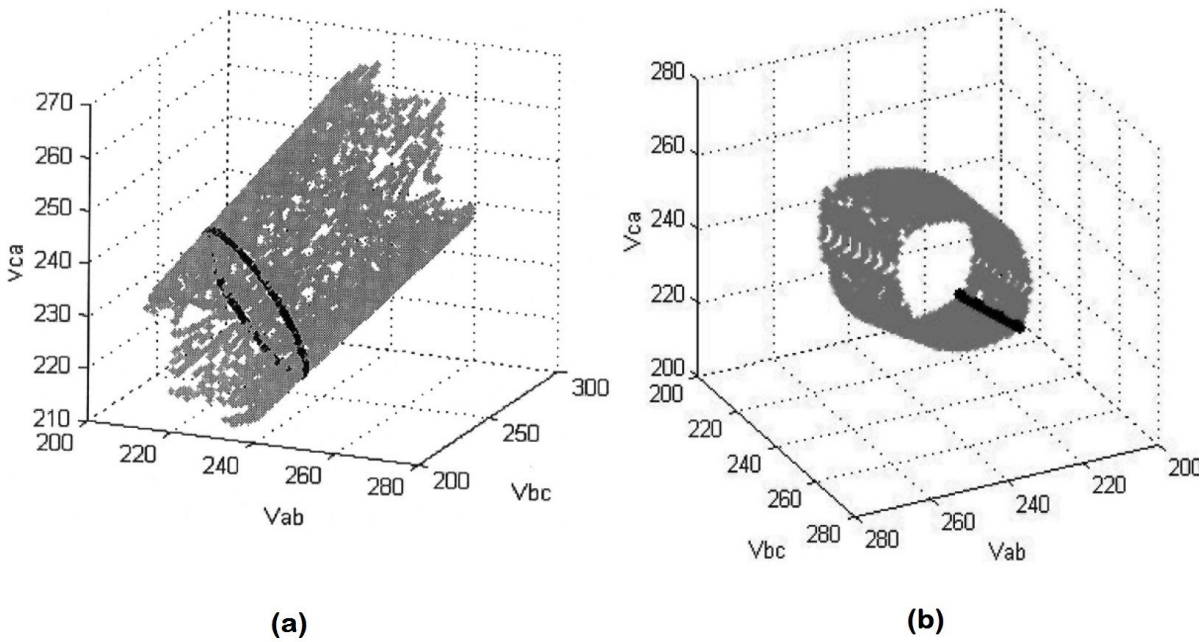

Figure 1-10. Terminal voltage variation of motor for VUF=6%. (a) with V_1=230 V, (b) with θ=120^o. [54].

which investigated the effect of simultaneous voltage unbalance and over or undervoltage on winding temperature and thermal loss of life of induction machines. The influence of angle of the CVUF was considered. The two studies showed that machines' saturated circuit property has a significant influence on the derating factor in the conditions of unbalanced voltage combined with over or undervoltage.

The latest research in regards to the induction machines derating issue was conducted by Anwari and Hiendro and published in 2010 [57]. In this research, a detailed symmetrical component mathematical procedure has been presented to estimate the efficiency of induction motor operating under unbalanced voltages with their associated phase angles. The only issue within the calculations was that the author didn't include the core and mechanical losses to estimate the output power of the machine under test.

The author used the complex voltage unbalance factor CVUF instead of VUF. The CVUF was presented as in (1.7).

$$k_v=\frac{V_{s2}}{V_{s1}}=k_v\angle\theta_v \tag{1.7}$$

where k_v is the magnitude of the CVUF and θ_v is the angle.

It was again shown that for a certain value of k_v, there are infinite combinations of terminal voltages. It was proposed to reduce the large range of terminal voltage variations by considering the phase angle and a new proposed factor which is called by the author "coefficient of unbalance" which was given the letter "f" and it is shown in (1.8).

$$V_{s1}=f\left(\frac{V_{ab}+a.V_{bc}+a^2.V_{ca}}{3}\right)\angle\theta_{s1} \tag{1.8}$$

where a is the Fortescue operator, $a=-\frac{1}{2}+j\frac{\sqrt{3}}{2}$, and $a^2=-\frac{1}{2}-j\frac{\sqrt{3}}{2}$

The study demonstrated an important comparison between the peak losses with balanced voltages when f=1, with under-unbalanced voltages when f<1, and with over-unbalanced voltages when f>1. For the example presented, the increase in the stator losses was 254% and 217%, and the increase in the rotor losses was 293% and 210%, for f=0.8 and f=1.2 respectively. This can indicate clearly that a motor operates in undervoltage unbalance condition can be under

high risk of overheating.

1.13. Impact of Harmonics in the Literature

Harmonics and their associated problems in induction motors were an area of interest for many scientists since 1920's. In 1929, the harmonic phenomenon was addressed as an unnecessary noise in electrical apparatus. Spooner and Foltz in [58] had investigated the problem of noise in electrical motors. In 1930, Hildebrand had another study regarding the only noise problem the harmonics can cause in induction motors [59]. In [60], Appleman proposed a solution to eliminate noise in small motors by having proper slot combinations, winding distribution, and skew to secure nearly sinusoidal wave form. In the 1940's, harmonics were still only a concern of the noise they caused in induction machines [61]. In the 1950's, researchers started to address the serious problem of losses in induction machines caused by harmonics due to increasing of the number of applications of induction machines with static frequency converter power supplies. In [62], Rawcliffe and Menon discussed the fact that all induction motors have magnetic power-losses at harmonic frequencies. They demonstrated a simple test for measuring the harmonic-frequency losses in induction motors as a separate quantity. Jain in [63] had used Fourier technique to analyze the voltage waveform that supplied to an induction machine. A very detailed mathematical technique to estimate the output power and torque with harmonic was presented. He found that, when an induction motor is fed by variable-frequency source which is often rich in harmonics, the distorted voltage modifies the motor operation considerably from that operating under conditions of pure sinusoidal voltages. He also noticed that, depending on the order, a harmonic component of voltage may contribute either positive, negative, or zero torque. Fourier analysis showed that (3n+1) order harmonics in the voltage waveform develop positive torques, while (3n+2) orders result in negative torques. (3n+3) orders produce no torque.

Klingshirn and Jordan presented a method in [64] for calculating harmonic currents and their associated losses in induction machines. The authors observed that the largest loss is in the rotor bars as a result of deep bar effect, and harmonic losses are almost independent of motor load. The applied voltage was assumed to have the expression shown in Eq(1.9) which is the voltage waveform that is most frequently encountred with 3-phase induction motors. It does not contain even and triplen harmonics.

$$v(t)=\sqrt{2}(V_1 \sin \omega t + V_5 \sin 5\omega t + V_7 \sin 7\omega t + \ldots + V_k \sin k\omega t) \quad (1.9)$$

Chalmers and Sarkar [65] highlighted the need for an accurate assessment of the time-harmonic losses when the input waveforms have a high harmonic content. They summarized the additional losses caused by harmonics in induction motors as follows:

(a) Stator copper losses when the harmonic current contribute to the total r.m.s. input current. Skin effect may be neglected in small wire-wound machines.
(b) Rotor copper losses. Skin effect must be taken into account as the rotor frequency is considered high.
(c) Core losses due to harmonic main fluxes.
(d) Losses due to skew-leakage fluxes.
(e) Losses due to end-leakage fluxes.
(f) Space-harmonic m.m.f. losses excited by time-harmonic currents. They might called high-frequency stray load losses.

As the development of static switching devices with high power ratings was leading to their increasing application in the control of induction machines, researchers started to search for new design of induction machine that can operate on rich harmonic power supply with minimum associated losses. McLean et al. in [66] and Buck in [67] investigated the reasons of loss of efficiency when conventional induction motors are supplied with square-wave voltages or subjected to PWM waveforms, and methods of design were described and presented to produce induction motors with comparable efficiency and output to those of sinusoidally fed machines.

A modified induction motor equivalent circuit which have additional resistances to account for the losses associated with stator and rotor leakage fluxes was proposed by Venkatesan and Lindsay in [68]. The modified equivalent circuit was used to calculate the losses considering stray iron losses, end leakage, and skew leakage. It was found that on full-load, time harmonic losses while running a 20 hp motor on six-step waveform were about 18 to 20 percent of the fundamental losses. Another interesting finding was that the harmonic stray losses greatly exceeded the fundamental stray losses. It was shown that harmonics of order (3k+2), where k is odd integer, produce MMFs rotating in the opposite direction to the fundamental field, whereas harmonics of order (3k+1), where k is even integer, produce MMFs rotating in the same direction as that of the fundamental field.

De Buck et al. in [69] proposed a model for estimating losses caused by harmonics in induction motors. The model was claimed to account for harmonics between 100 and 20000 Hz. Stator, rotor, and iron losses were estimated separately as a function of frequency. A penalization factor F_i or F_v were developed and they depend only on harmonic frequency and motor power rating.

In 1985, an IEEE Committee Report was written about the effects of power system harmonics on power system equipment and loads [70]. The problem of harmonics generation due to increasing applications of power electronic type devices which have nonlinear voltage current characteristics, and the increasing application of shunt capacitor banks for power factor correction and voltage regulation which results in an increased potential for resonant conditions that can magnify existing harmonic levels, were addressed in the report. The report divided the effect of voltage distortion into three general categories: (1) insulation stress; (2) thermal stress; and (3) disruption. The main purpose of the report was to examine the various equipment characteristics to determine the limiting factors in the operation of the equipment with system distortion present. In regards to motors, the report assumed that the harmonic components may be classified as stator winding loss, rotor winding loss, and stray loss, which are I^2R loss. The additional core loss due to voltage distortion is negligibly small.

It was also assumed that the rotor frequency at any harmonic is equal to the stator harmonic frequency. This assumption might overestimate the negative sequence losses, but underestimate the positive sequence losses. This assumption is reasonable as long the smallest harmonics ($2 \le n \le 4$) are not present.

The report proposed the harmonic losses P_h to be represented as

$$\frac{P_h}{P_{RL}} = k \sum_{n=5}^{\infty} \frac{V_n^2}{\sqrt[2]{n^3} V_1^2} \tag{1.10}$$

where P_{RL} is the machine loss at the rated point with sinusoidal supply, and n is the harmonic order. The approximate form of the proportionality constant k is

$$k = \frac{\left(\frac{T_{st}}{T_r}\right)\eta}{(1-s_r)(1-\eta)} \tag{1.11}$$

where T_{st} is the starting torque, and T_r, s_r, η are the machine torque, slip, and efficiency at rated point.

The report came up with a definition of Motor Distortion Index (MDI) by the following equation:

$$MDI=\frac{1}{V_1}\sqrt{\sum_{n=5}^{\infty}\frac{V_n^2}{\sqrt[2]{n^3}}} \tag{1.12}$$

The equation suggests that motors with a large deep bar or double cage effect would have the highest harmonic heating.

The need for derating induction motors operating under rich harmonic power supply was first mentioned by Cummings in [71] where he developed Harmonic Voltage Factor (HVF). The slip for any harmonic frequency was defined as

$$S_n=\frac{3k}{3k\pm1} \tag{1.13}$$

where k is even integer as balanced firing of converter and symmetrical loads are assumed. So, only odd harmonics will be exist as shown in Table 1-II.

Cummings used the equivalent circuit and the principle of superposition to evaluate the effect of harmonic voltage on induction motors. He approximated the harmonic equivalent circuit as shown in Figure 1-11. The resistance r_{1n} in the figure was considered to be equal to the dc resistance of the stator winding which is constant with frequency and varies with temperature. The resistance r_{LLn} represents the stary-load loss or any circulating or strand losses. The stator leakage reactance is proportional to frequency ($x_{1n}=nx_1$) where x_1 is the stator leakage reactance

Table 1-II. Time Harmonics and Rotation of their Associated Torques

n	**Harmonic Orders for Positive Sequence (3n+1)**	**Harmonic Orders for Negative Sequence (3n+2)**	**Harmonic Orders for Zero Sequence (3n+3)**
0	1	2	3
1	4	5	6
2	7	8	9
3	10	11	12
4	13	14	15
5	16	17	18
6	19	20	21
7	22	23	24

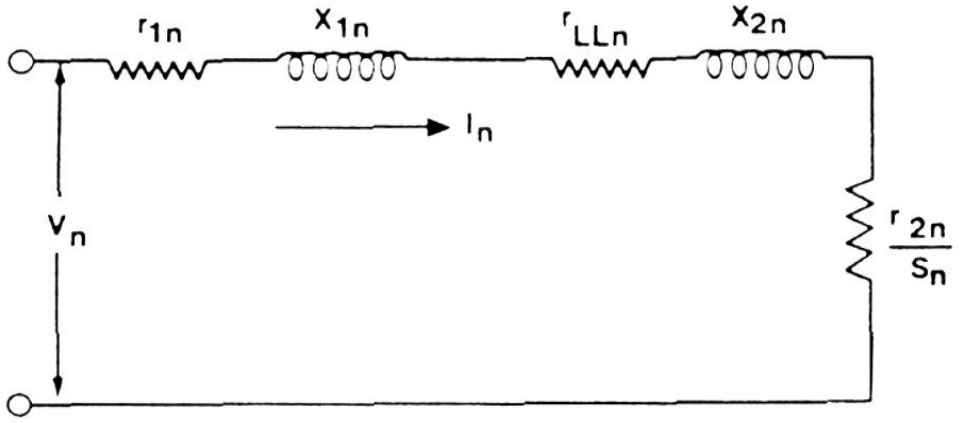

Figure 1-11. Harmonic equivalent circuit.

at fundamental frequency. The rotor resistance r_{2n} and rotor leakage reactance x_{2n} are a complex function of the frequency of the rotor current ($n \times f_{rated} \times S_n$) which is almost always $\leq$2 Hz for normal operation with 60 Hz rated frequency. At this low rotor current frequency, the skin effect or deep-bar effect is inactive. While for higher frequencies, the skin effect will take place which increases the rotor resistance and decreases the rotor leakage reactance. The r_{LLn} was assumed to be proportional to $n^{0.8}$ with sufficient accuracy due to its complex relationship with frequency.

The author developed a model to estimate the harmonic loss and Harmonic Voltage Factor which is

$$HVF=\sqrt{\sum_{n=5}^{\infty}\frac{V_n^2}{n}} \tag{1.14}$$

The relationship between total harmonic loss and HVF is

$$\Delta W_T \cong 35 \times (HVF)^2 \tag{1.15}$$

For thermal considerations, HVF has to be less than 0.045.

Kataoka et al. in [72] presented a method of measuring both the fundamental and time harmonic equivalent circuit parameters of inverter fed induction motors. The fundamental equivalent circuit per phase had the core loss resistance and the magnetizing reactance in series. While the harmonic equivalent circuit ignored the core loss and magnetizing branch. The method includes no-load and blocked-rotor tests, beside a dc stator winding resistance test. The authors use the no-load and blocked-rotor tests with both fundamental and harmonic voltages. The iron

loss resistance and the magnetizing inductance were measured at no-load with variable voltages at fundamental frequency. The rotor resistance and leakage inductance with harmonics were calculated by using the equivalent circuit with different applied frequencies.

With regards to the dominant loss in induction motors due to harmonics existence, it has been claimed in [64] that the largest loss is usually in the rotor bars due to the deep bar effect. While Undeland and Mohan in [73] found that iron losses are the dominant part of the additional motor losses due to the presence of harmonics.

Sen and Landa in [74] discussed derating of induction motors of NEMA design B of different output ratings due to different cases of harmonic distortion. According to IEEE Standard 519 [75], no derating of a motor would be necessary for a harmonic content of up to 5%. According to [75], the distortion factor DF which can be determined as

$$\text{DF}=\sqrt{\frac{\text{sum of squares of amplitudes of all harmonic voltages}}{\text{square of amplitude of fundamental voltage}}} \tag{1.16}$$

and it is used to establish harmonic limits. The study in [74] was based on three assumptions: (1) the motors are nonskewed, Y-connected, and ungrounded, (2) the analysis is limited to full-load steady-state operating conditions, and (3) the principle of superposition applies. The mechanical losses that comprise of friction and windage losses are assumed to be unaffected by voltage harmonic distortion. The stray-load losses were estimated based on a comprehensive study conducted by Alger et al. in [76]. The percent full-load losses for a typical standard NEMA design B machines were presented as

$P_{\text{mechanical}}$=0.09, P_{iron}=0.20, $P_{\text{stator copper loss}}$=0.37, $P_{\text{rotor copper loss}}$=0.18, P_{stray}=0.16.

The effect of harmonic voltages upon their orders were presented in [74] as shown Table 1-II which shows those time harmonics up to the 24^{th} order. It can be seen that all triplen harmonics have zero associated torque.

The formula used to derate the machines under test is

$$\text{Derating Factor}=1-\frac{\text{Output Power with Harmonics}}{\text{Output Power with Sinusoidal}} \tag{1.17}$$

The important outcomes of the study in [74] were that the second order harmonic have to be included on the harmonic distortion limits established by IEEE Standard 519, and derating in some cases should be considered for less than 5% harmonic distortion.

In 1993, a new report of the IEEE Task Force on the effects of harmonics on equipment was established [77]. The problem of overheating was again presented as the main problem caused by voltage distortion as the losses in electric machines are dependent upon the frequency spectrum of the applied voltage. The increase in motor operating temperature will cause a reduction of the motor operating life. It was stated that if the harmonics are time varying, the motor can tolerate higher peak distortion levels without significant increase in temperature. This is because the motor thermal time constant is much longer than the period of harmonic variation. The pulsating torque was diagnosed as a consequence of the interaction between the fundamental air gap flux and the fluxes produced by the harmonic currents in the rotor.

Lee et al. pointed out the reasons behind a rich harmonic power supply which are: (1) operation of power electronics devices, (2) operation of steel mills arc furnaces, and (3) resonance of shunt capacitors and/or series inductors [78]. Even when induction motors are driven by sinusoidal power supplies, the magnetic fields include many time harmonics which are caused by the phase band, stator and rotor slot ripple [79]. The authors in [78] used a real load test to investigate the effects of harmonics on the performance of induction motors under different Voltage Distortion Factors (VDF) in terms of efficiency, temperature rise, and pulsating torques. Three different VDFs, 5%, 10%, and 15%, were used to test a 3 hp, 3-phase induction motor for efficiency with different orders of harmonics. Associated useful figures were presented to show the effect of +ve, -ve, and zero sequences on the efficiency of the motor. It was noticed that the lower order harmonic (2nd order) resulted in lower efficiency, and the larger the VDF is, the lower the efficiency. The temperature rise was also observed, and again, the lower harmonic orders below 5 affect the performance of the motor more severely than the harmonic orders above 5. The study concluded that when studying the impact of harmonics on induction motors, both odd and even harmonics must be considered.

In [80], Jalilian et al. presented a method of measuring induction motor harmonic losses

by using the DCC (Double Chamber Calorimeter) technique. The idea is based on measuring the amount of heat dissipated from the machine while running under a rich harmonic power supply. It was mentioned that the calorimeter is capable of measuring motor losses up to 1 kW, including harmonic losses, with maximum uncertainty of ±15 W. This can give a clear idea that this approach can work with only small rated induction machines.

In another study of Jalilian et al. [81], it was found that lower order harmonics cause more losses in induction motors when compared against higher order harmonics. A weighted THD which varies with harmonic orders was presented as

$$\text{WTHD}=\sqrt{\sum \frac{V_n^2}{n^{0.8}}} \tag{1.18}$$

This WTHD was proposed to be used as an index of the amount of distortion allowed in the supplied voltage rather than THD which seems not to vary with different harmonic orders, although the severe effects of lower harmonic orders over the higher ones was shown.

Hildebrand and Boehrdanz in [82] studied the effects of pulse frequencies of PWM converters on the additional losses of induction motors caused by harmonics. They found that harmonic copper losses became significant with the increase of pulse frequencies, and those losses can be more distinct for skewed rotors.

Wheeler et al. in [83] introduced Harmonic Loss Factor (HLF) which measured in milliwatts per square volt (mW/V^2) which was considered to be an index of the amount of harmonic losses in induction motors. The relationship of the HLF with the applied frequency was shown. The harmonic loss for an induction motor under any operating condition was predicted from the HLF curve and the amount of distortion in the applied voltage.

Many researchers proposed circuit models to represent the induction motor equivalent that includes harmonics effects [61] [63] [72] [84]. Figure 1-12 and Figure 1-13 show the induction motor equivalent circuits of both fundamental and harmonic frequencies respectively.

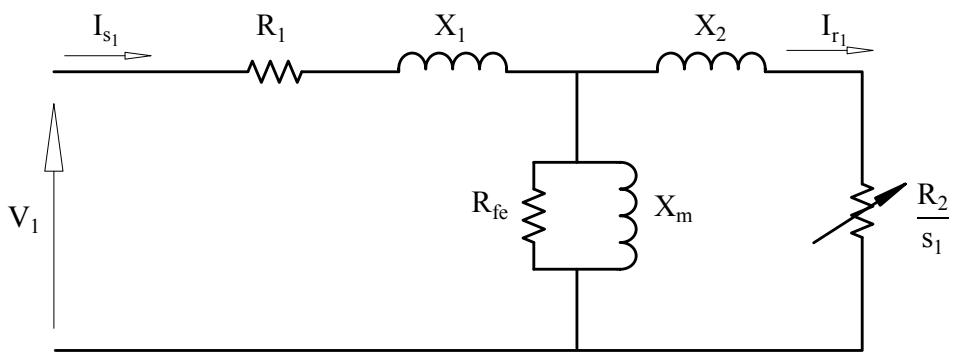

Figure 1-12. Equivalent circuit at fundamental frequency.

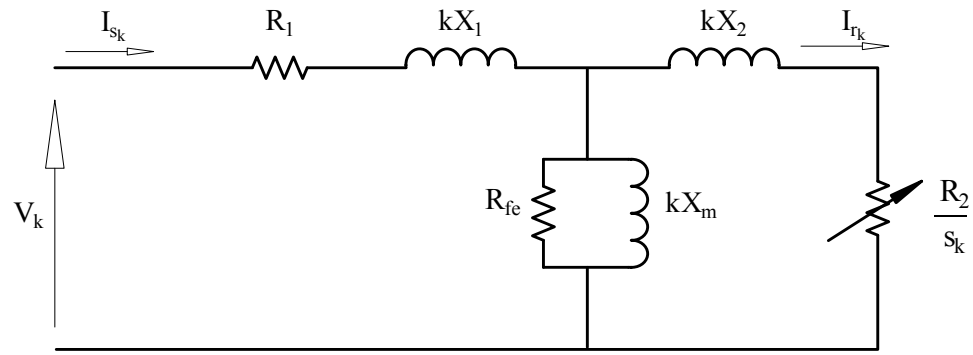

Figure 1-13. General equivalent circuit at harmonic frequencies.

1.14. Thesis Outline

This thesis is organized as follows:

Chapter 2

This chapter presents a novel algorithm for induction motor full-load and partial loads efficiency estimation from only no-load test. The algorithm is based on power calculations and it utilizes a large database of induction motors tested for efficiency in Laboratoire des Technologies de l'Énergie, Institut de Recherche, Hydro-Québec, Shawinigan, Québec, Canada [85]. The data has a wide range of motors' power rating and generously offered by Hydro-Québec as a contribution to the project. Another valuable set of data is received from BC Hydro, which includes the testing of 55 used (aged) induction motors [86]. The algorithm is validated by testing 196 induction motors of ratings ranged between 1 hp to 500 hp. The goal of the proposed algorithm is to be easily used in North America's electric motor service centers. This research work is well received when presented in CIGRÉ 2014 in Paris.

Chapter 3

This chapter introduces another novel algorithm for induction motors efficiency estimation which also based on no-load tests. The algorithm requires the availability of variable voltages as it is based on the saturation test recommended by IEEE 112^{TM}-2004. The algorithm also utilizes the Hydro-Québec/BC hydro data. The proposed algorithm is evaluated by testing eight induction motors and the results showed acceptable accuracy. The work is published in the IEEE Transactions on Energy Conversion journal.

Chapter 4

This chapter presents a developed software that includes both algorithms of Chapter 2 and Chapter 3 to create a useful industrial tool that can be used in electric motor service centers. The platform of the software is selected to be spreadsheets to make it affordable and user-friendly. The software is designed and upgraded upon feedbacks and comments that are received from technical monitors from several Canadian power companies. The software is evaluated and approved by the technical monitors and now it is being marketing by CEATI International Inc.

Chapter 5

This chapter presents an algorithm for in-situ induction motor efficiency estimation by using a combination of GA procedures with the IEEE Form 2-Method F1 calculations. The algorithm is also designed to utilize the Hydro-Québec/BC hydro data. The algorithm uses the measured stray load loss and hot temperature. It requires only one load point which is full-load with its corresponding rms values of voltage, current, and power obtained at the motor terminals. The speed estimation technique used needs the current signal acquisition of only one line. The algorithm is not only an in-situ efficiency determination tool; it can also be used as a promising tool for on-site efficiency estimation that might eliminate the need to the costly dynamometer procedure. The algorithm is evaluated and assessed by testing 30 induction motors of different kinds and power ratings. The results show an acceptable level of accuracy. The work is published in the IEEE Transactions on Energy Conversion journal as Early Accessed Article.

Chapter 6

This chapter proposes a novel algorithm for in-situ efficiency estimation of induction motors operating with unbalanced voltages by using a combination of GA procedure, IEEE Form 2-Method F1 calculations, and pre-tested motors. It is proven in Chapters 2 & 3 that using the assumed values of stray load loss can significantly increase the error and reduce the accuracy of the estimated efficiency. Hence, the proposed algorithm in this chapter is designed to utilize Hydro-Québec and BC hydro data. A strategy is proposed to assign an average value of stray load loss to the machine under test. The strategy is detailed in this chapter. The algorithm is also designed to use measured and assumed values of friction and windage losses. The algorithm requires only one load point which is full-load with its corresponding rms values of voltage, current, and power obtained at the motor terminals. The speed estimation technique that is used in this chapter needs the current signal acquisition of only one line. The algorithm is evaluated and assessed by 10 voltage unbalance tests and 2 test with balanced voltages using 2 small induction motors. The results are presented and show an acceptable level of accuracy. The goal of the study was to design a useful tool that can be used in industry to derate induction motors due to voltage unbalance.

Chapter 7

This chapter proposes another novel algorithm for in-situ efficiency estimation of induction motors that operate with distorted unbalanced voltages by using GA procedures, IEEE Form 2-Method F1 calculations, and by utilizing Hydro-Québec/BC hydro data. The novelty of the algorithm is demonstrated by using a new approach in determining the stray load loss and friction and windage losses based on a certain strategies and novel equations which are declared in this chapter. The algorithm requires only one load point which is full-load with its corresponding rms values of voltage, current, and power obtained at the motor terminals. The online speed estimation technique that is used in this chapter needs the current signal acquisition of only one line. The algorithm is evaluated and assessed by 50 tests of different combinations of voltage unbalance and harmonics performed with two small induction motors. The results are presented and show an acceptable level of accuracy. The algorithm is also validated for its consistency by 10 repeated tests with a very low coefficient of variation. The usability of the algorithm with balanced harmonics free voltages is demonstrated by testing the two machines and an acceptable accuracy is shown.

Chapter 8

This chapter presents the conclusions and future works.

1.15. Thesis Contributions

The contributions that achieved in this Ph.D. work are as follows:

I. In Chapter 2, a novel algorithm is designed to be easily used in any electric motor service center. It is based on only one no-load test and rms values. The algorithm is approved by technical monitors from several Canadian power companies. The algorithm is presented and well received in the CIGRÉ 2014 Conference and Exhibition in Paris, France [87].

M. Al-Badri and P. Pragasen, "A Novel Technique for Refurbished Induction Motors' Efficiency Estimation Based on," in *CIGRÉ 2014 Conference and Exhibition, Session 45, Paris*, 24-29 August 2014.

II. In Chapter 3, another novel algorithm is designed to be used in electric motor workshops. It is also based on no-load tests. The algorithm is approved by technical monitors from several Canadian power companies. The algorithm is published in IEEE Transactions on Energy Conversion journal [88].

M. Al-Badri, P. Pillay and P. Angers, "A Novel Algorithm for Estimating Refurbished Three-Phase Induction Motors Efficiency Using Only No-Load Tests," *Energy Conversion, IEEE Transactions on*, vol. 30, no. 2, pp. 615,625, June 2015.

III. In Chapters 2 & 3, an uncertainty study is conducted on both proposed algorithms of Chapters 2 & 3 to create credits to the outcome of both algorithms. The study is presented in 2014 IEEE International Conference on Power and Energy (PECon) in Kuching, Malaysia [89].

M. Al-Badri and P. Pragasen, "Evaluation of measurement uncertainty in induction machines efficiency estimation," in Power and Energy (PECon), 2014 IEEE International Conference on, Kuching, Malaysia, 1-3 Dec. 2014.

IV. In Chapters 4, a spreadsheet based software is developed to turn the two novel algorithms of Chapters 2 & 3 into a practical industrial tool. The software is approved by the technical monitors and it is being marketing now by CEATI International Inc.

V. In Chapters 5, a novel in-situ efficiency estimation algorithm is proposed. The algorithm has the potential to replace the expensive dynamometer procedure. The research work is published in IEEE Transactions on Energy Conversion journal [90].

Al-Badri, M.; Pillay, P.; Angers, P., "A Novel In Situ Efficiency Estimation Algorithm for Three-Phase IM Using GA, IEEE Method F1 Calculations, and Pretested Motor Data," *Energy Conversion, IEEE Transactions on* , (IEEE Early Access Articles).

VI. In Chapters 6, a novel algorithm for in-situ efficiency estimation of induction motors operating with unbalanced voltages is proposed. The algorithm has the potential to be a reliable tool for induction motors derating due to voltage unbalance. The research work is presented in IEEE International Electric Machines & Drives Conference in Coeur d'Alene, Idaho, USA in May 10-13, 2015. Upgraded version of this paper is submitted to IEEE Transactions on Industry Application.

VII. In Chapters 7, a novel algorithm for in-situ efficiency estimation of induction motors operating with unbalanced and distorted voltages is proposed. The algorithm has the potential to be a reliable tool for induction motors derating due to voltage unbalance and harmonics. A paper of the research work is submitted to the IEEE Transactions on Energy Conversion journal.

CHAPTER TWO

2. A Novel Technique for Induction Motors Full-Load and Partial Loads Efficiency Estimation from Only One No-Load Test

Full-load and partial load efficiency of 3-phase induction motors can be determined by using the dynamometer tests which is expensive, time consuming, and it is only available in well-equipped laboratories. There were few trials from engineers in the field and researchers to make the process of induction motor efficiency estimation applicable in electric motors service workshops [90] .

This chapter presents a novel method for estimating induction motor full-load and partial loads efficiency from only one no-load test. The objective of this research is to eliminate the need for the costly dynamometer method. The technique requires very limited data and can be applied in any electric motor service center in North America. Experimental and field results of testing a total of 196 induction motors are presented and the degree of accuracy is shown by comparing the estimated efficiencies against the measured values. The algorithm utilizes a database of a large number of induction motors tested for efficiency in the Laboratoire des Technologies de l'Énergie, Institut de Recherche, Hydro-Québec, Shawinigan, Québec, Canada. The data has a wide range of motor types and power ratings. Another set of data was received from BC hydro which includes a full test of 55 used (aged) induction motors. The database is utilized to estimate machine losses based on a certain pattern of losses distribution. The accuracy of the algorithm is verified by testing 196 of power rating from 1 hp to 500 hp. An acceptable level of accuracy is obtained. Error analysis and uncertainty study is conducted to give the reliability and credibility needed for the algorithm.

To turn the algorithm into a practical industrial tool that can be used in workshops, a user-friendly software was designed to handle both the algorithm and the database. To make the software affordable and cost effective, a spreadsheet was selected to be the platform of the software.

2.1. Introduction

In industrialized countries, electric motors utilize nearly two-thirds of the electricity generated [1], and hence, contribute to the global environmental problem which is represented by the emission of greenhouse gases [2]. Several Canadian and U.S. utilities have taken serious steps in implementing demand side management programs [3] to reduce both greenhouse gas effects and the cost of power that feeds this large population of electric motors.

In developing countries, a similar situation encountered, where a significant portion of the generated power is utilized by motors. Taking South Africa as an example, motorized systems account for up to 60% of the total electricity utilization [4].

In industry, only motors above 500 hp are usually monitored because of their high costs. However, motors below 500 hp make up 99.7% of the motors in service. These motors operate at approximately 60% of their rated load because of oversized installations or under-load conditions, and hence, they work at reduced efficiency which results in wasted energy [6]. Motor losses can represent a considerable cost over a long period due to high load factor [7].

Power costs are constantly rising at a rate that is even faster than both material and producer goods prices [8], many companies have hired energy managers whose sole purpose is to find practical ways to reduce power costs [9]. As an example, and according to the U.S. Department of Energy's (DOE) Office of Energy Efficiency and Renewable Energy (EERE), a large size paper mill could save an average of $659,000 a year through motor system efficiency [10]. In today's economy, it is more important than ever to optimize motor losses and keep the operating cost under control [8]. Efficient operation of electric motors can provide significant energy savings with benefits for both consumers and power utilities [11].

If a replacement decision of low efficient motor is taken as a result of the calculation of energy savings and payback periods that are based on nameplate motor efficiency or manufacturer's data only, this could lead to large errors [1], because the real efficiency of a motor is usually different from that value mentioned on its nameplate, as efficiency may decrease significantly due to aging or rewinding process [17], or it might not be given according to IEEE Std 112™ Method B [18].

A significant amount of research work have been conducted on the subject of induction motors' efficiency estimation. The following is a quick review of some of the major methods that are used in the field. Comprehensive reviews were conducted in [18], [20], and [13]. In the nameplate method, it is assumed that the efficiency of the motor is constant and always equal to the nameplate value. This method is inaccurate and could lead to large error since the nameplate data are rounded [14], plus other issues that are previously mentioned. Other researchers proposed using the slip method as an approach to determine the efficiency of a motor. This method relies on speed measurements, but it has been proven that it is not very accurate or useful due to the variations in motor nameplate data, line voltage unbalance, and temperature variation of the rotor [19]. Another approach to approximate motor efficiency is the current method, and again, this method was also proven impractical and inaccurate in [18], [20] and [13]. In the segregated loss method, the magnitudes of the five losses of induction motor, namely, stator copper loss, rotor copper loss, core loss, stray load loss, and friction and windage loss are estimated and then summed up and subtracted from the input power to determine the output power and hence the efficiency [20]. In the IEEE Std 112^{TM} -2004, the equivalent circuit methods F/F1 are presented [21]. In these methods, the test procedure is as follows:

- Measurement of cold resistance.
- Perform the no-load test.
- Conduct the impedance test.
- Determine the friction and windage losses.
- Determine the core loss.
- Extract the six parameters of the motor.
- Measure or assume the stray load loss.
- Estimate the efficiency.

The degree of the accuracy of this approach depends on how close the assumed hot temperature and stray load losses are to the real values. The wider the difference, the larger the error obtained in estimating the efficiency. Ontario Hydro proposed a modified version of the IEEE Std 112TM Method F1 [22]. A no-load test and a full-load test, both at rated voltage have

to be conducted. This method eliminates the need for a variable-voltage required by IEEE Std 112TM Method F1 [20]. The well-known air-gap equations are utilized for determining motor efficiency by a method called the air-gap torque method. In this method, the negative rotating torque caused by unbalance voltages and harmonics is considered. The major disadvantage of this method is that current and voltage waveforms are required as input data, besides software is required to analyze the field measurements [20]. Most, if not all, of those methods in the literature have been designed to work properly in well-equipped laboratories, where the required instrumentation and equipment are available. The authors of those works did not pay close attention to make their proposed methods applicable in the electric motor service centers where there is a need to have the rewound motors tested for efficiency before delivering them back in service. In [11], the authors proposed a technique for efficiency estimation for refurbished induction motors, but again, it was not feasible to be applied in any workshop due to the need for data acquisition measuring devices and a sophisticated and expensive software to handle the proposed technique.

In this chapter, a novel efficiency estimation technique for repaired, rewound, or any existing induction motor, is proposed. This would work in the technical environment of North America's electric service centers and tailored to available in such workshops of instrumentation. The proposed algorithm is named (Method A), and it works with very limited data obtained from only one no-load operating point run under a voltage equal or close to the rated voltage. Method A is designed to eliminate any need for voltage and current waveforms capturing devices as it uses only RMS values. To transfer the method into a practical tool to be used in the industry; a software has been designed based on a spreadsheet. The algorithm utilizes a large database of induction motors tested for efficiency in the Laboratoire des Technologies de l'Énergie, Institut de Recherche, Hydro-Québec, Shawinigan, Québec, Canada. The data has a wide range of motor power ratings [91]. Another valuable set of data is used from BC Hydro, which includes a full test of 55 used (aged) induction motors [86]. Applicability and feasibility of the method has been determined by technical visits made by the research team to some electric motor service centers in the Montréal region. Experimental and field results for testing 196 induction motors are presented and demonstrate the degree of accuracy of the proposed technique.

2.2. The Proposed Algorithm

Efficiency tests are necessary to establish a performance level that allows evaluation of the repaired and rewound motors [92] or any existing motor. Determination of refurbished motor's efficiency in laboratories is too expensive, although it can give precise efficiency estimation. A no-load based efficiency estimation of full-load and partial loads of the induction motor is the most suitable and applicable way to be used in electric motor service workshops. The simpler the requirements are, the easier the technique can be applied and be matched to the technical environment of those workshops where sophisticated equipment and software cannot be encountered. An algorithm is designed to work with very limited inputs of only one operating point with no load coupled to the motor shaft and with the motor running at rated or close to rated voltage, and with rated frequency. The algorithm relies mainly on induction motor powers calculation. The source of calculations is the nameplate data and RMS values of input voltage, input current, and input power. The DC resistance of the stator winding should be determined by using a DC resistance test that complies with section 5.4 of IEEE Std 112™-2004 [21] and section 8 of CAN/CSA Std C392-11 [93]. The temperature has to be measured during the DC resistance test using the recommended instruments in section 4.4 of IEEE Std 112™-2004 and section 8 of CAN/CSA Std C392-11. The value of the DC resistance should be corrected to the full-load temperature (Hot Temperature). With no load coupled to the motor; the measured input power should be equal to the total losses of the motor as the output power is assumed to be zero. The stator copper loss, friction and windage losses, and core loss comprise the no-load total losses. The mechanical rotational losses that consist of friction and windage losses, and the core loss can be determined by subtracting the stator loss from the input power. The algorithm assumes that the no-load mechanical rotational losses have the same value under full-load condition if voltage and frequency are the same [94]. The reason of making this assumption is because the algorithm has no way to separate the core loss and friction and windage losses as it has only one operating point. Stray load loss is estimated based on IEEE Std 112™-2004 and International Standard IEC 60034-2-1 [95] computing methodologies. Full-load total losses are estimated based on the nameplate data. Full-load efficiency is predicted based on the previous calculations and assumptions. The partial loads efficiencies are estimated based on relationships that are extracted based on a thorough investigation done on Hydro-Québec/BC hydro data. The flow chart of the proposed Method A's algorithm is shown in Figure 2-1.

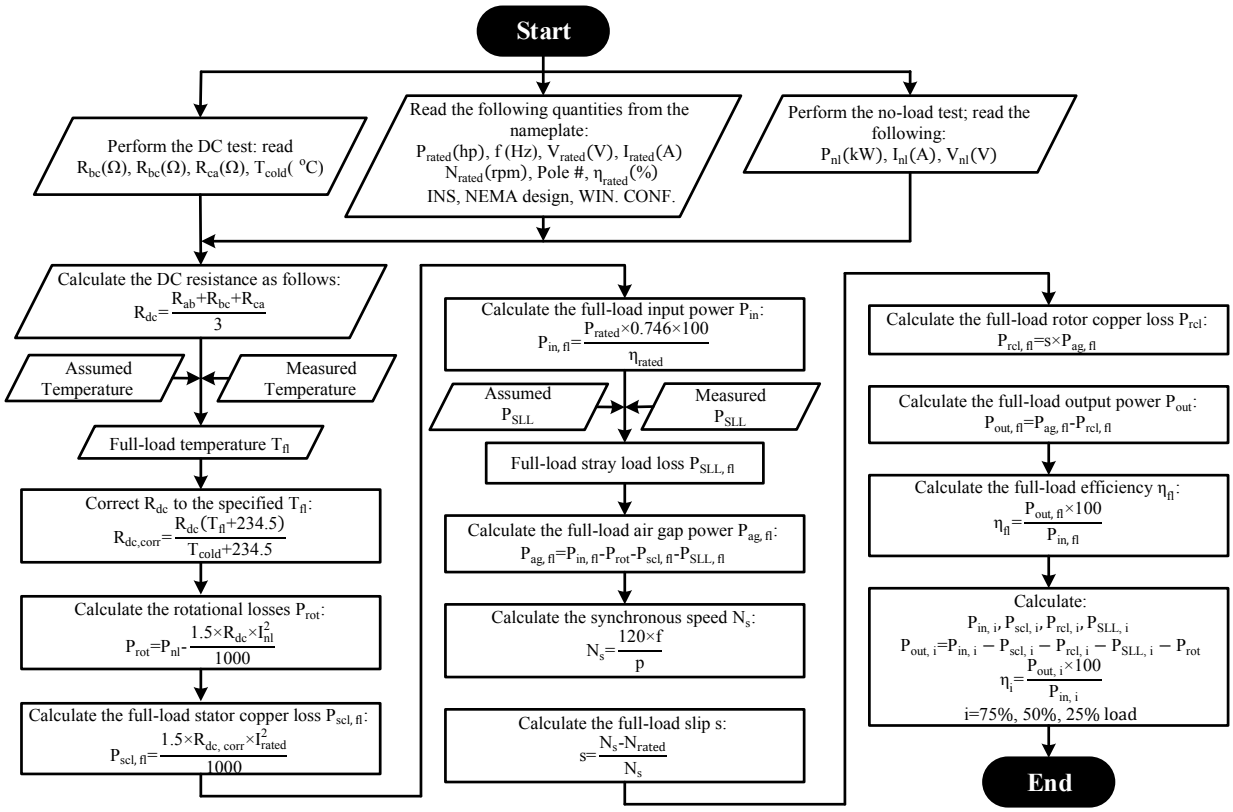

Figure 2-1. The proposed algorithm flow chart

2.2.1. Efficiency Estimation Procedure

The efficiency estimation procedure of Method A is as follows:

2.2.1.1. DC Test

The stator winding lead-to-lead resistance is measured among the three phases of the motor (i.e. R_{ab}, R_{bc}, R_{ca}). The average lead-to-lead dc resistance R_{dc} is calculated as in (2.1). During the measurement, the temperature T_{cold} is recorded.

$$R_{dc}=\frac{R_{ab}+R_{bc}+R_{ca}}{3} \tag{2.1}$$

2.2.1.2. Nameplate Data

Nameplate data is a necessary part of the algorithm. The rated voltage, rated current, rated power, rated speed, number of poles, efficiency, insulation class, NEMA design, and winding configuration should be read and recorded.

2.2.1.3. Performing the No-Load Test

The motor is run with no load coupled to the shaft at rated or close to rated voltage and with rated frequency shown on the nameplate. The input power reading should be stabilized, and the RMS values of input voltage, input current, and input power should be read and recorded.

2.2.1.4. Stator Resistance Correction for Temperature

The R_{dc} obtained from (2.1) should be corrected to the full-load temperature T_{fl} as in (2.2) and based on the insulation class of the machine and Table 2-I (if full-load temperature rise is not available) as recommended in IEEE Std 112™-2004.

$$R_{dc,corr} = \frac{R_{dc}(T_{fl}+K_1)}{T_{cold}+K_1} \tag{2.2}$$

where

K_1 is 234.5 for 100% IACS conductivity copper.

Table 2-I : Rated Temperature for Efficiency Calculations [21]

Class of insulation system	T_{fl} Temperature in ˚C Total temperature including 25˚C reference ambient
A	75
B	95
F	115
H	130

2.2.1.5. Estimation of Stator Copper Loss at Room Temperature

Stator Copper Loss at room temperature $P_{scl,a}$ can be calculated as in (2.3).

$$P_{scl,a}=1.5\times I_{nl}^2\times R_{dc} \tag{2.3}$$

2.2.1.6. Estimation of Mechanical Rotational Losses

Mechanical rotational losses P_{rl} will be estimated by subtracting the no-load stator copper loss from the no-load input power as in (2.4).

$$P_{rl}=P_{nl}-P_{scl,a} \tag{2.4}$$

2.2.1.7. Estimation of Full-Load Input Power

Full-load input power $P_{in,fl}$ can be estimated by using nameplate values of full-load output power P_{out} and full-load efficiency η_{fl} as in (2.5).

$$P_{in,fl}=\frac{P_{out}}{\eta_{fl}} \tag{2.5}$$

2.2.1.8. Estimation of Stray Load Loss

By investigating the testing data of wide range of machines of different power ratings (1-500 hp) offered by by Hydro-Québec and BC hydro, it has been found that, for motors of ratings larger than 40 hp, the value of Stray Load Loss P_{sll} can be better estimated by applying International Standard IEC 60034-2-1 computing methodology using (2.6). On the other hand, motors of ratings less than 40 hp, the stray load loss will be better assumed according to Table 1-I.

$$P_{sll}=P_{in,fl}\left[0.025\text{-}0.005\log_{10}\left(\frac{P_{out}}{1\text{kW}}\right)\right] \tag{2.6}$$

For the partial loads (i.e. 75%, 50%, and 25%), the stray load loss can be approximated by using the following formulas which are proposed in [90] and decided through a thorough check

upon the data.

$$P_{sll,75}=0.5556P_{sll,fl} \quad (2.7)$$

$$P_{sll,50}=0.2500P_{sll,fl} \quad (2.8)$$

$$P_{sll,25}=0.0625P_{sll,fl} \quad (2.9)$$

2.2.1.9. Estimation of Full-Load Stator Copper Loss

Full load stator copper loss $P_{scl,fl}$ can be calculated as in (2.10).

$$P_{scl,fl}=1.5\times I_{fl}^2\times R_{dc,corr} \quad (2.10)$$

For the partial loads (i.e. 75%, 50%, and 25%), stator copper loss can be approximated by using the following proposed formulas which are decided through a thorough check upon the data.

$$P_{scl,75}=0.608P_{scl,fl} \quad (2.11)$$

$$P_{scl,50}=0.335P_{scl,fl} \quad (2.12)$$

$$P_{scl,25}=0.1675P_{scl,fl} \quad (2.13)$$

2.2.1.10. Estimation of the Air Gap Power

Given one no-load operating point, there is no way to calculate the core and friction and windage losses. Hence, an assumption of using the same value of no-load mechanical rotational losses P_{rl} obtained in subsection 2.2.1.6 in full-load losses calculations would be acceptable [94]. Air gap power P_{ag} can be calculated as in (2.14).

$$P_{ag}=P_{in,fl}-P_{rl}-P_{scl,fl}-P_{sll} \quad (2.14)$$

2.2.1.11. Estimation of Synchronous Speed

Synchronous speed n_s can be estimated as in (2.15).

$$n_s = \frac{120 \times f_r}{p} \tag{2.15}$$

2.2.1.12. Estimation of Full-Load Slip

Full-Load slip S_{fl} can be estimated as in (2.16).

$$S_{fl} = \frac{n_s - n_{fl}}{n_s} \tag{2.16}$$

2.2.1.13. Estimation of Rotor Copper Loss

Full-load rotor copper loss $P_{rcl,fl}$ can be estimated as in (2.17).

$$P_{rcl,fl} = S_{fl} \times P_{ag} \tag{2.17}$$

For the partial loads (i.e. 75%, 50%, and 25%), the rotor copper loss can be approximated by using the following proposed formulas which are decided through a careful check upon the data.

$$P_{rcl,75} = 0.541 P_{rcl,fl} \tag{2.18}$$

$$P_{rcl,50} = 0.235 P_{rcl,fl} \tag{2.19}$$

$$P_{rcl,25} = 0.061 P_{rcl,fl} \tag{2.20}$$

2.2.1.14. Estimation of Mechanical Power

Mechanical power P_{mech} can be estimated as in (2.21).

$$P_{mech} = P_{ag} - P_{rcl,fl} \tag{2.21}$$

The mechanical output power represents the value of the estimated output power at full-load as in (2.22).

$$P_{out,ca} = P_{mech} \tag{2.22}$$

2.2.1.15. Estimation of Efficiency

Estimated efficiency η can be obtained as in (2.23).

$$\eta_i = \frac{P_{out,ca_i}}{P_{in_i}} \tag{2.23}$$

where i represents 100%, 75%, 50%, or 25% load.

2.2.2. Experimental Results and Analysis

Method A is applied on a group of different induction motors ranged from 3 to 150 hp. The results of the estimated efficiencies are tabulated in Table 2-II. The absolute error is calculated as in (2.24).

$$\text{Error} = \text{Measured Efficiency} - \text{Estimated Efficiency} \tag{2.24}$$

The errors shown in Table 2-II reflect a certain degree of accuracy. Although this level of accuracy obtained can be compromised by the limited input data that feed the algorithm, however, such errors make the technique unacceptable to be relied on when it is used to estimate efficiency in motor service centers especially for large power rating motors.

A thorough investigation into the source of error showed that two factors have large impact on the accuracy of the algorithm. The first factor is the estimated stray load loss P_{sll}, and the second factor is the assumed full-load temperature T_{fl}.

Table 2-II: Estimated Versus Measured Efficiencies

Motor Size (hp)	Measured Efficiency (%)	Estimated Efficiency (%)	Error (%)
3	79.61	78.59	1.02
7.5	90.79	89.55	1.24
25	92.80	92.07	0.73
50	92.80	91.68	1.12
60	94.80	94.02	0.78
100	95.50	93.81	1.69
150	93.60	92.76	0.84

2.2.2.1. Stray Loa Loss

According to IEEE Std 112™-2004, the stray load loss is that portion of the total loss in electrical machine not accounted for by the sum of the friction and windage loss, the stator copper loss, the rotor copper loss, and core loss. There are two ways to measure the stray load loss, *indirect measurement* and *direct measurement*. In the indirect measurement, the stray load loss is determined by measuring the total losses, and subtracting from these losses the sum of the friction and windage, core loss, stator copper loss, and rotor copper loss.

The remaining value is the stray load loss. In the direct measurement of the stray load loss, the fundamental frequency and the high frequency components of the stray load loss are determined and the sum of these two components is the total stray load loss [21]. The other procedure to determine the stray load loss according to IEEE Std 112™-2004 is to assume it. If the stray load loss is not measured, its value at rated load may be assumed to be the value as shown in Table 1-I, or it can be estimated according to International Standard IEC 60034-2-1 as in (2.6). Figure 2-2 elaborates a comparison between the estimated P_{sll} according to both standards and the measured values for five different induction motors. The wide difference between the assumed values of stray load loss and the measured values is very clear, especially for high power rating motors, which can prove that using the assumed value will significantly affect the value of the estimated efficiency and will lead to large errors.

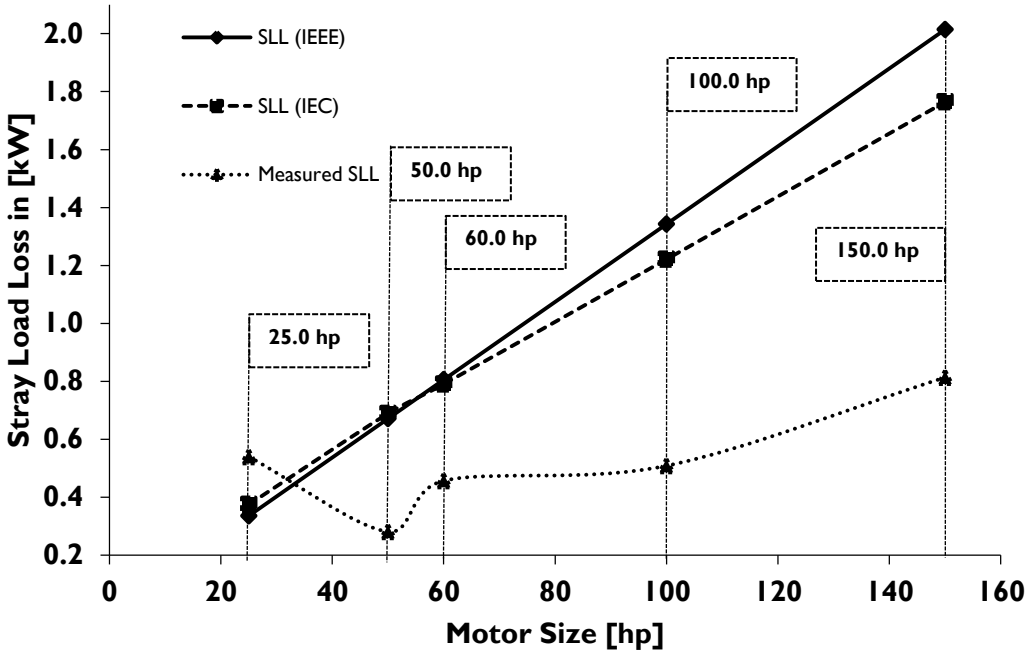

Figure 2-2. Estimated stray load loss versus measured values.
Source of measured data: Laboratoire des Technologies de l'Énergie, Institut de Recherche, Hydro-Québec.

2.2.2.2. Full-Load Temperature

Assuming the full-load temperature T_{fl} according to Table 2-I also contributes effectively to the degree of the estimated efficiency accuracy. This can be seen clearly by comparing the assumed full-load temperature of the above mentioned five induction motors with the measured values as illustrated in Figure 2-3. The full-load temperature is very critical in the efficiency estimation. It can be clearly noticed now that using the measured values of both stray load loss and full-load temperature instead of the assumed ones will dramatically reduce the errors shown in Table 2-II.

Hydro-Québec offered to support this research through providing an extremely valuable data of a large number and a wide range of induction motors tested in Laboratoire des Technologies de l'Énergie, Institut de Recherche, Hydro-Québec [91]. The data has been integrated in the algorithm, and whenever the motor under test is similar to any of the Hydro-Québec tested motors, the algorithm will use the measured values of stray load loss and full-load

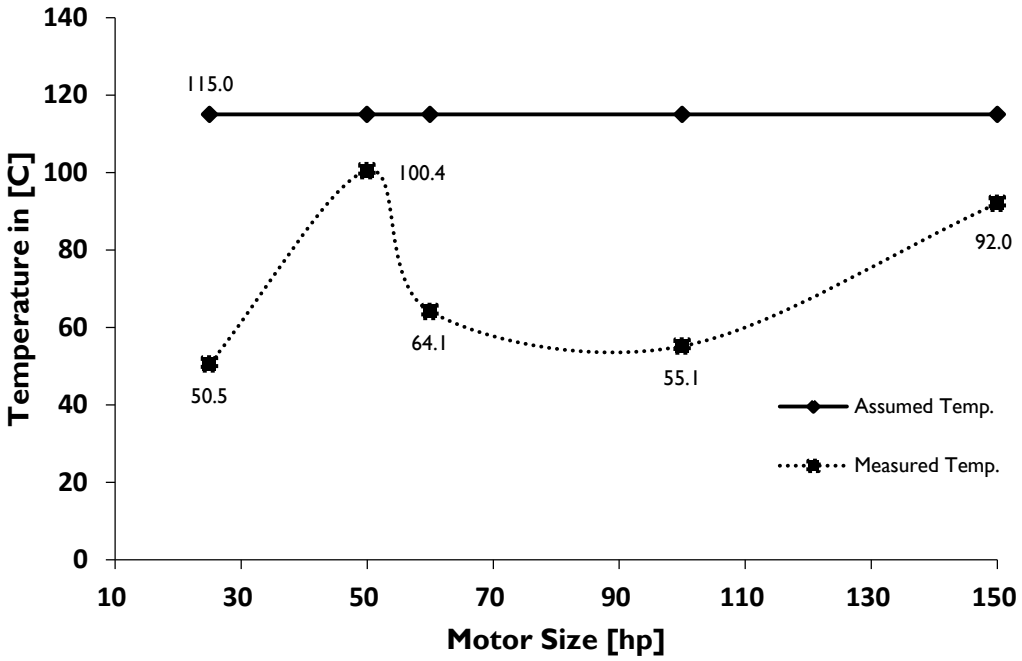

Figure 2-3. Assumed versus measured full-load temperature.
Source of measured data: Laboratoire des Technologies de l'Énergie, Institut de Recherche, Hydro-Québec.

temperature instead of the assumed values. The algorithm is designed to initiate the search process within the data by checking whether the power rating of the motor under test matches any of Hydro-Québec tested motors. Then it will pick up the value of the measured full-load

temperature of a similar motor within the data if the motor under test and the Hydro-Québec tested motor are similar in any of the following 4 conditions:

- Number of poles and insulation class.
- Rated voltage and insulation class.
- Insulation class.
- Rated voltage, no. of poles, and insulation class.

Other than the above mentioned conditions, the algorithm will use the assumed value of temperature according to IEEE Std 112™-2004 as presented previously in Table 2-I. On the other hand, and in regards to the stray load loss, the algorithm is designed to start the search process within the data by checking whether the power rating of the motor under test matches any of

Table 2-III: Estimated Versus Measured efficiency by Utilizing Hydro-Québec Measured P_{sll} and T_{fl}

Motor Size (hp)	Measured Efficiency (%)	Estimated Efficiency (%)	Error (%)
3	79.61	80.09	-0.48
7.5	90.79	90.73	0.06
25	92.80	93.30	-0.50
50	92.80	92.93	-0.13
60	94.80	94.74	0.06
100	95.50	95.01	0.49
150	93.60	93.42	0.18

Hydro-Québec tested motors. Then, if the similarity is found, the algorithm will pick up the value of the measured full-load stray load loss from the data if the motor under test and the motor within the data are similar in any of the following 2 conditions:

- Rated voltage and insulation class.
- Rated voltage, no. of poles, and insulation class.

Other than that, the algorithm will use the assumed value of stray load loss according to Table 1-I, or according to the formula as previously shown in (2.6), depending on the power rating of the motor as discussed previously. Finally, if the power rating of the motor under test has no similarity with any of Hydro-Québec data, the algorithm is designed to use the assumed values of both full-load temperature and full-load stray load loss. Results of the estimated efficiency of the seven motors are tabulated in Table 2-III after integrating the Hydro-Québec data in the algorithm. By comparing the errors of Table 2-II and those of Table 2-III, it is clear that a very good improvement has occurred when the measured values of both stray load loss and full-load temperature were used instead of the assumed values. Although method A is expected to give a less accurate value of full-load efficiency due to its very limited data of having only one operating point and with no ability to segregate the core loss and friction and windage losses, but with the aid of the valuable data of Hydro-Québec, this method could give an acceptable value of the estimated efficiency of those seven motors with a maximum deviation of (-0.50) and minimum of (0.06). Though, it can be considered as an acceptable technique to estimate the full-load efficiency from only one no-load operating point and with minimal requirement of instrumentations.

2.2.3. Algorithm Validation (196 Motors Tested)

Method A requires the following data to be fed to the software: Line-to-line stator resistance, winding temperature, nameplate data, or no-load input voltage (rated voltage, or any voltage level that is close to the rated voltage in case of having fixed level of voltages out of transformer taps), input current, and input power. By having all of those required data, Method A is validated by providing the estimated efficiencies of 196 induction motors.

Figure 2-4 shows the experimental setup for 5.0 hp induction motor direct test.

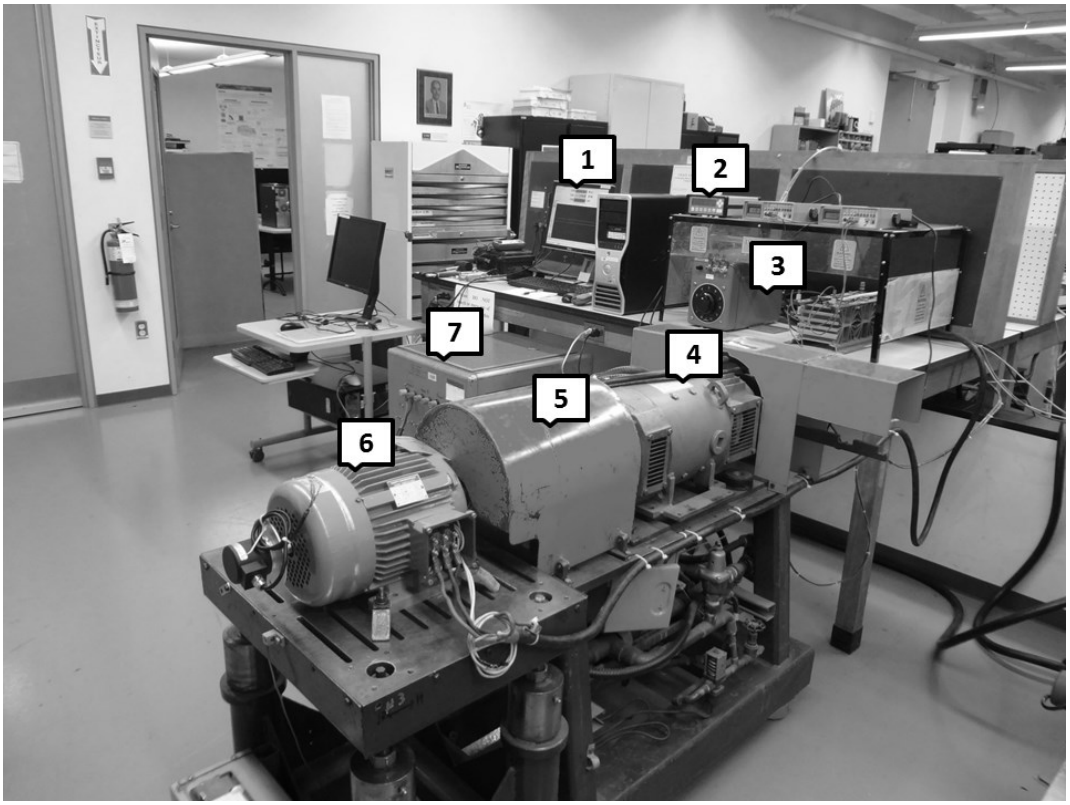

Figure 2-4. The experimental setup for testing 5.0 hp induction motor: 1, programmable power supply control unit; 2, multi-channel signal conditioner; 3, field control unit; 4, 13 kW dynamometer; 5, torque transducer; 6, 5.0 hp IM; 7, resistor bank.
Photo is a courtesy of Concordia University.

The following Table 2-IV shows the test results of the 196 tested motors tested using the proposed algorithm.

Table 2-IV. Testing Results of 196 Induction Motors Tested with Method A

Nameplate							Measured Efficiency [%]				Estimated Efficiency [%]				Error [%]			
VOLTS	POWER [hp]	AMPS	RPM	DESIGN	INS	EFF [%]	100%	75%	50%	25%	100%	75%	50%	25%	100%	75%	50%	25%
460	1	1.4	1745	B	F	84.4	84.4	83.6	80.3	68.0	84.8	85.0	83.1	74.5	0.40	1.37	2.81	6.49
460	1	1.5	1740	B	F	84.4	84.4	83.8	80.8	70.4	84.1	84.1	81.8	72.0	0.30	0.25	0.91	1.67
575	1	1.2	1720	B	F	81.9	81.9	81.5	78.2	66.7	81.1	81.7	80.0	70.7	0.84	0.20	1.73	4.01
575	1	1.1	1745	B	F	84.7	84.7	84.4	82.1	72.8	85.8	86.0	84.3	76.4	1.13	1.58	2.17	3.57
575	1	1.1	1745	B	F	84.8	84.8	84.5	81.7	72.6	86.6	87.1	85.9	79.5	1.78	2.64	4.21	6.84
575	1	1.15	1750	B	F	86.5	86.6	87.1	85.8	77.3	86.4	87.6	87.5	83.2	0.17	0.49	1.66	5.95
575	1	1.16	1745	B	F	83.2	83.2	82.6	79.3	67.5	83.4	83.2	80.6	70.2	0.13	0.67	1.33	2.66
575	1	1.16	1745	B	F	83.3	83.3	82.6	79.4	67.5	83.4	83.2	80.6	70.2	0.08	0.57	1.24	2.62
575	1	1.2	1715	B	F	78.7	78.8	77.9	73.5	63.0	79.3	79.7	77.3	66.2	0.49	1.74	3.79	3.21
575	1	1.2	1740	B	F	85.0	85.0	85.0	82.8	74.4	84.5	85.4	84.6	78.4	0.47	0.48	1.83	4.00
460	1.5	2	3490	B	F	85.8	85.8	85.2	82.5	80.2	85.4	85.2	82.6	72.9	0.33	0.04	0.15	7.33
575	1.5	1.64	1725	B	F	82.2	82.1	82.4	80.5	71.5	82.1	82.8	81.3	72.8	0.04	0.40	0.83	1.32
575	1.5	1.64	1725	B	F	82.5	82.4	82.6	80.7	71.7	82.0	82.7	81.2	72.7	0.40	0.09	0.55	1.00
460	2	3	1180	B	F	87.3	87.3	87.1	84.9	76.8	87.5	87.6	85.9	78.6	0.23	0.53	0.97	1.88
460	2	2.5	3490	B	F	88.3	88.3	88.0	85.9	82.5	87.3	87.4	85.8	78.6	1.03	0.58	0.09	3.88
460	2	2.4	3500	B	F	85.6	85.6	85.4	83.0	78.7	86.8	86.4	83.9	74.5	1.20	1.00	0.83	4.16
575	2	2.36	1740	B	F	82.6	82.5	82.8	81.0	72.0	83.9	84.0	81.9	72.5	1.38	1.16	0.90	0.49
575	2	2.36	1740	B	F	84.5	84.4	84.5	82.5	74.4	84.3	84.6	82.9	74.5	0.12	0.15	0.41	0.11
575	2	2.2	1735	B	F	85.2	85.2	85.3	83.4	75.0	84.3	85.1	84.0	77.2	0.83	0.19	0.65	2.19
460	3	4.5	1180	B	F	88.4	88.4	87.4	84.5	75.2	88.5	88.0	85.5	76.8	0.07	0.51	0.96	1.65
460	3	3.8	1750	B	F	87.7	87.7	87.5	85.5	77.8	87.5	87.4	85.5	77.6	0.28	0.13	0.02	0.13
575	3	3.6	1760	B	B	87.2	87.2	86.8	84.4	75.3	87.3	87.5	85.8	78.6	0.11	0.65	1.48	3.35
575	3	3.35	1720	B	F	85.7	85.5	87.2	87.6	83.9	84.8	86.8	87.5	84.7	0.62	0.44	0.10	0.77
575	3	3	3510	B	F	84.9	84.9	83.9	80.2	71.6	85.4	84.6	81.2	69.7	0.54	0.69	1.07	1.97
575	3	3	3510	B	F	84.7	84.7	83.8	80.2	72.1	85.3	84.4	81.0	69.3	0.61	0.69	0.81	2.80
575	3	3.1	1745	B	F	86.5	86.5	85.9	83.3	74.1	86.4	86.1	83.8	74.7	0.16	0.18	0.51	0.62
460	5	6.7	1740	B	F	85.0	85.0	85.3	83.7	75.9	85.5	85.7	83.9	75.9	0.53	0.40	0.21	0.05
460	5	6.5	1750	B	F	89.0	88.9	90.0	89.9	86.1	87.8	89.2	89.5	86.6	1.08	0.76	0.41	0.50

Nameplate							Measured Efficiency [%]				Estimated Efficiency [%]				Error [%]			
VOLTS	POWER [hp]	AMPS	RPM	DESIGN	INS	EFF [%]	100%	75%	50%	25%	100%	75%	50%	25%	100%	75%	50%	25%
460	5	6.7	1740	B	F	87.7	87.7	88.1	87.1	81.2	86.7	87.4	86.6	80.9	1.05	0.73	0.48	0.26
460	5	6.5	1750	B	F	87.4	87.4	87.7	86.2	79.0	86.4	87.1	86.2	80.3	1.07	0.61	0.06	1.24
460	5	6.5	1750	B	F	88.0	87.8	88.7	88.3	83.7	87.2	88.3	88.1	84.1	0.67	0.42	0.16	0.39
575	5	5.1	1730	B	B	86.6	86.7	87.2	86.0	78.9	86.1	87.0	86.3	80.8	0.58	0.27	0.27	1.85
575	5	5.23	1736	B	F	86.4	86.5	87.4	86.5	79.9	85.9	87.2	87.1	82.9	0.62	0.22	0.56	2.98
460	7.5	10.2	1740	B	B	86.9	86.8	87.8	87.4	82.5	86.0	87.3	87.2	83.0	0.85	0.49	0.20	0.55
460	7.5	10.5	1180	B	F	89.9	89.9	90.0	88.7	83.8	90.3	90.4	89.2	83.8	0.39	0.41	0.51	0.06
575	7.5	7.9	1760	B	F	89.1	89.1	89.6	89.2	85.3	89.4	90.0	89.4	84.9	0.34	0.41	0.14	0.34
575	7.5	7.5	1750	B	F	86.5	86.5	87.4	87.0	81.9	86.8	87.7	87.2	82.3	0.30	0.26	0.16	0.39
575	7.5	6.9	3545	B	F	89.4	89.4	88.9	86.7	79.0	89.9	89.2	86.8	78.5	0.45	0.32	0.04	0.56
575	7.5	7.2	1750	B	F	87.8	87.8	88.4	87.7	82.6	87.6	88.2	87.5	82.2	0.24	0.14	0.25	0.46
460	10	12.1	1760	B	F	91.1	91.0	92.1	92.5	91.0	90.9	91.9	92.2	90.1	0.04	0.16	0.32	0.84
460	10	12.4	1755	B	F	89.5	89.4	90.5	90.6	87.6	90.0	90.8	90.7	87.4	0.66	0.36	0.10	0.19
460	10	11.5	1750	B	F	89.9	89.7	90.9	91.1	88.6	89.1	90.3	90.5	87.9	0.62	0.60	0.55	0.62
460	10	12.1	1755	B	F	90.0	89.8	91.1	91.4	89.1	89.8	90.9	91.2	88.7	0.04	0.19	0.28	0.42
460	10	12.4	1755	B	F	90.2	90.1	91.1	91.5	89.1	90.3	91.3	91.3	88.6	0.24	0.13	0.16	0.50
460	10	12	1745	B	F	90.1	90.1	90.9	90.8	87.7	89.8	90.6	90.5	87.2	0.29	0.28	0.32	0.47
460	15	16.6	3550	B	F	88.7	88.7	88.3	86.4	79.0	89.3	88.5	85.9	77.0	0.60	0.20	0.48	2.04
460	15	16.6	3550	B	F	91.7	91.6	91.7	90.7	86.7	91.6	91.5	90.3	85.1	0.03	0.19	0.42	1.55
575	15	15.8	1760	B	F	91.6	91.6	92.2	92.0	88.8	91.6	92.3	92.0	89.1	0.01	0.07	0.07	0.25
575	15	15	1775	B	F	92.3	92.3	92.3	91.3	86.4	92.0	92.1	91.2	86.8	0.31	0.19	0.10	0.39
460	20	25.2	1175	B	F	91.2	91.2	92.1	92.0	89.2	91.3	92.0	91.9	89.2	0.14	0.02	0.10	0.01
460	20	25.2	1175	B	F	91.2	91.2	92.0	91.9	88.9	91.1	91.8	91.6	88.7	0.12	0.17	0.23	0.26
460	20	26.5	1760	B	B	88.6	88.7	89.5	89.3	85.6	87.9	89.1	89.2	86.0	0.77	0.44	0.08	0.40
460	20	26.5	1760	B	B	88.7	88.6	89.6	89.3	85.5	87.9	89.1	89.2	86.0	0.71	0.45	0.12	0.53
575	20	18.8	1760	A	F	90.4	90.3	91.5	91.7	89.2	91.4	92.1	92.0	89.1	1.11	0.64	0.22	0.13
575	20	18.4	1760	B	F	92.7	92.6	93.2	93.1	90.5	91.6	92.4	92.5	90.1	0.99	0.77	0.63	0.41
575	20	18.8	1760	B	F	91.1	91.1	91.8	91.5	88.1	91.1	91.7	91.2	87.6	0.00	0.11	0.25	0.43
575	20	19.4	1770	B	F	92.4	92.3	93.2	93.3	91.1	92.3	93.0	92.9	90.6	0.01	0.21	0.32	0.46
460	25	30	1770	B	F	93.9	93.9	94.5	94.6	92.5	93.7	94.3	94.4	92.6	0.14	0.17	0.21	0.11

Nameplate							Measured Efficiency [%]				Estimated Efficiency [%]				Error [%]			
VOLTS	POWER [hp]	AMPS	RPM	DESIGN	INS	EFF [%]	100%	75%	50%	25%	100%	75%	50%	25%	100%	75%	50%	25%
460	25	28	3545	B	F	91.4	91.4	91.9	91.2	87.1	91.5	91.8	91.1	87.1	0.06	0.07	0.13	0.08
575	25	25	1780	B	F	92.4	92.3	92.5	91.8	87.0	92.5	92.6	91.6	87.3	0.18	0.06	0.18	0.30
575	25	25	1780	B	F	92.8	92.8	93.0	92.3	88.1	92.8	92.9	92.1	88.2	0.07	0.13	0.20	0.07
460	30	38	1755	B	B	90.9	90.9	92.0	92.1	89.6	90.4	91.5	91.8	89.7	0.46	0.46	0.33	0.01
460	30	32.9	3555	B	F	91.1	91.1	90.7	88.9	82.2	91.4	90.9	88.9	81.9	0.39	0.16	0.05	0.31
460	30	36	1770	B	F	92.7	92.6	92.8	92.0	87.6	92.4	92.7	91.9	88.2	0.20	0.11	0.03	0.61
575	30	27.9	1765	B	F	92.4	92.4	93.0	92.7	89.5	92.8	93.2	92.8	89.7	0.46	0.27	0.06	0.22
575	30	29.2	1773	B	F	94.7	94.7	95.0	94.7	92.1	94.3	94.7	94.6	92.6	0.39	0.26	0.11	0.53
575	30	28.2	1775	B	B	93.9	93.9	94.4	94.4	92.1	94.0	94.5	94.3	92.2	0.11	0.02	0.05	0.16
460	40	47	1750	B	F	93.0	93.0	93.2	92.6	88.8	91.9	92.4	91.9	88.6	1.07	0.86	0.71	0.25
460	40	48	1765	B	B	89.3	89.2	90.1	89.9	86.0	88.5	89.6	89.5	86.2	0.72	0.56	0.36	0.21
460	40	48	1770	B	F	93.5	93.5	93.8	93.2	90.2	93.2	93.5	93.0	89.9	0.37	0.35	0.22	0.34
575	40	37.5	1775	B	B	93.8	93.8	94.2	93.9	91.0	93.5	93.9	93.5	90.9	0.33	0.32	0.37	0.13
575	40	37	1770	B	F	93.6	93.5	94.1	94.0	91.4	93.5	94.0	93.7	91.3	0.02	0.12	0.25	0.12
575	40	38	1180	B	F	93.5	93.5	93.4	92.3	87.7	93.0	93.1	92.2	88.2	0.50	0.36	0.09	0.48
575	45	42	1780	B	F	90.6	90.6	90.0	87.9	80.4	90.6	90.0	87.8	80.3	0.04	0.01	0.09	0.07
460	50	62	1765	B	B	89.8	89.8	90.7	90.6	86.7	89.3	90.5	90.7	88.1	0.46	0.24	0.10	1.40
460	50	58	1770	B	F	94.4	94.4	94.9	94.9	93.1	93.6	94.3	94.4	92.8	0.74	0.64	0.53	0.29
460	50	58	1770	B	F	93.3	93.3	93.8	93.5	90.5	93.0	93.5	93.2	90.6	0.30	0.36	0.36	0.09
460	50	60	1760	B	B	92.2	92.2	92.2	91.1	85.9	90.7	91.1	90.4	86.0	1.47	1.08	0.76	0.10
575	50	50.5	1770	B	F	92.5	92.5	93.0	92.7	89.2	92.5	93.1	92.9	90.3	0.01	0.09	0.21	1.01
575	50	47.1	1770	B	F	93.4	93.4	93.8	93.5	90.4	93.1	93.5	93.2	90.5	0.31	0.27	0.25	0.03
575	50	45.6	1775	B	F	92.7	92.7	93.5	93.7	91.7	93.5	94.0	93.8	91.6	0.73	0.44	0.14	0.13
575	50	46.2	1770	B	F	94.4	94.4	94.8	94.5	92.2	93.9	94.4	94.3	92.3	0.49	0.37	0.24	0.08
460	60	71	1770	B	F	93.3	93.3	94.0	94.1	91.8	92.6	93.3	93.4	91.4	0.73	0.68	0.69	0.41
460	60	70	1780	B	F	92.5	92.5	93.0	92.7	89.3	92.6	93.0	92.6	89.5	0.14	0.02	0.10	0.14
575	60	57.1	1780	A	F	94.2	94.1	94.5	94.3	91.6	93.7	94.1	93.9	91.6	0.41	0.40	0.41	0.02
575	60	55	1770	B	F	90.8	90.7	90.9	89.8	84.2	90.9	90.8	89.4	83.7	0.14	0.09	0.44	0.48
460	75	86	1780	B	F	94.5	94.5	95.1	95.1	93.1	94.9	95.3	95.1	93.3	0.42	0.22	0.02	0.17
460	75	85	1780	B	F	94.5	94.5	94.9	94.7	92.4	94.8	95.0	94.7	92.4	0.33	0.16	0.01	0.01

Nameplate							Measured Efficiency [%]				Estimated Efficiency [%]				Error [%]			
VOLTS	POWER [hp]	AMPS	RPM	DESIGN	INS	EFF [%]	100%	75%	50%	25%	100%	75%	50%	25%	100%	75%	50%	25%
460	75	90.6	1765	B	F	94.4	94.3	94.8	94.7	92.3	94.0	94.5	94.4	92.3	0.32	0.30	0.28	0.00
460	75	82	3580	A	F	94.4	94.3	94.2	93.3	89.2	94.5	94.3	93.2	89.3	0.16	0.07	0.01	0.12
575	75	68	1780	B	F	94.4	94.3	94.8	94.8	92.6	94.2	94.7	94.6	92.7	0.09	0.10	0.19	0.11
575	75	70	1777	B	F	92.1	92.1	92.2	91.4	86.7	92.3	92.4	91.3	86.8	0.26	0.13	0.11	0.13
460	100	116	1780	B	F	95.0	95.0	95.1	94.5	90.6	93.9	94.2	93.8	91.2	1.08	0.91	0.66	0.58
460	100	112	1780	B	F	95.0	95.0	95.3	95.1	93.1	94.3	94.8	94.6	92.7	0.68	0.55	0.44	0.36
550	100	96	1170	B	F	92.2	92.2	92.7	92.4	88.7	92.3	92.8	92.3	89.1	0.09	0.04	0.08	0.36
575	100	93	1770	B	F	93.6	93.6	93.7	92.9	89.0	93.1	93.2	92.5	88.7	0.52	0.45	0.40	0.25
575	100	90	1770	B	F	93.4	93.4	93.5	92.7	88.7	93.1	93.2	92.4	88.5	0.25	0.26	0.33	0.23
575	100	90.2	1780	B	F	93.4	93.4	93.9	93.6	90.8	93.9	94.2	93.8	91.1	0.53	0.30	0.15	0.27
575	125	113.4	1780	B	F	96.0	96.0	96.1	95.5	94.7	95.1	95.4	95.1	93.2	0.95	0.77	0.42	1.55
575	125	107	1785	B	F	94.5	94.4	94.8	94.5	92.0	95.0	95.1	94.6	92.0	0.55	0.31	0.07	0.07
575	125	113	1778	B	F	93.9	93.9	94.0	93.4	89.7	94.1	94.1	93.2	89.5	0.24	0.09	0.15	0.17
575	125	116	1780	B	F	94.8	94.8	94.9	94.4	91.2	94.8	94.9	94.3	91.5	0.00	0.04	0.09	0.32
460	150	166	1783	C	F	93.8	93.7	93.9	93.2	89.7	94.6	94.5	93.5	89.7	0.89	0.57	0.27	0.04
460	150	175	1785	B	F	95.3	95.2	95.2	94.5	91.0	95.1	95.0	94.2	91.0	0.16	0.19	0.30	0.00
575	150	138.4	1780	B	F	94.4	94.3	94.5	93.8	90.1	94.5	94.5	93.7	90.3	0.18	0.05	0.08	0.22
575	150	132	1785	B	F	95.7	95.7	96.0	95.8	94.0	95.6	95.9	95.6	93.9	0.06	0.10	0.17	0.09
575	150	140	1780	B	F	94.3	94.3	94.0	92.8	88.1	93.7	93.5	92.3	87.8	0.58	0.54	0.52	0.29
460	200	230	1788	B	F	95.0	94.9	95.0	94.5	91.3	95.0	95.0	94.3	91.3	0.09	0.02	0.18	0.03
460	200	223	1785	B	F	95.7	95.7	95.9	95.5	94.2	95.5	95.7	95.4	93.4	0.18	0.18	0.14	0.84
460	200	235	1790	B	F	95.2	95.2	95.0	93.9	89.9	95.0	94.9	93.9	90.4	0.22	0.13	0.03	0.48
575	200	181	1780	B	F	94.3	94.3	94.0	92.6	87.3	94.2	93.8	92.4	87.7	0.17	0.13	0.11	0.47
575	200	176.9	1775	B	F	95.8	95.8	95.9	95.4	92.6	95.1	95.3	94.9	92.7	0.64	0.52	0.41	0.00
575	200	182	1785	B	F	95.9	95.9	96.1	95.7	93.4	95.8	95.9	95.6	93.6	0.12	0.19	0.11	0.18
575	200	182.1	1780	B	F	93.5	93.5	93.5	92.4	87.5	93.7	93.5	92.3	87.8	0.19	0.02	0.15	0.26
575	200	179	1780	B	F	95.3	95.3	95.7	95.5	93.6	95.5	95.8	95.6	93.8	0.25	0.12	0.04	0.18
575	200	179	1780	B	F	96.7	96.7	96.9	96.8	95.4	95.9	96.3	96.3	95.2	0.75	0.60	0.42	0.25
575	200	179.1	1785	B	F	94.7	94.7	95.1	94.7	92.6	95.1	95.3	94.8	92.4	0.46	0.23	0.08	0.21
460	250	274	1785	B	F	95.5	95.4	95.5	94.9	92.1	95.3	95.4	94.8	92.2	0.16	0.15	0.15	0.05

Nameplate							Measured Efficiency [%]				Estimated Efficiency [%]				Error [%]			
VOLTS	POWER [hp]	AMPS	RPM	DESIGN	INS	EFF [%]	100%	75%	50%	25%	100%	75%	50%	25%	100%	75%	50%	25%
460	250	284	1785	B	F	95.1	95.1	95.3	94.8	92.3	95.1	95.2	94.7	92.3	0.02	0.07	0.08	0.01
575	250	232	3550	B	F	90.3	90.3	90.4	88.9	82.6	90.6	90.4	88.8	82.6	0.28	0.00	0.07	0.00
460	300	430	1780	B	F	95.6	95.6	95.7	95.2	92.7	94.7	95.0	94.6	92.3	0.93	0.75	0.59	0.35
460	300	329	1785	B	F	95.4	95.4	95.7	95.5	93.4	95.5	95.7	95.5	93.7	0.09	0.02	0.04	0.27
575	300	268	1790	B	F	95.2	95.2	95.1	94.2	92.2	95.3	95.1	94.2	90.8	0.07	0.03	0.02	1.35
460	350	402	1790	B	F	94.9	94.9	94.8	93.9	89.9	95.0	94.9	93.9	90.3	0.16	0.08	0.02	0.41
575	350	320	1775	B	F	93.4	93.4	93.6	92.8	88.6	93.5	93.5	92.7	89.0	0.00	0.03	0.07	0.42
575	400	353	1788	B	F	95.0	95.0	95.0	94.4	91.3	95.0	95.0	94.3	91.3	0.08	0.02	0.11	0.00
575	500	446	1789	B	F	96.6	96.6	96.6	95.9	93.0	96.6	96.5	95.8	93.4	0.07	0.12	0.10	0.35
575	500	465	1185	B	F	94.7	94.7	94.8	94.2	91.1	94.4	94.5	94.0	91.1	0.33	0.27	0.18	0.01
460	15	17.2	1760	B	F	91.0	90.6	91.2	90.7	86.5	90.4	90.8	90.1	85.8	0.25	0.39	0.57	0.68
575	25	25	1780	B	F	94.1	92.0	92.8	92.8	90.3	93.0	93.3	92.7	89.4	0.99	0.46	0.13	0.93
575	50	50.5	1770	B	F	93.0	92.8	93.1	92.6	89.2	92.6	93.2	93.0	90.5	0.23	0.06	0.39	1.27
575	60	55.9	1790	B	F	95.0	94.8	94.9	93.9	91.0	94.5	94.7	94.2	91.5	0.28	0.21	0.28	0.51
440	100	120.4	1780	B	F	94.5	95.5	95.5	94.9	92.1	95.1	95.2	94.7	92.2	0.44	0.30	0.19	0.09
460	150	174	1780	B	F	93.6	93.6	93.4	92.1	87.1	93.5	93.4	92.3	88.1	0.10	0.00	0.20	1.00
230	7.5	17.7	1755	B	F	91.7	90.5	91.2	90.8	86.9	90.5	91.6	91.9	89.8	0.03	0.38	1.08	2.87
460	7.5	8.85	1755	B	F	91.7	91.4	91.6	91.5	88	89.8	90.7	90.6	87.5	1.65	0.92	0.90	0.54
208	3	10.3	1740	B	B	81.0	80.1	79.8	77.1	65	79.8	79.9	77.2	65.6	0.28	0.13	0.14	0.56
460	75	91.4	1785	A	F	95.4	95.7	95.9	95.5	93.1	95.7	95.9	95.6	93.7	0.06	0.04	0.07	0.59
460	75	91.4	1785	A	F	95.4	95.4	95.6	95.2	92.6	95.6	95.8	95.4	93.3	0.24	0.19	0.21	0.63
460	75	92	1770	B	B	93.0	92.3	92.9	92.8	90.1	92.1	92.8	92.8	90.5	0.24	0.11	0.02	0.42
460	100	119	1775	B	B	93.0	92.9	93.6	93.7	91.6	92.5	93.3	93.4	91.6	0.32	0.31	0.23	0.02
460	100	120	1780	B	B	93.0	93.2	93.4	92.6	88.7	92.6	92.9	92.3	89.0	0.61	0.46	0.26	0.35
460	75	92	1770	B	B	92.0	91.7	92.2	91.8	88.4	91.7	92.3	92.1	89.1	0.09	0.14	0.22	0.66
460	75	92	1770	B	B	92.0	92.2	92.7	92.5	89.3	91.8	92.5	92.4	89.7	0.37	0.24	0.12	0.48
460	50	56.5	1760	B	B	91.0	90.6	92.0	92.6	91.5	91.4	92.4	92.6	90.6	0.75	0.38	0.01	0.90
460	75	84	1785	B	F	95.4	94.3	95.0	95.2	93.7	95.4	95.7	95.6	94.0	1.05	0.71	0.36	0.26
460	75	84	1785	B	F	95.4	94.3	95.1	95.4	94.2	95.5	95.9	95.8	94.4	1.14	0.75	0.38	0.25
460	75	84	1785	B	F	95.4	94.6	95.3	95.6	94.3	95.5	95.9	95.8	94.4	0.86	0.54	0.26	0.16

Nameplate							Measured Efficiency [%]				Estimated Efficiency [%]				Error [%]			
VOLTS	POWER [hp]	AMPS	RPM	DESIGN	INS	EFF [%]	100%	75%	50%	25%	100%	75%	50%	25%	100%	75%	50%	25%
460	75	84	1785	B	F	95.4	95.0	95.6	95.7	94.1	95.5	95.8	95.7	94.3	0.42	0.27	0.06	0.11
460	150	175	1780	B	F	95.8	96.3	96.4	96.0	93.7	95.4	95.7	95.5	93.7	0.86	0.67	0.47	0.00
460	75	90	1775	B	B	91.7	92.1	92.9	92.8	90.1	92.4	93.0	92.9	90.4	0.35	0.17	0.03	0.23
460	75	90	1775	B	B	91.7	91.4	92.4	92.6	90.0	91.8	92.6	92.6	90.3	0.45	0.21	0.09	0.38
460	100	117	1780	B	B	90.0	89.6	90.3	89.7	85.2	91.8	91.8	90.6	85.7	2.25	1.55	0.94	0.58
460	100	118	1775	B	F	90.2	91.0	90.9	89.5	83.4	90.9	90.8	89.2	83.2	0.05	0.10	0.27	0.15
460	75	89	1775	B	F	95.4	95.2	95.4	95.0	92.4	95.0	95.3	95.0	92.8	0.22	0.14	0.01	0.44
460	75	85.1	1775	B	F	95.4	94.7	94.8	94.2	90.9	94.5	94.6	94.0	91.1	0.17	0.13	0.13	0.18
460	150	175	1783	B	F	95.8	95.5	96.0	96.1	94.8	96.0	96.3	96.2	94.9	0.51	0.33	0.11	0.12
460	75	89	1775	B	F	95.4	95.2	95.5	95.2	92.9	95.1	95.5	95.2	93.4	0.10	0.06	0.06	0.49
460	150	175	1783	B	F	95.8	95.6	96.1	96.1	94.6	95.9	96.2	96.1	94.7	0.28	0.15	0.02	0.08
460	150	165	1785	B	F	96.2	96.3	96.6	96.4	94.5	95.9	96.1	96.0	94.4	0.49	0.41	0.38	0.12
460	50	58.8	1775	B	F	94.5	94.9	95.4	95.4	93.7	94.0	94.7	94.9	93.7	0.91	0.70	0.49	0.04
460	75	87.1	1785	B	F	95.4	94.5	94.8	94.5	91.9	95.0	95.1	94.6	92.0	0.46	0.30	0.10	0.19
460	75	89	1760	B	F	92.0	91.5	92.2	92.0	88.6	92.7	93.0	92.3	88.7	1.18	0.74	0.35	0.19
460	75	86	1781	B	F	95.0	93.7	94.3	94.3	92.0	94.5	94.8	94.6	92.3	0.84	0.53	0.28	0.29
460	75	87	1775	B	F	93.0	92.4	92.8	92.1	88.2	93.1	93.1	92.3	88.3	0.63	0.38	0.14	0.19
460	150	170	1780	B	F	95.8	96.3	96.5	96.1	94.1	95.7	96.0	95.8	94.2	0.65	0.51	0.32	0.08
460	150	170	1780	B	F	95.8	96.1	96.2	96.0	93.9	95.6	95.9	95.8	94.1	0.41	0.30	0.22	0.20
460	75	82.3	1775	B	F	95.4	95.1	95.6	95.5	93.6	94.7	95.2	95.2	93.7	0.40	0.36	0.22	0.14
460	75	82.3	1775	B	F	95.4	95.2	95.6	95.6	93.7	94.7	95.2	95.3	93.8	0.45	0.31	0.26	0.13
460	150	166	1770	B	F	93.5	93.1	93.7	93.5	90.6	93.7	94.0	93.5	90.7	0.64	0.35	0.08	0.06
460	150	167	1759	B	F	92.9	92.9	93.2	92.7	89.1	92.8	93.1	92.4	88.9	0.10	0.16	0.26	0.19
460	75	89	1775	B	F	93.0	94.0	94.7	94.8	93.0	94.5	95.0	95.0	93.4	0.52	0.30	0.18	0.40
460	100	113	1780	B	F	95.0	94.7	95.1	94.8	92.3	94.2	94.6	94.4	92.2	0.48	0.46	0.38	0.07
460	50	60	1770	B	F	91.7	91.7	91.8	90.6	85.2	91.7	91.7	90.6	85.7	0.05	0.03	0.03	0.51
460	50	60	1770	B	B	91.0	91.1	91.6	91.1	86.9	91.4	91.8	91.1	87.2	0.22	0.15	0.05	0.32
460	150	178	1775	B	F	95.0	95.0	95.2	94.6	91.8	94.6	94.8	94.3	91.7	0.38	0.38	0.33	0.09
460	75	93	1780	B	B	95.2	92.5	92.3	90.9	85.6	91.7	91.7	90.4	85.3	0.83	0.64	0.51	0.27
460	150	174	1780	B	F	93.6	93.8	93.8	92.9	88.7	93.7	93.6	92.6	88.6	0.11	0.19	0.26	0.13

Nameplate							Measured Efficiency [%]				Estimated Efficiency [%]				Error [%]			
VOLTS	**POWER** [hp]	**AMPS**	**RPM**	**DESIGN**	**INS**	**EFF** [%]	**100%**	**75%**	**50%**	**25%**	**100%**	**75%**	**50%**	**25%**	**100%**	**75%**	**50%**	**25%**
460	75	86	1775	B	F	95.4	94.9	95.4	95.3	93.3	94.8	95.3	95.2	93.6	0.12	0.09	0.04	0.35
460	75	86	1775	B	F	95.4	94.8	95.3	95.3	93.4	94.8	95.3	95.3	93.7	0.01	0.00	0.01	0.31
460	75	90	1780	B	B	93.0	92.4	93.0	92.6	89.4	92.8	93.1	92.6	89.4	0.33	0.07	0.06	0.01
460	75	92	1770	B	F	92.0	91.6	91.7	90.7	85.7	92.0	92.0	90.8	85.9	0.37	0.22	0.11	0.20
460	75	93	1780	B	F	93.0	92.6	92.6	91.5	86.7	92.8	92.7	91.7	87.2	0.19	0.16	0.15	0.44
460	150	180	1775	B	F	93.0	93.1	93.1	92.0	87.5	93.4	93.2	92.0	87.4	0.29	0.14	0.05	0.08
460	150	171	1780	B	B	91.5	91.3	91.0	89.3	83.2	91.4	91.0	89.1	82.5	0.17	0.01	0.23	0.65
460	100	116	1775	B	F	92.0	91.7	92.4	92.1	88.9	92.5	92.9	92.4	89.1	0.90	0.54	0.25	0.17
460	50	58	1770	B	F	92.0	91.6	92.4	92.4	89.6	92.1	92.7	92.5	89.7	0.46	0.25	0.03	0.09
460	100	115	1785	B	F	94.1	94.0	94.8	95.1	93.8	94.9	95.4	95.4	94.0	0.91	0.61	0.27	0.17
460	50	60	1770	B	F	94.1	91.6	92.2	92.0	88.6	92.2	92.6	92.0	88.5	0.67	0.38	0.08	0.09
460	75	90	1775	B	F	93.0	92.5	92.9	92.6	89.2	93.3	93.5	92.8	89.4	0.82	0.54	0.24	0.27
460	150	174	1785	B	F	93.0	94.7	94.8	94.3	91.3	94.7	94.9	94.3	91.5	0.07	0.04	0.00	0.23
460	75	89.4	1775	B	F	91.0	91.1	91.4	90.5	85.7	92.3	92.2	90.9	85.9	1.27	0.84	0.45	0.21
460	150	174	1785	B	F	93.0	94.5	94.7	94.3	91.4	94.8	94.9	94.4	91.7	0.29	0.20	0.08	0.29
460	100	112	1785	B	F	93.0	93.5	94.2	94.4	92.6	94.2	94.7	94.6	92.7	0.79	0.49	0.16	0.04
460	100	112	1785	B	F	94.0	93.5	94.3	94.4	92.6	94.1	94.6	94.5	92.6	0.61	0.33	0.07	0.01

2.3. Error Analysis and Uncertainty

The accuracy of an estimated efficiency is highly dependent on the accuracy of power measurements, both electrical and mechanical [96]. This reflects the importance of conducting an uncertainty study to give the necessary credits to any declared estimated values of efficiency. The three components (i.e. the methodology, the instruments, and the personnel) are the main sources of error that compose the general form of the measurement error represented by (2.25).

$$\zeta=\zeta_m+\zeta_i+\zeta_p \tag{2.25}$$

where, ζ is the measurement error, ζ_m is the methodological error, ζ_i is the instrumental error, and ζ_p is the personnel error [97].

Two error estimation techniques are used in this study for the evaluation of the uncertainty results of the proposed method. These techniques are, WCE (Worst-Case Estimation), and RPBE (Realistic Perturbation-Based Estimation). The WCE is based on the assumption that the maximum error of a measurement occurs when the possible maximum uncertainties of all the instruments used present simultaneously in the measurement system [97] [98] [99]. In this method, the effect of each error source will be taken into account separately. For an output variable y (i.e. motor efficiency) of a complex system (e.g. induction motor), the maximum error ε_y can be determined using (2.26).

$$\varepsilon_y=\sum_{i=1}^{n} I_{x_i}\varepsilon_{x_i}+\frac{1}{y}\sum_{j=1}^{m} W_{z_j} z_j \tag{2.26}$$

where I_{x_i} is the influence coefficient of the input variable x_i and can be determined by using (2.27).

$$I_{x_i}=\frac{\varepsilon_y}{\varepsilon_{x_i}}=\frac{x_i}{y}\times\frac{\partial f}{\partial x_i} \tag{2.27}$$

W_{z_j} is the influence coefficient of the additive noise z_j.

For a complex system, like an induction motor, the explicit expressions of the derivatives are not available, the influence coefficient of each input variable can be approximated by applying a small perturbation in the corresponding input variable and measuring the change in the output variable [99]. The RPBE method is introduced in [98], [99], and [100] as a technique that

improves the results obtained from the WCE. The effects of the individual instrumentation errors are discriminately accounted for according to their corresponding influence coefficient, hence, the estimate of the measurement error is more realistic [99].

In [97] it has been shown that for a uniformly distributed errors, the relative error in the output variable y can be determined using (2.28).

$$\varepsilon_y = \sqrt{\sum_{i=1}^{n} \left(I_{x_i} \varepsilon_{x_i}\right)^2 + \frac{1}{y^2} \sum_{j=1}^{m} \left(W_{z_j} z_j\right)^2} \tag{2.28}$$

The relationship between an input and output variable can be investigated by applying a small change in the input, and observing the influence coefficient on the output. The significance of the input variable can be obtained by multiplying its influence coefficient by its corresponding measurement accuracy. When all error sources are added up using (2.28), the overall realistic error in the output variable will be obtained.

In order to achieve a proper uncertainty study with regard to the proposed Method A algorithm, the actual motor efficiencies must be measured and their accuracies must be guaranteed [99] [98] [100]. In this section, the two techniques (i.e. WCE, and RPBE) will be used to investigate the uncertainty of the measured and estimated motor efficiencies.

Three different induction motors are chosen and their nameplates are manifested in Table 2-V. The three motors are tested for efficiency using the direct measurements (dynamometer procedure). Method A is used to estimate the efficiencies of the same three tested motors.

To extract the value of every required influence coefficient, the change in the output variable (i.e. motor efficiency) is plotted against the corresponding perturbation in the input variable. Method A utilizes a very limited input data, and the only input variables accounted for are the input power, the stator resistance, and the stray load loss. For the direct measurements, the

Table 2-V. Nameplate Details of Three Induction Motors

Motor Size (hp)	Rated Voltage (V)	Rated Current (A)	Rated Speed (rpm)	No. of Poles	INS.	Design
5	220	13	1730	4	H	B
7.5	230	17.7	1755	4	F	B
7.5	460	8.85	1755	4	F	B

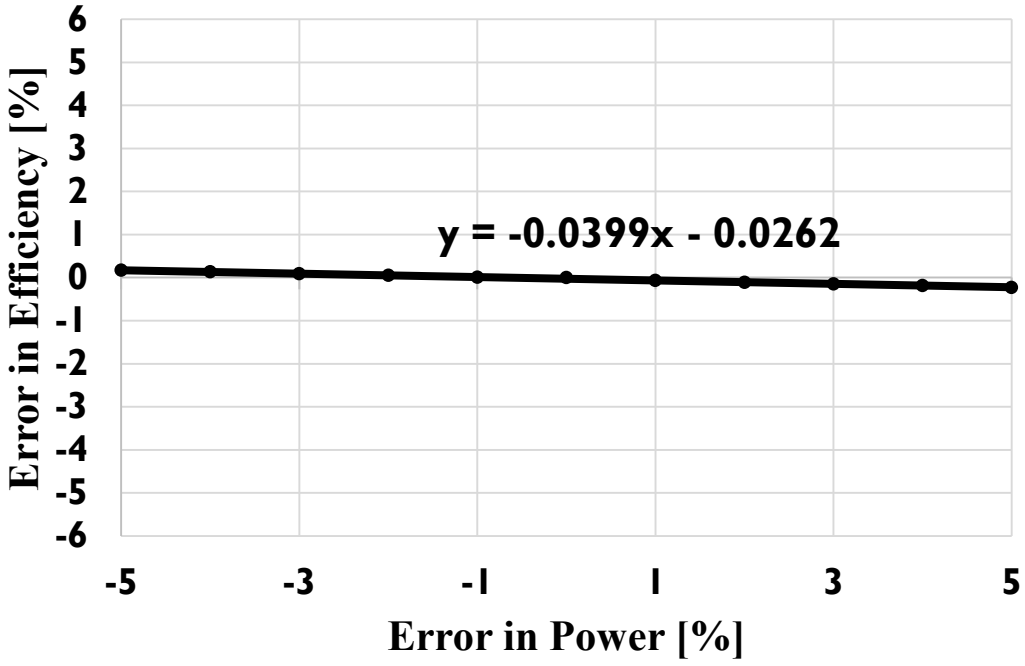

Figure 2-5. Influence coefficient of input power, Method A measurements (I_p=-0.0399).

input variable involve in the uncertainty are the input power, shaft torque, and rotor speed. Figure 2-5 shows the graph produced to help extract the influence coefficient of the input power of the 5.0 HP, 220 V induction motor by using Method A. The final results obtained for the three tested motors of the direct measurements and the Method A measurements, by using WCE and RPBE techniques are tabulated in Table 2-VI. The results show that the average levels of uncertainty of Method A measurements are ±0.028%, and ±0.02% by using WCE and RPBE respectively. Such levels of uncertainty within the estimated efficiencies by using Method A can give a good credit to the proposed algorithm.

2.4. Summary

In this chapter, a novel technique is proposed for estimating induction machines full-load and partial loads efficiencies from only one no-load test. The technique runs with very limited data and measurements that can easily performed in any electric motor service centers. The algorithm is designed to be applied in any motor repair shop. The algorithm utilizes an extremely valuable test data that is received from Hydro-Québec and BC Hydro which significantly improved the outcome of the proposed algorithm. The data is utilized in assigning the measured stray load loss and full-load temperature to the motor under test based on certain similarity with the motors of the data. The data is also utilized to propose new formulas to estimate the partial load stray load loss, stator copper loss, and rotor copper loss.

A detailed flow chart of the proposed algorithm is presented in subsection 2.2. All related formulas are also presented.

The advantages of using measured stray load loss and full-load temperature in lieu of the assumed values are discussed and the algorithm accuracy improvement is shown in subsections 2.2.2.1 and 2.2.2.2 respectively.

A total of 196 induction motors were tested using the proposed algorithm as part of the algorithm validation. The results are presented in subsection 2.2.3.

To evaluate the estimated efficiency values obtained by the proposed algorithm, an uncertainty study is conducted and showed acceptable levels of uncertainty by using the WCE and RPBE techniques. The results are introduced in subsection 2.3.

Table 2-VI. Uncertainty Results of the Three Tested Induction Motors

Tested Induction Motor	**Uncertainty of the Measured Efficiency [±%]**		**Uncertainty of the Estimated Efficiency (Method A) [±%]**	
	WCE [±%]	**RPBE [±%]**	**WCE [±%]**	**RPBE [±%]**
5.0 HP, 220 V	1.0417	0.6115	0.0350	0.0254
7.5 HP, 230 V	0.9004	0.5517	0.0260	0.0198
7.5 HP, 460 V	1.1664	0.6978	0.0238	0.0147

The proposed algorithm can be deemed to have enough confidence to be used in the industry to give acceptable motor efficiency prediction.

CHAPTER THREE

3. A Novel Algorithm for Estimating Refurbished Three-Phase Induction Motors Efficiency Using Only No-Load Tests

Induction motors fail due to many reasons and many are rewound two or more times during their lifetimes. It is generally assumed that a rewound motor is not as efficient as the original motor. Precise estimation of efficiency of a refurbished motor or any existing motor is crucial in industries for energy savings, auditing and management. Full-load and partial load efficiency can be measured by using the dynamometer. This work presents a novel technique for estimating refurbished induction motors' full-load and partial loads efficiencies from only no-load tests. The technique can be applied in any electric motor workshop and eliminates the need for the dynamometer procedure. It also eliminates the need for the locked-rotor test. Experimental and field results of testing 8 induction motors are presented and the degree of accuracy is shown by comparing the estimated efficiencies against the measured values. To provide the necessary credits to the proposed technique, an error analysis is conducted to investigate the level of uncertainty through testing three induction motors, and the results of uncertainty of the direct measurements and no-load measurements using the proposed technique are presented.

3.1. Introduction

In the industrialized countries, electric motors utilize nearly two-thirds of the electricity generated [1], hence, they contribute to the global environmental problem which is represented by the emission of greenhouse gases [2]. Several Canadian and U.S. utilities have taken serious steps in implementing demand side management programs [3] to reduce both greenhouse gas effects and the cost of power that feeds this tremendous population of electric motors. In developing countries, a similar situation encountered, where a significant portion of the generated power is utilized by motors. Taking South Africa as an example, motorized systems account for up to 60% of the total electricity utilization [4].

In industry, only motors above 500 hp are usually monitored because of their high costs.

However, motors below 500 hp make up 99.7% of the motors in service. These motors operate at approximately 60% of their rated load because of oversized installations or under-load conditions, and hence, they work at reduced efficiency which results in wasted energy [6]. Motor losses can represent a considerable cost over a long period due to high load factor [7].

Power costs are constantly rising at a rate that is even faster than both material and producer goods prices [8], many companies have hired energy managers whose sole purpose is to find practical ways to reduce power costs. As an example, and according to the U.S. Department of Energy's (DOE) Office of Energy Efficiency and Renewable Energy (EERE), a large size paper mill could save an average of $659,000 a year through motor system efficiency [10]. If a replacement decision of low efficient motor is taken as a result of the calculation of energy savings and payback periods that are based on nameplate motor efficiency or manufacturer's data only, this could lead to large errors [1], because the real efficiency of a motor is usually different from that value mentioned on its nameplate, as efficiency may decrease significantly due to aging or rewinding [17], or it might not be given according to IEEE Std 112^{TM} Method B [18]. To make a correct decision and select the optimal retrofit scenario, engineering staff should be able to estimate the efficiency of motors under test with the least possible error. This demand from industry drives practical work and research on the development and enhancement of methods for induction motors efficiency estimation [1].

The key point in estimating the efficiency of an induction motor is to identify the 6 electrical parameters of the machine. In [101], an offline deterministic method was used to identify moment of inertia, mechanical losses, and the electrical parameters for large induction machines based on DOL (Direct-On-Line) starting and slowdown tests performed under no-load conditions. The approximated machine model was used in this work. The core loss resistance is ignored. The proposed method is only applicable to large motors as the large mass of such machines can allow the rotor to stall for a time that will be enough to obtain some of the electrical parameters that is usually extracted from a locked-rotor test. This method lacks a proper validation, beside it is not applicable in all kind of electric motor workshops.

Parameter identification from starting no-load low-voltage test was proposed in [102]. The core loss resistance was also ignored. The method utilizes the variation of impedance versus slip, with the help of least mean square (LMS) and particle swarm optimization (PSO) to obtain

the required electrical and mechanical parameters. Data acquisition equipment and sophisticated software make the method inapplicable to be used properly in normal electric workshops. In [11], a method was proposed to extract the electrical parameters of induction machines from no-load and start-up tests. Again, the need for data logging equipment and sophisticated software to run the proposed technique makes the method inapplicable in normal electric workshops. A comprehensive review of induction motor parameter estimation techniques was conducted in [103].

Currently, the dynamometer method is the most reliable procedure that is being followed in the industry to test induction motor performance. However, this procedure is expensive and it is only available in well-equipped laboratories. There is also no-load/locked-rotor test. This test needs full control on the voltage, beside proper instrumentation to achieve a mechanically secured and safe locked-rotor condition. These instrumentations are widely different for different motor sizes. Using line-to-line single phase supply autotransformer to provide continuous voltage regulation to the input voltage during the locked-rotor test is an option in some electric workshops, but was not available in the workshops visited as part of this study. Hence, there is a need for practical and cost-effective procedure that can be applied easily in workshops.

In this chapter, a novel efficiency estimation technique for repaired, rewound, or any existing induction motor, is proposed to match the technical environment of electric motor service workshops. It is tailored to what is really available in these workshops in terms of instrumentation and equipment. The algorithm works with very limited data obtained from a DC test (including cold temperature measurement), a minimum 5 no-load operating points, and one speed measurement. The algorithm is designed to eliminate any need for voltage and current waveforms capturing devices as it uses only rms values which is accounted for as one good advantage of the proposed algorithm. To transfer the method into a practical tool to be used in the industry; software has been designed based on spreadsheets and using Visual Basic® programming to implement the algorithm. The proposed method eliminates the need for sophisticated software that is unlikely to be available in the workshops. The algorithm utilizes a large database of induction motors tested for efficiency in the Laboratoire des Technologies de l'Énergie, Institut de Recherche, Hydro-Québec, Shawinigan, Québec, Canada. The data has a wide range of motor power ratings. Another valuable set of testing data is received from BC hydro, which includes a full test of 55 used (aged) induction motors [86]. Applicability and

feasibility of the method has been supported by technical visits made by the research team to electric motor service centers in the Montréal area. Experimental and field results of testing 8 induction motors are presented and demonstrate the degree of accuracy of the proposed technique.

3.2. The Proposed Algorithm

The algorithm is designed to deal with only rms values of voltage, current, and power that can be obtained using suitable measuring instruments which comply with IEEE Std 112™-2004 [21] and Canadian standard CAN/CSA C392-11 [93].

The required input data for running the proposed algorithm are:

- DC resistance of the stator windings.
- Temperature of the stator winding.
- Nameplate details.
- Minimum of 5 different rms values of no-load voltage, no-load current, and no-load input power.

In IEEE Std 112™-2004, a method called Efficiency Test Method F1-Equivalent Circuit is proposed. This method estimates induction motor's efficiency based on calculation of the machine's equivalent circuit parameters by using no-load test data and an impedance test (Method 3). This proposed method is based on IEEE Std 112™-2004 Efficiency Test Method F1-Equivalent Circuit. The parameters of the machine are extracted based on Method 3 (reduced voltage slip test) of the IEEE Std 112™-2004. The equivalent circuit of the machine is shown in Figure 3-1. In order to find the parameters of the machine from the voltage, current, and the power measurements, without performing a low frequency locked-rotor test, the data of multiple operating points is required. The multiple operating points are created by reducing the voltage and thus changing the slip of the machine in the no-load condition. Once the parameters are accurately defined for the rated condition, the slip and the input power of the machine under rated load and any partial load can be found based on solving the equivalent circuit of the machine iteratively. Knowing the real rated slip of the machine and the right value of the rated input

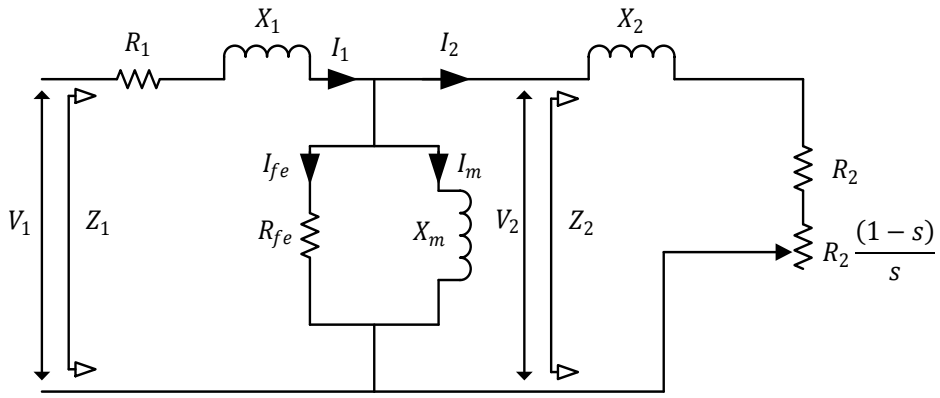

Figure 3-1. Induction motor equivalent circuit.

power will lead to more accurate estimation of the efficiency [21]. The algorithm is designed to work with limited data from running the motor with no load coupled to the shaft and with voltages started from rated voltage or value close to rated voltage, down to the point where further voltage reduction causes the current to increase. Per phase stator winding resistance $R_{1,cold}$ (cold resistance) should be determined by using a DC test that complies with section 5.4 of IEEE Std 112™-2004 and section 5.7 of Canadian standard CAN/CSA C392-11 [93].

The temperature T_{cold} has to be measured during the DC test using the recommended instruments in section 4.4 of IEEE Std 112™-2004. The value of $R_{1,cold}$ will be corrected to the full-load temperature T_{fl}.

The measured input power is the total losses in the motor at no-load and these losses consist of the stator copper loss, friction and windage losses, and core loss, in addition to the stray load loss.

The friction and windage losses and the core losses may be determined according to sections 5.5.4 and 5.5.5 of the IEEE Std 112™-2004 respectively, or section 7.1.7 of Canadian standard CAN/CSA C390-10 [104].

Stray load loss is estimated based on International Standard IEC 60034-2-1 computing methodology for induction motors larger than 40 hp as it is assumed to have better accuracy. For motors smaller than 40 hp, stray load loss is assumed according to IEEE Std 112™-2004 methodology [88].

Full-load and partial load efficiencies are predicted based on the previous calculations and

assumptions.

It is useful to show induction motor power flow and its corresponding losses as illustrated in Figure 3-2.

The test procedure as recommended in the IEEE Std 112™-2004 is as follows:

3.2.1. DC Resistance Test

The stator winding lead-to-lead resistance is measured among the three phases of the motor (i.e. R_{ab}, R_{bc}, R_{ca}). The average lead-to-lead dc resistance R_{dc} is calculated according to (2.1). During the measurement, the temperature T_{cold} is recorded.

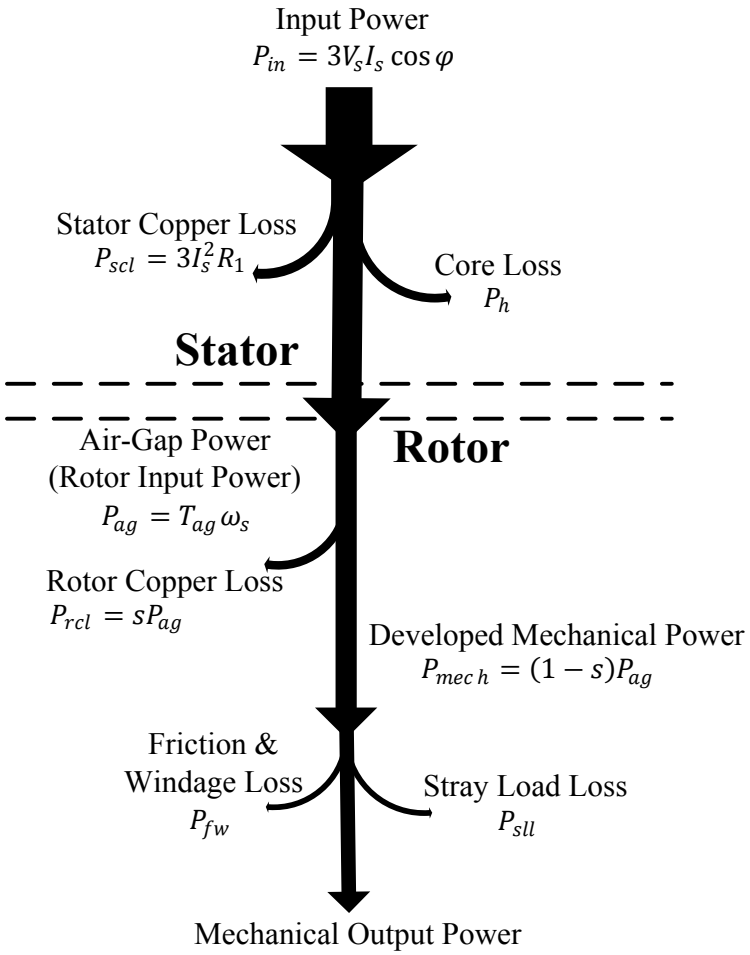

Figure 3-2. Induction motor power flow.

3.2.2. Nameplate Details

Nameplate details are necessary part of the algorithm. Rated voltage, rated current, rated power, rated speed, number of poles, efficiency, insulation class, NEMA design, and winding configuration, all will be included in the algorithm.

3.2.3. Performing the No-Load Test

The no-load test is performed by running the motor with no load coupled to the shaft. This test is used to separate the no-load losses by running the uncoupled motor with different voltage levels starting from 125% of rated voltage down to the point where further voltage reduction increases the current. Temperature, voltage, current, and input power are to be read and recorded during each voltage point. An outcome of this test is to determine the Stator Copper Loss, Friction and Windage Losses, and Core Loss.

By connecting the induction motor under the no-load test to a balanced 3-phase voltage supply and running the motor until the input power is stabilized, a minimum of six different voltage values are required [104]. By reading and recording voltage, current, and input power using suitable RMS meters, the no-load data would be tabulated and used in certain calculations to separate stator copper loss, core loss, and friction and windage losses. The no-load stator copper loss of operating point (i) $P_{scl,i}$ is calculated by (3.1).

$$P_{scl,i}=1.5\times I_{nl,i}^2\times R_{dc} \tag{3.1}$$

where,

$I_{nl,i}$ is the no-load current of the operating point (i).

i=1,2,3,4,5,6 (six operating points with different voltage levels, 1 refers to the maximum voltage, 6 refers to the minimum voltage).

By subtracting $P_{scl,i}$ from $P_{in,i}$ (total input power at the operating point (i)) and plotting the power versus squared phase voltage at the last three or four voltage points, and by performing linear regression, the friction and windage losses can be determined. Figure 3-3 shows the losses curve of a 7.5hp induction machine. The friction and windage losses value (12.868W) is shown in the second term of the linear function (y=0.0022x+12.868) appeared on the figure.

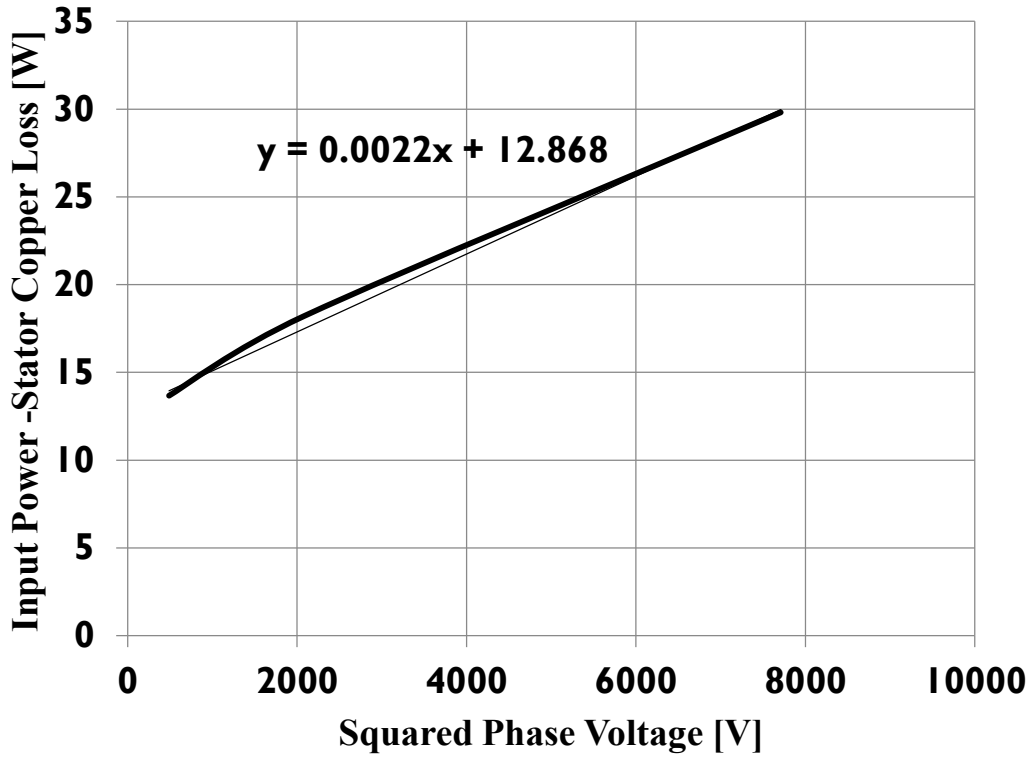

Figure 3-3. Friction & Windage losses separation for 7.5hp

3.2.4. Impedance Test

An Impedance Test is used to determine the value of each parameter of the equivalent circuit. Method 3 of the IEEE Std 112™-2004 standard is chosen as it matches the no-load condition. From the no-load data, a curve is drawn for total calculated reactance versus phase voltage. The highest point of this curve is used as the total no-load reactance per phase ($X_1 + X_m$) which is equal to (81.629 Ω) as shown in Figure 3-4. This result belongs to the same example mentioned in subsection 3.2.3 and is used in calculations of the reduced voltage slip test.

From the reduced slip test data (i.e. the lowest voltage point 6), the total impedance per phase and the power factor are calculated. The phase angle ($\theta_{1,i}$) of the input current, the apparent resistance of the total per phase circuit ($R_{a,i}$), and the total apparent reactance ($X_{a,i}$) can be calculated as shown in (3.2) through (3.4).

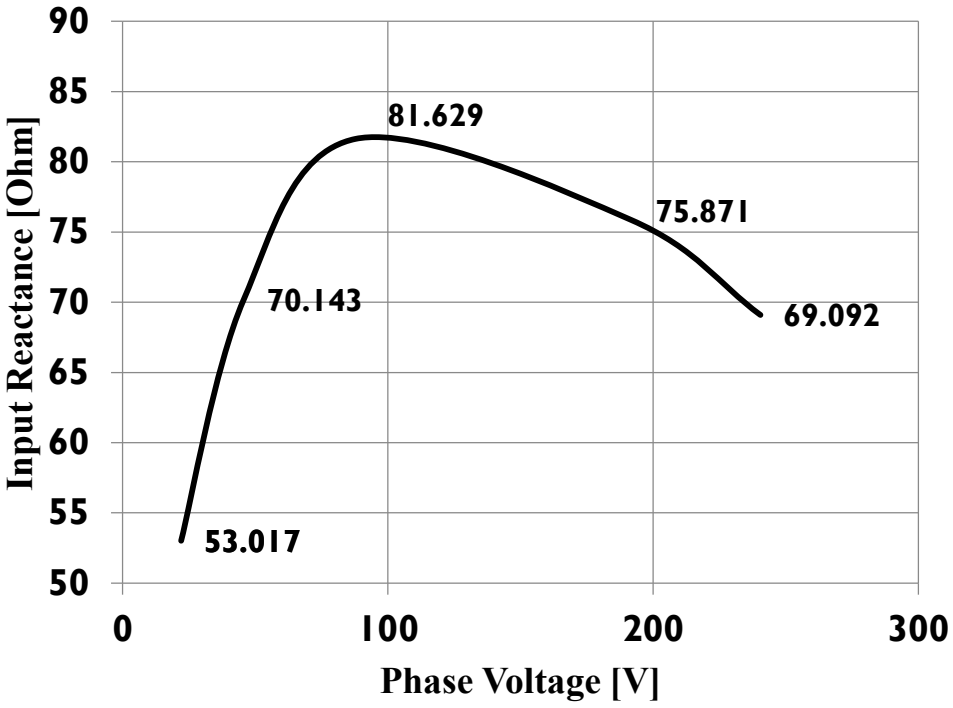

Figure 3-4. Input reactance vs. phase voltage for 7.5 hp

Equations (39) through (58) in section 5.9.4.2 (pp29) of the IEEE Std 112™-2004 were checked and some typing errors have been found. Equations (3.2) through (3.23) of this paper are a corrected presentation of the above mentioned equations of the standard.

$$\theta_{1,6}=-\cos^{-1}(PF_6) \tag{3.2}$$

$$R_{a,6}=Z_{a,6}\times\cos(-\theta_{1,6}) \tag{3.3}$$

$$X_{a,6}=Z_{a,6}\times\sin(-\theta_{1,6}) \tag{3.4}$$

The value of ($X_{a,i}$) determined from (3.4) is used as the first estimate of the sum (X_1+X_2). According to the machine design, a value for the ratio (X_1/X_2) can be obtained according to Table 3-I. Based on the ratio and X_1+X_2. (X_1) can be calculated as shown in (3.5).

$$X_1=X_{a,i}\frac{(X_1/X_2)}{1+(X_1/X_2)} \tag{3.5}$$

Table 3-I : Ratio of (X_1/X_2) [21]

Design class	X_1/X_2
A	1.00
B	0.67
C	0.43
D	1.00
Wound rotor	1.00

Using the maximum value of total no-load reactance $(X_1+X_m)_i$, the value of the magnetizing reactance (X_m) can be approximated as shown in (3.6).

$$X_m=(X_1+X_m)_i-X_1 \tag{3.6}$$

Per phase stator winding resistance has to be determined according to (3.7) and (3.8).

In case of a delta (Δ) connected motor,

$$R_{1,cold}=1.5\times R_{dc} \tag{3.7}$$

In case of a star (Y) connected motor

$$R_{1,cold}=0.5\times R_{dc} \tag{3.8}$$

From the no-load data and for the reduced slip voltage, $V_{2,6}$ (6 refers to the operating point 6) can be calculated according to (3.9).

$$V_{2,6}=\sqrt{\left[V_{1,6}-I_{1,6}\left(R_{1,cold}\cos\theta_{1,6}-X_1\sin\theta_{1,6}\right)\right]^2+\left[I_{1,6}\left(R_{1,cold}\sin\theta_{1,6}+X_1\cos\theta_{1,6}\right)\right]^2} \tag{3.9}$$

The angle ($\theta_{2,i}$) is calculated according to (3.10).

$$\theta_{2,6}=\tan^{-1}\left(\frac{-I_{1,6}\left(R_{1,cold}\sin\theta_{1,6}+X_1\cos\theta_{1,6}\right)}{V_{1,6}-I_{1,6}\left(R_{1,cold}\cos\theta_{1,6}-X_1\sin\theta_{1,6}\right)}\right) \tag{3.10}$$

The following equations are used to calculate necessary values needed in equivalent circuit parameters determination.

$$I_{m,6}=V_{2,6}/X_m \tag{3.11}$$

$$R_{fe,6}=V_{2,6}^2/\left(P_{h,6}/3\right) \tag{3.12}$$

$$G_{fe,6} = 1/R_{fe,6} \tag{3.13}$$

$$I_{fe,6} = V_{2,6}/R_{fe,6} \tag{3.14}$$

$$I_{2,6} = \sqrt{\left[I_{1,6}\cos\theta_{1,6} - I_{m,6}\sin\theta_{2,6} - I_{fe,6}\cos\theta_{2,6}\right]^2 + \left[I_{1,6}\sin\theta_{1,6} + I_{m,6}\cos\theta_{2,6} - I_{fe,6}\sin\theta_{2,6}\right]^2} \tag{3.15}$$

$$X_2 = \left(-V_{1,6}I_{1,6}\sin\theta_1 - I_{1,6}^2X_1 - I_{m,6}^2X_m\right)/I_{2,6}^2 \tag{3.16}$$

$$X_{a,i} = X_1 + X_2 \tag{3.17}$$

Equations (3.5) through (3.17) must be repeated using the initial ratio of (X_1/X_2) as used in (3.5) and the new value of $(X_{a,i})$ obtained from (3.17) and continue until stable values of (X_1) and (X_2) are achieved within 0.1%.

$$Z_{2,6} = V_{2,6}/I_{2,6} \tag{3.18}$$

$$s = n_s - n_{r,i}/n_s \tag{3.19}$$

$$R_{2,cold} = s\sqrt{Z_{2,6}^2 - X_2^2} \tag{3.20}$$

Using the value of the total reactance $(X_1+X_m)_i$ from the rated voltage no-load test, the following is calculated.

$$X_m = (X_1 + X_m)_1 - X_1 \tag{3.21}$$

where X_m has a new value which is different from that obtained from (3.6).

The algorithm will use the variable operating points and will estimate the nominal voltage and its associated no-load input power, no-load input current, power factor, input reactance $(X_1+X_m)_1$, and core losses $P_{h,1}$. The estimation is based on a curve fitting approach. Those estimated values will be used in the following equations. This curve fitting procedure plays an important role in the accuracy of the estimated value of efficiency. Moreover, it makes the algorithm very immune to voltage fluctuations (over or undervoltage) in the power supply.

$$V_{2,1} = \sqrt{\left[V_{1,1} - I_{1,1}\left(R_{1,cold}\cos\theta_{1,1} - X_1\sin\theta_{1,1}\right)\right]^2 + \left[I_{1,1}\left(R_{1,cold}\sin\theta_{1,1} + X_1\cos\theta_{1,1}\right)\right]^2} \tag{3.22}$$

$$G_{fe,1} = P_{h,1} / 3V_{2,1}^2 \tag{3.23}$$

$$R_{fe,1} = 1 / G_{fe,1} \tag{3.24}$$

The values of $\theta_{1,i}$, X_2, X_m, and $R_{fe,i}$ obtained from (3.2), (3.16), (3.21), and (3.24) respectively, are used in the equivalent circuit. The rotor resistance $R_{2,cold}$ from (3.20) and the stator resistance $R_{1,cold}$ will be corrected to the full-load temperature using (3.25) based on insulation class of the machine and Table 2-I (if full-load temperature rise is not available) as recommended in IEEE Std 112™-2004, before using them in the equivalent circuit. R_1 and R_2 will refer to the corrected values of $R_{1,cold}$ and $R_{2,cold}$ respectively.

$$R_1 = \frac{R_{1,cold}(T_{fl} + K_1)}{T_{cold} + K_1} \tag{3.25}$$

where,

K_1 is 234.5 for 100% IACS conductivity copper.

3.2.5. Stray Load Loss

If the motor under test has the same:

- rated voltage & insulation class, or
- rated voltage & number of poles & insulation class

of any of the motor within the supporting data, the algorithm will use the measured stray load loss of the data. Otherwise, stray load loss is to be assumed according to Table 1-I based on IEEE Std 112™-2004 or IEC 60034-2-1 [95] standards.

It has been noticed that estimating stray load loss (P_{sll}) based on IEC 60034-2-1 standards could give better result for motors rating larger than 40 hp. P_{sll} will be estimated by using (2.6).

By having the full-load value of the stray load loss; the 75%, 50%, and 25% load stray load losses will be determined according to (2.18), (2.19), and (2.20) respectively [90].

3.2.6. Test Method F1

This test should be performed by using a group of equations that are set in Calculation Form F2. 9.13, Page 72 of IEEE Std 112™-2004. Those equations must be followed to estimate the efficiency. The equations are as follows:

Slip is to be assumed for each load point. It is calculated using (3.19).

$$Z_2=\sqrt{(R_2/s)^2+X_2^2} \tag{3.26}$$

$$G_2=(R_2/s)/Z_2^2 \tag{3.27}$$

$$G=G_2+G_{fe} \tag{3.28}$$

$$B_2=-\left(X_2/Z_2^2\right) \tag{3.29}$$

$$B_m=-(1/X_m) \tag{3.30}$$

$$B=B_2+B_m \tag{3.31}$$

$$Y_2=\sqrt{G^2+B^2} \tag{3.32}$$

$$R_g=G/Y_2^2 \tag{3.33}$$

$$R=R_1+R_g \tag{3.34}$$

$$X_g=-\left(B/Y_2^2\right) \tag{3.35}$$

$$X=X_1+X_g \tag{3.36}$$

$$Z=\sqrt{R^2+X^2} \tag{3.37}$$

$$I_1=V_1/Z \tag{3.38}$$

$$I_2=I_1/\sqrt{Z_2^2\times Y_2^2} \tag{3.39}$$

$$P_s=3I_1^2R \tag{3.40}$$

$$P_r=3I_2^2(R_2/s) \tag{3.41}$$

$$P_{scl}=3I_1^2R_1 \tag{3.42}$$

$$P_h=3I_1^2\left(G_{fe}/Y_2^2\right) \tag{3.43}$$

$$P_{rcl}=sP_r \tag{3.44}$$

$$P_t=P_{scl}+P_h+P_{rcl}+P_{fw}+P_{sll} \tag{3.45}$$

$$P_{cov}=P_s-P_t \tag{3.46}$$

Finally, the efficiency is estimated by using (3.47).

$$\eta=(P_{cov}/P_s)\times 100 \tag{3.47}$$

where,

Z_2 is the rotor impedance.

G_2 is the rotor conductance.

G is the rotor and magnetic conductance .

B_2 is the rotor susceptance.

B_m is the magnetizing susceptance.

B is the rotor & magnetic circuit susceptance.

Y_2 is the rotor and magnetizing circuit admittance.

R_g is the rotor & magnetizing circuit resistance.

R is the total resistance of the equivalent circuit.

X_g is the rotor and magnetizing circuit reactance.

X is the total reactance of the equivalent circuit.

Z is the total impedance of the equivalent circuit.

I_1 is the stator current.

I_2 is the rotor current.

P_s is the stator power.

P_r is the rotor power.

P_{scl} is the stator copper loss.

P_h is the core loss.

P_{rcl} is the rotor copper loss.

P_t is the total loss.

P_{cov} is the converted power.

η is the estimated efficiency.

3.3. Experimental Results and Analysis

The proposed algorithm has been applied to test 7 induction motors of different ratings (3-150hp). Out of the seven motors tested, the algorithm failed to estimate the efficiency of three motors as shown in Table 3-II. The proposed algorithm is supposed to be able to deal with all kinds and sizes of induction motors. A deep investigation was made to determine the cause of the failure, and in which part of the algorithm it occurs. To be able to determine the source of the problem and to pinpoint the place where it occurs, a flow chart of the proposed method is shown in Figure 3-5 which illustrates the flow of the whole process. There are two iteration processes. The first one is during the extraction of the motor parameters.

Table 3-II. Efficiency estimation using the proposed algorithm

Motor Size (hp)	**Efficiency estimation using the proposed algorithm**
3.0	Succeeded
7.5	**Failed**
25	Succeeded
50	**Failed**
60	**Failed**
100	Succeeded
150	Succeeded

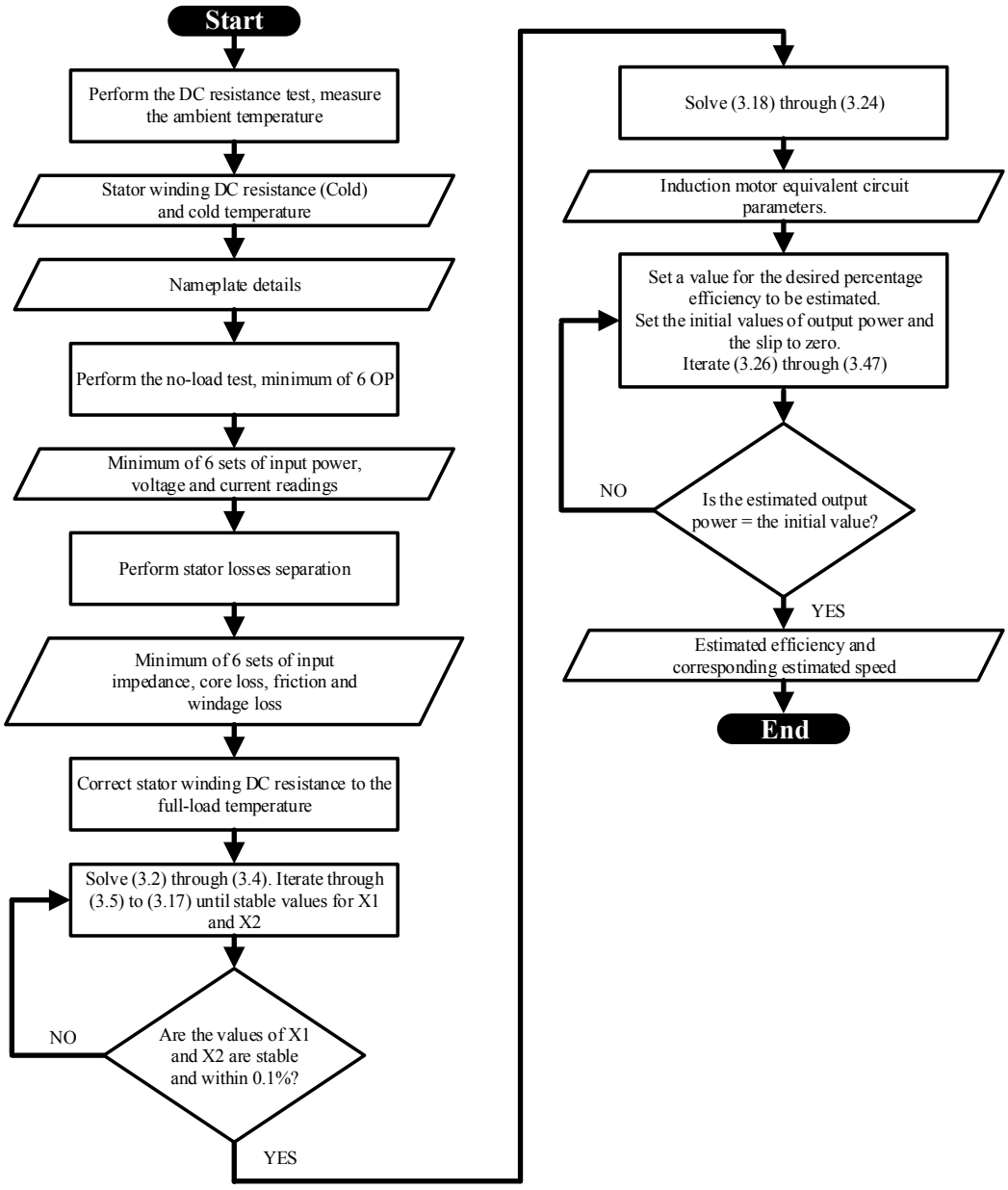

Figure 3-5. Algorithm flow chart

The second iteration is for estimating the efficiency. The estimated parameters of the seven motors are as shown in Table 3-III. Having all the parameters extracted for all the seven motors means that the process went through the first iteration successfully. That indicates that the algorithm fell into an infinite loop within the second iteration. The second iteration starts with initial values of zero for both output power and slip, which means that the initial value of the rotor speed is the synchronous speed of the motor. The speed will be decreased by 1 r.p.m. for

Table 3-III. Estimated equivalent circuit parameters

Motor Size (hp)	R_1 (Ω)	X_1 (Ω)	R_{fe} (Ω)	X_m (Ω)	R_2 (Ω)	X_2 (Ω)
3.0	0.7837	1.7397	204.73	19.175	0.5004	2.5966
7.5	0.8144	18.549	820.27	52.499	0.4862	27.684
25	0.8740	7.7979	2825.1	116.63	0.3584	11.638
50	0.4899	5.1212	1344.6	39.900	0.3724	7.6436
60	0.2858	4.0768	1808.1	53.304	0.0947	6.0847
100	9.6098	0.9767	646.73	18.710	6.0182	1.4578
150	7.5329	0.7997	512.49	19.128	4.2646	1.1937

each iteration; so the slip and the output power will increase accordingly. The iteration will stop when certain conditions are met, that is when the estimated output power reaches the desired percentage of the rated output power of the motor. Failing to meet the foregoing set conditions means that the declared equivalent circuit parameters are not correct.

It was noticed that with the 3 failed motors, the calculated value of the input reactance which is used in (6) leads to a high extracted value of X_1 and hence X_2 as shown in Table 3-III. If those high values of X_1 and X_2 are used in the IEEE Method F1 equations (28) through (49), and if the output of the equations is observed carefully, it can be seen that those high values of X_1 and X_2 will result in a low value of R in (36), high value of X in (38), low value of I_1 in (40), and hence, low value of the input power P_s in (42). This low value of P_s will make the output power P_{cov} in (48) very low (it might even have negative value when the P_s is less than the total losses), and in this case, it cannot reach the expected value of the motor output power. As (28) through (49) are part of an iterative process to estimate the efficiency, this means that the process will fall into an infinite loop.

From the previous analysis, it can be seen that the key factor in extracting realistic values for X_1 and X_2 is the value of the input reactance of the motor at the lowest voltage operating point. To further reduce the value of the input reactance, a suitable low voltage must be reached which will further increase the value of the input current. As the variable voltages in electric motor repair workshops is determined by fixed values of transformer taps; there is no way to reach the required low voltage, and hence, a mathematical approach was proposed in this work to solve the problem. The seven motors were run through five different levels of voltages. The input reactance values of the motors are tabulated in Table 3-IV. The table also shows a ratio of the maximum to the minimum values of the input reactance of every motor within the tested group.

Table 3-IV. Input reactance vs. voltage for seven induction motors

%V	3 hp	7.5 hp	25 hp	50 hp	60 hp	100 hp	150 hp
100%	20.64	70.57	124.42	45.02	57.38	19.68	19.92
80%	29.21	76.67	138.77	58.53	61.47	23.10	21.20
37%	29.99	80.21	147.23	62.74	62.63	24.75	16.89
19%	18.89	68.48	97.81	53.76	40.69	17.00	5.48
9%	4.552	41.62	20.74	16.84	11.31	3.03	2.68
$\frac{X_{max}}{X_{min}}$	**6.588**	**1.927**	**7.098**	**3.725**	**5.538**	**8.168**	**7.911**

By comparing the ratio values of the seven motors, it can be noticed that the three motors which the algorithm failed to estimate their efficiencies have smaller values of (X_{max}/X_{min}) compared to the others. It can be said that the smaller value of (X_{min}) the bigger value of the ratio.

Per phase input impedance of the motor can be calculated as follows:

$$Z_{in} = V_{\varphi}/I_{\varphi} \tag{3.48}$$

where V_{φ} and I_{φ} are phase voltage and phase current respectively.

The power factor (PF) is estimated by using (3.49)

$$PF = P_{in}/\left(\sqrt{3}V_{in}I_{in}\right) \tag{3.49}$$

where V_{in} and I_{in} are input line voltage and input line current respectively.

Hence, the input reactance can be estimated using (3.50)

$$X_{in} = \frac{V_{\varphi}}{I_{\varphi}}\sqrt{1\text{-}PF^2} \tag{3.50}$$

Based on (3.50) the only way to reduce the value of the minimum input reactance is by pushing up the value of the current. It is mentioned in subsection 3.2.3 that the minimum point during the no-load run is the point where further voltage reduction increases the current. Although that point is reached with the three failed motors, but still, the minimum reactance shows a relatively high value, hence, a low value of (X_{max}/X_{min}). It means that further voltage reduction is needed in the case of those three motors to achieve higher current and smaller value of (X_{min}). The 7.5 hp induction motor is one of the motors in the failed group and has one of the

Table 3-V. Input voltage vs. input reactance of 7.5 hp motor

%V	X_{in}
100%	71.240
80%	77.530
37%	82.663
19%	72.104
9%	39.668
5.9%	21.089
$\frac{X_{max}}{X_{min}}$	**3.919**

lowest values of (X_{max}/X_{min}). The motor tested with the voltages shown in Table 3-V with its corresponding input reactances.

Another further reduction in voltage (5.9%), the (X_{max}/X_{min}) is still within the low range (3.919) and yet, the machine failed again to go through the algorithm successfully. To bring up the (X_{max}/X_{min}) value, another voltage reduction is applied (4.57%) and the voltage versus input reactance results are tabulated in Table 3-VI. With 4.57% of the rated voltage (230V) of the 7.5 hp induction motor, the value of (X_{max}/X_{min}) reached (6.86) which is considered to be within the preferred range. This value allowed the motor to go through the algorithm successfully. In one of the workshops, it was found that the lowest voltage that can be accessed is around 9% of the rated voltage of the network (usually 600V for industrial sector). In this case, reaching a low value as in the case of 4.57% of the rated voltage mentioned above in Table 3-VI is not usually allowable. The task now is how to adjust the algorithm to work with what is available in those motor service centers in terms of voltage supplies.

Table 3-VI. Input voltage vs. input reactance of 7.5 hp

%V	X_{in}
100%	69.669
80%	76.378
37%	81.562
19%	72.961
9%	39.414
4.57%	11.885
$\frac{X_{max}}{X_{min}}$	**6.86**

3.4. Modified Method

The lower point of voltage is limited with the lowest value that can be reached through the transformer taps. An alternative solution is proposed here. A mathematical approach to the problem is found to access a lower point within the input reactance versus phase voltage. The proposed mathematical solution to the problem is by fitting a curve to the multiple no-load operating points. The curve's equation will be utilized to calculate the proper input reactance that can make the value of (X_{max}/X_{min}) to fall within the accepted range which is decided to be > 6.

The value of (6) is determined through extensive experimental tests and based on values of (X_{max}/X_{min}) shown in Table 3-IV.

So, the algorithm is further modified to go through the following steps before declaring the six parameters of the machine:

1. In case that the value of (X_{max}/X_{min}) is less than 6, the algorithm will further check the following conditions:

    a. If (X_{max}/X_{min}) is greater than 1 and less than 2, then the algorithm will go down with the voltage and keep checking on the value of (X_{min}), till (X_{max}/X_{min}) will be equal or greater than 12. A new value of minimum input reactance will be obtained here ($X_{min, new}$).

    b. If (X_{max}/X_{min}) is greater than 2 and less than 4, then the algorithm will go down with the voltage and keep checking on the value of (X_{min}), till (X_{max}/X_{min}) will be equal or greater than 11. A new value of minimum input reactance will be obtained here ($X_{min, new}$).

    c. If (X_{max}/X_{min}) is greater than 4 and less than 6, then the algorithm will go down with the voltage and keep checking on the value of (X_{min}), till (X_{max}/X_{min}) will be equal or greater than 9.

    The values 12, 11, and 9 in a, b, and c respectively were decided after extensive tests run on many machines.

2. A new value of minimum input reactance ($X_{min, new}$) will be obtained according to (a, b, or c).

3. New value of X_1 will be calculated according to (3.51).

$$X_{1,\,new}=X_{min,\,new}\left(\left(\frac{X_1}{X_2}\right)\Big/\left(1+\frac{X_1}{X_2}\right)\right) \tag{3.51}$$

New value of X_2 will be calculated according to (3.52).

$$X_{2,\,new}=X_{1,\,new}\Big/\left(\frac{X_1}{X_2}\right) \tag{3.52}$$

These new values $X_{1,\,new}$ and $X_{2,\,new}$ will replace the previous extracted values by equations (3.2) through (3.24).

3.5. Algorithm's Validation

A group of 8 motors are tested by using the modified method. The validation is achieved by using 5 and 6 operating points. The measured and estimated efficiencies by using 5 no-load operating points are tabulated in Table 3-VII. The measured and estimated efficiencies by using 6 no-load operating points are tabulated in Table 3-VIII. Both tables show the absolute error which is the difference between the measured and the estimated values of efficiency. It can be clearly noticed that having 6 no-load operating points gives higher accuracy of the estimated efficiencies compared to 5 operating points.

Table 3-VII. Measured vs. Estimated efficiency for 8 Induction Motors (Proposed method, 5 OP)

Motor Size (hp)		**100%**	**75%**	**50%**	**25%**
3.0	Measured %η	80.4	79.1	75.6	63.9
	Estimated %η	80.2	79.7	76.5	65.4
	%Error	**0.20**	**-0.60**	**-0.90**	**-1.50**
7.5	Measured %η	90.5	91.2	90.8	86.9
	Estimated %η	90.1	91.1	91.0	87.3
	%Error	**0.40**	**0.10**	**-0.20**	**-0.40**
15	Measured %η	90.6	91.2	90.7	86.5
	Estimated %η	90.1	90.9	90.5	86.5
	%Error	**0.50**	**0.30**	**0.20**	**0.00**
25	Measured %η	92.0	92.8	92.8	90.3
	Estimated %η	92.7	93.4	92.8	89.3
	%Error	**-0.70**	**-0.60**	**0.00**	**1.00**
50	Measured %η	92.8	93.1	92.6	89.2
	Estimated %η	92.2	92.7	92.1	88.3
	%Error	**0.60**	**0.40**	**0.50**	**0.90**
60	Measured %η	94.8	94.9	93.9	91.0
	Estimated %η	94.3	94.7	94.4	92.8
	%Error	**0.50**	**0.20**	**-0.50**	**-1.80**
100	Measured %η	95.5	95.5	94.9	92.1
	Estimated %η	95.1	95.4	94.9	93.0
	%Error	**0.40**	**0.10**	**0.00**	**-0.90**
150	Measured %η	93.6	93.4	92.1	87.1
	Estimated %η	93.4	93.6	92.7	88.4
	%Error	**0.20**	**-0.20**	**-0.60**	**-1.30**

Table 3-VIII. Measured vs. Estimated efficiency for 8 Induction Motors (Proposed method, 6 OP)

Motor Size (hp)		100%	75%	50%	25%
3.0	Measured %η	80.4	79.1	75.6	63.9
	Estimated %η	80.6	79.6	75.6	63.9
	%Error	**-0.20**	**-0.50**	**0.00**	**0.00**
7.5	Measured %η	90.5	91.2	90.8	86.9
	Estimated %η	90.4	91.4	91.4	88.5
	%Error	**0.10**	**-0.20**	**-0.60**	**-1.60**
15	Measured %η	90.6	91.2	90.7	86.5
	Estimated %η	90.8	91.4	90.9	86.7
	%Error	**-0.20**	**-0.20**	**-0.20**	**-0.20**
25	Measured %η	92.0	92.8	92.8	90.3
	Estimated %η	92.7	93.4	92.9	89.4
	%Error	**-0.70**	**-0.60**	**-0.10**	**0.90**
50	Measured %η	92.8	93.1	92.6	89.2
	Estimated %η	92.3	92.7	92.1	88.4
	%Error	**0.50**	**0.40**	**0.50**	**0.80**
60	Measured %η	94.8	94.9	93.9	91.0
	Estimated %η	94.2	94.7	94.3	92.8
	%Error	**0.60**	**0.20**	**-0.40**	**-1.80**
100	Measured %η	95.5	95.5	94.9	92.1
	Estimated %η	95.1	95.4	95.0	93.1
	%Error	**0.40**	**0.10**	**-0.10**	**-1.00**
150	Measured %η	93.6	93.4	92.1	87.1
	Estimated %η	93.4	93.6	92.7	88.4
	%Error	**0.20**	**-0.20**	**-0.60**	**-1.30**

3.6. Error Analysis and Uncertainty

The same error analysis techniques that is described in subection 2.3, and the same three induction motors are used to demonstrate the uncertainty of the proposed Method B. Figure 3-6 shows the experimental setup and the apparatus used to run both the dynamometer and the no-load tests. To extract the value of every required influence coefficient, the change in the output variable (i.e. motor efficiency) is plotted against the corresponding perturbation in the input variable. Figure 3-7 shows the graph produced to help extracting the influence coefficient of the input power of the 5.0 hp, 220 V induction motor by using the algorithm. The final results obtained for the three tested motors of the direct measurements and the proposed method measurements, by using WCE and RPBE techniques are tabulated in Table 3-IX. The results show that the average levels of uncertainty of the algorithm measurements are ±0.028%, and ±0.02% by using WCE and RPBE respectively. The extracted influence factors for the input

voltage, input current, shaft torque, and stray load loss are all zero. The other influence factors of input power, rotor speed, stator resistance, and friction and windage losses were very low. This resulted in a low uncertainty of the estimated efficiencies. Such a low level of uncertainty within the estimated efficiencies gives some confidence to the proposed algorithm.

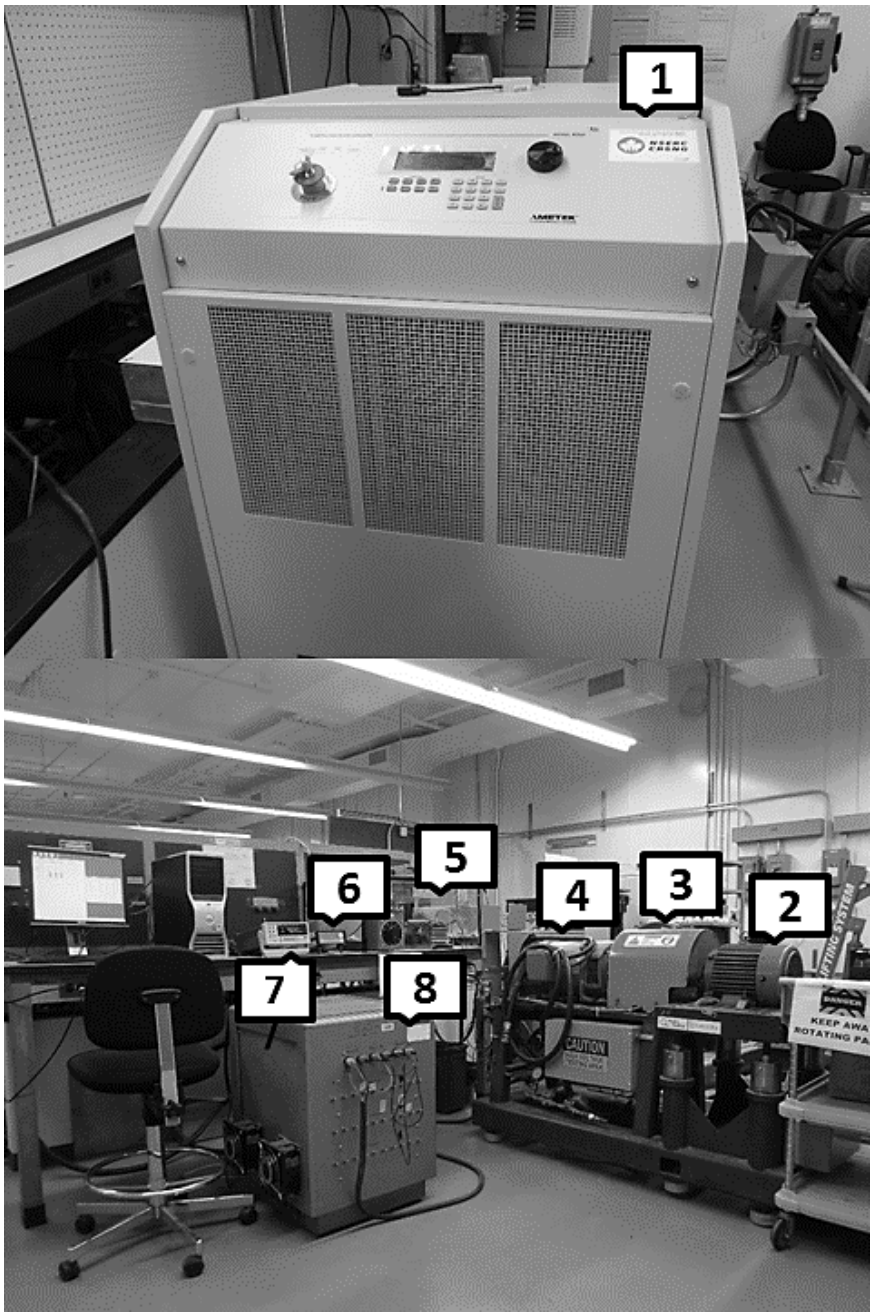

Figure 3-6. Motor testing experimental setup; 1, programmable power supply; 2, 3.0 hp induction motor; 3, torque transducer; 4, dynamometer; 5, field control unit; 6, multi-channel signal conditioner; 7, high resolution dc multimeter; 8, Resistor bank.
Photo is a courtesy of Concordia University.

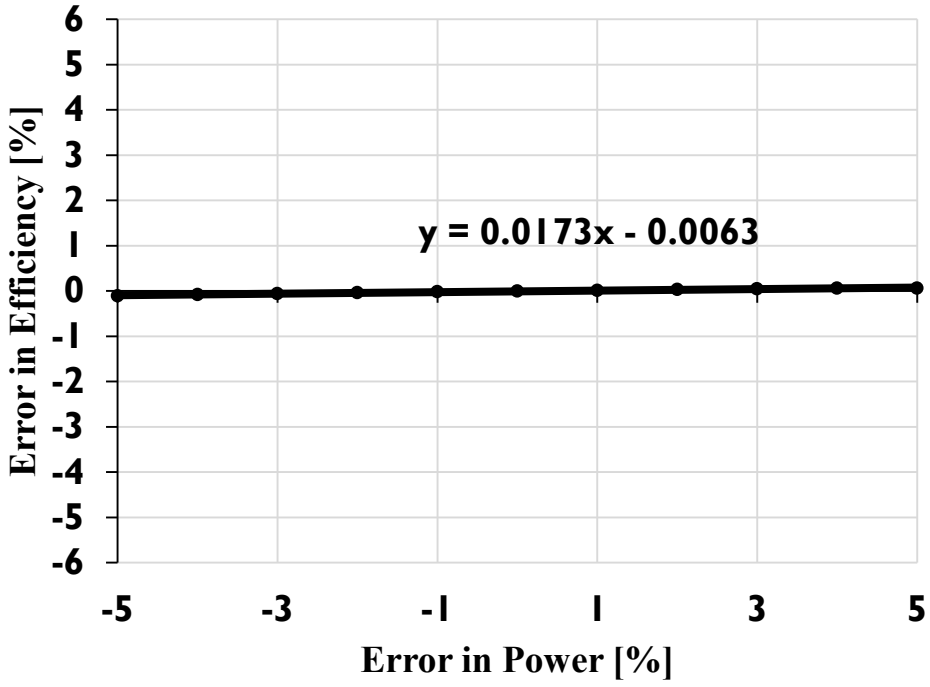

Figure 3-7. The proposed method measurements, FL (5.0 hp): I_P=0.0173

Table 3-IX. Uncertainty Results of the Three Tested Induction Motors

Tested Induction Motor	Uncertainty of the Measured Efficiency [±%]		Uncertainty of the Estimated Efficiency (Proposed method) [±%]	
	WCE [±%]	RPBE [±%]	WCE [±%]	RPBE [±%]
5.0 HP, 220 V	1.0417	0.6115	0.0359	0.0250
7.5 HP, 230 V	0.9004	0.5517	0.0503	0.0314
7.5 HP, 460 V	1.1664	0.6978	0.0310	0.0203

3.7. Summary

In this chapter, a novel technique is proposed for a refurbished induction machines efficiency estimation. The technique is called “Method B”. Method B is designed to run with very limited data and measurements that can usually be encountered in electric motor service centers. Method B is also designed to be easily applied in any motor repair workshop.

It was found that the IEEE Std 112™-2004-Method 3 is not capable of dealing with the

limitations of the variable voltage source in electric motor repair workshops. However, the IEEE Std 112™-2004-Method 3 succeeded to deal with the majority of the motors tested (8 motors), but on the other hand, it failed with some motors.

In this chapter, a modification is proposed to the IEEE Std 112™-2004-Method 3 that takes into account the equipment limitations and capabilities in normal motor repair workshops. In other words, the IEEE Std 112™-2004-Method 3 is designed to work only in well-equipped laboratories, while the proposed Method B is designed to be applicable in North American electric motor service centers.

A detailed procedure of the proposed method with its flow chart are presented in section 3.2 and its subsections.

The algorithm utilizes a valuable data received from Hydro-Québec and BC hydro by using the measured full-load temperature and stray load loss values in lieu of the assumed ones. Having this data, has improved the performance and the output of the algorithm to acceptable levels of performance. 8 induction motors of size range from 3-to-150 hp were tested using the designed software. The results were presented and showed acceptable accuracy.

To evaluate the estimated efficiency values obtained by the proposed algorithm, an uncertainty study was conducted and showed acceptable levels of uncertainty by using the WCE and RPBE techniques. The level of uncertainty within the estimated efficiencies obtained by using the proposed method provides confidence to the proposed algorithm and the software can be used in industry with some confidence. The proposed algorithm is designed to work with only 60 Hz induction motors. It does not work with machines of different frequency or different types of rotors.

CHAPTER FOUR

4. Developed Software

Concordia University signed a contract with a Canadian company (CEATI International Inc.) to develop a user-friendly software that can be utilized as an industrial tool for three-phase, 60 Hz induction motors efficiency estimation. The tool has to be totally applicable in North America electric motors service centers. The project title is "*Estimating Motor Efficiency of Three Phase A.C. Motors Using Standard No-Load Tests*". Senior engineers from Hydro-Québec, BC hydro, SaskPower, and Manitoba Hydro were appointed as technical monitors for the project. Professor Pragasen Pillay of Concordia University was the Principle Investigator of the project.

The two proposed algorithms (i.e. Method A & Method B) were approved after a very careful and thorough assessment and evaluation process done by the technical monitors of the project. It was decided that spreadsheets should be the software platform in order to make the proposed tool affordable by the electric motor workshops. The two algorithms and the Hydro-Québec and BC hydro supporting data were all to be integrated in the software.

Visual Basic® programming was used to create an interactive front panel. This allows entering of the required data and obtaining the estimated value of the motor's efficiency. The software is also designed to produce useful graphs and data. The software is approved by the technical monitors.

4.1. Introduction to Visual Basic

The name BASIC is an acronym for Beginner's All-purpose Symbolic Instruction Code. BASIC was first developed in the early 1960s as a way to teach programming techniques to college students. BASIC caught on quickly and is available in hundreds of dialects for many types of computers. BASIC has evolved and improved over the years. For example, in many early implementations, BASIC was an *interpreted* language. Each line was interpreted before it was executed, causing slow performance. Most modern dialects of BASIC allow the code to be *compiled* — converted to machine code which results in faster and more efficient execution.

BASIC gained quite a bit of respectability in 1991 when Microsoft released Visual Basic

for Windows. This product made it easy for the masses to develop stand-alone applications for Windows. Visual Basic has very little in common with early versions of BASIC, but Visual Basic is the foundation on which VBA was built.

Excel 5 was the first application on the market to feature Visual Basic for Applications (VBA). VBA is best thought of as Microsoft's common application scripting language, and it's included with most Office 2010 applications and even in applications from other vendors [105].

4.2. Building up the Software

At the first stage of building the software, it was suggested to have two separate versions of the software, one for Method A, and the other for method B. It is commonly known that the first step of the process of building a software is to design the front panel. The front panel was built by using the GUI technique. It has to include all the necessary cells to enter the machine data and its test measurements. The following are a group of figures that show the first version of the proposed software (Method A).

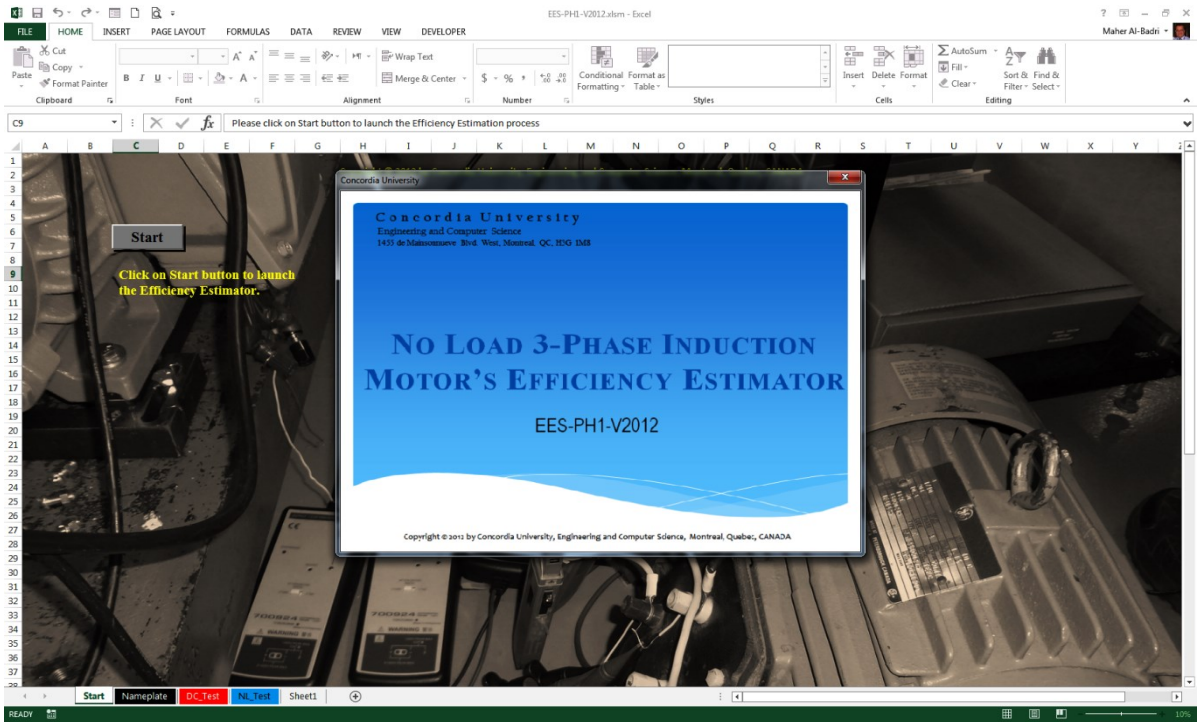

Figure 4-1. A splash screen of the software.

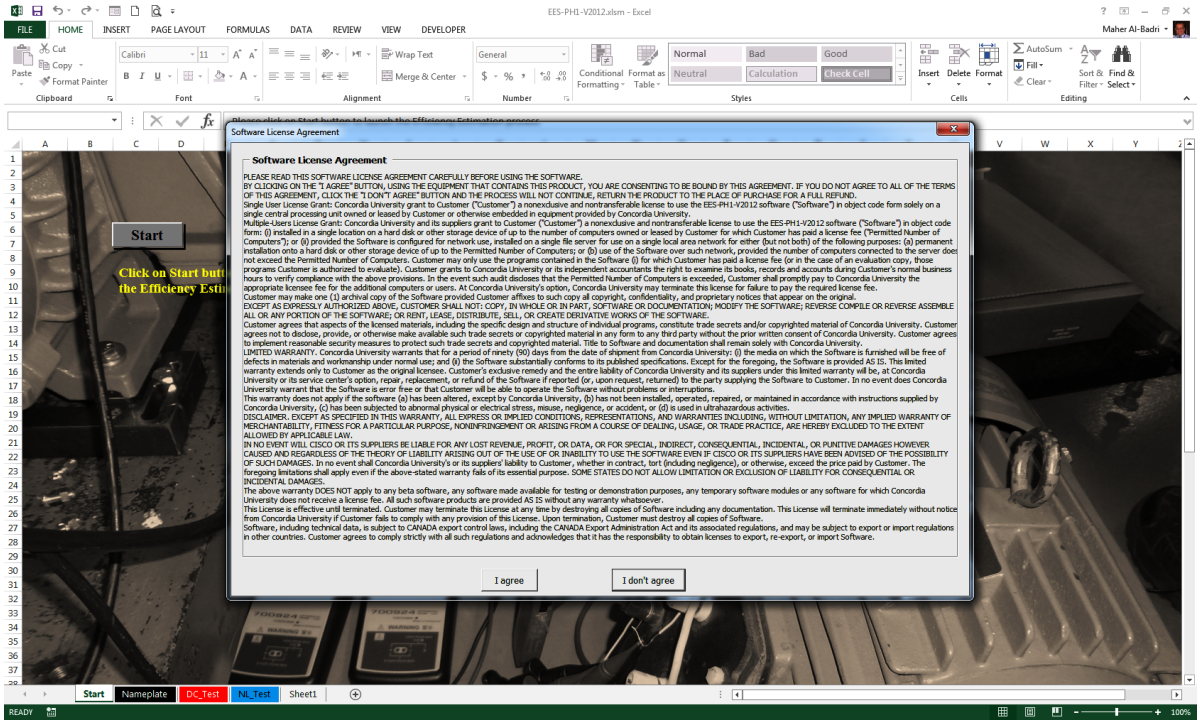

Figure 4-2. The software license agreement window.

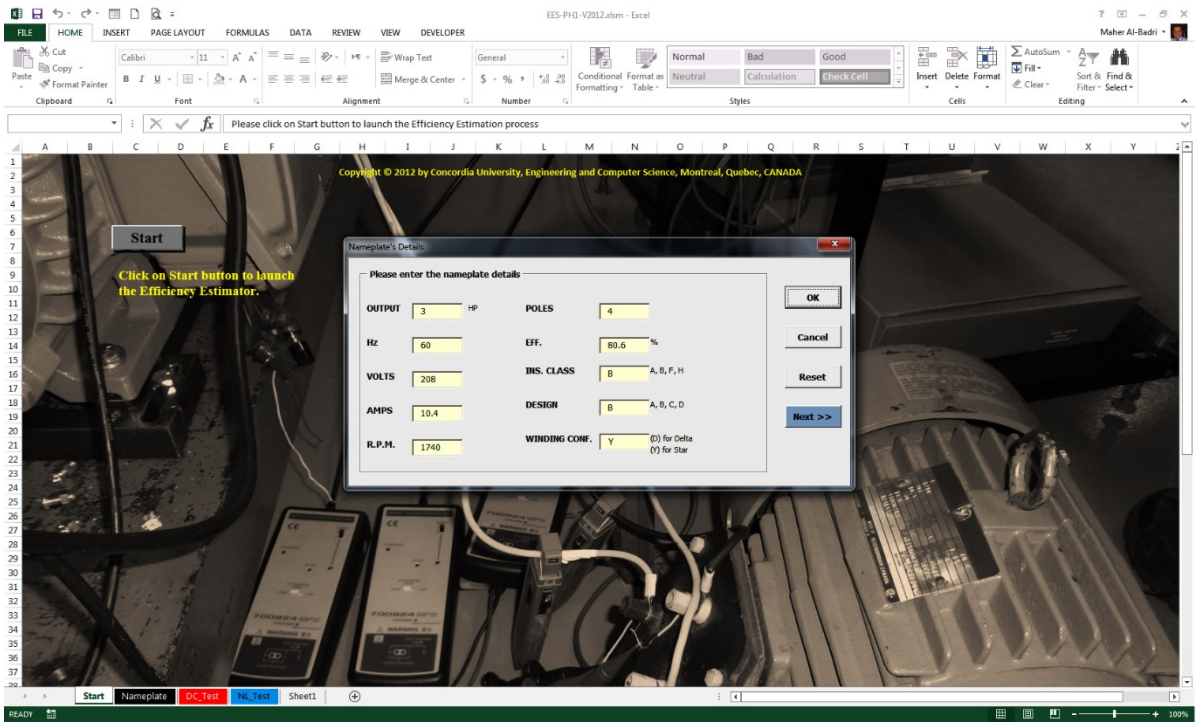

Figure 4-3. The Nameplate Details window filled up with the 3 hp machine data.

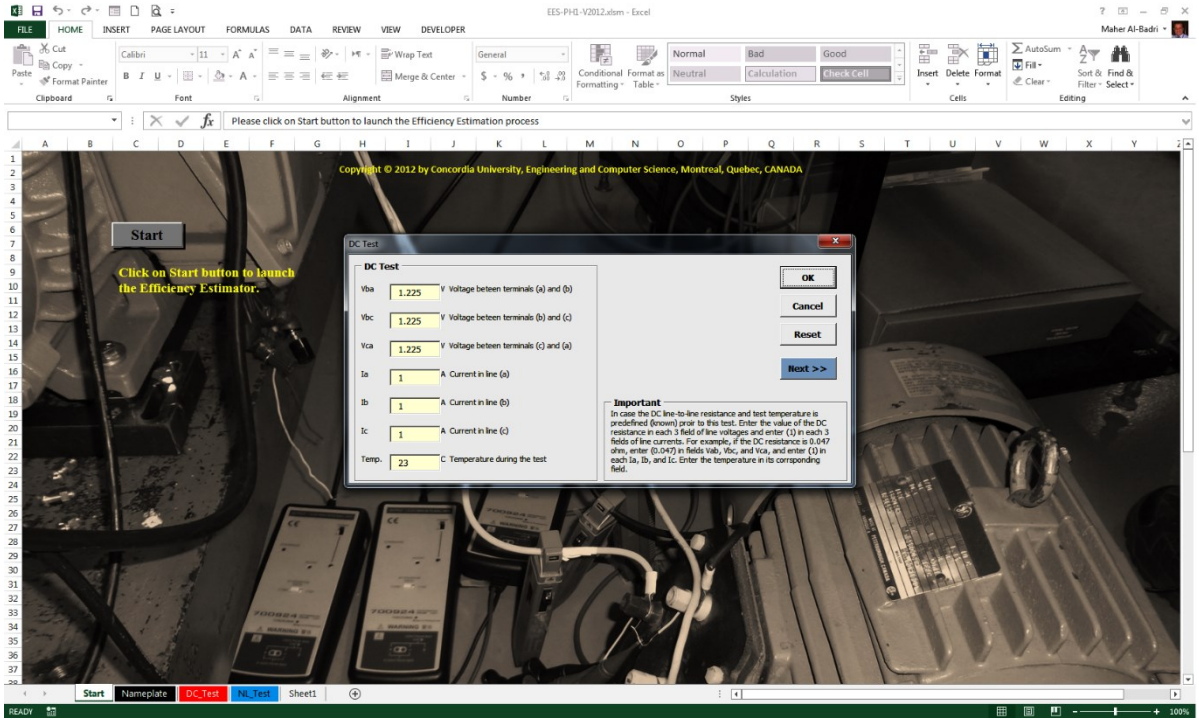

Figure 4-4. The DC Test window filled up with the 3 hp machine data.

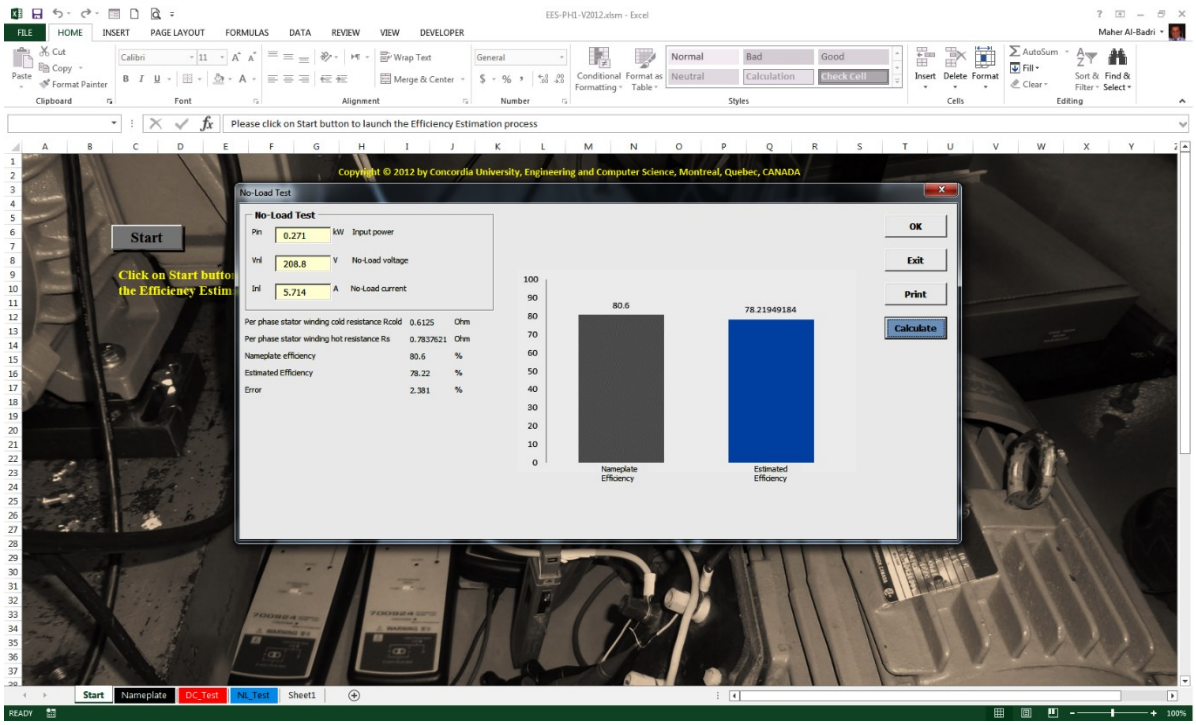

Figure 4-5. The No-Load Method A Test window shows the final efficiency results of the 3 hp machine.

Later on, the technical monitors suggested that the software should be of one version that includes both Method A and Method B and the front panel should be only one piece rather than three separated windows and it consists of all test sections (i.e. DC Test, Nameplate Details, Method A measurements, and Method B Measurements). The following Figure 4-6 shows the modified software. Figure 4-7 shows only the front panel for clearer details.

An Exit and Print buttons were suggested to be added to the software to help the user to have a printout copy of the final test results and to exit via the software GUI and not through the main spreadsheets window. The software was modified accordingly. Figure 4-7 shows the modified software.

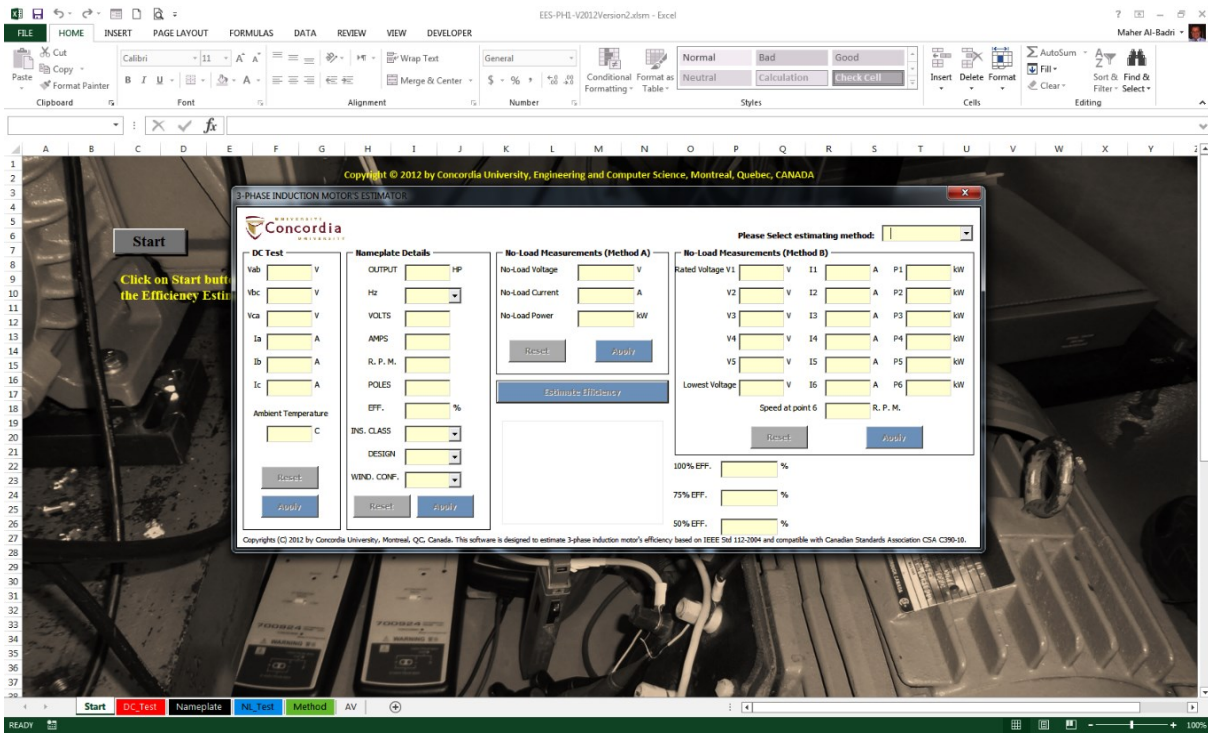

Figure 4-6. The modified software of one front panel.

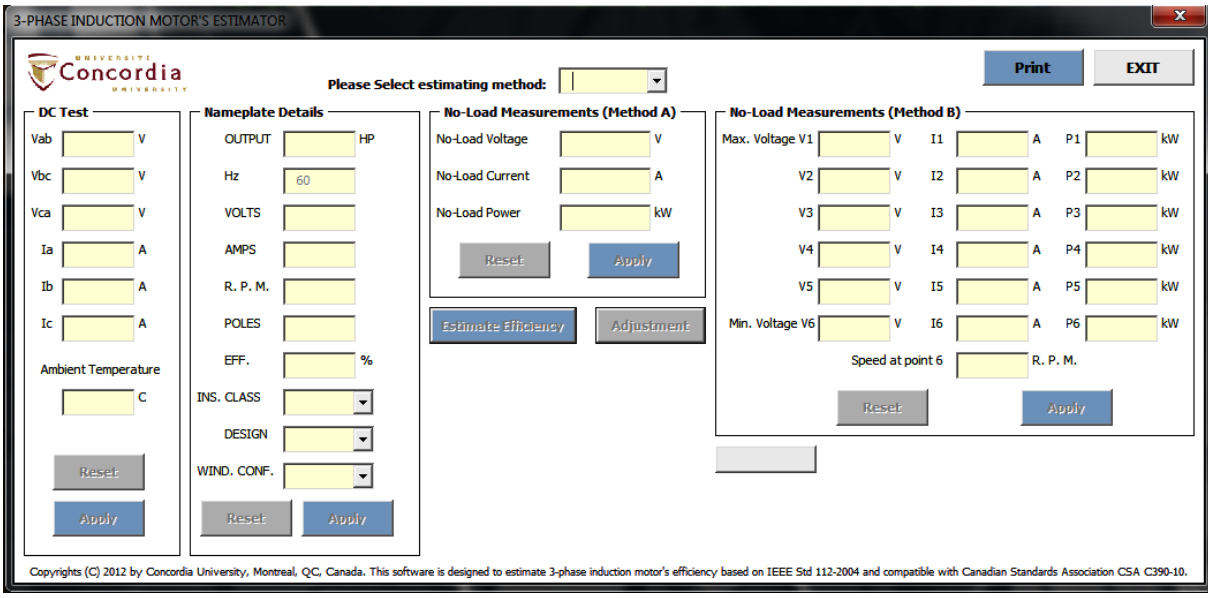

Figure 4-7. Print and Exit buttons are added to the front panel.

The logos of the sponsor Canadian companies were suggested to be added to the software front panel. A button to display the User's Guide is also proposed. The software was modified accordingly. Figure 4-8 shows the modified software.

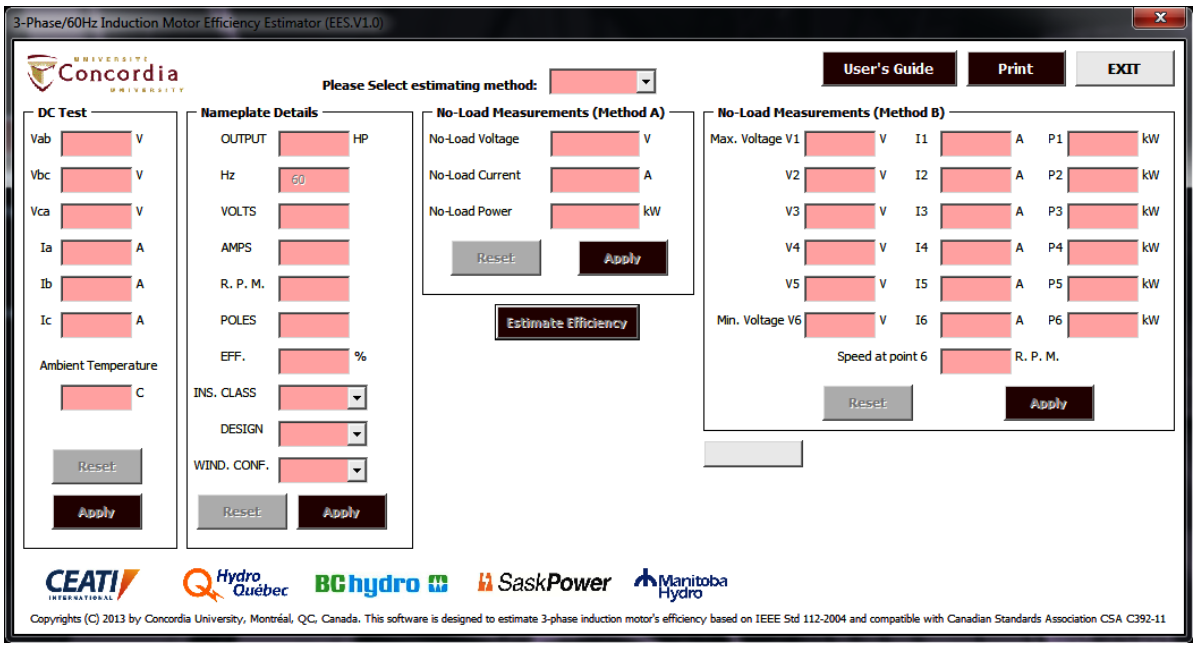

Figure 4-8. The companies' logos appear on the software.

The technical monitors also suggested that the DC test should include two procedures:

1. DC test with voltage and current measurements of the three stator windings.
2. DC test that is carried out by an ohmmeter.

It was also suggested that the user should be able to save a test data and its associated results. The user should also be able to import pre-tested machine measurements into the software without the need of entering the data again. Hence, two buttons were added. One is named “Save Data As” whereby the data can be saved in both .xls and .xlsx extensions. The second added button was named “Import Data” helps the user of importing data of a pre-tested machine into the software. It was also suggested that the user has the option of hiding the front panel. Hence a button named “Hide” is added to the software.

More than 10,000 coding lines were added to turn the software into a smart version where a checking process on all entered data is carried out once the user clicks on a newly added button named “Check”. The user cannot proceed to the efficiency estimation process unless all data are checked to be relative. Any abnormal data entered will trigger a message box from the software asking the user to make sure of the data that been entered.

The technical monitors finally asked that an additional important feature must be added to the software. The feature is that, once the efficiency estimation process is finished, the user must be informed about the nominal and minimum efficiency the tested machine has to have according to the ANSI/NEMA MG 1-2011 standard [15]. Data of Table 12-11 (Full-load efficiencies of energy efficient motors (random wound)) and Table 12-12 (Full-load efficiencies for 60 Hz premium efficiency electric motors rated 600 volts or less (random wound)) of the mentioned standard were added to the software to be utilized to implement the new feature. The final version of the software had a total of 21050 coding lines. A detailed User’s Guide was produced with all illustrative picture that describe the procedure of using the software and handling the required tests. The following are group of figures that show the latest version of the software which is approved by the technical monitors.

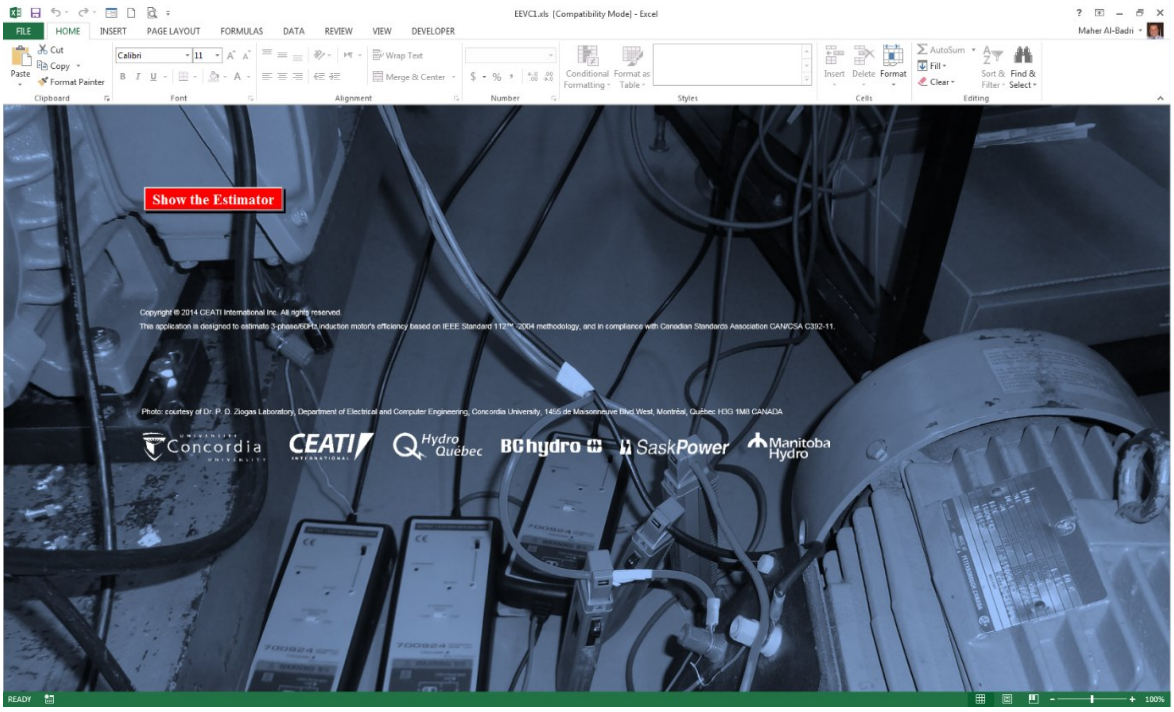

Figure 4-9. The main window of the software
Copyrights © CEATI International Inc.

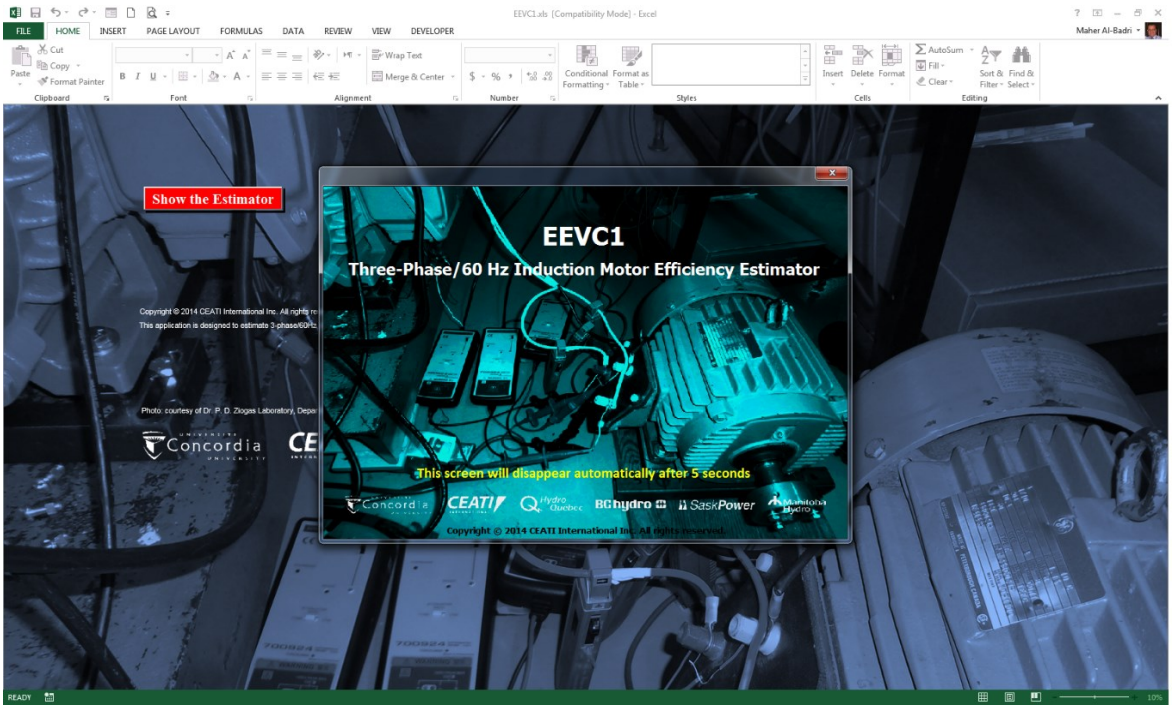

Figure 4-10. A splash screen shows up when the software launches.
Copyrights © CEATI International Inc.

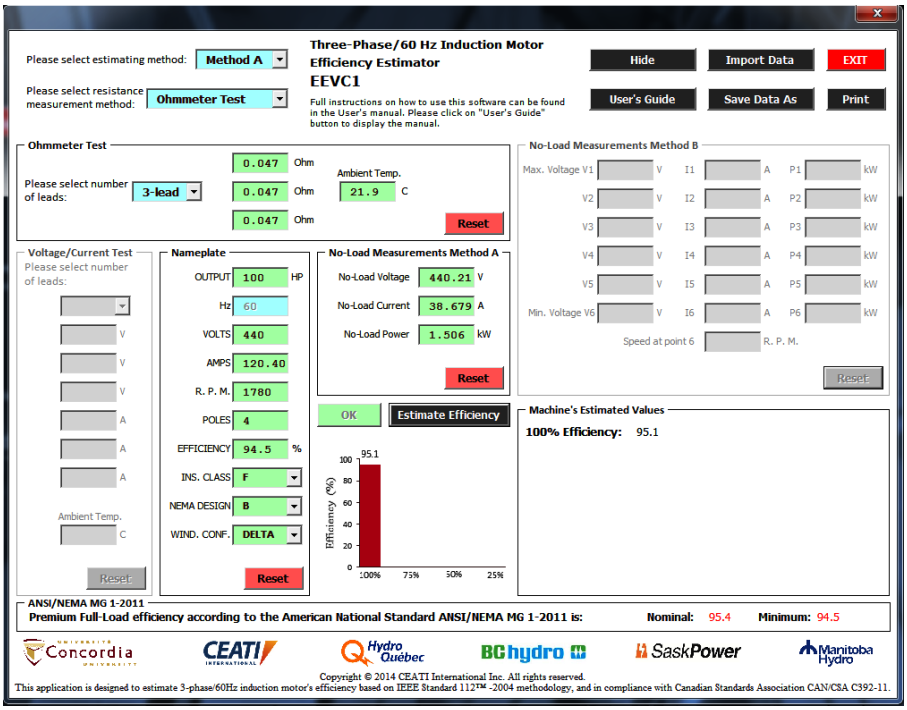

Figure 4-11. A 100 hp motor test results by using Method A.
Copyrights © CEATI International Inc.

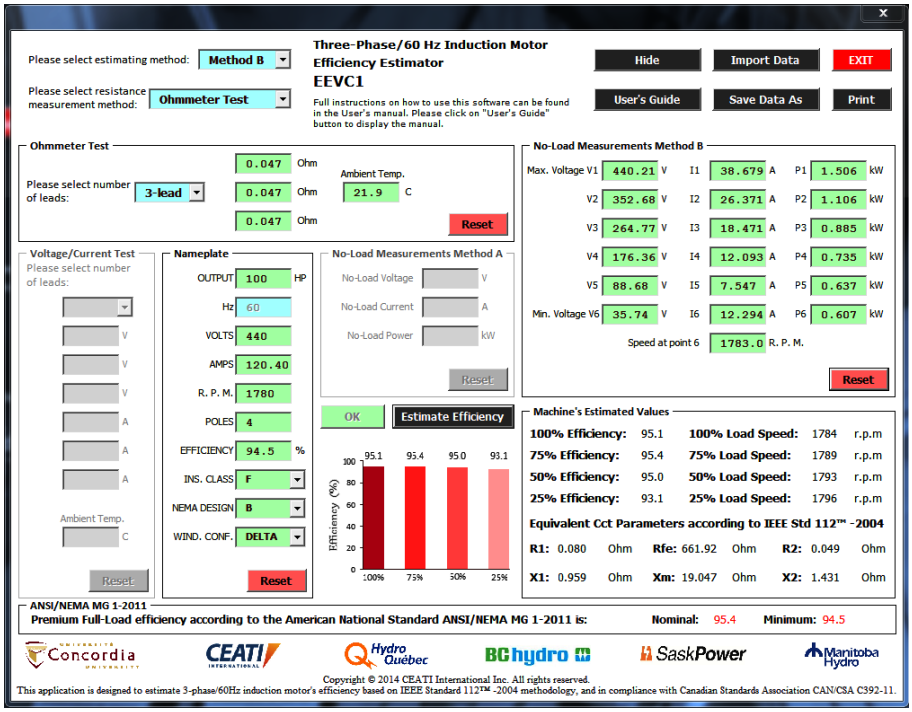

Figure 4-12. The 100 hp motor test results by using Method B.
Copyrights © CEATI International Inc.

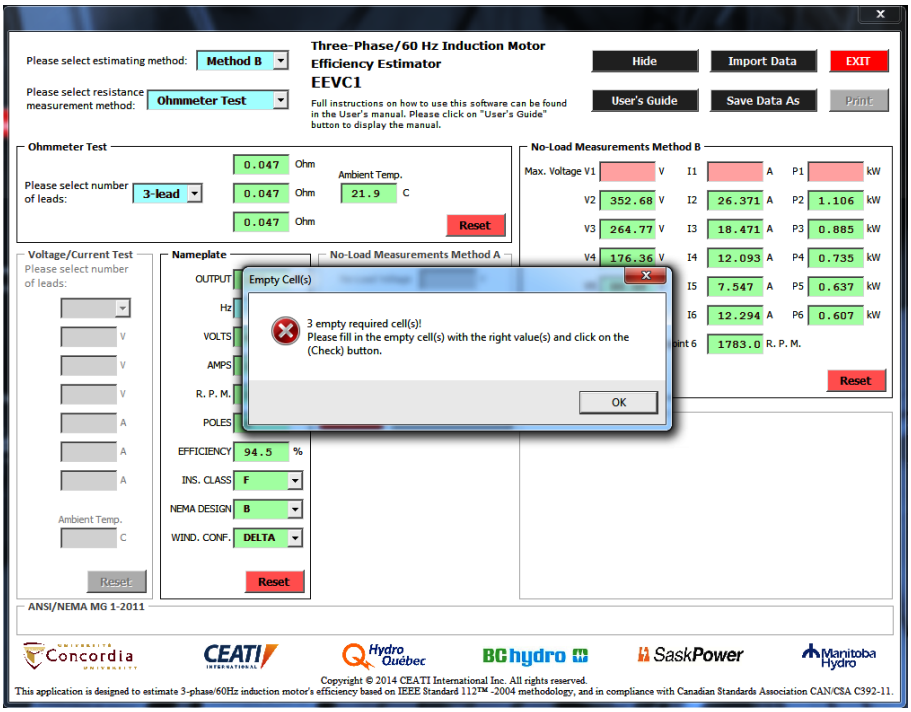

Figure 4-13. A message box triggered due to 3 empty cells.
Copyrights © CEATI International Inc.

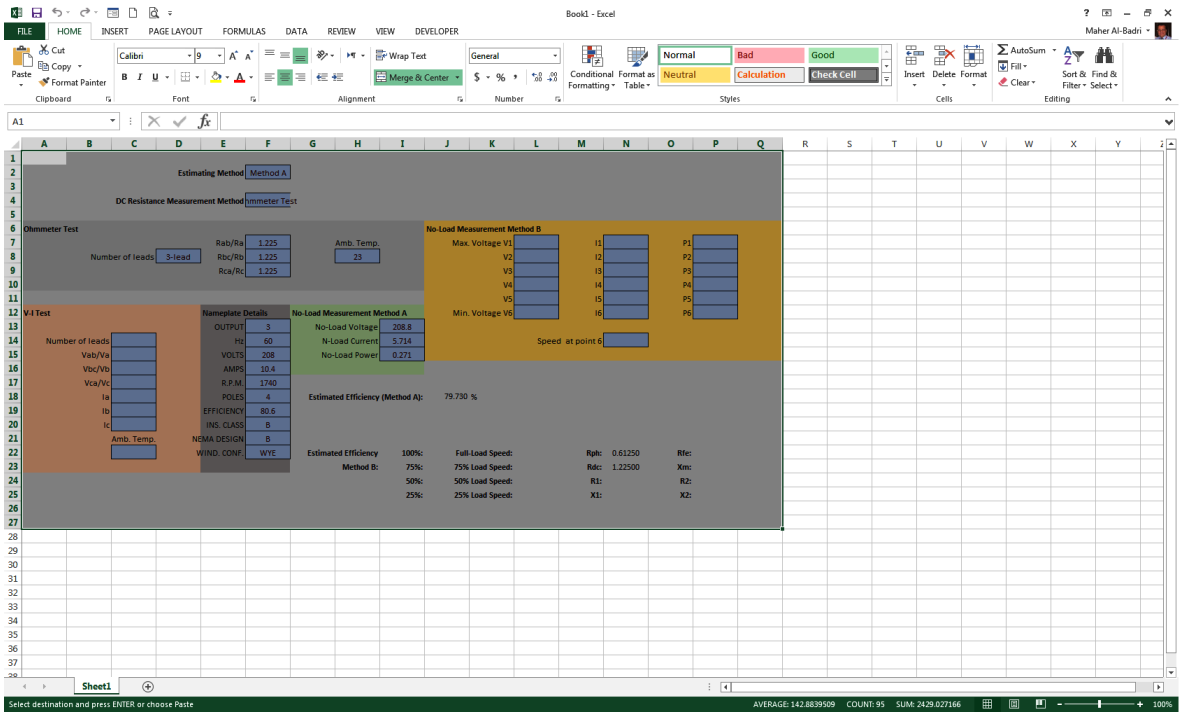

Figure 4-14. A generated test spreadsheet by the software to save a test results.
Copyrights © CEATI International Inc.

4.3. Summary

A software is developed to utilize the two proposed algorithms in chapters 2 & 3 and the supporting data. The software is aimed to be a practical industrial tool that can be used in any electric motor service center in North America. The software was under a thorough monitoring and assessing process by a technical monitors team selected by a group of Canadian Power Companies who sponsored the project. The software has come through many different stages of upgrading process by including many useful suggestions of the technical monitors. The latest version of the software comprises of 21050 coding lines. The latest version was approved by the technical monitors and it is currently a copyright of CEATI International Inc.

CHAPTER FIVE

5. A Novel In-Situ Efficiency Estimation Algorithm for Three-Phase IM Using GA, IEEE Method F1 Calculations and Pre-Tested Motor Data

The precise estimation of efficiency of induction motors is crucial in industries for energy savings, auditing, and management. This chapter presents a novel method for in situ induction motors efficiency estimation by applying the genetic algorithm and utilizing IEEE Form F2-Method F1 calculations with pretested motor data. The method requires a dc test, full-load operating point rms voltages, currents, input power, and speed measurements. The proposed algorithm uses a sensorless technique to determine motor speed. The algorithm is not only an in situ tool; it can also be used as an on-site efficiency estimation tool that might replace the expensive dynamometer procedure. The method was validated by testing 30 induction motors.

5.1. Introduction

Electrical motors below 500 hp make up 99.7% of the motors in service. These motors operate at approximately 60% of their rated load because of oversized installations or under-load conditions, and hence, they work at reduced efficiency which results in wasted energy [6] and additional cost. Motor losses can represent a considerable cost over a long period due to high load factor [7].

Power costs rise at a rate that is even faster than both material and producer good prices [8]. Many companies have hired energy managers whose sole purpose is to find practical ways to reduce power costs. These managers noticed that electric motors can present a major potential for cost reduction [9]. One approach to efficiently reduce wasted energy in the industrial sector and control the cost of the utilized power is by retrofitting standard efficient (SE) motors with energy efficient (EE) motors [3]. The Energy Act of 1992 mandates that most types of commonly used electric motors manufactured as of October 1997 or later must be energy efficient designs [12].

If a replacement decision of low efficient motor is taken as a result of calculation of energy savings and payback periods that are based on nameplate motor efficiency or manufacturer's data only, this could lead to large errors [1]. The real efficiency of a motor is

usually different from that value mentioned on its nameplate, as efficiency may decrease significantly due to aging or rewinding [17], or it might not be given according to the IEEE Std 112TM Method B [18]. To make a correct decision and select the optimal retrofit scenario, engineering staff should be able to estimate the efficiency values of the motors under test with the least possible error. This demand from industry stimulates practical work and research on the development and enhancement of techniques for induction motors efficiency estimation [1], with some of the research reported in [18], [20], and [13].

Torque and speed measurements are necessary to estimate the efficiency of an induction motor. However, when an efficiency estimation is required for a running (in-situ) induction motor which its operation is not allowed to be disturbed due to an ongoing critical industrial process, torque is not available.

Identifying the six parameters of induction motor is also a well-known procedure to estimate the efficiency. The six parameters of the per phase equivalent circuit which models the induction motor can be extracted by using the no-load/locked rotor test, or by using the IEEE Std 112 impedance test-method 3. Nevertheless, both procedures are not applicable in the above mentioned in-situ case.

In such a situation, the Genetic Algorithm (GA) is found to be one of the successful tools to identify the six parameters of the induction machine. Many research works employed the GA to estimate those parameters based on available operating data of the motor.

The GA was employed in [106] to identify induction motor parameters from load tests. The proposed algorithm needed at least two different values of slip, which means two loading points. The model used was modified by connecting the magnetizing leakage reactance X_m and the iron loss resistance R_{fe} in series. In [107], several versions of the GA were used to help find the induction motor parameters for small (5 hp), medium (50 hp) and large (500 hp) induction motors. The core loss resistance is omitted in the IM model used in this work, but the stator resistance is estimated rather than measured. A comparison of the estimated parameter values against the actual values was demonstrated. It was concluded that one of the versions gave extremely good results. The GA applicability to in-situ efficiency determination was demonstrated in [1]. Three different methods were presented in this work; Method I utilizes only full-load input parameters that are used for motor parameter determination. This method showed

around a 3% deviation from the actual efficiency. Method II needs different load points and this approach did improve the robustness of the GA, but did not lead to better results in motor parameters and efficiency. In Method III, the nameplate output power is used as an additional full-load input parameter for the GA. This approach did improve the outcome of the GA by reducing the deviation to less than 1% [1]. In [17], another in-situ IM efficiency estimation approach which employed the GA was proposed. The approach needed multiple load points to have a noticeable improvement in accuracy and repeatability. It was concluded that this method is sensitive to the number of load points and to their separation. Thermal equilibrium was needed for each load point for good estimation of the resistive components. Other research works on the GA application in induction motor parameters determination can be found in [108], [109], [110], [111] and [112].

In this chapter, a novel in-situ efficiency estimation using the GA, the IEEE Form F2-Method F1 calculations, and pre-tested motors data is proposed. The algorithm utilizes a database of a large number of induction motors tested for efficiency in the Laboratoire des Technologies de l'Énergie, Institut de Recherche, Hydro-Québec, Shawinigan, Québec, Canada. The data has a wide range of motor type and power ratings. Another valuable data set was received from BChydro, which includes a full test of 55 used (aged) induction motors. The database was used to specify the full-load temperature, the stray load loss, and the friction and windage loss. The algorithm is designed to not only be used as an in-situ tool; it is also built to be used as an on-site efficiency estimation tool that might replace the expensive dynamometer procedure. Applicability and feasibility of the method were approved by testing 30 induction motors.

5.2. The Genetic Algorithm

The GA is an optimization and search technique based on the principles of genetics and natural selection [113]. The GA is used to solve a system of nonlinear equations. It uses objective functions based on a performance criterion to calculate an error [107]. There are two versions of GA; the binary GA which represents variables as an encoded binary string, and the continuous GA which works with the continuous variables. This study adopts the continuous GA as it is faster than the binary GA because the chromosomes do not need to be decoded [113]. Figure 5-1 is an overview of the continuous GA used in this research work. The first step in the process is

building a fitness function and defining a chromosome as an array of variables. A chromosome of certain number of variables (N_{var}) can be represented as in (5.1)

$$\text{Chromosome}=[P_1, P_2, \ldots.., P_{N_{var}}] \tag{5.1}$$

where P_i is a variable.

An initial population is generated with random values of the variables, and each chromosome within the population size is checked for its fitness through the fitness function.

The algorithm assumes that the cold resistance and cold temperature of the stator winding are predetermined. The value of rotor leakage reactance X2 can be determined by identifying the value of the stator leakage reactance X1 and the NEMA design of the motor according to Table 3-I. Four parameters out of six are to be determined; the stator leakage reactance X1, the core loss resistance Rfe, the magnetizing leakage reactance Xm, and the rotor resistance R2. Those four parameters compose the four variables of each chromosome in the GA as in (5.2)

$$\text{Chromosome}=[X_1, R_{fe}, X_m, R_2\ ] \tag{5.2}$$

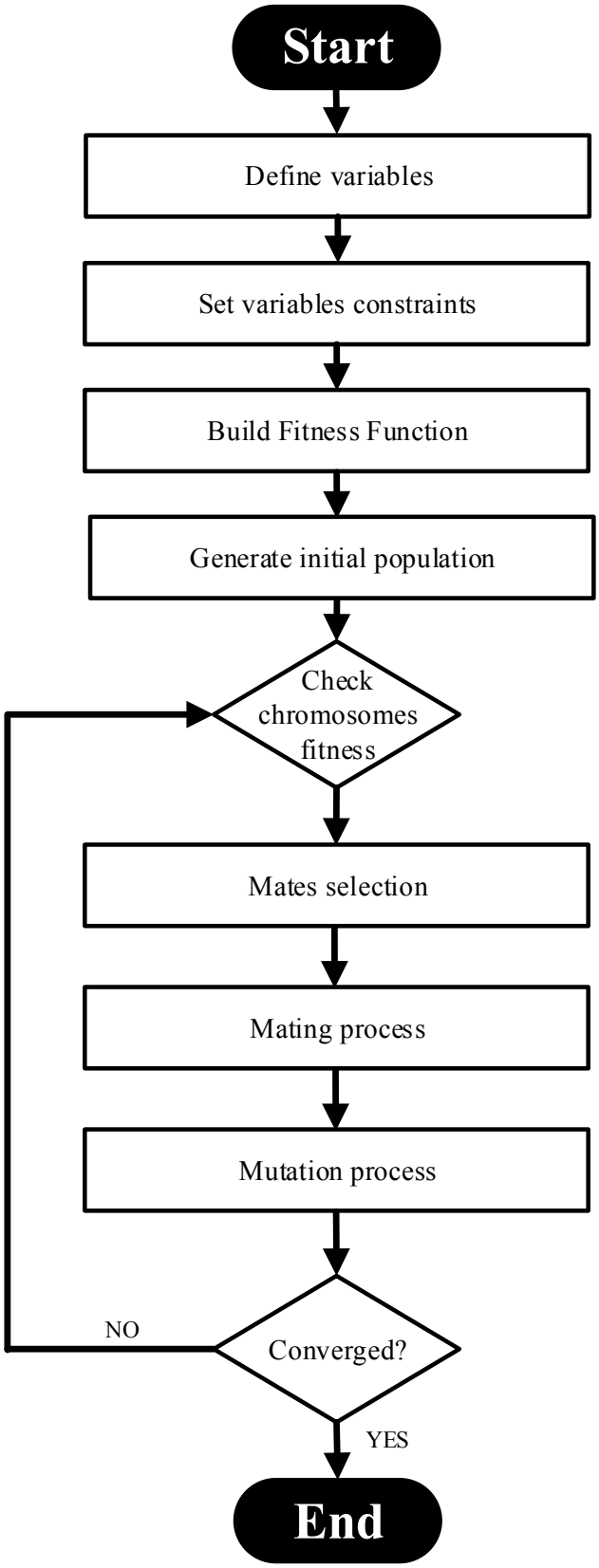

Figure 5-1. The Genetic Algorithm flow chart.

5.3. The Proposed Algorithm

A detailed flow chart of the proposed algorithm is illustrated in Figure 5-2. The algorithm starts with predetermined values of the stator winding cold resistance R_{cold} and cold temperature T_{cold}. The algorithm uses the nameplate details, full-load rms measured values for line-to-line voltage, line current, input power, and one line current signal captured by a data acquisition measuring device of at least 10 seconds length and preferably of 10 microsecond sampling time.

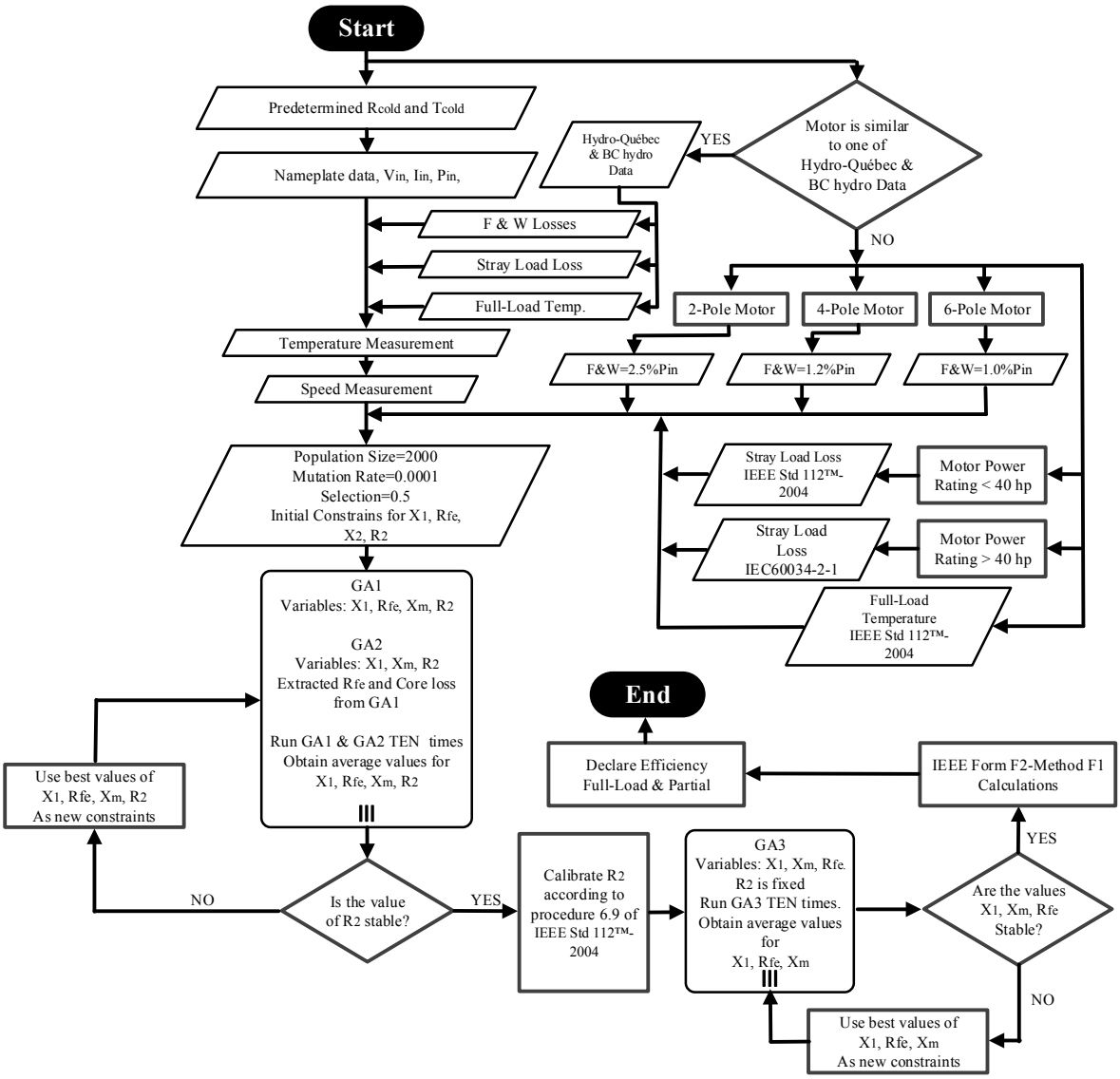

Figure 5-2. The proposed algorithm flow chart

5.3.1. Stray Load Loss, FL Temperature, and Friction & Windage Losses Determination

The values of stray load loss and full-load temperature are required by the algorithm. According to the IEEE Std 112™-2004, the stray load loss is that portion of the total loss in the electrical machine not accounted for by the sum of the friction and windage loss (F&W), the stator copper loss, the rotor copper loss and core loss. There are two ways to measure the stray load loss, indirect measurement and direct measurement. In the indirect measurement, the stray load loss is determined by measuring the total losses and subtracting from these losses the sum of the F&W, core loss, stator copper loss and rotor copper loss. The remaining value is the stray load loss. In the direct measurement of the stray load loss, the fundamental frequency and the high frequency components of the stray load loss are determined and the sum of these two components is the total stray load loss [21]. The other procedure to determine the stray load loss according to the IEEE Std 112™-2004 is to assume it. If the stray load loss is not measured, its value at rated load may be assumed to be the value as shown in Table 1-I, or it can be estimated according to the International Standard IEC 60034-2-1 [95] as in (2.6).

With the advantage of having the test data of a large number of motors that was provided by Hydro-Québec and BC hydro; a comparison was made between the measured and the assumed values of both stray load loss and full-load temperature showed that there is a wide difference between the real (measured) stray load loss and its corresponding assumed value according to the IEEE Std 112™-2004 or the IEC60034-2-1 standards. This can be clearly seen in Figure 5-3, which illustrates the results of 4 medium induction motors. Taking the 500 hp machine as an example, the IEEE standards overestimate the stray load losses by 257.83% while the IEC standards overestimate the mentioned loss by 215.78%. However, in IEC60034-2-1, it is stated in a note that the stray loss load curve generated does not represent an average value of stray load loss but an upper envelope of a large number of measured values, and in most cases it may yield greater additional load losses than the direct stray load loss measurements methods described in the standard [95]. Such a difference can significantly increase the error in the estimated efficiency and reduce the accuracy. The second factor that may significantly affect the accuracy of the estimated efficiency is the difference between the assumed and measured full-load temperature as illustrated in Figure 5-4 where it can be seen that for the 200 hp machine, the IEEE standards assumed temperature overestimates the measured value by 143.23% [90]. Hence, the advantage of the data will be utilized in enhancing the accuracy of the proposed algorithm by using the

measured values in lieu of the assumed ones whenever it is applicable.

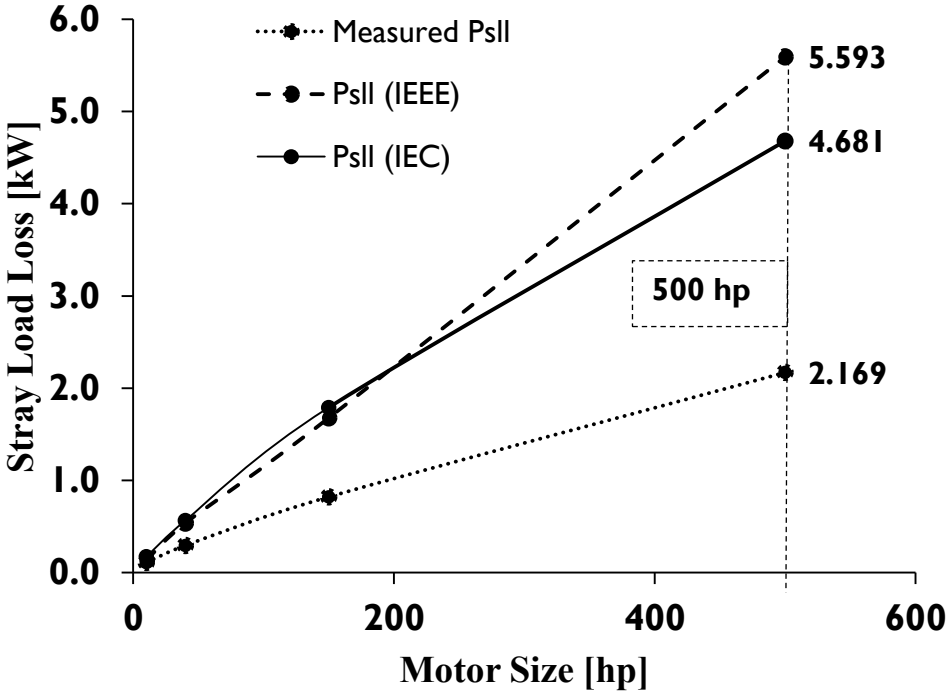

Figure 5-3. Estimated stray load loss versus measured values.
Source of measured data: Laboratoire des Technologies de l'Énergie, Institut de Recherche, Hydro-Québec.

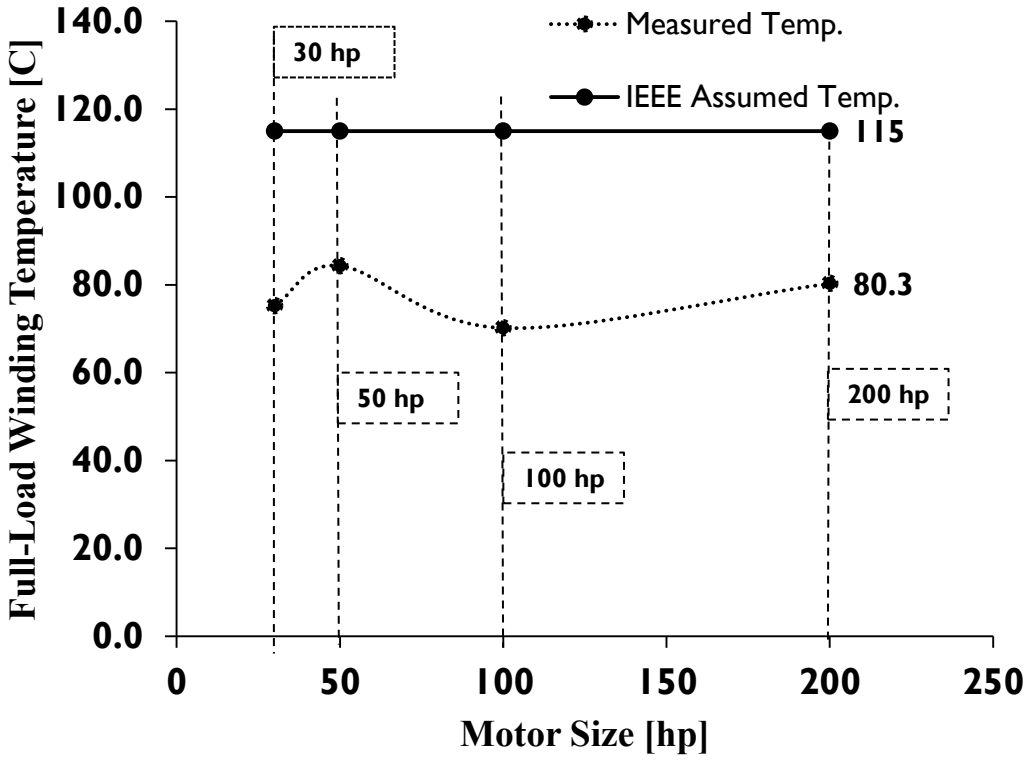

Figure 5-4. Assumed versus measured full-load temperature.
Source of measured data: Laboratoire des Technologies de l'Énergie, Institut de Recherche, Hydro-Québec.

The strategy is based on the following criteria that will be used to determine:

- friction and windage losses,
- stray load loss and
- full-load temperature.

5.3.1.1. Motor has similarity with Hydro-Québec/ BC hydro data

In this case, the algorithm will search the data using the following strategy:

- If number of poles is similar, the measured F&W will be used.
- If the rated voltage and insulation class are similar, the measured stray load loss will be used.
- If the rated voltage, number of poles, and insulation class are all similar, the

measured stray load loss will be used.

- If the number of poles and insulation class are similar, the measured full-load temperature will be used.
- If the rated voltage and insulation class are similar, the measured full-load temperature will be used.
- If the rated voltage, number of poles and insulation class are similar, the measured full-load temperature will be used.

It is important to mention that it was found that using the measured stray load loss and full-load temperature instead of the assumed values, based on only rated voltage and insulation class, will still give better efficiency estimation.

5.3.1.2. Motor has no similarity with Hydro-Québec/ BC hydro data

In this case, the algorithm will follow a different strategy as follows:

- If number of poles is 2, then the F&W will be calculated as in (5.3)

$$P_{fw}=2.5\%\times P_{in,fl} \tag{5.3}$$

- If number of poles is 4, then the F&W will be calculated as in (5.4)

$$P_{fw}=1.2\%\times P_{in,fl} \tag{5.4}$$

- If number of poles is 6, then the F&W will be calculated as in (5.5)

$$P_{fw}=1.0\%\times P_{in,fl} \tag{5.5}$$

where, P_{fw} is the friction and windage loss.

The percentage values of input power in (5.3), (5.4), and (5.5) are determined by a thorough check made on the Hydro-Québec/ BC hydro data.

- If the motor power rating is less than 40 hp, the stray load loss shall be estimated according to Table 1-I.
- If the motor power rating is larger than or equal to 40 hp, the stray load loss is

estimated according to (2.6).

The 40 hp threshold is determined by a thorough check made on the Hydro-Québec/ BC hydro data.

The full-load temperature is assumed according to Table 2-I. The data was further investigated to come out with another practical finding that is useful for identifying certain values of stray load loss of partial loads. The formulas are as previously shown in Chapter 2, subsection 2.2.1.8.

It is very important to clarify that all similarity criteria mentioned above are only considered if, and only if, the motor under test and the data motor are of the same power rating.

5.3.2. Stator Windings Temperature Measurement

Temperature measurement plays an important role in the efficiency estimation process. On-line temperature measurement applications for induction machines temperature monitoring and protection are commercially available and cost-effective. The technique is to intermittently inject a low level of dc current into the stator winding without causing unacceptable torque pulsations in the machine, and using the dc voltage and current to estimate the value of stator resistance which can reflect the value of temperature compared to the reference cold resistance R_{cold} and its associated cold temperature T_{cold}. This technique was described and validated in [114] and [115]. In this study, the values of R_{cold} and T_{cold} are assumed to be known from data sheets or tests done during motor turn off. The stator resistance is measured online and translated to temperature as in (5.6).

$$T_{hot}=\frac{K_1(R_{hot}-R_{cold})+T_{cold}R_{hot}}{R_{cold}} \tag{5.6}$$

where,

K_1 is 234.5 for 100% IACS conductivity copper;

T_{hot} is the estimated hot temperature;

R_{hot} is the measured hot resistance;

T_{cold} is the measured cold temperature;

R_{cold} is the measured cold resistance.

5.3.3. Sensorless Speed Measurement Technique

Full-load speed is a critical input that is required by the proposed algorithm. The algorithm was designed to work where the industrial process is not interrupted. Hence, a speed measurement technique that estimates the speed through the input current signal is needed and proposed. The speed estimation throughout utilizing the motor slot harmonics was the area of interest of many researchers. The following is a brief review of major research works pertaining to the sensorless speed estimation. In [116], a technique of utilizing the harmonics generated in the stator voltages of inverter fed three-phase squirrel-cage induction motors in extracting the slip frequency was proposed. The idea was based on the slot harmonics being independent of electromagnetic parameters of the motor except for a frequency of the rotating flux. The Fast Fourier Transform (FFT) technique was utilized in [117] to improve speed detection of inverter fed induction motors through the stator current signal. The method implies another algorithm to determine the number of rotor slots as a key component required by the method. The researchers claimed that the technique was successful in detecting speeds under different load conditions including load levels down to near no-load conditions and over a wide range of inverter output frequencies. In [118], an improved technique of speed measurement utilizing the motor current harmonics which arise from stator core ovality, rotor shaft misalignment, bearing wear, or rotor bar resistance variations was proposed. The technique does not require any user input. The current harmonics can be described by (5.7)

$$f_{sh}=f_1\left\{(kR+n_d)\left(\frac{1-s}{p}\right)+n_\omega\right\} \tag{5.7}$$

where,

f_{sh} is the current harmonic frequency;

f_1 is the source frequency;

k=0,1,2....; R is the number of rotor slots;

n_d=0,±1,…, is the order of rotor eccentricity;

s is per unit slip;

p is the number of pole pairs;

n_ω=±1,±3,…, is the airgap mmf harmonic order.

Results of different sampling time and frequency source were illustrated and compared against speed measurements with an optical tachometer showed maximum deviation of 4.4 rpm and minimum of 0.9 rpm. In [119], the Motor Current Signature Analysis (MCSA) was implemented in Labview. The MCSA is an electric machinery monitoring technology developed by the Oak Ridge National Laboratory (ORNL) in 1990 which is based on the recognition that a conventional electric motor can also act as an efficient and permanently connected transducer that detects small time dependent motor load variations and converts them into electric current signals that flow along the feeder cable of the motor. The current signal was acquired and fed into a demodulation process that was followed by Fast Fourier Transform (FFT) to obtain the spectrum in the frequency domain. The spectrum clearly showed the component of interest which is the motor speed. A comparison of spectrum estimation techniques for sensorless speed detection in induction machines was conducted in [120].

In this chapter, the speed detection technique is based on an adaptive notch filter algorithm which was proposed in [121], where all mathematical principles and the governing equations can be found. The advantage of this algorithm is that it does not use slots or slots harmonics, hence slots number is not required.

The block diagram of the proposed filter is shown in Figure 5-5.

The μ parameters shown in the block diagram are important to be identified according to the current drawn by the motor and shall be adjusted due to the following conditions:

$$0<\mu_1<2f_1$$

$$0<\mu_2<\left(\frac{2f_1}{A}\right)^2$$

where, A is the amplitude of the current signal.

The choice of μ_3 is interdependent on the choice of μ_2. One may choose the value of μ_3 such that the product of $\mu_2\mu_3$ becomes of the same order of magnitude as μ_1 [121]. One line current signal was obtained by a data acquisition measuring device with a sampling time of 10 microseconds, and fed to the notch filter to extract the main component. Noise filtering and the Fast Fourier Transform (FFT) were used to extract the frequency which was used to calculate the required slip according to (5.8) which is derived from (5.7) in [118]

$$f_{sh}=f_1\left(1\pm\frac{1-s}{p}\right) \tag{5.8}$$

Based on (5.8), the estimated speed will have a certain range due to the ± sign within the

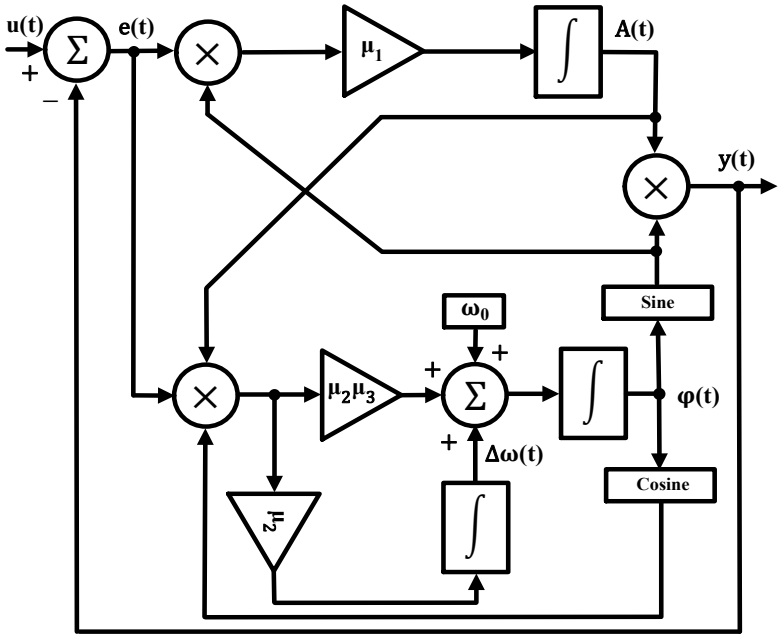

Figure 5-5. Block diagram of the notch filter [121].

equation. Figure 5-6 shows the range of the detected full-load speed of 3 hp, 208 V induction motor. The average value of 1741 and 1747 rpm was calculated to be 1744 rpm and declared as the estimated speed. The estimated speed has 1.1 rpm absolute error when compared with the 1743 rpm measured by contactless tachometer. The results of other partial loads speed of the same motor are shown in Table 5-I.

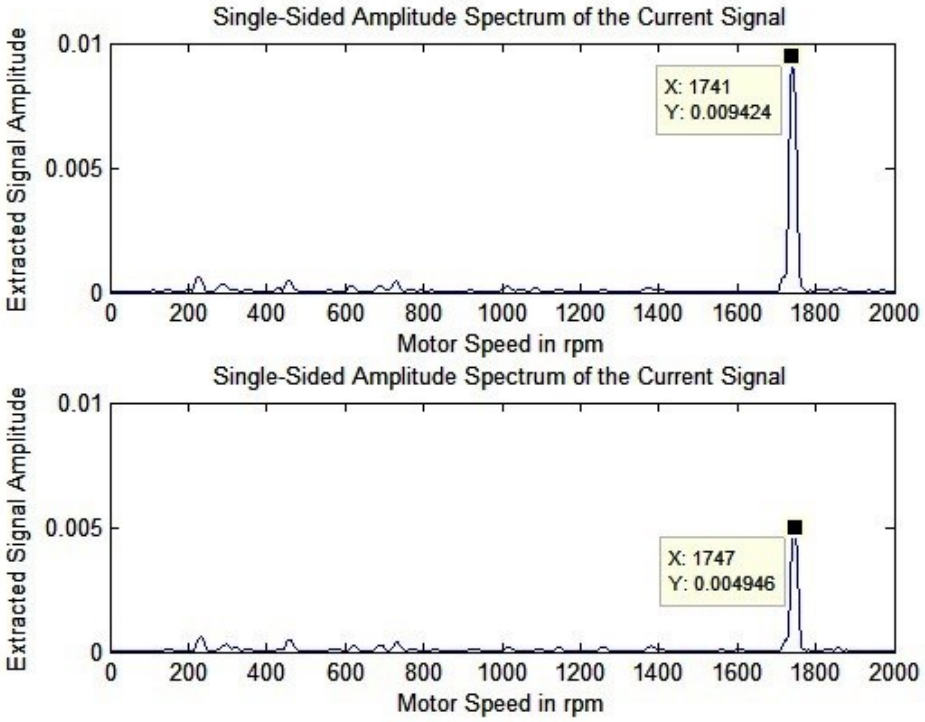

Figure 5-6. The range of estimated full-load speed of 3 hp, 208 V induction motor

Table 5-I. Estimated Against Measured Speeds

Loads [%]	Measured Speed [rpm]	Estimated Speed [rpm]
100%	1743	1744
75%	1761	1760.5
50%	1774	1774
25%	1787.5	1788

5.3.4. Extracting the Induction Motor Unknown Parameters

So far, all the required data which is needed to run the GA were collected. The task now

is to estimate the remaining unknown motor parameters, i.e. X_1, R_{fe}, X_m, and R_2 by using the GA technique. Three GAs were designed to extract the required parameters. The fitness functions of the three GAs were built based on the induction motor equivalent circuit detailed in [21] and shown in Figure 5-7.

The following equations are used in the three GA fitness functions

$$Y_m=\frac{1}{jX_m}+\frac{1}{R_{fe}} \tag{5.9}$$

$$Y_2=\frac{1}{\frac{R_2}{s}+jX_2} \tag{5.10}$$

$$Z_2=\frac{1}{Y_m+Y_2} \tag{5.11}$$

$$Z_1=R_1+jX_1 \tag{5.12}$$

$$Z=Z_1+Z_2 \tag{5.13}$$

$$I_s=\frac{V_{ph}}{Z} \tag{5.14}$$

$$I_r=I_s\left[\frac{1/(Y_m+Y_2)}{1/Y_2}\right] \tag{5.15}$$

$$I_m=I_s-I_r \tag{5.16}$$

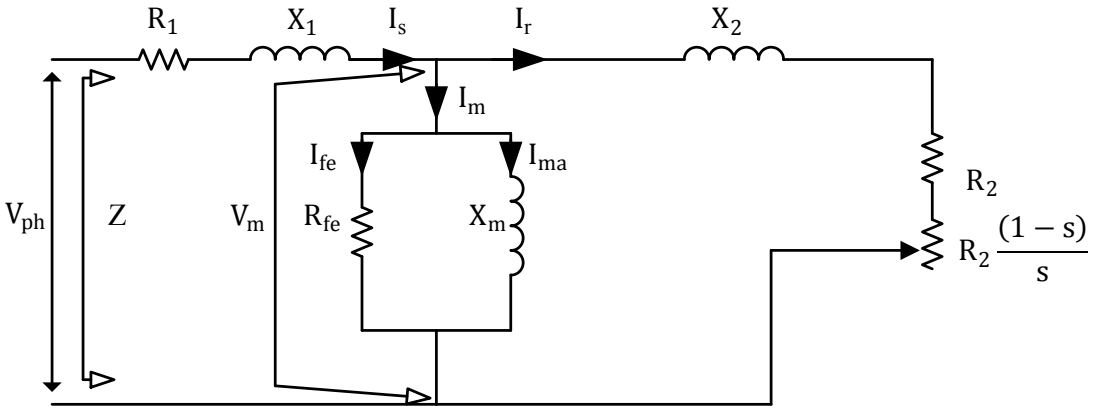

Figure 5-7. Per phase induction motor equivalent circuit

$$V_m = \frac{I_m}{Y_m} \tag{5.17}$$

where,

Y_m is per phase admittance of the magnetizing branch;

X_m is per phase leakage reactance of the magnetizing branch;

R_{fe} is per phase iron loss resistance;

Y_2 is per phase admittance of the rotor;

R_2 is per phase rotor resistance;

X_2 is per phase rotor leakage reactance;

s is the slip;

Z_2 is per phase impedance of both the rotor and the magnetizing branches;

Z_1 is per phase stator impedance;

R_1 is per phase stator resistance;

Z is per phase total impedance;

V_{ph} is phase voltage;

I_s is per phase stator current;

I_r is per phase rotor current;

I_m is per phase total magnetizing current;

V_m is per phase magnetizing voltage.

The stator and rotor resistances shall be corrected to the full-load temperature T_{fl} according to (5.18) and (5.19)

$$R_{1,corr} = \frac{R_1(T_{fl}+K_1)}{T_{cold}+K_1} \tag{5.18}$$

$$R_{2,corr} = \frac{R_2(T_{fl}+K_2)}{T_{cold}+K_2} \tag{5.19}$$

The total core loss, stator copper loss, and rotor copper loss will be estimated as in (5.20), (5.21) and (5.22) respectively

$$P_h = 3\frac{V_m^2}{R_{fe}} \tag{5.20}$$

$$P_{scl}=3I_s^2R_{1,corr} \tag{5.21}$$

$$P_{rcl}=3I_r^2R_{2,corr} \tag{5.22}$$

where,

P_h is total core loss;

P_{scl} is total stator copper loss;

P_{rcl} is total rotor copper loss.

Total losses will be determined by (5.23)

$$P_{total}=P_h+P_{scl}+P_{rcl}+P_{fw}+P_{sll} \tag{5.23}$$

where,

P_{total} is the total losses;

P_{fw} is the friction & windage losses.

The output power can be estimated by using (5.24)

$$P_{out}=P_{in,fl}-P_{total} \tag{5.24}$$

where,

P_{out} is the output power;

$P_{in,fl}$ is the measured input power.

The input power will be estimated according to (5.25)

$$P_{in,\,calc}=3real(V_{ph}I_s^*) \tag{5.25}$$

where,

$P_{in,\,calc}$ is the calculated input power;

I_s^* is the conjugate of the stator phase current.

The three GAs have the same error functions as described in (5.26), (5.27), (5.28), (5.29) and (5.30)

$$f_1=\frac{real(I_{sm})-real(I_s)}{real(I_{sm})} \tag{5.26}$$

$$f_2=\frac{\text{imag}(I_{sm})-\text{imag}(I_s)}{\text{imag}(I_{sm})} \tag{5.27}$$

$$f_3=\frac{P_{in,\,fl}-P_{in,\,calc}}{P_{in,\,fl}} \tag{5.28}$$

$$f_4=\frac{\theta_1-\theta_2}{\theta_1} \tag{5.29}$$

$$f_5=\frac{P-P_{out}}{P} \tag{5.30}$$

where,

I_{sm} is the measured per phase stator current;

θ_1 is the measured phase angle of the input current;

θ_2 is the per phase impedance phase angle;

P is nameplate power.

The fitness function which has the maximum value of 1 is as in (5.31)

$$ff=\frac{1}{1+\sum_{i=1}^{5} f_i} \tag{5.31}$$

The three GAs are run in the following sequence and certain observations should be done carefully to guarantee best results of the algorithm. In GA1, the core loss will be approximated by using (5.32)

$$P_{h,\,calc}=P_{in,\,fl}-P-P_{scl}-P_{rcl}-P_{fw}-P_{sll} \tag{5.32}$$

The approximated core loss $P_{h,\,calc}$ is compared against the total core loss P_h of (5.20). This comparison is utilized to adjust the constraints of R_{fe}. The values of both R_{fe} and P_h from GA1 are used as fixed values in GA2. This makes R_2 converge to a stable value. Hence, GA2 works with only three variables (i.e. X_1, X_m, and R_2). The values of the 4 variables of 10 consecutive runs of both GA1 and GA2 are tabulated and values of best fitness are used as new constraints for both GA1 and GA2. A new round of 10 runs follows, and this process iterates until a stable value of R_2 is achieved.

Figure 5-8 shows that the GA can reach a stable fitness value after about the 50^{th} generation.

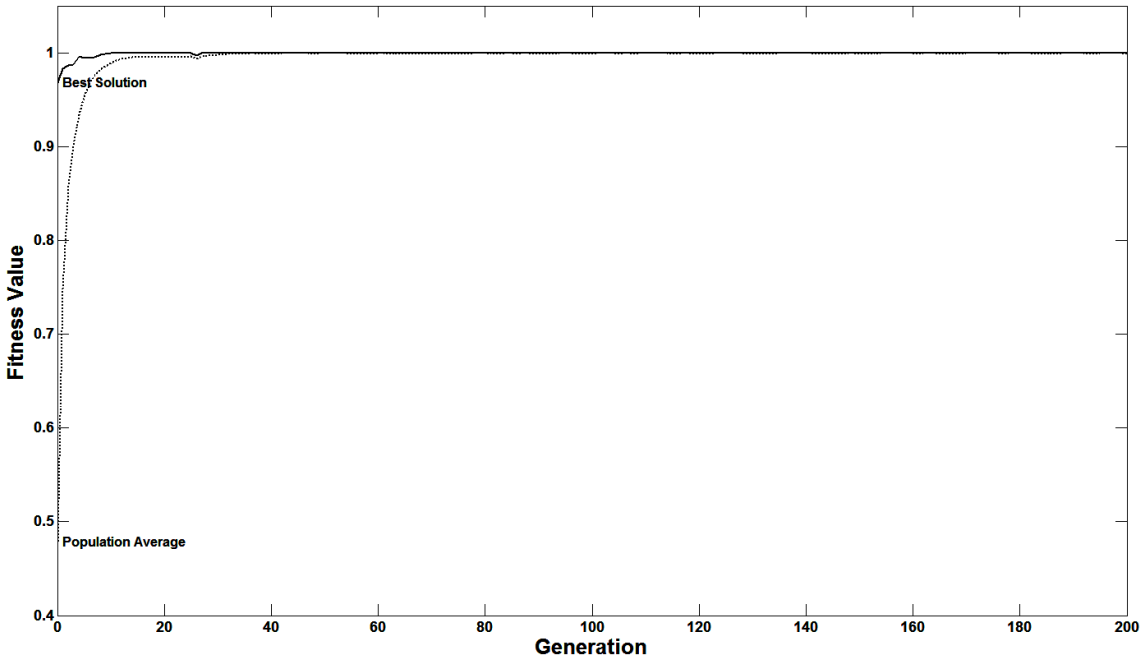

Figure 5-8. Fitness of the objective function

5.3.5. Rotor Resistance Calibration

As input power is primarily a function of R_2/s , the value of R_2 shall be calibrated according to the IEEE Std 112™-2004 procedure described in section 6.9 of the standard. An iteration process shall start with an assumed value of R_2/s. The value of R_2/s is adjusted for each iteration until the calculated value of input power P_s and input current I_1 both agree with the measured values of input current and input power within 1%.

The value of R_2 is then transferred and fixed in GA3. This makes other variables reach stable values. Hence, GA3 also has 3 variables (i.e. X_1, X_m, and R_{fe}). GA3 will run, and the best values of the three variables after each 10 runs will be used as new constraints until stable values are achieved and the 4 parameters of the induction machine are declared. R_1 is already known, and X_2 will be determined based on Table 2-I.

5.3.6. IEEE Form F2-Method F1 for Full-Load and Partial Load Efficiency Estimation

The six motor parameters are used to estimate the full-load and other partial loads by using the IEEE Form F2-Method F1 calculations [21]. The value of stray load loss for 75%, 50% and 25% loads are as proposed in (2.7) - (2.9) respectively.

5.4. Experimental Results and Analysis

A 3.0 hp induction machine with a nameplate as detailed in Table 5-II was tested using the proposed algorithm. The test was conducted by using a programmable power supply, a 13 kW dynamometer driven by a field control unit and supplied with a torque transducer, a multi-channel signal conditioner, and high resolution digital dc voltmeter which is used to display the dc analog output of the multi-channel signal conditioner which corresponds to the value of the applied torque. The dynamometer load is a resistor bank. The DC test was performed on the machine and the stator cold resistance and cold temperature were measured and recorded. The motor was run for 8 hours to reach its temperature stability. The hot temperature was measured by using the resistance procedure. One line current signal was needed to be acquired by using a data acquisition device to be used in the speed detection technique. The speed was also measured by using a contactless tachometer just for evaluation purpose. Table 5-III shows the machine measured efficiencies and their corresponding speeds. The data was transferred to the designed algorithm and the six parameters were extracted and tabulated in Table 5-IV. Those parameters were used in IEEE Form 2-Method F1 calculations, and the full-load efficiency and other partial loads efficiencies were declared as shown in Table 5-V. It can be noticed from Table 5-V that the full-load and partial loads speeds can be also estimated by using IEEE Form 2-Method F1. The table also shows the absolute errors of both efficiency and speed compared with the results of Table 5-IV.

5.5. Algorithm Validation (30 Motors Tested)

The proposed algorithm is applied in testing 30 induction motors of different kinds and power ratings. All motors are of 60 Hz rated frequency. All values of stray load loss and full-load temperature used in testing the 30 machines are the measured values obtained from the

supporting data associated to the algorithm.

Figure 5-9 shows the experimental setup of testing 3.0 hp machine in Dr. P. D. Ziogas Laboratory of Concordia University.

The results are tabulated and shown in Table 5-VI. The proposed algorithm shows an acceptable level of accuracy when the estimated efficiencies are compared to their associated measured values.

The other factor which is important in the validation process of the proposed algorithm is the level of consistency of the extracted parameters with terminal voltage and current measurements. To demonstrate this consistency, 17 out of the 30 tested motor are selected. The proposed method is used to extract the parameters of each induction motor. The parameters are used in the IEEE per phase equivalent circuit of Figure 5-7. The measured per phase voltage is applied to the circuit, and the input current is calculated. The results are shown in Table 5-VII.

Table 5-II. Nameplate Details of 3 hp Motor

Hp	**VOLTS**	**AMPS**	**RPM**
3	208	10.3	1740
POLES	**EFF.**	**INS.**	**DESIGN**
4	80.6	B	B

Table 5-III. 3 hp Measured Efficiencies and Speeds

Load [%]	**Speed [rpm]**	**Efficiency [%]**
100%	1743	80.1
75%	1761	79.8
50%	1774	77.1
25%	1787	65.0

Table 5-IV. Six Parameters of the Tested Motor

R_1	X_1	R_{fe}	X_m	X_1	R_2
0.81167	0.21068	253.826	18.3924	0.31445	0.49923

Table 5-V. 3 hp Estimated Efficiencies and Speeds

Load [%]	**Speed [rpm]**	**Error [rpm]**	**Efficiency [%]**	**Error [%]**
100%	1744	1	80.7	0.6
75%	1759	2	79.8	0.0
50%	1773	2	76.2	0.9
25%	1786	1	65.4	0.4

The percentage of deviation of the calculated current from the measured value is presented in the table. It can be seen that the highest error (deviation) is with motor number 22 (i.e. 125 hp) where the error is found to be 4.19%. As per the table of accuracy in Table 5-VI, the percentage error of the estimated full-load efficiency of the motor number 22 is 0.3%, which is within the acceptable range of error. It means that even with high deviation of calculated input current compared to the measured value, the percentage error of the estimated efficiency is still within the acceptable level.

This validation gives credibility to the proposed tool and demonstrates the level of confidence in the capability of the tool in estimating induction machine efficiency without the presence of the measured value. It also gives credits to the applicability of the tool in industry.

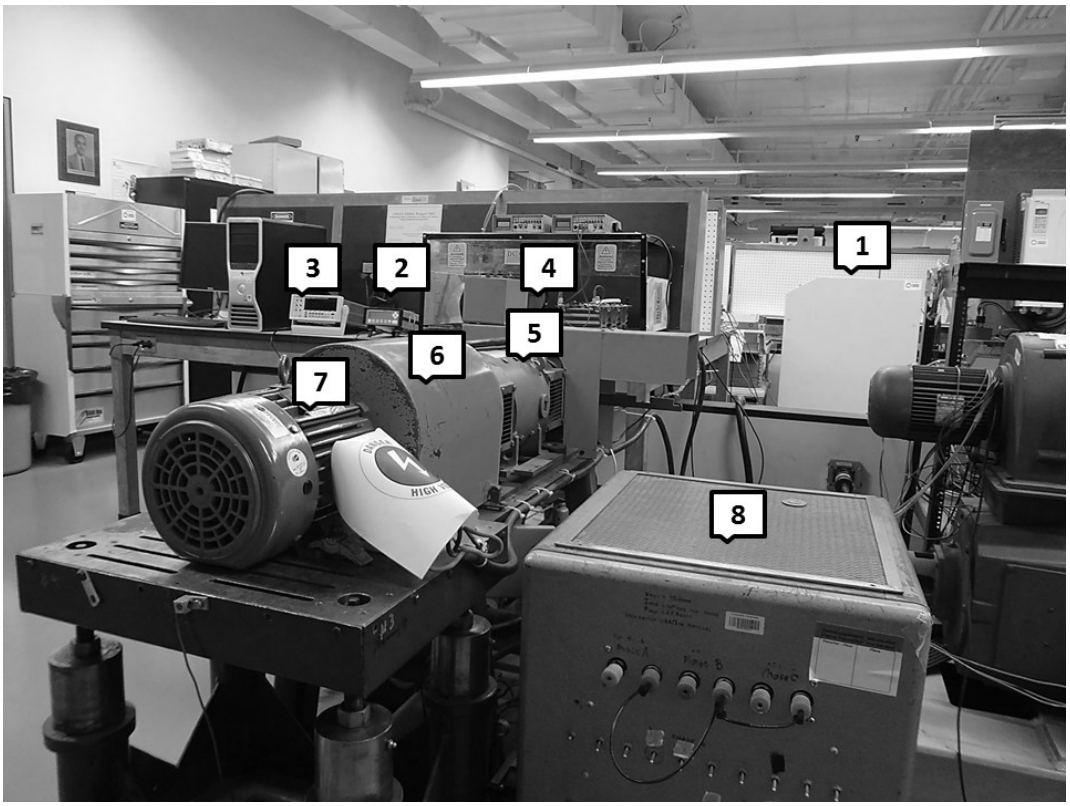

Figure 5-9. The experimental setup for testing 3.0 hp induction motor: 1, programmable power supply; 2, multi-channel signal conditioner; 3, high-resolution dc voltmeter; 4, field control unit; 5, 13 kW dynamometer; 6, torque transducer; 7, 3.0 hp IM; 8, resistor bank.
Photo is a courtesy of Concordia University.

Table 5-VI. Measured versus Estimated Efficiency of 30 Induction Motors

No.	Nameplate						Measured Efficiency				Estimated Efficiency				Absolute Error			
	VOLTS	HP	AMPS	RPM	DESIGN	INS	100%	75%	50%	25%	100%	75%	50%	25%	100%	75%	50%	25%
1	460	1	1.4	1745	B	F	84.4	83.6	80.3	68.0	84.7	83.8	79.5	67.1	0.3	0.2	0.7	0.9
2	460	1	1.5	1740	B	F	84.4	83.8	80.8	70.4	84.8	83.9	80.5	70.7	0.4	0.1	0.4	0.3
3	575	1	1.2	1720	B	F	81.9	81.5	78.2	66.7	82.8	81.6	77.7	66.3	0.9	0.1	0.6	0.4
4	575	1	1.1	1745	B	F	84.7	84.4	82.1	72.8	84.9	84.1	81.0	71.0	0.2	0.3	1.1	1.8
5	575	1	1.1	1745	B	F	84.8	84.5	81.7	72.6	85.2	84.5	81.6	72.0	0.3	0.0	0.1	0.6
6	575	1	1.2	1750	B	F	86.6	87.1	85.8	77.3	87.6	87.5	85.5	77.3	1.0	0.4	0.3	0.0
7	575	1	1.2	1745	B	F	83.2	82.6	79.3	67.5	83.8	82.7	78.6	66.3	0.5	0.1	0.7	1.2
8	575	1.5	1.6	1725	B	F	82.1	82.4	80.5	71.5	82.9	82.7	79.8	69.7	0.8	0.3	0.7	1.9
9	460	2	3	1180	B	F	87.3	87.1	84.9	76.8	87.9	86.5	82.6	72.5	0.6	0.5	2.3	4.2
10	460	2	2.5	3490	B	F	88.3	88.0	85.9	82.5	88.8	88.4	86.0	82.8	0.5	0.4	0.1	0.3
11	208	3	10	1740	B	B	80.1	79.8	77.1	65.0	80.7	80.0	76.4	65.7	0.6	0.2	0.7	0.7
12	460	5	6.5	1750	B	F	88.9	90.0	89.9	86.1	89.2	89.5	88.4	83.3	0.3	0.5	1.5	2.8
13	460	7.5	8.9	1755	B	B	91.0	91.7	91.4	87.8	90.3	91.4	91.4	88.3	0.7	0.3	0.0	0.5
14	575	7.5	6.9	3545	B	F	89.4	88.9	86.7	79.0	89.3	88.4	85.5	76.3	0.1	0.5	1.2	2.7
15	460	10	12	1745	B	F	90.1	90.9	90.8	87.7	90.4	90.8	90.0	85.6	0.3	0.1	0.8	2.1
16	575	15	16	1760	B	F	91.6	92.2	92.0	88.8	91.9	92.4	91.5	87.0	0.3	0.2	0.5	1.8
17	460	20	25	1175	B	F	91.2	92.1	92.0	89.2	91.6	92.2	91.3	87.8	0.4	0.1	0.7	1.4
18	460	50	58	1770	B	F	94.4	94.9	94.9	93.1	94.8	95.3	95.1	92.7	0.5	0.4	0.1	0.3
19	460	60	70	1780	B	F	92.5	93.0	92.7	89.3	93.0	93.3	92.4	88.3	0.5	0.3	0.3	1.0
20	460	75	82	3580	A	F	94.3	94.2	93.3	89.2	94.5	94.3	92.9	88.3	0.1	0.0	0.3	0.9
21	575	100	93	1770	B	F	93.6	93.7	92.9	89.0	93.6	93.3	92.0	88.2	0.1	0.4	0.9	0.8
22	575	125	107	1785	B	F	94.4	94.8	94.5	92.0	94.7	95.0	94.2	92.0	0.3	0.2	0.3	0.1
23	575	150	132	1785	B	F	95.7	96.0	95.8	94.0	96.0	96.2	95.9	94.2	0.4	0.2	0.0	0.2
24	460	200	235	1790	B	F	95.2	95.0	93.9	89.9	95.8	95.7	94.8	91.4	0.6	0.7	0.9	1.5
25	460	250	284	1785	B	F	95.1	95.3	94.8	92.3	95.3	95.4	94.5	93.1	0.2	0.1	0.3	0.8
26	460	300	329	1785	B	F	95.4	95.7	95.5	93.4	95.6	95.9	95.6	92.4	0.3	0.2	0.0	1.0
27	460	350	402	1790	B	F	94.9	94.8	93.9	89.9	95.1	95.0	94.2	90.7	0.2	0.2	0.3	0.8
28	575	400	353	1788	B	F	95.0	95.0	94.4	91.3	95.2	95.2	94.2	90.6	0.2	0.2	0.2	0.7
29	575	500	446	1789	B	F	96.6	96.6	95.9	93.0	96.8	96.6	96.2	93.5	0.2	0.0	0.2	0.5
30	575	500	465	1185	B	F	94.7	94.8	94.2	91.1	94.8	94.8	93.7	91.2	0.0	0.0	0.5	0.1

Table 5-VII. Measured versus Calculated Input Full-Load Currents

No.	Nameplate						Measured Full-Load Current (A)	Calculated Full-Load Current (A)	Error (%)
	VOLTS	HP	AMPS	RPM	DESIGN	INS			
1	460	1	1.4	1745	B	F	1.504	1.543	2.60
2	460	1	1.5	1740	B	F	1.450	1.470	1.33
3	575	1	1.2	1720	B	F	1.186	1.201	1.22
4	575	1	1.1	1745	B	F	1.208	1.197	0.88
11	208	3	10	1740	B	B	9.834	9.802	0.32
14	575	7.5	6.9	3545	B	F	7.176	7.065	1.54
16	575	15	16	1760	B	F	15.460	15.194	1.72
17	460	20	25	1175	B	F	24.449	24.263	0.76
18	460	50	58	1770	B	F	55.835	56.454	1.11
19	460	60	70	1780	B	F	70.243	70.868	0.89
20	460	75	82	3580	A	F	84.708	86.614	2.25
21	575	100	93	1770	B	F	92.233	91.672	0.61
22	575	125	107	1785	B	F	111.008	115.660	4.19
23	575	150	132	1785	B	F	134.669	137.094	1.80
25	460	250	284	1785	B	F	281.539	288.071	2.32
26	460	300	329	1785	B	F	326.995	338.358	3.48
30	575	500	465	1185	B	F	462.953	467.838	1.06

5.6. Summary

In this chapter, a novel algorithm for in-situ induction motor efficiency estimation by using a combination of GA procedures and the IEEE Form 2-Method F1 calculations is proposed. It was shown that using the assumed values of stray load loss and hot temperature can significantly increase the error and reduce the accuracy of the estimated efficiency. Hence, the algorithm was designed to utilize test data of large number of induction motors provided by Hydro-Québec and BC hydro. The algorithm uses the measured stray load loss and hot temperature. The algorithm requires only one load point which is full-load with its corresponding rms values of voltage, current, and power obtained at the motor terminals.

The genetic algorithm is briefly introduced in subsection 5.2.

A detailed flow chart of the proposed algorithm is presented in subsection 5.3.

The impact of using the assumed values of stray load loss and full-load temperature instead of the measured values and the strategy of assigning these values are illustrated in subsection 5.3.1.

Novel formulas of estimation the friction and windage losses are presented in subsection 5.3.1.2.

The speed estimation technique that is detailed in subsection 5.3.3 which is used in the proposed algorithm needs the current signal acquisition of only one line.

The algorithm is extensively evaluated and assessed by testing 30 induction motors of different kinds and power ratings. The results are presented in subsection 5.5. and showed an acceptable level of accuracy.

The algorithm is not only deemed an in-situ efficiency determination tool; it can also be used as a promising tool for on-site efficiency estimation that might eliminate the need to the costly dynamometer procedure.

CHAPTER SIX

6. A Novel Full-Load Efficiency Estimation Technique for Induction Motors Operating with Unbalanced Voltages

This chapter presents a novel algorithm for in situ full-load efficiency estimation of induction motors operating with unbalanced voltages. The goal of this research work is to design a reliable in situ efficiency estimation tool that can be used in industry to not only estimate induction motors efficiency, but also to help derate induction motors operating with unbalanced voltages. The proposed technique utilizes the genetic algorithm, IEEE Form F2-Method F1 calculations and pre-tested motor data. The method requires a DC test, full-load rms voltages, currents, input power and speed measurement. The proposed algorithm uses a sensorless on-line speed measurement technique. The algorithm is evaluated by testing two induction motors with different voltage unbalance conditions. The results show acceptable accuracy. The repeatability of the algorithm is assessed. The usability of the algorithm with balanced voltages is also evaluated.

6.1. Introduction

Induction motors are designed to operate with balanced voltages. Voltage unbalance increases rotor losses which results in stator and rotor temperature rises that can cause serious ill effects on the three-phase induction motors, such as, reduction in output torque, vibration and overheating that lead to a reduction on insulation life of the machine [35]. IEEE attributes the excessive temperatures in parts of the rotor of induction motors to the excessive unbalanced negative sequence currents [37]. The fact that there are only sporadic reports of motor failures due to voltage unbalance is because many motors operating in the industry are less than fully loaded, and this can provide the needed thermal margin which will allow those motors to operate with a voltage unbalance condition without failure [38]. The voltage unbalance can exist by unsymmetrical transformer windings or transmission impedances, unbalanced loads, large single-phase loads [39], incomplete transposition of transmission lines, open delta transformer connections [78], blown fuses on three-phase capacitor bank, operation of single-phase loads at

different times, or defective transformers in power systems.

Induction motors are always prone to stresses due to voltage unbalance as there is no power supply that can be perfectly balanced. In power systems which supply large single-phase loads, the level of unbalance can be considerably large [36]. According to ANSI/NEMA MG 1-2011, it is not recommended to operate induction motors with voltage unbalance above 5% [15]. The severe effect of voltage unbalance on the performance of the induction motors was the area of interest of many researchers since 1930's of the last century [45] where there was a trial to analyze the performance of three-phase induction motor operating under unbalanced voltages by using the equivalent circuit and the symmetrical component. In the 1950's, some other useful approaches to the same issue were presented [46] [47] [48] [49]. In [50], it was concluded that the temperature rise above balanced operating temperature is due to an increase in copper loss. It was demonstrated that the negative sequence current has the worst effect in terms of heating the motor, rather than an equal value of positive sequence and that is due to the low negative sequence rotor resistance. It was noticed that core loss and friction and windage losses remain essentially independent of unbalance of negative sequence voltage that is less than 15%. It was also observed that negative sequence components cause vibration that may be injurious to bearings, to insulation, and to interconnecting mechanical parts of the machine. Important studies was conducted in [51] where three 5 hp, 220 volts, 1800 rpm, and of NEMA design type B, from different manufacturers were tested for temperature rise. To derate the machines, they were run under fixed unbalance and different loads. Two different methods were used to measure the winding temperature: (a) Change in winding resistance, and (b) thermocouples. The exact temperature at shut-off was extrapolated by having many resistance measurements for different elapsed time readings. 14 thermocouples were used to determine the hot spots. The negative sequence voltage was the main parameter that was used to derate the three motors. This study concluded that there is a need for a severe reduction in the rating of induction motors when operated with unbalanced line voltages. Important curves were produced in [34] which show the relationship between the percentage of voltage unbalance and the percentage of increase of motor losses and motor heating. In [52], a useful study stated that "*It is not sufficient to merely know the percent voltage unbalance, but it is equally important to know how they are unbalanced*". In this study, a detailed mathematical technique to analyze the performance of an induction motor under unbalanced voltages was presented. The proposed technique shortened the conventional

mathematical equations needed to achieve the same performance analysis on the machine. The study concluded that, besides what mentioned above of the importance of knowing the manner of the unbalanced voltages and its marked effect on the increase in losses, the rotor losses increase at a faster rate than the stator losses as the voltages become more unbalanced. The analysis included only the magnitude of the positive and negative sequence voltages without considering the effect of the angle on the performance of the machines.

The Genetic Algorithm (GA) is an evolutionary procedure that is successfully employed in studying the performance of induction motors. The GA is a very practical tool in on-line induction motor efficiency estimation. It is used to identify the electrical parameters of the machine which is an important requirement to accurately estimate the efficiency. The application of the GA in evaluating the performance of induction motors is presented and validated in many research works [1], [41], and [104]-[110].

In this chapter, a novel technique for in situ efficiency estimation of three-phase induction motors operating with unbalanced voltages, utilizing the GA, IEEE Form F2-Method F1 calculations and pre-tested motors data is proposed. The algorithm utilizes a database of large number of induction motors tested for efficiency in the Laboratoire des Technologies de l'Énergie, Institut de Recherche, Hydro-Québec, Shawinigan, Québec, Canada. The data has a wide range of motor type and power ratings. Another set of data was received from BC hydro which includes a full test of 55 used (aged) induction motors. The database is utilized to specify the stray load loss and the friction and windage loss for induction motors that have similarities with the motors within the data. Applicability and feasibility of the method are approved by testing 2 induction motors under different levels of voltage unbalance. The repeatability of the algorithm is assessed. The usability of the algorithm with balanced voltages is also evaluated.

6.2. The Proposed Algorithm

The proposed algorithm utilizes the Genetic Algorithm (GA) which was introduced and discussed in Chapter 5. The proposed algorithm assumes that the cold resistance and cold temperature of the stator winding of the induction motor under test are predetermined from data sheets or during a turn off. The value of rotor leakage reactance X_2 can be determined by identifying the value of the stator leakage reactance X_1 and the NEMA design of the motor

according to Table I. Four parameters out of six are to be identified; the stator leakage reactance X_1, the core loss resistance R_{fe}, the magnetizing leakage reactance X_m, and the rotor resistance R_2. Those four parameters represent the four variables of each chromosome in the GA as in (6.1)

$$\text{Chromosome}=[X_1, R_{fe}, X_m, R_2] \tag{6.1}$$

A flow chart that fully pictures the proposed algorithm is illustrated in Figure 6-1. The first input to the algorithm is the predetermined values of the stator winding cold resistance R_{cold}, and cold temperature T_{cold}. Then, the algorithm is fed with the nameplate details, full-load rms measured values for three line-to-line voltages, three line currents, total input power and one line current signal acquired by data logging device of at least 10 seconds length and preferably of 10 microsecond sampling time.

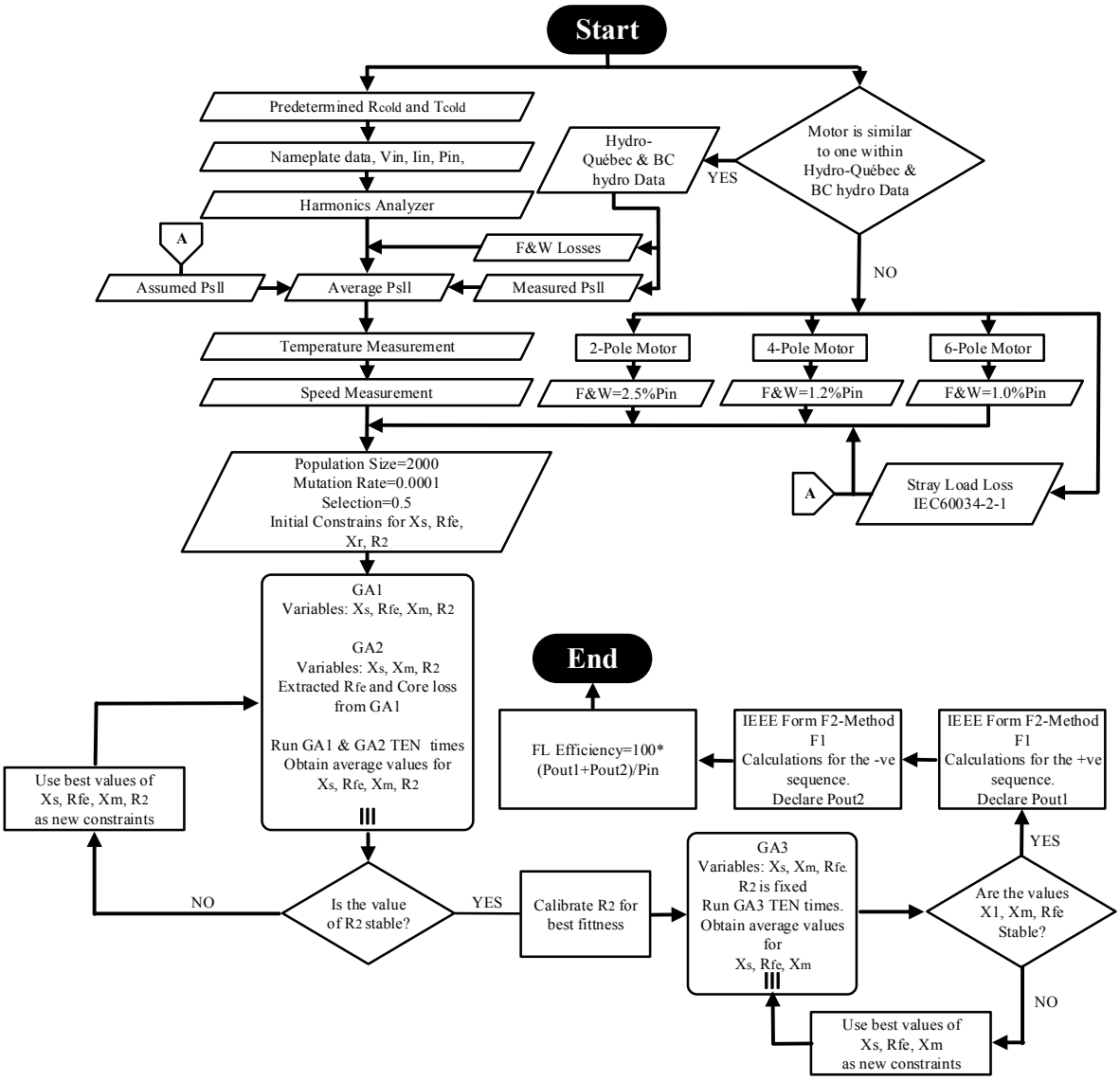

Figure 6-1. The proposed algorithm flow chart

6.2.1. Determination of Full-Load Stray Load Loss and Friction and Windage Losses

The stray load loss determination plays an important role in the precise evaluation of the motor efficiency. In [122], IEEE 112-B was considered the most suitable standard for the stray-load loss measurements and both IEC 34-2 and JEC 37 overestimate the motor efficiency because they define, instead of measuring, the stray-load losses. On the other hand, IEEE 112-B also assumes the stray load loss based on the motor power rating in case the measurement cannot be performed, and again, the assumed values seem to overestimate the real stray load loss which will not allow the correct efficiency value to be obtained [123]. This is in line with the results

presented in a study conducted by the authors of this work [88]. However, the stray load loss measurements are not simple to perform and they are severely influenced by the measurement errors.

Stray load loss of a particular motor is affected by the magnitude and the angle of voltage unbalance factor, and due to the unlimited voltage unbalance combinations, where each has different effects on the machine in terms of losses, and hence, each combination produces a different value of stray load loss; this situation creates a large amount of uncertainty in the estimation of the stray load loss. The proposed algorithm is designed to perform in-situ where stray load loss measurements is not allowed due to the intrusive nature of those measurements. Based on this and on the above mentioned discussion, it is proposed in this paper to utilize the measured values of the stray load loss in the data of Hydro-Québec and BC hydro to have a reasonable approximation of the stray load loss. The measured stray load loss of the data is based on balanced power tests, so it can be considered as an underestimated value if compared to the stray load loss of the same machine when operating with unbalanced voltages. On the other hand, if the stray load loss is calculated according to the International Standard IEC 60034-2-1 [95] as in (2.6), its value will be overestimated as discussed above. Hence, the better approximation of the stray load loss is by taking the average of both measured and calculated values. The strategy to assign the measured stray load loss from the data is as follows:

6.2.1.1. Motor Has Similarity with the Data

Whenever data is mentioned, it means the Hydro-Québec/BC hydro data.

If the motor under test is similar to any of the data's motors, the algorithm will search the data using the following strategy:

- If power, rated voltage, and insulation class are similar, the measured stray load loss will be used.
- If power, rated voltage, number of poles, and insulation class are all similar, the measured stray load loss will be used.

6.2.1.2. Motor Has No Similarity with the Data

In this case, the stray load loss will be assumed according to (2.6).

6.2.2. Determination of Friction & Windage Losses

The extra heating in induction motors operating with unbalanced voltages is due to the increase in copper loss. The negative sequence current has a worse effect in terms of heating the motor. The core loss and friction and windage losses remain essentially independent of unbalance of negative sequence voltage that is less than 15% [50]. In this study, all tests were conducted within the 5% limit of unbalance which is set by NEMA. The proposed algorithm follows the following strategy in estimating the friction and windage losses.

6.2.2.1. Motor Has Similarity with the Data

- If power and number of poles is similar, the measured F&W will be used.

6.2.2.2. Motor Has No Similarity with the Data

In this case, the algorithm will follow a different strategy which is similar to that presented in Chapter 5. The strategy is as follows:

- If number of poles is 2, then the F&W will be calculated as in (5.3).
- If number of poles is 4, then the F&W will be calculated as in (5.4).
- If number of poles is 6, then the F&W will be calculated as in (5.5).

6.2.3. Sensorless Speed Measurement Technique

Speed measurement plays a key role in the process of induction motors efficiency estimation. Measuring the speed by an intrusive procedure is not allowed in many industrial situations. On-line speed measurement is the suitable way to deal with such a situation. The algorithm utilizes the same on-line speed measurement technique that was presented and discussed in Chapter 5, subsection 5.3.3.

6.2.4. Stator Windings Temperature Measurement

Determination of the stator winding temperature is one of the important factors in the process of a precise induction motors efficiency estimation. Due to the in situ nature of the proposed algorithm, the same procedure that was presented in Chapter 5, subsection 5.3.2 to determine the stator winding temperature is followed.

6.2.5. Determination of Positive and Negative Sequence Components

The three unsymmetrical line-to-line voltages are measured and recorded. They are used in the following group of equations to determine the three unsymmetrical per phase voltages and the positive and negative sequence voltages with their defined angles [124] [125]. The angle of V_{ab} is predefined as in (6.2)

$$\theta_{ab}=0^{o} \tag{6.2}$$

The angles of V_{bc} and V_{ca} are calculated by using the cosine law as follows:

$$\theta_{V_{ab-bc}}=\cos^{-1}\left(\frac{V_{ab}^2+V_{bc}^2-V_{ca}^2}{2V_{ab}V_{bc}}\right) \tag{6.3}$$

$$\theta_{V_{bc-ca}}=\cos^{-1}\left(\frac{V_{bc}^2+V_{ca}^2-V_{ab}^2}{2V_{bc}V_{ca}}\right) \tag{6.4}$$

$$\theta_{V_{bc}}=-180^{o}+\theta_{V_{ab-bc}} \tag{6.5}$$

$$\theta_{V_{ca}}=\theta_{V_{ab-bc}}+\theta_{V_{bc-ca}} \tag{6.6}$$

The positive and negative sequence voltages V_1 and V_2 are calculated as in (6.7)

$$\begin{bmatrix}V_1\\V_2\end{bmatrix}=D^{-1}\begin{bmatrix}V_{ab}\\V_{bc}\end{bmatrix} \tag{6.7}$$

where,

$$D=\begin{bmatrix}1-a^2 & 1-a\\a^2-a & a-a^2\end{bmatrix} \tag{6.8}$$

where, a = -0.5+j0.866

The three unsymmetrical per phase voltages V_a, V_b and V_c are calculated as in (6.9)

$$\begin{bmatrix} V_a \\ V_b \\ V_c \end{bmatrix} = A \begin{bmatrix} 0 \\ V_1 \\ V_2 \end{bmatrix} \tag{6.9}$$

where,

$$A = \begin{bmatrix} 1 & 1 & 1 \\ 1 & a^2 & a \\ 1 & a & a^2 \end{bmatrix} \tag{6.10}$$

To make V_a to be the reference vector, the absolute value of the angle of V_a is added to all other vectors to redefine new angles as follows:

$$\theta_{V_{a,\,new}} = \theta_{V_a} + |\theta_{V_a}| = 0^o \tag{6.11}$$

$$\theta_{V_{b,\,new}} = \theta_{V_b} + |\theta_{V_a}| \tag{6.12}$$

$$\theta_{V_{c,\,new}} = \theta_{V_c} + |\theta_{V_a}| \tag{6.13}$$

$$\theta_{V_{ab,\,new}} = \theta_{V_{ab}} + |\theta_{V_a}| \tag{6.14}$$

$$\theta_{V_{bc,\,new}} = \theta_{V_{bc}} + |\theta_{V_a}| \tag{6.15}$$

$$\theta_{V_{ca,\,new}} = \theta_{V_{ca}} + |\theta_{V_a}| \tag{6.16}$$

$$\theta_{V_{1,\,new}} = \theta_{V_1} + |\theta_{V_a}| \tag{6.17}$$

$$\theta_{V_{2,\,new}} = \theta_{V_2} + |\theta_{V_a}| \tag{6.18}$$

The angles of the three input currents are determined as follows:

$$\theta_{I_a} = \cos^{-1} \left| \frac{P_a}{V_a I_a} \right| \tag{6.19}$$

$$\theta_{I_b} = \cos^{-1} \left| \frac{P_b}{V_b I_b} \right| \tag{6.20}$$

$$\theta_{I_c} = \cos^{-1} \left| \frac{P_c}{V_c I_c} \right| \tag{6.21}$$

where,

P_a is the measured input power of phase a;

V_a is the calculated voltage of phase a;

I_a is the measured input current of phase a;

P_b is the measured input power of phase b;

V_b is the calculated voltage of phase b;

I_b is the measured input current of phase b;

P_c is the measured input power of phase c;

V_c is the calculated voltage of phase c;

I_c is the measured input current of phase c.

The positive and negative sequence currents are identified as follows:

$$\begin{bmatrix} 0 \\ I_1 \\ I_2 \end{bmatrix} = A^{-1} \begin{bmatrix} I_a \\ I_b \\ I_c \end{bmatrix} \tag{6.22}$$

where,

$$A^{-1} = \frac{1}{3} \begin{bmatrix} 1 & 1 & 1 \\ 1 & a & a^2 \\ 1 & a^2 & a \end{bmatrix} \tag{6.23}$$

6.2.5.1. Example Calculations

As an example for the above mentioned calculations and to know the magnitude and angle of the voltage unbalance, let the three line-to-line voltages at the terminals of a motor of 460 V rated voltage be as follows:

$$V_{ab}=473 \text{ V}$$

$$V_{bc}=460 \text{ V}$$

$$V_{ca}=434 \text{ V}$$

By applying the procedure described in subsection 6.2.5, the calculated per phase three voltages and the positive and negative voltages will be as follows:

$$V_a=260.89 \text{ V}\angle -28.94^{o}$$

$$V_b=275.34 \text{ V}\angle -152.71^{o}$$

$$V_c=253.02\ V\angle -86.29^o$$

$$V_1=262.92\ V\angle -31.79^o$$

$$V_2=13.16\ V\angle 68.50^o$$

To make V_a as the reference, a value of $+28.94^o$ must be added to the three phases which will result in the following redefined phasors:

$$V_a=260.89\ V\angle 0^o$$

$$V_b=275.34\ V\angle -123.77^o$$

$$V_c=253.02\ V\angle 115.23^o$$

$$V_1=262.92\ V\angle -2.84^o$$

$$V_2=13.16\ V\angle 97.44^o$$

The percentage complex voltage unbalance factor can be determined as in

$$CVUF=100\frac{\overline{V_2}}{\overline{V_1}} \tag{6.24}$$

By substituting the obtained complex values of the positive and negative voltages into (6.24), the results will be as follows:

$$CVUF=0.05\angle 100.28^o$$

6.2.6. Identifying the Electrical Parameters

All the required data which is needed to run the GA are acquired so far. According to the algorithm flow chart in **Error! Reference source not found.**, the unknown motor parameters, .e. X_1, R_{fe}, X_m, and R_2, are to be identified by using the GA technique. Three GAs were designed to extract the required parameters. The fitness function for each GA was built based on the positive sequence equivalent circuits shown in Figure 6-2(a). The negative sequence equivalent circuit is shown in Figure 6-2(b).

The following equations that are derived from the positive sequence equivalent circuit are used in the three GAs fitness functions.

$$Y_m = \frac{1}{jX_m} + \frac{1}{R_{fe}} \tag{6.25}$$

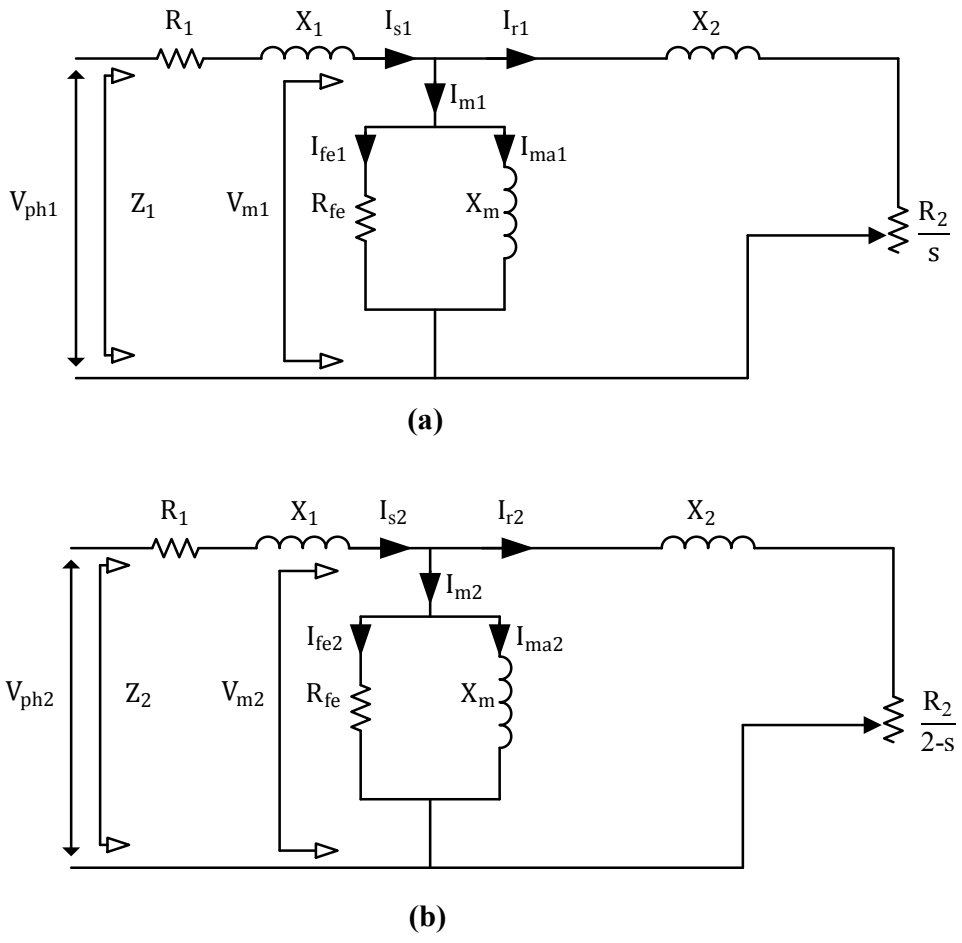

Figure 6-2. Induction machine exact equivalent circuit with unbalanced voltages; (a) Positive Sequence; (b) Negative sequence [132].

$$Y_r = \frac{1}{\frac{R_2}{s_1} + jX_2} \tag{6.26}$$

$$Z_r = \frac{1}{Y_m + Y_r} \tag{6.27}$$

$$Z_1 = R_1 + jX_1 \tag{6.28}$$

$$Z = Z_1 + Z_r \tag{6.29}$$

$$I_{s_1} = \frac{V_{ph_1}}{Z} \tag{6.30}$$

$$I_{r_1} = I_{s_1}\left[\frac{1/(Y_m + Y_r)}{1/Y_r}\right] \tag{6.31}$$

$$I_{m_1} = I_{s_1} - I_{r_1} \tag{6.32}$$

$$V_{m_1} = \frac{I_{m_1}}{Y_m} \tag{6.33}$$

$$Z_m = \frac{V_{ph_1}}{I_{s_{1m}}} \tag{6.34}$$

where,

Y_m is per phase admittance of the magnetizing branch;

X_m is per phase leakage reactance of the magnetizing branch;

R_{fe} is per phase iron loss resistance;

Y_r is per phase admittance of the rotor;

R_2 is per phase rotor resistance;

X_2 is per phase rotor leakage reactance;

s_1 is the slip;

Z_r is per phase impedance of both the rotor and the magnetizing branches;

Z_1 is per phase stator impedance;

R_1 is per phase stator resistance;

Z is per phase total impedance;

V_{ph_1} is the positive sequence phase voltage;

I_{s_1} is the positive per phase estimated stator current;

I_{r_1} is the positive per phase estimated rotor current;

I_{m_1} is the positive per phase estimated total magnetizing current;

V_{m_1} is the positive per phase estimated magnetizing voltage;

Z_m is the positive sequence per phase impedance calculated based on measured positive sequence current;

$I_{s_{1m}}$ is the measured positive sequence current.

The stator and rotor resistances are to be corrected to the full-load temperature T_{fl} according to (6.35) and (6.36)

$$R_{1,corr}=\frac{R_1(T_{fl}+K_1)}{T_{cold}+K_1} \tag{6.35}$$

$$R_{2,corr}=\frac{R_2(T_{fl}+K_2)}{T_{cold}+K_2} \tag{6.36}$$

The total core loss, stator copper loss and rotor copper loss are estimated as in (6.37), (6.38) and (6.39) respectively

$$P_h=3\frac{V_{m_1}^2}{R_{fe}} \tag{6.37}$$

$$P_{scl}=3I_{s_1}^2R_{1,corr} \tag{6.38}$$

$$P_{rcl}=3I_{r_1}^2R_{2,corr} \tag{6.39}$$

where,

P_h is total core loss;

P_{scl} is total stator copper loss;

P_{rcl} is total rotor copper loss.

Total losses will be determined by (6.40)

$$P_{total}=P_h+P_{scl}+P_{rcl}+P_{fw}+P_{sll} \tag{6.40}$$

where,

P_{total} is the total losses;

P_{fw} is the friction & windage losses.

The output power can be estimated by using (6.41)

$$P_{out}=P_{in,fl}-P_{total} \tag{6.41}$$

where,

P_{out} is the output power;

$P_{in,fl}$ is the measured input power.

The total input power will be calculated according to (6.42) and (6.43)

$$P_{in,\ calc1}=3real(V_{ph_1} I^{*}_{s1m}) \tag{6.42}$$

$$P_{in,\ calc2}=3real(V_{ph_1} I^{*}_{s_1}) \tag{6.43}$$

where,

$P_{in,\ calc1}$ is the calculated input power from measured current;

I^{*}_{s1m} is the conjugate of the positive sequence measured stator current;

$P_{in,\ calc2}$ is the calculated input power from calculated current;

$I^{*}_{s_1}$ is the conjugate of the positive sequence estimated stator current in (6.30).

The two values of the input power are used to produce an error function as in (6.46). The three GAs have the same error functions as described in (6.44), (6.45), (6.46), (6.47), and (6.48)

$$f_1=\frac{real(I_{s1m})-real(I_{s_1})}{real(I_{s1m})} \tag{6.44}$$

$$f_2=\frac{imag(I_{s1m})-imag(I_{s_1})}{imag(I_{s1m})} \tag{6.45}$$

$$f_3=\frac{P_{in,\ calc1}-P_{in,\ calc2}}{P_{in,\ calc1}} \tag{6.46}$$

$$f_4=\frac{\theta_{Z_m}-\theta_Z}{\theta_{Z_m}} \tag{6.47}$$

$$f_5=\frac{P-P_{out}}{P} \tag{6.48}$$

where,

θ_{Z_m} is the angle of the measured input impedance Z_m;

θ_Z is the angle of the calculated input impedance Z;

P is nameplate power.

The fitness function which has the maximum value of 1 is as in (6.49)

$$ff=\frac{1}{1+\sum_{i=1}^{5} f_i} \tag{6.49}$$

The three GAs are to be run in the following sequence, and certain observations should be done carefully to guarantee best results of the algorithm. In GA1, the core loss is approximated by using (6.50)

$$P_{h,\,calc}=P_{in,\,fl}-P_{out}-P_{scl}-P_{rcl}-P_{fw}-P_{sll} \tag{6.50}$$

The approximated core loss $P_{h,\,calc}$ is compared against the total core loss P_h of (6.37). This comparison is utilized to adjust the constraint of R_{fe}. The values of both R_{fe} and P_h from GA1 are used as fixed values in GA2. This makes R_2 converge to a stable value. Hence, GA2 works with only three variables (i.e. X_1, X_m and R_2). The values of the 4 variables of 10 consecutive runs of both GA1 and GA2 are tabulated and the values of best fitness are used as new constraints for both GA1 and GA2. New round of 10 runs follows, and this process iterates until a stable value of R_2 is achieved.

6.2.7. Rotor Resistance Calibration

The value of R_2 that is transferred to GA3 shall be carefully calibrated until the best fitness of GA3 is acquired. This makes other variables reach stable values. Hence, GA3 will also have 3 variables (i.e. X_1, X_m, and R_{fe}). GA3 iterates, and the best fitness of the three variables after each 10 runs is used as new constraints until stable values are achieved and the 4 parameters of the induction machine is declared. R_1 is already known, and X_2 will be determined based on Table 3-I.

6.2.8. IEEE Form F2-Method F1calculations

The six motor parameters are used in IEEE Form F2-Method F1 calculations to estimate positive sequence output power P_{cov1} as illustrated in the following equations (6.51) through (6.71)

$$Z_2=\sqrt{(R_2/s_1)^2+X_2^2} \tag{6.51}$$

$$G_2=(R_2/s_1)/Z_2^2 \tag{6.52}$$

$$G=G_2+G_{fe} \tag{6.53}$$

$$B_2=-\left(X_2/Z_2^2\right) \tag{6.54}$$

$$B_m=-(1/X_m) \tag{6.55}$$

$$B=B_2+B_m \tag{6.56}$$

$$Y_2=\sqrt{G^2+B^2} \tag{6.57}$$

$$R_g=G/Y_2^2 \tag{6.58}$$

$$R=R_1+R_g \tag{6.59}$$

$$X_g=-\left(B/Y_2^2\right) \tag{6.60}$$

$$X=X_1+X_g \tag{6.61}$$

$$Z=\sqrt{R^2+X^2} \tag{6.62}$$

$$I_1=V_{ph1}/Z \tag{6.63}$$

$$I_2=I_1/\sqrt{Z_2^2\times Y_2^2} \tag{6.64}$$

$$P_s=3I_1^2R \tag{6.65}$$

$$P_r=3I_2^2(R_2/s_1) \tag{6.66}$$

$$P_{scl}=3I_1^2R_1 \tag{6.67}$$

$$P_h=3I_1^2\left(G_{fe}/Y_2^2\right) \tag{6.68}$$

$$P_{rcl}=s_1 P_r \tag{6.69}$$

$$P_t=P_{scl}+P_h+P_{rcl}+P_{fw}+P_{sll} \tag{6.70}$$

$$P_{cov1}=P_s-P_t \tag{6.71}$$

$$s_2=2-s_1 \tag{6.72}$$

The positive sequence slip s_1 is replaced with the negative sequence slip s_2 of (6.72), and the positive sequence phase voltage V_{ph1} is replaced with the negative sequence phase voltage V_{ph2} that was calculated in (6.7), and the same equations (6.51) through (6.71) are used to estimate the negative sequence output power P_{cov2}. The friction and windage and the stray load loss that are shown in (6.70) are excluded from the calculations of total negative sequence losses. Finally, the full-load efficiency will be estimated by using (6.73)

$$\eta=\frac{P_{cov1}+P_{cov2}}{P_s}\times 100 \tag{6.73}$$

where,

Z_2 is the rotor impedance;

G_2 is the rotor conductance;

G is the rotor and magnetic conductance;

B_2 is the rotor susceptance;

B_m is the magnetizing susceptance;

B is the rotor & magnetic circuit susceptance;

Y_2 is the rotor and magnetizing circuit admittance;

R_g is the rotor & magnetizing circuit resistance;

R is the total resistance of the equivalent circuit;

X_g is the rotor and magnetizing circuit reactance;

X is the total reactance of the equivalent circuit;

Z is the total impedance of the equivalent circuit;

I_1 is the stator current;

I_2 is the rotor current;

P_s is the stator power;

P_r is the rotor power;

P_{scl} is the stator copper loss;

P_h is the core loss;

P_{rcl} is the rotor copper loss;

P_t is the total loss;

P_{cov1} is the positive sequence converted power;

P_{cov2} is the negative sequence converted power;

s_1 is the positive sequence slip;

s_2 is the negative sequence slip;

η is the estimated efficiency.

6.3. Experimental Results and Analysis

An experimental setup shown in Figure 6-3 is used to test a 7.5 hp induction motor. The nameplate details are tabulated in Table 6-I.

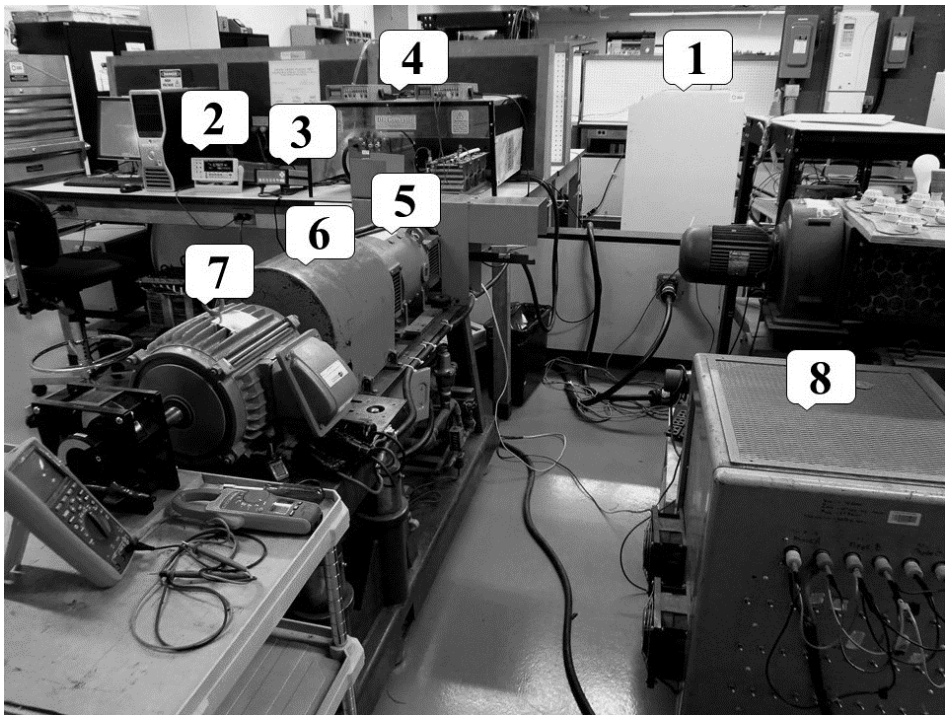

Figure 6-3. The experimental setup for testing 7.5 hp induction motor: 1, programmable power supply; 2, high resolution digital dc voltmeter; 3, multi-channel signal conditioner; 4, field control unit; 5, dynamometer; 6, torque transducer; 7, 7.5 hp IM; 8, resistor bank.
Photo is a courtesy of Concordia University.

Table 6-I. Nameplate Details of 7.5 hp Motor

Hp	**VOLTS**	**AMPS**	**RPM**
7.5	460	8.85	1755
POLES	**EFF.**	**INS.**	**DESIGN**
4	91.7	F	B

The test was conducted by using a programmable power supply, 13kW dynamometer driven by a field control unit and supplied with torque transducer, multi-channel signal conditioner and high resolution dc voltmeter which is used to display the dc analog output of the multi-channel signal conditioner which corresponds to the value of the applied torque. The dynamometer load is a resistor bank. The DC test was performed and the stator cold resistance and cold temperature were measured and recorded. The motor was run for 8 hours to reach its temperature stability. The hot temperature was measured by using the resistance procedure where the cold temperature is taken as a reference and the value of the hot resistance is translated to hot temperature as in (5.6). The line-to-line voltages, line currents, and total input power were measured by using rms measuring devices. One line current signal is needed to be acquired by using a data logging device for the purpose of speed measurement. The speed was also measured by using contactless tachometer for validation purpose. Voltage unbalance of 5% was created by the programmable power supply and applied on the machine for one hour and the full-load efficiency was measured and recorded. The data of the test is illustrated in Table 6-II.

Table 6-II. Test Data of 7.5 hp Machine

$\mathbf{V_{ab}}$ [V]	$\mathbf{V_{bc}}$ [V]	$\mathbf{V_{ca}}$ [V]	$\mathbf{I_a}$ [A]	$\mathbf{I_b}$ [A]	$\mathbf{I_c}$ [A]
473.05	459.95	433.92	10.616	11.212	5.703
$\mathbf{P_a}$ [W]	$\mathbf{P_b}$ [W]	$\mathbf{P_c}$ [W]	$\mathbf{PF_a}$	$\mathbf{PF_b}$	$\mathbf{PF_c}$
2685	2364	1251	0.970	0.770	0.870
$\mathbf{N_r}$ [rpm]	$\mathbf{P_{FW}}$ [W]	$\mathbf{P_{SLL}}$ [W]	$\mathbf{T_{FL}}$ [^{o}C]	$\mathbf{T_{cold}}$ [^{o}C]	$\mathbf{R_{1,cold}}$ [Ω]
1757.5	17.785	108.68	67.89	22.1	2.55

The data is transferred to the proposed algorithm and the six parameters including the corrected stator resistance are identified and sorted in Table 6-III.

Table 6-III. Electrical Parameters of 7.5 hp Machine

R_1 [Ω]	X_1 [Ω]	R_{fe} [Ω]	X_m [Ω]	R_2 [Ω]	X_2 [Ω]
3.005	2.474	4153	201.7	2.300	3.693

Those parameters are to be used in IEEE Form 2-Method F1 calculations, i.e. equations (6.51) through (6.71), and the full-load efficiency is declared and compared to the measured value and illustrated in Table 6-IV. As it can be seen from Table 6-IV, the estimated efficiency is close to the measured value.

Table 6-IV. Full-Load Efficiency of 7.5 hp Machine Under 5% UV

Measured Efficiency [%]	**Estimated Efficiency** [%]	**Absolute Error**
88.7	88.3	0.4

6.4. The Proposed Algorithm Validation

The 7.5 hp machine was tested for full-load and partial loads efficiency. The machine was also tested for efficiency at different values of voltage unbalance (i.e. 1%, 2%, 3%, 4%, and 5% of VU).

A 3.0 hp induction motor is also tested by the dynamometer method and the proposed algorithm under the same pattern of voltage unbalance described above. The impact of unbalance on the 3.0 hp machine is illustrated in Figure 6-4. The severe impact of the 5% VU on the performance of the machine can be easily noticed where the full-load efficiency degraded from 80.7% under balanced voltages to 79.1% under 5% unbalance.

The results of both 3.0 and 7.5 hp machines are shown in Table 6-V and Table 6-VI respectively. The maximum deviation of the estimated efficiency when compared to the measured value is 0.4% for both 3.0 hp and 7.5 hp respectively. This range of error reflects an acceptable accuracy. Although the algorithm is validated through 10 different voltage unbalance tests with acceptable accuracy, the algorithm still needs additional validation by testing medium and large size induction motors.

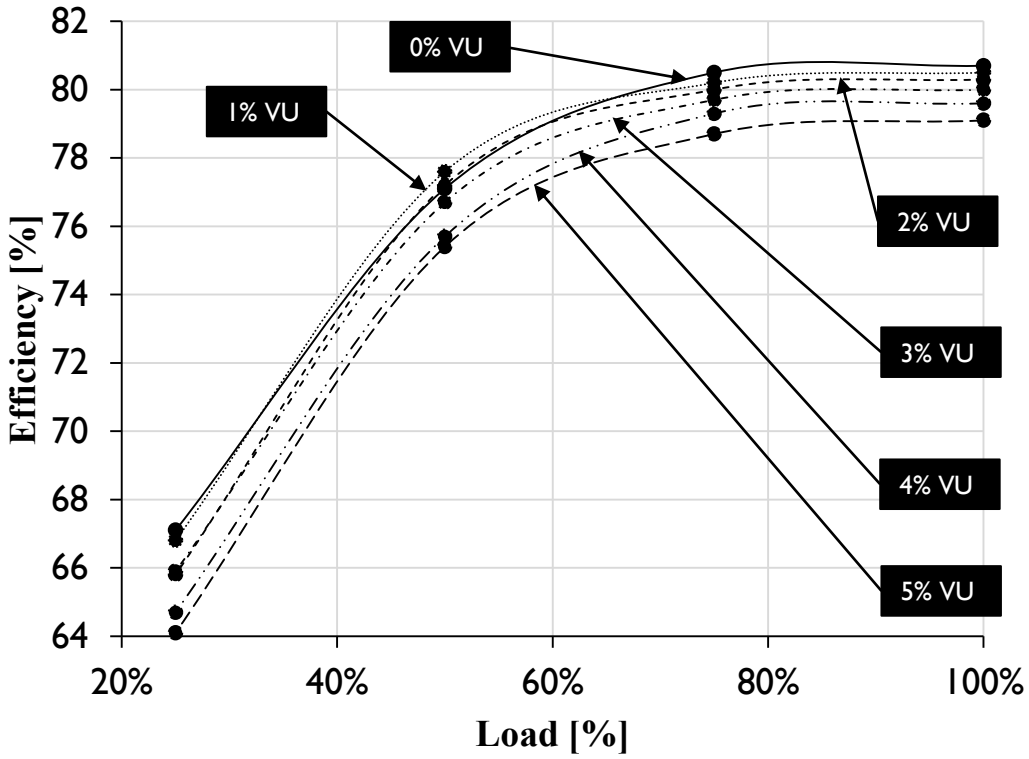

Figure 6-4. Impact of unbalance on the 3.0 hp machine performance

Table 6-V. Measured vs. estimated efficiency of 3.0 hp motor

Unbalance [%]	**Measured Efficiency** [%]	**Estimated Efficiency** [%]	**Absolute Error** [%]
1	80.7	80.5	0.2
2	80.6	80.6	0.0
3	80.6	80.2	0.4
4	79.7	79.6	0.1
5	79.0	79.1	0.1

Table 6-VI. Measured vs. estimated efficiency of 7.5 hp motor

Unbalance [%]	**Measured Efficiency** [%]	**Estimated Efficiency** [%]	**Absolute Error** [%]
1	90.4	90.1	0.3
2	90.2	89.8	0.4
3	89.9	89.6	0.3
4	89.3	89.0	0.3
5	88.7	88.3	0.4

6.4.1. Usability of the Proposed Algorithm with Balanced Supplied Voltages

The usability of the proposed algorithm to estimate the efficiency of induction motors that operate with balanced voltages is demonstrated by testing the 7.5 hp and 3.0 hp machines. The results are shown in Table 6-VII. The acceptable accuracy obtained can give another credit to the proposed technique and demonstrate the level of confidence in the capability of the technique under different electrical environments.

Table 6-VII. Estimated Efficiency with Balanced Voltages

Motor Size [hp]	**Measured Efficiency** [%]	**Estimated Efficiency** [%]	**Absolute Error** [%]
7.5	91.0	90.3	0.7
3.0	80.7	80.3	0.4

6.4.2. Repeatability of the Proposed Algorithm

The efficiency test by using the proposed algorithm of the 7.5 hp machine that operates with 5% voltage unbalance is repeated ten times. The results are tabulated in Table 6-VIII. The coefficient of variation C_V is used as one of the statistical concepts to compare relative dispersion of data [126]. The coefficient of variation is defined as the ratio of the standard deviation σ to the mean value $\bar{e}$ expressed as a percentage as in (6.74)

$$C_v = 100\frac{\sigma}{\bar{e}} \tag{6.74}$$

The coefficient of variation obtained for the data shown in Table 6-VIII is 13.13% which can prove the consistency of the results obtained by the proposed algorithm.

Table 6-VIII. Ten Repeated Tests by Using the Proposed Algorithm

No.	Measured FL Efficiency [%]	Estimated FL Efficiency [%]	Absolute Error [%]
1	88.70	88.32	0.38
2		88.22	0.48
3		88.31	0.39
4		88.26	0.44
5		88.30	0.40
6		88.29	0.41
7		88.22	0.48
8		88.33	0.38
9		88.23	0.47
10		88.15	0.55

6.5. Summary

In this chapter, an algorithm for in situ efficiency estimation of induction motors operating with unbalanced voltages by using a combination of GA procedure, IEEE Form 2-Method F1 calculations, and pre-tested motors is proposed. It was proven in chapter 1 that using the assumed values of stray load loss can significantly increase the error and reduce the accuracy of the estimated efficiency. Hence, the algorithm was designed to utilize test data of a large number of induction motors provided by Hydro-Québec and BC hydro.

The proposed algorithm and its detailed flow chart is presented in subsection 6.2.

The strategy on how to assign the value of stray load loss and friction and windage losses are detailed in subsection 6.2.1. The strategy is to assign an average value of stray load loss to the machine under test when the motor under test has similarity with the supporting data. New proposed formulas to determine the friction and windage losses are detailed in the mentioned subsection.

An extensive procedure is presented in subsection 6.2.5 for the determination of positive and negative sequence components. This procedure is used to determine the phase voltages and their associated angles of a certain level of unbalance in the programmable power supply. An

example calculations are given in subsection 6.2.5.1.

The algorithm requires only one load point which is full-load with its corresponding rms values of voltage, current, and power obtained at the motor terminals.

The same speed estimation technique that is presented in Chapter 5 is used in this study and it needs the current signal acquisition of only one line.

The algorithm is evaluated and assessed by 10 voltage unbalance tests and the accuracy of the results is shown.

The usability of the algorithm with balanced voltages is investigated by testing the 3.0 hp and 7.5 hp machines and the results with acceptable accuracy are presented in subsection 0.

The repeatability of the proposed algorithm is also investigated in subsection 6.4.2. The results showed a 13.13% coefficient of variation.

The goal of the study was to design a useful tool that can be used in industry to derate induction motors due to voltage unbalance.

CHAPTER SEVEN

7. A Novel In Situ Efficiency Estimation Algorithm for Three-Phase Induction Motors Operating with Distorted Unbalanced Voltages

Three-phase power supply can never be completely clean of distortion or voltage unbalance. Unbalanced voltages and harmonics have detrimental impacts on the performance of induction motors. The efficiency estimation process can be a difficult task with the existence of voltage unbalance and harmonics. In this chapter, a novel algorithm for *in situ* full-load efficiency estimation for induction motors operating with distorted unbalanced voltages is proposed. The proposed technique utilizes the genetic algorithm, IEEE Form F2-Method F1 calculations and pre-tested motors data. The method requires a stator winding dc resistance measurement, full-load rms voltages, currents, input power and speed measurement. The proposed algorithm uses a sensorless online speed measurement. The technique is evaluated by testing 2 induction motors with different combinations of voltage unbalance and total harmonic distortion. The results showed acceptable accuracy. The technique may be used as a potential industrial tool that can help derate induction motors upon the presence of voltage unbalance and harmonics distortion.

7.1. Introduction

Three-phase induction motors can perform well up to their design limits if they are supplied with balanced sinusoidal voltages. However, power supplies nowadays can never be balanced or clean of harmonics. Voltage unbalance can exist by (1) unbalanced loads, (2) unsymmetrical transformer windings or transmission impedances, (3) large single-phase loads [39], (4) incomplete transposition of transmission lines, (5) open delta transformer connections [78], (6) blown fuses on three-phase capacitor bank, (7) operation of single-phase loads at different times, or (8) defective transformers in power systems [41]. On the other hand, harmonics presence in a power supply is due to: (1) operation of power electronics devices, (2) operation of steel mills arc furnaces, and (3) resonance of shunt capacitors and/or series inductors [78]. Stator and rotor temperature rises due to voltage unbalance can cause detrimental effects on

the three-phase induction motors, such as, reduction in output torque, vibration and overheating that lead to a reduction on insulation life of the machine [35]. The excessive temperatures in parts of the rotor of induction motors are attributed to the excessive unbalanced negative sequence currents [37]. Induction motors are always prone to stresses due to voltage unbalance as there is no power supply that can be perfectly balanced due to the previously mentioned reasons. According to the American National Standard ANSI/NEMA MG 1-2011, it is not recommended to operate induction motors with voltage unbalance above 5% [15]. The serious effect of voltage unbalance on the performance of the induction motors was the area of interest of many researchers since 1930's of the last century [45] where there was a trial to analyze the performance of three-phase induction motor operating under unbalanced voltages by using the equivalent circuit and the symmetrical component. In [50], it was demonstrated that the negative sequence current has the worse effect in terms of heating the motor, rather than an equal value of positive sequence and that is due to the high negative sequence rotor resistance. It was noticed that core loss and friction and windage losses remain essentially independent of unbalance of negative sequence voltage that is less than 15%. Unbalance voltage related vibration and its injurious effects to bearings, to insulation, and to interconnecting mechanical parts of the machine was also reported. Voltage unbalance is defined differently according to the national Electrical Manufacturers Association (NEMA), IEEE and IEC standards. Those definitions are detailed and discussed in [127]. In [52], it was stated that "*It is not sufficient to merely know the percent voltage unbalance, but it is equally important to know how they are unbalanced*". This important point stimulates researches to come up with what is called Complex Voltage Unbalance Factor (CVUF) where the magnitude and angle of the unbalance factor are both taken into account [54] [128].

The other issue that has serious impact on the performance of induction machines is the presence of harmonics in the supplied three-phase voltages. When a motor is operated on a bus with harmonic content, its efficiency will be reduced. The harmonics increase the electrical losses which decrease efficiency. The increase in losses results in an increase in motor temperature, which further reduces the efficiency [15]. Harmonics and their associated problems in induction motors were the area of interest of many scientists since 1920's. In 1929, the harmonic phenomenon was addressed as an unnecessary noise in electrical apparatus [58]. In the 1950's, researchers started to address the serious problem of losses in induction machines caused by

harmonics due to increasing of the number of applications of induction machines with static frequency converter power supplies. In [62], the fact that all induction motors have magnetic power-losses at harmonic frequencies was discussed. A simple test for measuring the harmonic-frequency losses in induction motors as a separate quantity was demonstrated. In [63], Fourier technique was utilized to analyze the voltage waveform that supplies an induction machine. A very detailed mathematical technique to estimate the output power and torque with harmonic was presented. It was found that, when an induction motor is fed by variable-frequency source which is often rich in harmonics, the distorted voltage modifies the motor operation considerably from that operating under conditions of pure sinusoidal voltages. It was also noticed that, depending on the order, a harmonic component of voltage may contribute either positive, negative, or zero torque. Fourier analysis showed that (3n+1) order harmonics in the voltage waveform develop positive torques, while (3n+2) orders result in negative torques. On the other hand, (3n+3) orders produce no torque, where n is any integer number. Each harmonic order has its own slip as presented in [129].

In 1985, an IEEE Committee Report was written about the effects of power system harmonics on power system equipment and loads [70]. The problem of harmonics generation due to increasing applications of power electronic type devices which have nonlinear voltage current characteristics, and the increasing application of shunt capacitor banks for power factor correction and voltage regulation which results in an increased potential for resonant conditions that can magnify existing harmonic levels, were addressed in the report. The report divided the effect of voltage distortion into three general categories: (1) insulation stress, (2) thermal stress, and (3) disruption. The main purpose of the report was to examine the various equipment characteristics to determine the limiting factors in the operation of the equipment with system distortion present. In regards to motors, the report assumed that the harmonic components may be classified as stator winding loss, rotor winding loss, and stray loss. The additional core loss due to voltage distortion is negligibly small.

To estimate the efficiency of an induction motor, measurements of torque and speed are essential. Such a kind of measurements is not available when efficiency estimation is required for a running (*in situ*) machine and when any disruption of its operation is not allowed.

Identifying the six parameters of the per phase equivalent circuit of the induction motor is

also a well-known procedure for efficiency determination. The six parameters can be identified by using the no-load/locked rotor test, or by using the IEEE Std. 112 impedance test-method 3. Nevertheless, both procedures are not applicable in the above mentioned *in situ* case. The Genetic Algorithm (GA) is found to be one of the successful tools to help identify the six parameters of the induction machine in *in situ* situation. Many research works employed the GA to estimate those parameters based on available operating data of the motor. The GA was employed in [106] to identify induction motor parameters from load tests. The proposed algorithm needed at least two different values of slip, which means two loading points. The model used was modified by connecting the magnetizing leakage reactance X_m and the iron loss resistance R_{fe} in series. In [107], several versions of the GA were used to help find the induction motor parameters for a small (5 hp), medium (50 hp) and large (500 hp) induction motors. The core loss resistance is omitted in the IM model used in this work. The stator resistance is estimated rather than measured. A comparison of the estimated parameter values against the actual values was demonstrated. It was claimed that one of the versions gave extremely good results. The GA applicability to *in situ* efficiency determination was also demonstrated in [1]. Three different methods were presented in this work; Method I utilizes only full-load input parameters that are used for motor parameter determination. This method showed around a 3% deviation from the actual efficiency. Method II needs different load points and this approach did improve the robustness of the GA, but did not lead to better results in motor parameters and efficiency. In Method III, the nameplate output power is used as an additional full-load input parameter for the GA. This approach did improve the outcome of the GA by reducing the deviation to less than 1% [1]. Other research works on the GA application in induction motor parameters determination can be found in [17], and [106]-[110].

In this chapter, a novel technique for *in situ* efficiency estimation of three-phase induction motors operating with a combination of unbalanced voltages and harmonics, utilizing the GA, IEEE Form F2-Method F1 calculations and pre-tested motors data is proposed. The algorithm utilizes a database of large number of induction motors tested for efficiency in the Laboratoire des Technologies de l'Énergie, Institut de Recherche, Hydro-Québec, Shawinigan, Québec, Canada. The data has a wide range of motor types and power ratings. Another set of data was received from BC hydro which includes a full test of 55 used (aged) induction motors. The database is utilized to specify the stray load loss and the friction and windage loss for induction

motors that have similarities with the tested motors of the data. Applicability and feasibility of the method are approved by testing 2 induction motors under different combinations of voltage unbalance and total harmonic distortion.

7.2. The Proposed Algorithm

The proposed algorithm utilizes the Genetic Algorithm which was introduced in Chapter 5. The per phase stator winding cold resistance and cold temperature of the induction motor under test are assumed to be predetermined from data sheets or tests performed during motor turn off. The value of rotor leakage reactance X_r is determined by identifying the value of the stator leakage reactance X_s and the NEMA design of the motor according to Table 3-I of the IEEE Std 112-2004 [21]. Hence, only four parameters out of six are to be identified; (1) the stator leakage reactance X_s, (2) the core loss resistance R_{fe}, (3) the magnetizing leakage reactance X_m, and (4) the rotor resistance R_r. Each chromosome in the designed GA consists of four variables; each variable represents one of the above mentioned parameters as in (7.1)

$$\text{Chromosome}=[X_s, R_{fe}, X_m, R_r] \tag{7.1}$$

A detailed flow chart of the proposed algorithm is illustrated in Figure 7-1. The algorithm is first fed with the predetermined values of the stator winding cold resistance R_{cold}, and cold temperature T_{cold}. The nameplate details, full-load rms measured values for three line-to-line voltages, three line currents, total input power and one line current signal acquired by data logging device of at least 10 seconds length and preferably of 10 microsecond sampling time are also required input.

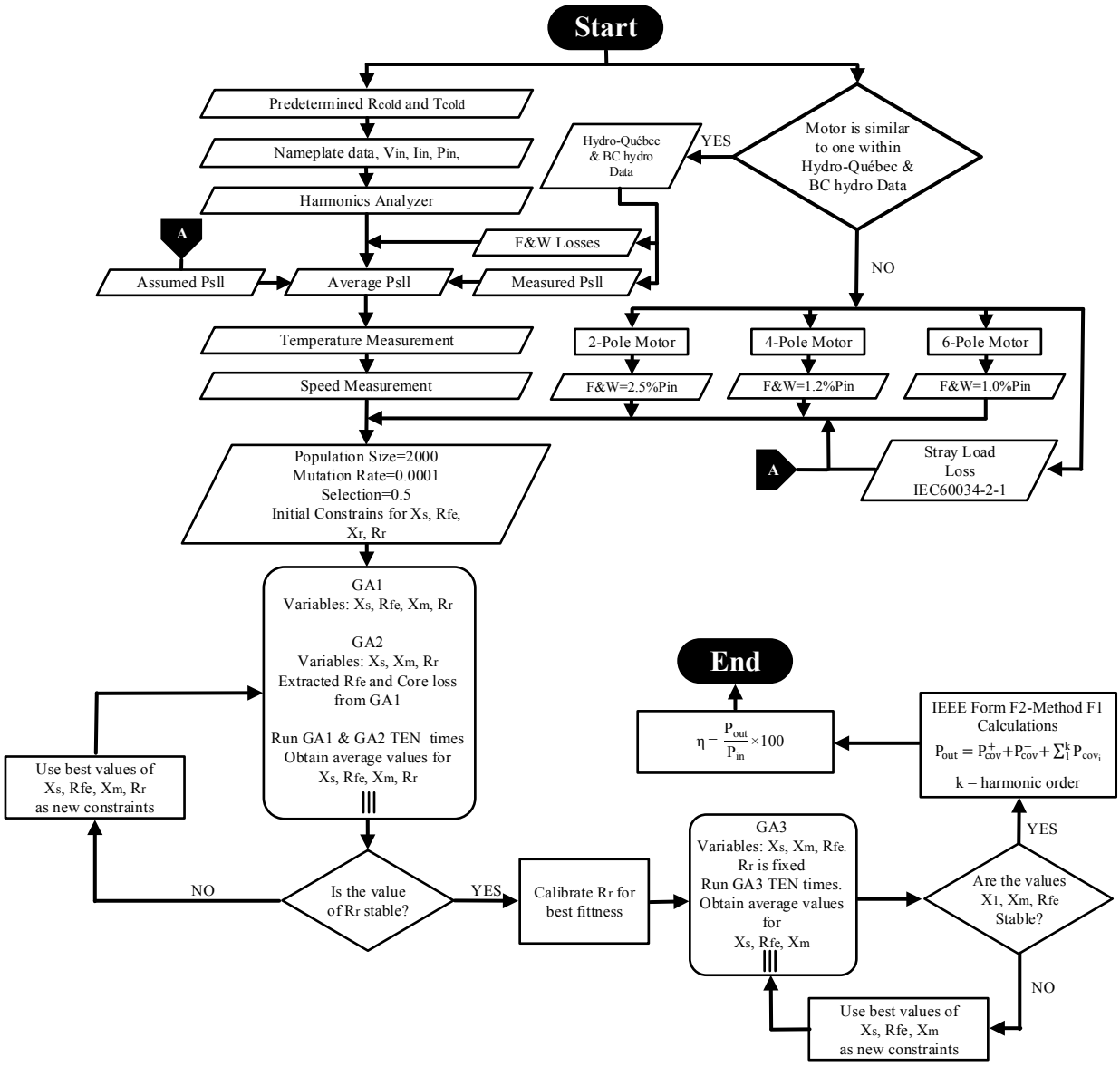

Figure 7-1. The proposed algorithm flow chart

7.2.1. Determination of Full-Load Stray Load Loss

Stray load loss consists of many loss components within the stator and rotor that involves number of slots, slot opening shape, stator winding distribution, rotor construction, skewing and saturation, and eccentricity of the air gap [130]. Determining the value of stray load loss in an induction motor is one of the important requirements for having accurate efficiency estimation process. An indirect efficiency measurement can be deemed more accurate if the stray load loss is

accurately determined [131]. In [122], IEEE 112-B was introduced to be the most suitable standard for the stray load loss measurements and both IEC 34-2 and JEC 37 overestimate the motor efficiency because their procedures define the stray load loss instead of measuring it. However, IEEE 112-B also assumes the stray load loss based on the motor power rating in case the measurement cannot be conducted. The assumed values seem to overestimate the real stray load loss which will not allow the precise efficiency value to be acquired [123]. This is in line with the results presented in detail in a study conducted by the authors of this psper [88]. Figure 7-2 illustrates a comparison between measured values of stray load loss of 4 induction motors and their assumed values according to IEEE and IEC standards. Taking the 500 hp motor as an example, it can be seen from the values shown on the figure that IEEE and IEC standards overestimate the value of stray load loss by 257.83% and 215.78% respectively. Nevertheless, the stray load loss measurements are not easy process to perform and they are severely influenced by the measurement errors.

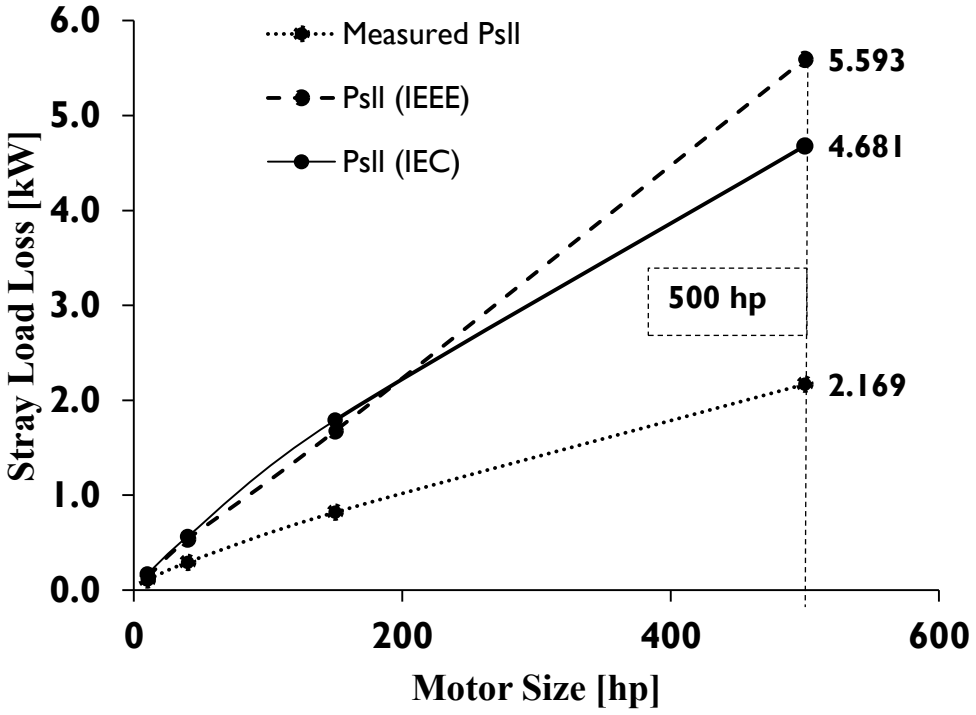

Figure 7-2. Measured and assumed stray load loss
Source of measured data: the Laboratoire des Technologies de l'Énergie, Institut de Recherche, Hydro-Québec, Shawinigan, Québec.

Stray load loss of a particular motor is affected by voltage unbalance, and due to the unlimited voltage unbalance combinations, where each has different effects on the machine in terms of losses, and hence, each combination produces a different value of stray load loss; this situation creates a large amount of uncertainty in the estimation of the stray load loss. The proposed algorithm is designed to perform in *in situ* where stray load loss measurement is not allowed due to the intrusive nature of the measurements. Hence, in this paper, it is proposed to utilize measured values of the stray load loss in the data of Hydro-Québec and BC hydro to have a reasonable approximation of the stray load loss. The measured stray load loss of the data is based on balanced power tests, so it can be considered as an underestimated value if compared to the stray load loss of the same machine when operating with unbalanced voltages. On the other hand, the stray load loss is calculated according to the International Standard IEC 60034-2-1 [95] as in (2.6) or assumed based on IEEE as in Table 1-I.

Using (2.6) or Table 1-I overestimates the value of stray load loss as discussed above. Hence, the better approximation of the stray load loss is by taking the average of both measured and assumed values.

To assign the stray load loss value, the following strategy is applied:

7.2.1.1. Motor Has Similarity with the Data

Whenever data is mentioned, it means Hydro-Québec and BC hydro data.

If the motor under test is similar to a motor within the data, the algorithm will use the following strategy:

- If power, rated voltage, and insulation class are all similar, the measured stray load loss will be assigned.
- If power, rated voltage, insulation class, and number of poles are all similar, the measured stray load loss will be assigned.

7.2.1.2. Motor Has No Similarity with the Data

In such a case, the only option to estimate the stray load loss is to assume it using (2.6).

7.2.2. Determination of Friction & Windage Losses

Two types of losses remain essentially independent of unbalance of negative sequence voltage that is less than 15%. They are core loss and friction and windage losses [50]. In this study, all tests were conducted within the limit of 5% unbalance which is set by NEMA. To accurately estimate the efficiency, friction and windage losses are to be determined and accounted for. The proposed algorithm follows the following strategy in estimating friction and windage losses:

7.2.2.1. Motor Has Similarity with the Data

If power and number of poles are similar, the measured friction and windage losses will be used.

7.2.2.2. Motor Has No Similarity with the Data

In such a case, the algorithm uses a different strategy [90] which is as follows:

- If number of poles is 2, then the friction and windage losses will be calculated as in (5.3).
- If number of poles is 4, then the friction and windage losses will be calculated as in (5.4).
- If number of poles is 6, then the friction and windage losses will be calculated as in (5.5).

7.2.3. Online Speed Measurement

Speed measurement is one of the key elements in the efficiency estimation process. In *in situ* situation, a non-intrusive procedure for speed measurement is required. An online speed measurement technique that estimates motor speed through the input current signal is utilized in this paper. The speed detection technique is based on an adaptive notch filter algorithm that was proposed in [121], where all mathematical principles and the governing equations can be found. The accuracy of the technique was previously presented in Chapter 5, subsection 5.3.3.

7.2.4. Online Stator Windings Temperature Measurement

Unbalanced voltages and harmonics bring a lot of stress on induction motors due to the excessive losses and the resulting heat. Temperature measurement plays an important role in the efficiency estimation procedure. Determination of the stator winding temperature is one of the important factors in the process of a precise induction motors efficiency estimation. Due to the in situ nature of the proposed algorithm, the same procedure that presented in Chapter 5, subsection 5.3.2 to determine the stator winding temperature is used.

7.2.5. Identifying the Electrical Parameters

The acquired values of stray load loss, friction and windage losses, stator winding dc resistance and its associated temperature, speed, and input power, voltage and current for the three phases are used to run the GA which is utilized to extract the unknown motor parameters, i.e. X_s, R_{fe}, X_m, and R_r. Three GAs are designed to extract the required parameters. The three GAs have the same fitness functions which are built based on the positive sequence equivalent circuits shown in Figure 7-3.

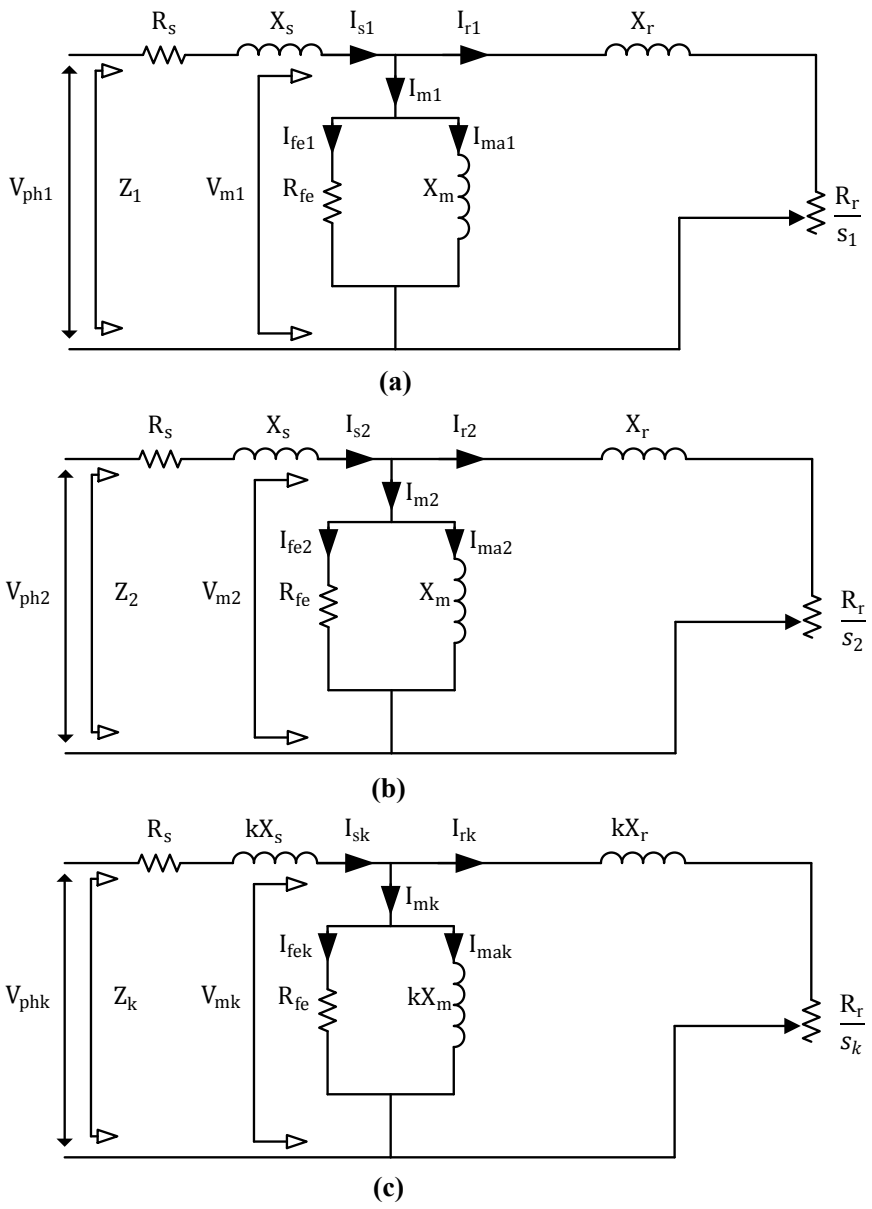

Figure 7-3. Induction machine equivalent circuit with unbalanced voltages; (a) Positive Sequence; (b) Negative sequence; (c) Harmonics.

The negative sequence equivalent circuit and the harmonics-based equivalent circuit are also shown. The following equations are used in the three GAs fitness functions.

$$Y_m = \frac{1}{R_{fe}} + \frac{1}{jX_m} \tag{7.2}$$

$$Y_r = \frac{1}{\frac{R_r}{s_1} + jX_r} \tag{7.3}$$

$$Z_r = \frac{1}{Y_m + Y_r} \tag{7.4}$$

$$Z_s = R_s + jX_s \tag{7.5}$$

$$Z_1 = Z_s + Z_r \tag{7.6}$$

$$I_{s_1} = \frac{V_{ph_1}}{Z_1} \tag{7.7}$$

$$I_{r_1} = I_{s_1}\left[\frac{1/(Y_m + Y_r)}{1/Y_r}\right] \tag{7.8}$$

$$I_{m_1} = I_{s_1} - I_{r_1} \tag{7.9}$$

$$V_{m_1} = \frac{I_{m_1}}{Y_m} \tag{7.10}$$

$$Z_{m_1} = \frac{V_{ph_1}}{I_{s_{1m}}} \tag{7.11}$$

where,

Y_m is per phase admittance of the magnetizing branch;

X_m is per phase leakage reactance of the magnetizing branch;

R_{fe} is per phase iron loss resistance;

Y_r is per phase admittance of the rotor;

R_r is per phase rotor resistance;

X_r is per phase rotor leakage reactance;

s_1 is the positive sequence slip;

Z_r is per phase impedance of both the rotor and the magnetizing branches;

Z_s is per phase stator impedance;

R_s is per phase stator resistance;

X_s is per phase stator leakage reactance;

Z_1 is per phase positive sequence total impedance;

V_{ph_1} is the positive sequence phase voltage;

I_{s_1} is the positive per phase estimated stator current;

I_{r_1} is the positive per phase estimated rotor current;

I_{m_1} is the positive per phase estimated total magnetizing current;

V_{m_1} is the positive per phase estimated magnetizing voltage;

Z_{m_1} is the positive sequence per phase impedance calculated based on measured positive sequence current;

$I_{s_{1m}}$ is the measured positive sequence current;

k is harmonic order.

The subscripts 1, 2, and k refer to the positive sequence, negative sequence, and harmonics components respectively.

The stator and rotor resistances are to be corrected to the full-load temperature T_{fl} according to (7.12) and (7.13)

$$R_{s,corr}=\frac{R_s(T_{fl}+K_1)}{T_{cold}+K_1} \tag{7.12}$$

$$R_{r,corr}=\frac{R_r(T_{fl}+K_2)}{T_{cold}+K_2} \tag{7.13}$$

The total core loss, stator copper loss and rotor copper loss are estimated as in (7.14), (7.15) and (7.16) respectively

$$P_h=3\frac{V_{m_1}^2}{R_{fe}} \tag{7.14}$$

$$P_{scl}=3I_{s_1}^2R_{s,corr} \tag{7.15}$$

$$P_{rcl}=3I_{r_1}^2R_{r,corr} \tag{7.16}$$

where,

P_h is total core loss;

P_{scl} is total stator copper loss;

P_{rcl} is total rotor copper loss.

Total losses will be determined by (7.17)

$$P_{total}=P_h+P_{scl}+P_{rcl}+P_{FW}+P_{sll} \tag{7.17}$$

where,

P_{total} is the total losses;

P_{FW} is the friction & windage losses.

The output power can be estimated by using (7.18)

$$P_{out}=P_{in,fl}-P_{total} \tag{7.18}$$

where,

P_{out} is the output power;

$P_{in,fl}$ is the measured input power.

The total input power will be calculated according to (7.19) and (7.20)

$$P_{in,\ calc1}=3real(V_{ph_1} I^*_{s1m}) \tag{7.19}$$

$$P_{in,\ calc2}=3real(V_{ph_1} I^*_{s_1}) \tag{7.20}$$

where,

$P_{in,\ m}$ is the calculated input power from measured current;

I^*_{s1m} is the conjugate of the positive sequence measured stator current;

$P_{in,\ calc}$ is the calculated input power from estimated current;

$I^*_{s_1}$ is the conjugate of the positive sequence estimated stator current in (7.7).

The two values of the input power are used to build an error function as in (7.23). The three GAs have the same error functions as described in (7.21), (7.22), (7.23), (7.24) and (7.25)

$$f_1=\frac{real(I_{s1m})-real(I_{s_1})}{real(I_{s1m})} \tag{7.21}$$

$$f_2=\frac{imag(I_{s1m})-imag(I_{s_1})}{imag(I_{s1m})} \tag{7.22}$$

$$f_3=\frac{P_{in,\,m}-P_{in,\,calc}}{P_{in,\,m}} \tag{7.23}$$

$$f_4=\frac{\theta_{Z_m}-\theta_Z}{\theta_{Z_m}} \tag{7.24}$$

$$f_5=\frac{P-P_{out}}{P} \tag{7.25}$$

where,

θ_{Z_m} is the angle of the measured input impedance Z_m;

θ_Z is the angle of the calculated input impedance Z;

P is nameplate power.

The fitness function which has the maximum value of 1 is as in (7.26)

$$ff=\frac{1}{1+\sum_{i=1}^{5} f_i} \tag{7.26}$$

The three GAs are to be run in the following sequence, and a certain observations should be carefully done to guarantee best results of the algorithm:

In GA1, the core loss is approximated by using (7.27)

$$P_{h,\,calc}=P_{in,\,fl}-P_{out}-P_{scl}-P_{rcl}-P_{FW}-P_{sll} \tag{7.27}$$

The approximated core loss $P_{h,calc}$ is compared with the total core loss P_h of (7.14). This comparison is utilized to adjust the constraints of R_{fe}. The values of both R_{fe} and P_h from GA1 are used as fixed values in GA2. This makes R_r to converge to a stable value. Hence, GA2 works with only three variables (i.e. X_s, X_m and R_r). The values of the 4 variables of 10 consecutive runs of both GA1 and GA2 are checked and the values of best fitness are used as new constraints for both GA1 and GA2. New round of 10 runs follows, and this process iterates until a stable value of R_r is acquired.

7.2.6. Rotor Resistance Calibration

The value of R_r is transferred to GA3. This value is to be very carefully calibrated until the best fitness of GA3 is achieved. Having the best value of R_r makes other variables reach stable values. Hence, GA3 will also have 3 variables (i.e. X_s, X_m, and R_{fe}). GA3 iterates, and the best fitness of the three variables after each 10 runs is used as new constraints until stable values are achieved and the 4 parameters of the induction machine are declared. R_s is already measured, and X_r will be determined based on Table 3-I.

7.2.7. IEEE Form F2-Method F1 Calculations

The IEEE Form F2-Method F1 calculations is a powerful tool in induction motor efficiency estimation. The whole set of equations can be found in IEEE Std 112-2004 [21]. The calculations form is used to estimate the output power of each individual equivalent circuit, i.e. the positive sequence equivalent circuit, the negative sequence equivalent circuit, and the equivalent circuit of each harmonic exists in the supplied voltage. Power analyzer can be used to identify the harmonic order and its rms value. The obtained six parameters are used in the output power calculations for each equivalent circuit. For the positive sequence output power calculation, the calculated per phase positive sequence voltage V_{ph1} and slip s_1 are used. For the negative sequence output power calculation, the calculated per phase negative sequence voltage V_{ph2} and slip s_2 are used. The slip s_2 is determined according to (7.28)

$$s_2=2-s_1 \tag{7.28}$$

For each harmonic order, the per phase voltage used is the rms value of the particular harmonic. The slip for each harmonic equivalent circuit is determined based on the torque associated to the harmonic, whether it is positive or negative torque as shown in Table 1-II.

Equations (7.29) and (7.30) are used to calculate the positive and negative harmonic slip respectively [129].

$$s_k^+=(1-k)+ks_1 \tag{7.29}$$

$$s_k^-=(1+k)-ks_1 \tag{7.30}$$

where k is the harmonic order.

The friction and windage losses and the stray load loss are only used in the positive sequence output power calculation. Finally, the full-load efficiency will be estimated by using (7.31)

$$\eta = \frac{P_{cov}^{+} + P_{cov}^{-} + \sum_{i=2}^{k} P_i}{P_{in,fl}} \times 100 \tag{7.31}$$

where,

P_{cov}^{+} is the positive sequence converted power;

P_{cov}^{-} is the negative sequence converted power;

P_i is the harmonic output power;

η is the estimated efficiency.

7.3. Experimental Results and Analysis

The impact of the unbalanced and distorted voltages on the performance of induction motors are demonstrated by testing a 7.5 hp, 460 V induction motor. The motor is tested for efficiency under different loads and different levels of voltage unbalance. The deterioration in the performance of the machine is illustrated in Figure 7-4(a) where the full-load efficiency, for example, is decreased from 91.4% with balanced voltages to 88.7% with 5% unbalance. The same motor is tested with balanced voltages and different Total Harmonic Distortion (THD_V). The impact of the harmonics presence in the supplied voltages is shown in Figure 7-4(b) where it can be clearly seen how the full-load efficiency is deteriorated from 91.07% with 0.15% THD_V to 89.72% with 9.86% THD_V.

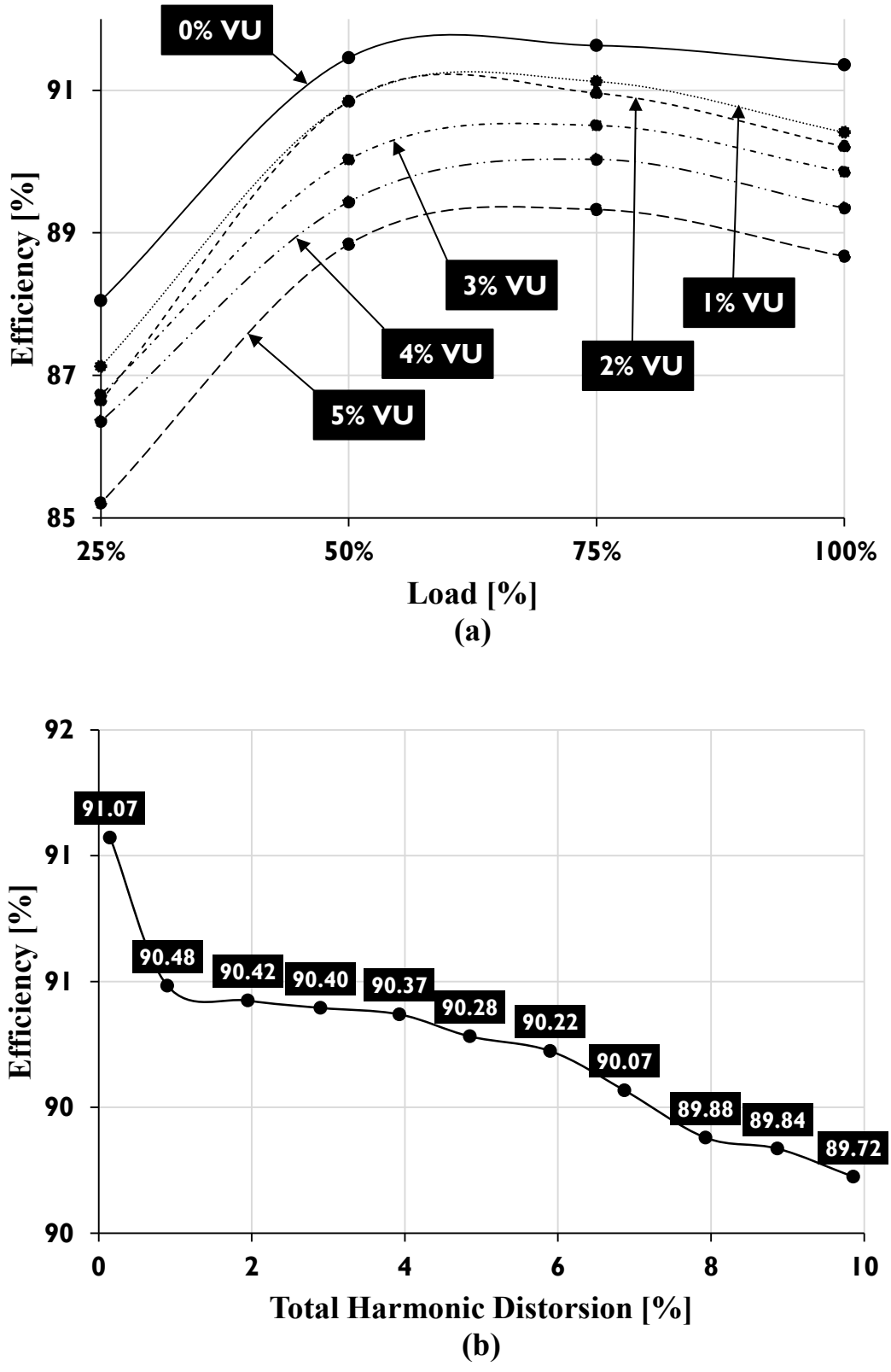

Figure 7-4. Impact of (a) unbalanced voltages and (b) harmonics on the performance of a 7.5 hp machine.

The tests are performed by using a programmable power supply whereby the unbalanced voltages and harmonics are created; a 13kW dynamometer driven by a field control unit and supplied with torque transducer; multi-channel signal conditioner and high resolution dc voltmeter which is used to display the dc analog output of the multi-channel signal conditioner which corresponds to the value of the applied torque. The dynamometer load is a resistor bank. The experimental setup is shown in Figure 7-5.

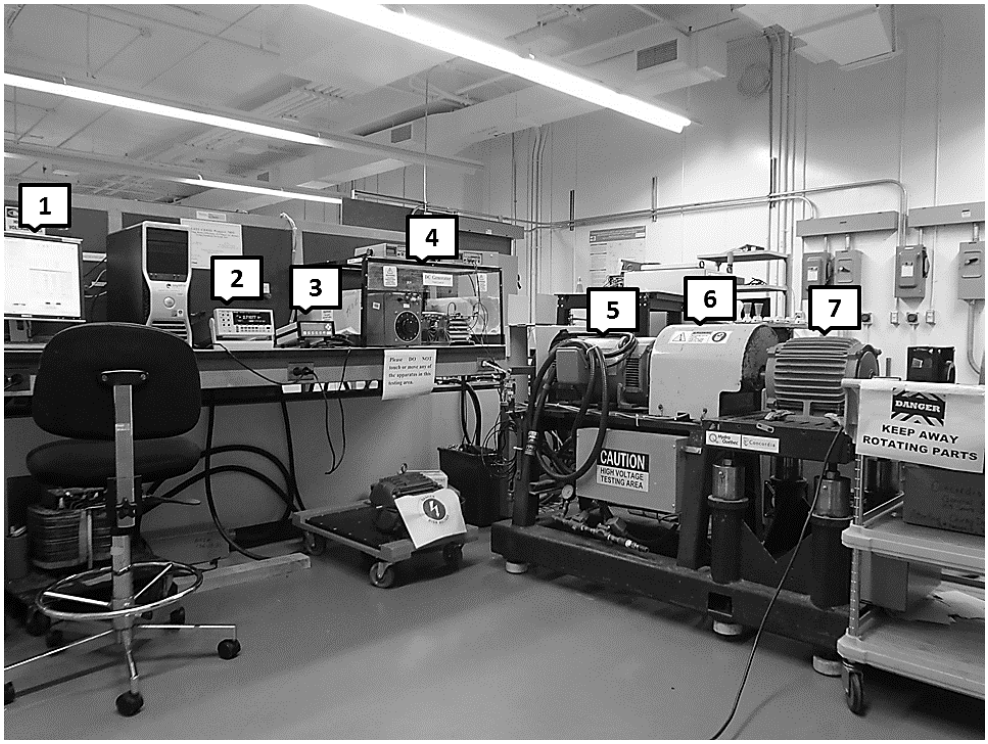

Figure 7-5. The experimental setup for testing 7.5 hp, 460 V induction motor; 1, programmable power supply; 2, high resolution digital dc voltmeter; 3, multi-channel signal conditioner; 4, field control unit; 5, DC generator; 6, torque transducer; 7, 7.5 hp motor.
Photo is a courtesy of Concordia University

To obtain the necessary data to run the proposed algorithm, the dc test is performed and the stator cold resistance and cold temperature are measured and recorded. The motor is run for 8 hours to reach its temperature stability. 5% THD_V and 5% voltage unbalance are applied on the machine for 1 hour by using the programmable power supply. Then, the hot temperature is measured by using the resistance procedure where the cold temperature is taken as a reference and the value of the hot resistance is translated to hot temperature as in (5.6). The line-to-line voltages, line currents, and total input power are measured by using rms measuring devices. One line current signal is needed to be acquired by using a data logging device for the purpose of

online speed measurement. The speed is also measured by using contactless tachometer for validation purpose. The efficiency is measured and recorded. The friction and windage losses and stray load loss are measured for this machine. The parameters of the machine are extracted by using the three stages of GA. The efficiency is estimated by using the positive and negative sequence equivalent circuits in addition to harmonic equivalent circuit for each harmonic that is present in the supplied voltage. The results are shown in Table 7-I

Table 7-I. Test Data and Results of 7.5 hp Machine

V_{ab} [V]	V_{bc} [V]	V_{ca} [V]	I_a [A]	I_b [A]	I_c [A]
479.96	459.83	440.14	10.969	10.659	5.732
P_a [W]	P_b [W]	P_c [W]	PF_a	PF_b	PF_c
2777	2182	1307	0.950	0.740	0.900
N_r [rpm]	P_{FW} [W]	P_{SLL} [W]	T_{FL} [°C]	T_{cold} [°C]	$R_{1,cold}$ [Ω]
1759	17.785	108.68	73.42	22.1	2.55
R_1 [Ω]	X_1 [Ω]	R_{fe} [Ω]	X_m [Ω]	R_2 [Ω]	X_2 [Ω]
3.06	1.669	5416	188.78	2.285	2.491

THD_V [%]	Unbalance [%]	Measured Efficiency [%]	Estimated Efficiency [%]	Absolute Error
4.87	5	89.2	88.1	1.1

7.4. The Proposed Algorithm Validation

The 7.5 hp machine and another 3.0 hp induction motor were tested under the same set of combination THD_V and voltage unbalance. The required dc tests, and measurements of speed, full-load temperature, and terminals current, voltage, and power were performed and data were collected. The full-load efficiency of the induction motors is measured under each case. The programmable power supply was used to create the required distorted and unbalanced voltages. The harmonics index used was the THD_V and it was created within the range of 0% up to the 5% limit of THD_V in the voltage which is set by IEEE [75]. The voltage unbalance was formed within the range of 1% up to 5% limit which is set by NEMA. The programmable power supply setup and the three-phase currents waveforms produced by a 5% voltage unbalance and 4.86% THD_V distorted three-phase voltages are shown in Figure 7-6. As it can be seen from Figure 7-6, the 5^{th}, 2^{nd}, and 4^{th} harmonic are chosen to shape up the input voltage signal. The reason of

having the 5th harmonic is that this order has the worst effect on the machine performance as demonstrated in Figure 7-7 which showed results of extensive tests conducted on the 7.5 hp induction motor by using different harmonic orders and their effects on the performance of the machine. It is clearly shown that the 5th harmonic has the worst impact on the full-load efficiency of the machine.

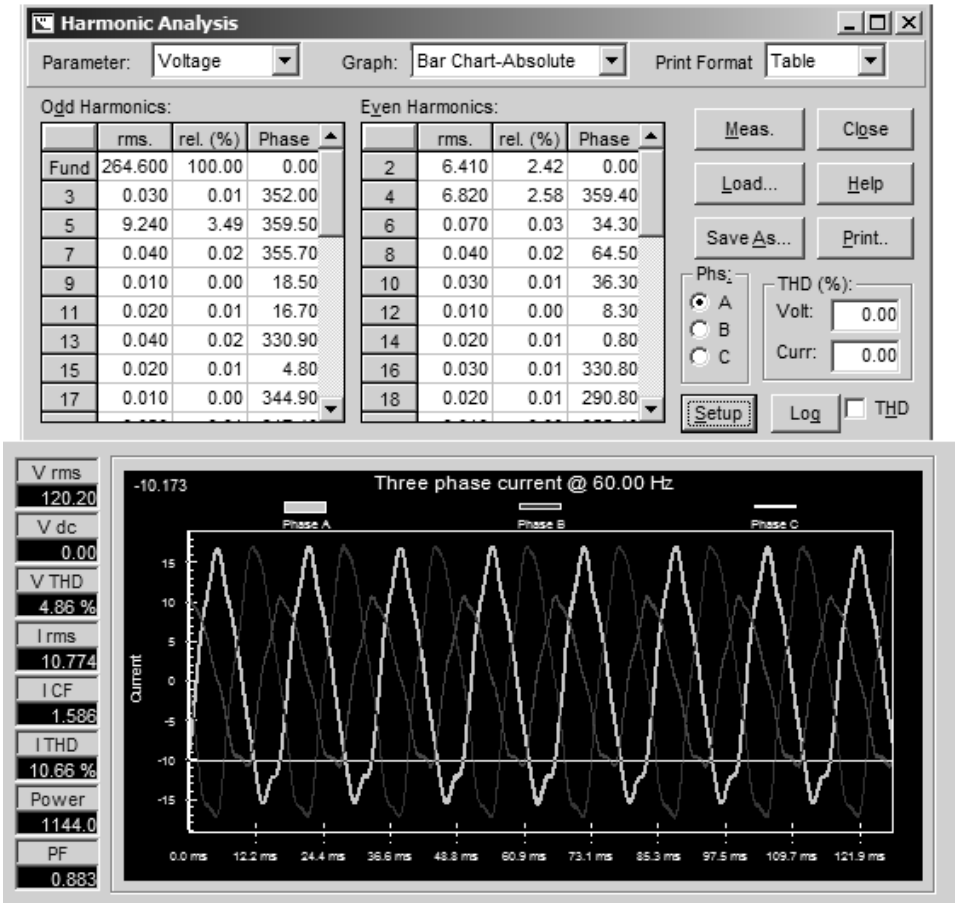

Figure 7-6. Programmable power supply setup for creating 5% voltage unbalance and 4.86% Total Harmonic Distortion

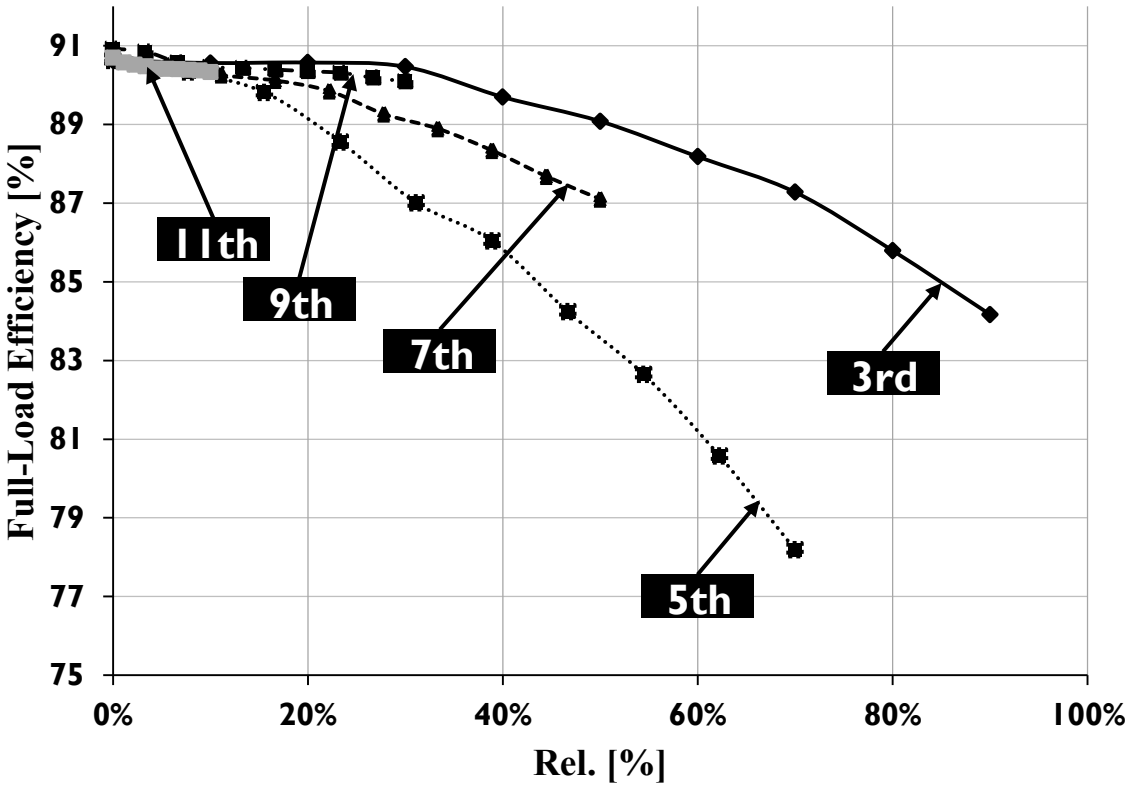

Figure 7-7. Impact of harmonics on the 7.5 hp induction motor.

In [78], as mentioned previously in Chapter 1, the impact of the 2nd harmonic on the performance of the tested machine was investigated and the paper concluded that when studying the impact of harmonics on induction motors, both odd and even harmonics must be considered. That was the reason of implying the 2nd harmonic in this study. The 4th harmonic was also implied to have a positive sequence torque as per Table 1-II.

The results of 50 tests are shown in Table 7-II. The measured efficiency is compared with the estimated value. The absolute error is declared for each case. The maximum error obtained in testing the 7.5 hp machine is 1.1%, and the minimum is 0.3%. On the other hand, the 3.0 hp machine tests show a maximum error of 0.2% and a minimum of 0.0%. Such a level of accuracy can be acceptable in induction motor efficiency estimation field.

Table 7-II. Measured vs. Estimated Efficiency of 7.5 hp and 3.0 hp Machines

Unbalance [%]	3.0 hp				7.5 hp			
	THD_V [%]	**Measured Efficiency** [%]	**Estimated Efficiency** [%]	**Absolute Error** [%]	**THD_V** [%]	**Measured Efficiency** [%]	**Estimated Efficiency** [%]	**Absolute Error** [%]
1%	0.97	80.7	80.6	0.1	0.98	91.1	90.8	0.3
	1.91	80.6	80.6	0.0	1.89	91.0	90.7	0.3
	2.99	80.5	80.5	0.0	2.89	91.0	90.7	0.3
	3.93	80.4	80.3	0.1	3.94	91.0	90.7	0.3
	4.86	80.3	80.3	0.0	4.98	91.0	90.7	0.3
2%	0.97	80.6	80.5	0.1	0.93	91.1	90.7	0.4
	1.91	80.5	80.5	0.0	1.89	91.0	90.6	0.4
	2.99	80.4	80.3	0.1	2.95	91.0	90.6	0.4
	3.93	80.3	80.1	0.2	3.93	91.0	90.6	0.4
	4.86	80.2	80.2	0.0	4.84	90.9	90.5	0.4
3%	1.02	80.2	80.2	0.0	0.95	90.6	90.2	0.4
	1.92	80.0	80.0	0.0	1.95	90.4	90.0	0.4
	2.97	80.0	80.0	0.0	2.93	90.4	90.0	0.4
	3.88	80.0	80.0	0.0	3.99	90.4	90.0	0.4
	4.87	79.9	79.9	0.0	4.87	90.6	90.2	0.4
4%	1.00	79.7	79.7	0.0	0.94	89.9	89.5	0.4
	1.94	79.7	79.7	0.0	1.90	89.9	89.5	0.4
	2.97	79.6	79.6	0.0	2.89	89.9	89.5	0.4
	3.90	79.5	79.5	0.0	3.96	89.8	89.4	0.4
	4.90	79.4	79.5	0.1	4.90	89.7	89.3	0.4
5%	0.96	79.2	79.2	0.0	0.95	89.5	88.7	0.8
	1.95	79.2	79.1	0.1	1.90	89.4	88.5	0.9
	2.92	79.1	79.0	0.1	2.90	89.4	88.4	1.0
	3.92	78.9	78.9	0.0	3.99	89.2	88.1	1.1
	4.86	78.7	78.7	0.0	4.87	89.2	88.1	1.1

7.5. Repeatability of the Proposed Algorithm

The efficiency test by using the proposed algorithm of the 7.5 hp machine that operates with 5% THD_V and 5% voltage unbalance is repeated ten times. The results of the 10 tests did not show any difference with one decimal point of efficiency. Hence, 4 decimal points are shown to demonstrate the difference. The results are tabulated in Table 7-III.

Table 7-III. Ten Repeated Tests of 7.5 hp Machine

THD_V [%]	**Measured Efficiency** [%]	**Estimated Efficiency** [%]	**Absolute Error** [%]
4.87	89.2	88.1196	1.0804
		88.1195	1.0805
		88.1196	1.0804
		88.1196	1.0804
		88.1182	1.0818
		88.1174	1.0826
		88.1196	1.0804
		88.1204	1.0796
		88.1196	1.0804
		88.1196	1.0804

The coefficient of variation C_V is used as one of the statistical concepts to compare relative dispersion of data [126]. The coefficient of variation is defined as the ratio of the standard deviation σ to the mean value $\bar{e}$ expressed as a percentage as in (7.32)

$$C_v = 100\frac{\sigma}{\bar{e}} \tag{7.32}$$

The coefficient of variation obtained for the data shown in Table 7-III is 0.0793% which can prove the consistency of the results obtained by the proposed algorithm.

7.6. Usability of the Proposed Algorithm with Undistorted Balanced Supplied Voltages

The usability of the proposed algorithm to estimate the efficiency of induction motors that operate with balanced and undistorted supply voltages is demonstrated by testing the 7.5 hp and 3.0 hp machines. The results are shown in Table 7-IV. The acceptable accuracy obtained as shown in Table 7-IV can give another credit to the proposed technique and demonstrate the level of confidence in the capability of the technique under different electrical environments.

It is important to mention that the proposed algorithm still needs to be validated by testing medium and large size machines.

Table 7-IV. Estimated Efficiency with 0% THDV and 0% Voltage Unbalance

Motor Size [kW]	**Measured Efficiency** [%]	**Estimated Efficiency** [%]	**Absolute Error** [%]
5.5	91.3	91.0	0.3
2.2	80.7	80.7	0.0

7.7. Summary

An algorithm for *in situ* efficiency estimation of induction motors that operate with distorted unbalanced voltages by using GA procedures, IEEE Form 2-Method F1 calculations, and by utilizing data of pre-tested motors is proposed in this chapter.

In subsection 7.2, the proposed algorithm and its detailed flow chart are introduced.

The algorithm is designed to utilize a test data of large number of induction motors provided by Hydro-Québec and BC hydro. The novelty of the algorithm is demonstrated by using a new approach in determining the stray load loss and friction and windage losses based on a certain strategy and novel equations which were declared in subsection 7.2.1.

The algorithm requires only one load point which is full-load with its corresponding rms values of voltage, current, and power obtained at the motor terminals.

The same online speed estimation technique that is presented in Chapter 5 is used in this study and it needs the current signal acquisition of only one line.

The experimental results of applying the proposed algorithm in testing a 7.5 hp induction motor are discussed in subsection 7.3.

The algorithm is evaluated and assessed by 50 tests of different combinations of voltage unbalance and harmonics done with two small induction motors. The results were presented and showed an acceptable level of accuracy as demonstrated in subsection 7.4.

The algorithm is also validated for its consistency by 10 repeated tests with a very low coefficient of variation of 0.0793% as shown in subsection 7.5.

The usability of the algorithm with balanced harmonics free voltages is demonstrated by testing the two machines and an acceptable accuracy is obtained as illustrated in subsection 7.6.

CHAPTER EIGHT

8. Conclusions and Future Works

This Ph.D. work is devoted to designing induction motor efficiency estimation algorithms that can be turned into reliable and practical tools to be used in industry. Hence, the level of both accuracy and uncertainty are important issues to evaluate the proposed algorithms in this research work. This chapter concludes this work and also suggests some future work.

8.1. Conclusions

Induction motors are deemed the backbone of industry. They use two-thirds of the total electrical energy generated in industrialized countries. Motors are prone to fail due to many reasons and many are rewound two or more times during their lifetimes. Estimation of the efficiency of a refurbished motor or any existing motor is crucial in industries for energy savings, auditing and management.

Full-load and partial load efficiency can be determined by using the dynamometer procedure which is a highly expensive way and available only in well-equipped laboratories. An inexpensive and easily applied procedure for efficiency estimation is a target of researchers and engineers in the field.

In Chapter 1, the objectives of this Ph.D. work was introduced and a review of the efficiency estimation techniques in the literature was presented. It was also shown that derating induction motors with voltage unbalance and/or harmonics is a necessary procedure to protect the machines from premature failure. It was also discussed that to derate a machine, its efficiency under balanced sinusoidal voltages is required to be determined. The efficiency of that machine under unbalanced voltages and/or harmonics is also required to determine the derating factor.

Chapters 2 and 3 of this thesis were devoted to design two novel methods for estimating repaired, refurbished, or any existing induction motors efficiency.

In Chapter 2, the proposed Method A for estimating induction machines full-load and partial load efficiencies from only one no-load test was presented. It was shown that the

technique can run with very limited data and measurements, which can easily be performed in any electric motor service centers. The algorithm was designed to be applied in any motor repair workshop. The algorithm utilizes an extremely valuable test data that was received from Hydro-Québec and BC Hydro which significantly improved the outcome of the proposed algorithm. The data was utilized in assigning the measured stray load loss and full-load temperature to the motor under test based on certain similarity with the motors of the data. The data was also utilized to propose new formulas to estimate the partial load stray load loss, stator copper loss, and rotor copper loss.

The advantages of using measured stray load loss and full-load temperature instead of the assumed values were discussed and the algorithm accuracy improvement were also discussed and analyzed.

A total of 196 induction motors were tested by using the proposed algorithm as part of the algorithm validation and the results obtained were with acceptable accuracy.

To evaluate the estimated efficiency values obtained by the proposed algorithm, an error analysis study was conducted and showed acceptable levels of uncertainty by using the WCE and RPBE techniques

In Chapter 2, it was concluded that the proposed algorithm can be deemed to have enough confidence to be used in the industry to give acceptable motor efficiency prediction. The algorithm was presented and well received in the CIGRÉ 2014 Conference and Exhibition in Paris, France [87].

In Chapter 3, Method B was proposed for refurbished induction machine efficiency estimation. Method B was designed to run with very limited data and measurements that can usually be encountered in electric motor service centers. Method B was also designed to be easily applied in any motor repair workshop.

It was found that the IEEE Std 112™-2004-Method 3 was not capable of dealing with the limitations of the variable voltage source in electric motor repair workshops. However, the IEEE Std 112™-2004-Method 3 succeeded to deal with the majority of the motors tested (8 motors), but on the other hand, it failed with some motors. Hence, a modification was proposed to the IEEE Std 112™-2004-Method 3 that takes into account the equipment limitations and capabilities in normal motor repair workshops. In other words, the IEEE Std 112™-2004-Method

3 was designed to work only in well-equipped laboratories, while the proposed Method B was designed to be applicable in electric motor service centers.

The proposed algorithm utilizes the Hydro-Québec/BC hydro data by using the measured full-load temperature and stray load loss values in lieu of the assumed ones. Having this data, improved the performance and the output of the algorithm to acceptable levels of performance. Eight induction motors of size range from 3-to-150 hp were tested using the designed software. The results were presented and showed acceptable accuracy.

As a necessary part of the evaluation of the estimated efficiency values obtained by the proposed algorithm, an uncertainty study was conducted and showed acceptable levels of uncertainty by using the WCE and RPBE techniques. The level of uncertainty within the estimated efficiencies obtained by using the proposed method provides confidence to the proposed algorithm and the software can be used in industry with some confidence.

Chapter 4 was devoted to the developed software which utilizes the two proposed algorithms of chapters 2 & 3 and the supporting data. The software was aimed to be a practical industrial tool that can be used in any electric motor service center in North America. The software went through a monitoring and assessing process by the technical monitors team which was selected by a group of Canadian Power Companies who sponsored the project. The software underwent many different stages of upgrading by including many useful suggestions of the technical monitors. The latest version was approved by the technical monitors and it is currently a copyright of CEATI International Inc.

In Chapter 5, a novel algorithm for in-situ induction motor efficiency estimation using a combination of GA procedures and the IEEE Form 2-Method F1 calculations was proposed. It was shown that using the assumed values of stray load loss and hot temperature can significantly increase the error and reduce the accuracy of the estimated efficiency. Hence, the algorithm was designed to utilize the Hydro-Québec/BC hydro data. The algorithm uses the measured stray load loss and hot temperature. The algorithm requires only one load point which is full-load with its corresponding rms values of voltage, current, and power obtained at the motor terminals. The algorithm uses online speed measurement technique to determine the speed of the motor under test.

The algorithm was extensively evaluated and assessed by testing 30 induction motors of

different kinds and power ratings. The results were presented and showed an acceptable level of accuracy.

The algorithm was not only deemed as an in-situ efficiency determination tool; it can also be used as a promising tool for on-site efficiency estimation that might eliminate the need to the costly dynamometer procedure.

Induction motors are designed to operate with balanced voltages. Voltage unbalance increases rotor losses which results in stator and rotor temperature rises that can cause serious ill effects on the three-phase induction motors, such as, reduction in output torque, vibration and overheating that lead to a reduction on insulation life of the machine. Hence, Chapter 6 was devoted to designing an algorithm for in situ efficiency estimation of induction motors operating with unbalanced voltages by using a combination of GA procedure, IEEE Form 2-Method F1 calculations, and pre-tested motors is proposed. The algorithm was designed to utilize the Hydro-Québec/BC hydro data.

An extensive procedure was presented in this chapter for the determination of positive and negative sequence components. This procedure was used to determine the phase voltages and their associated angles of a certain level of unbalance in the programmable power supply.

The same speed estimation technique that was presented in Chapter 5 was used in this chapter.

The algorithm was evaluated and assessed by 10 voltage unbalance tests and the accuracy of the results was shown.

The usability of the algorithm with balanced voltages was investigated by testing the 3.0 hp and 7.5 hp machines and the results showed acceptable accuracy.

The repeatability of the proposed algorithm was also investigated and the results showed a 13.13% coefficient of variation.

The goal of the study was to design a useful tool that can be used in industry to derate induction motors due to voltage unbalance.

Three-phase power supply can never be completely clean of distortion or voltage unbalance. Unbalanced voltages and harmonics have detrimental impacts on the performance of induction motors. The efficiency estimation process can be a difficult task with the existence of

voltage unbalance and harmonics. Hence, Chapter 7 was allocated to demonstrate a proposed novel algorithm for *in situ* efficiency estimation of induction motors that operate with distorted unbalanced voltages by using GA procedures, IEEE Form 2-Method F1 calculations, and by utilizing data of pre-tested motors is proposed in this chapter.

The algorithm was designed to utilize the Hydro-Québec/BC hydro data. The novelty of the algorithm was demonstrated by using a new approach in determining the stray load loss and friction and windage losses based on a certain strategy and novel equations.

The same online speed estimation technique that was discussed in Chapter 5 was used to determine the speed of the motor under test.

The algorithm was evaluated and assessed by 50 tests of different combinations of voltage unbalance and harmonics done with two small induction motors. The results showed an acceptable level of accuracy.

The repeatability of the algorithm was also validated by 10 repeated tests with a very low coefficient of variation of 0.0793%.

The usability of the algorithm with balanced harmonics free voltages was demonstrated by testing the two machines with an acceptable accuracy.

8.2. Proposed Future Works

In this section, suggested future works are proposed based on the acquired experiences throughout this Ph.D. work.

8.2.1. Minimizing the Load Test Time

As mentioned in this thesis, testing a machine by using the direct method (dynamometer procedure) requires long time. Full-load temperature stability can be reached after around eight hours of running the machine with 100% load. To reach another point of stability with new load, measurement can only be taken after around one hour of applying the required load.

It will definitely be useful if an algorithm can be designed to predict the performance of the machine under any partial load with quick measurement without waiting for the time required

for temperature stability.

8.2.2. Hot Spot Determination

Determination motor temperature plays an important role in estimating its efficiency. The procedure that was followed to determine the temperature in Chapters 5, 6, and 7 was through stator resistance measurement which is then needed to be translated into a temperature. Hence, it would be useful to develop an online algorithm that could precisely predict the hot spot of a running machine.

8.2.3. Identification of Machine's Parameters

In this thesis, the genetic algorithm was used in in-situ efficiency estimation of induction motors. Although the GA has been used successfully in induction machine efficiency estimation; it is known that there are few other evolutionary techniques that can be used for the same purpose, and some were used in some similar studies like the Bacterial Forging Algorithm (BFA).

It would be very useful if a comparison study can be achieved by estimating the efficiency of some induction motors using different types of evolutionary methods and investigating the advantages and disadvantages of each technique in terms of accuracy and speed.

8.2.4. Stray Load Loss Estimation

Determination of stray load loss is a key point in induction motors efficiency estimation. In this work, and by the advantage of having the Hydro-Québec/BC hydro data, the stray load loss could be estimated with some good approximation compared to the measured value for motors that have similarity with the data tested motor. Nevertheless, motors with no similarity will be assigned the assumed stray load loss as per IEEE and IEC standards which overestimate the measured value and hence contribute significantly to the inaccuracy of the estimated efficiency. It is very important to the field of induction motor performance evaluation that a new approach to be designed for stray load loss determination that can give better results than IEEE and IEC standards.

REFERENCES

[1] P. Pillay, V. Levin, P. Otaduy and J. Kueck, "In-situ induction motor efficiency determination using the genetic algorithm," *IEEE Transactions on Energy Conversion,* vol. 13, no. 4, pp. 326,333, Dec 1998.

[2] P. Pillay and K. A. Fendley, "The contribution of energy efficient motors to demand and energy savings in the petrochemical industry," *IEEE Transactions on Power Sytems,* vol. 10, no. 2, pp. 1085,1093, May 1995.

[3] P. Pillay, "Applying energy-efficient motors in the petrochemical industry," *IEEE Industry Applications Magazine,* vol. 3, no. 1, pp. 32,40, Jan/Feb 1997.

[4] H. M. Mzungu, M. J. Manyage, M. A. Khan, P. Barendse, T. L. Mthombeni and P. Pillay, "Application of induction machine efficiency testing standards in South Africa," in *IEEE International Electric Machines and Drives Conference, 2009. IEMDC '09*, Miami, FL, USA, May 2009.

[5] W. Hubbi and O. Goldberg, "A new method for quality monitoring of induction motors," *IEEE Transactions on Energy Conversion,* vol. 8, no. 4, pp. 726,731, Dec 1993.

[6] B. Lu, T. G. Habetler and R. G. Harley, "A Nonintrusive and In-Service Motor-Efficiency Estimation Method Using Air-Gap Torque With Considerations of Condition Monitoring," *IEEE Transactions on Industry Applications,* vol. 44, no. 6, pp. 1666,1674, Nov/Dec 2008.

[7] M. Gigante, "Rewind of Large Electric Motors for the Petroleum Industry," *IEEE Transactions on Industry and General Applications,* Vols. IGA-2, no. 2, pp. 125,131, March 1966.

[8] D. C. Montgomery, "The Motor Rewind Issue-A New Look," *IEEE transactions on Industry Applications,* Vols. IA-20, no. 5, pp. 1330,1336, Sep/Oct 1984.

[9] J. C. Hirzel, "Impact of Rewinding on Motor Efficiency," in *IEEE Pulp and Paper Industry Technical Conference*, Jun 1994.

[10] "United States Industrial Electric Motor Systems Market Opportunities Assessment," The U.S. Department of Energy's (DOE) Office of Energy Efficiency and Renewable Energy (EERE), Washington, DC, 2002.

[11] A. Siraki, P. Pillay and P. Angers, "Full Load Efficiency Estimation of Refurbished Induction Machines From No-Load Testing," *IEEE Transactions on Energy Conversion,* vol. 28, no. 2, pp. 317,326, June 2013.

[12] B. H. Campbell, "Failed Motors: Rewind or Replace?," *IEEE Industry Applications Magazine,* vol.

3, no. 1, pp. 45,50, Jan/Feb 1997.

[13] J. S. Hsu, J. D. Kueck, M. Olszewski, D. A. Casada, P. J. Otaduy and L. M. Tolbert, "Comparison of induction motor field efficiency evaluation methods," *IEEE Transactions on Industry Applications,* vol. 34, no. 1, pp. 117,125, Jan/Feb 1998.

[14] Y. El-Ibiary, "An accurate low-cost method for determining electric motors' efficiency for the purpose of plant energy management," *IEEE Transactions on Industry Applications,* vol. 39, no. 4, pp. 1205,1210, July/Aug 2003.

[15] ANSI/NEMA, "American National Standard Motors and Generators, ANSI/NEMA MG 1-2011, Revesion of ANSI/NEMA MG 1-2010," American National Standards Institute, Inc., 2011.

[16] C. Paes Salomon, W. C. Santana, L. E. Borges da Silva, E. L. Bonaldi, L. E. de Lacerda de Oliveira, J. Guedes Borges da Silva, G. Lambert-Torres and A. R. Donadon, "An air-gap torque based method for efficiency evaluation using pso to estimate a new concept of stator resistance including the losses effect," in *IEEE International Instrumentation and Measurement Technology Conference (I2MTC)*, Minneapolis, MN, 6-9 May 2013.

[17] A. Charette, J. Xu, A. Ba-Razzouk, P. Pillay and V. Rajagopalan, "The use of the genetic algorithm for in-situ efficiency measurement of an induction motor," *Power Engineering Society Winter Meeting, 2000. IEEE,* vol. 1, pp. 392,397, 2000.

[18] B. Lu, T. G. Habetler and R. G. Harley, "A survey of efficiency-estimation methods for in-service induction motors," *IEEE Transactions on Industry Applications,* vol. 42, no. 4, pp. 924,933, July/Aug 2006.

[19] J. R. Holmquist, J. A. Rooks and M. E. Richter, "Practical approach for determining motor efficiency in the field using calculated and measured values," *IEEE Transactions on Industry Applications,* vol. 40, no. 1, pp. 242,248, Jan/Feb 2004.

[20] J. D. Kueck, "Development of a method for estimating motor efficiency and analyzing motor condition," in *Pulp and Paper Industry Technical Conference*, Portland, Main, June 1998.

[21] "IEEE Standard Test Procedure for Polyphase Induction Motors and Generators," IEEE Std 112-2004 (Revision of IEEE Std 112-1996), 2004.

[22] "In-plant Electric Motor Loading and Efficiency Techniques," Ontario Hydro, 1990.

[23] "A Guide to AC Motor Repair and Replacement," (EASA) Electrical Apparatus Service Association, Inc. , 1999.

[24] R. H. Weiss, "Selecting and specifying a large AC motor rewind system," in *Pulp and Paper Industry Technical Conference*, Hyannis, MA, U.S., June 1993.

[25] W. P. Brithinee, "Electric motor repair industry update," *IEEE Electrical Insulation Magazine,* vol. 9, no. 4, pp. 23,24, July/Aug 1993.

[26] "QUALITY ELECTRIC MOTOR REPAIR: A GUIDEBOOK FOR ELECTRIC UTILITIES," Bonneville Power Administration, Portland, OR, Aug 1995.

[27] "INDUSTRIAL MOTOR REPAIR IN THE UNITED STATES," Bonneville Power Administraion, Portland, OR, Aug 1995.

[28] C. A. Sterling, "Prevalence of Components Necessary for Electrical Demand Side Management Savings Persistance in the Albertan Industrial Market Sector," University of Alberta, 1996.

[29] H. W. Penrose, "Anatomy of an energy efficient electric motor rewind," *IEEE Electrical Insulation Magazine,* vol. 13, no. 1, pp. 14,19, Jan/Feb 1997.

[30] B. H. Maru and C. H. Wennerstorm, "Effect of Modifications on the Efficiency of AC Induction Motors," *IEEE Transactions on Industry Applications,* Vols. IA-19, no. 6, pp. 1019,1023, Nov/Dec 1983.

[31] W. Cao and K. J. Bradley, "Assessing the impacts of rewind and repeated rewinds on induction motors: is an opportunity for Re-designing the machine being wasted?," *IEEE Transactions on Industry Applications,* vol. 42, no. 4, pp. 958,964, July-Aug. 2006.

[32] S.-Y. Huang and Y.-J. Wang, "Analysis of a three-phase induction motor under voltage unbalance using the circle diagram method," in *Power Con 2004. International Conference on Power System Technology*, 21-24 Nov. 2004.

[33] P. Pillay and P. Hofmann, "Derating of induction motors operating with a combination of unbalanced voltages and over or undervoltages," *IEEE Transactions on Energy Conversion,* vol. 17, no. 4, pp. 485,491, December 2002.

[34] R. F. Woll, "Effect of Unbalanced Voltage on the Operation of Polyphase Induction Motors," *IEEE Transactions on Industry Applications,* Vols. IA-11, no. 1, pp. 38,42, Jan. 1975.

[35] J. M. Corres, J. Bravo, F. J. Arregui and I. Matias, "Unbalance and harmonics detection in induction motors using an optical fiber sensor," *IEEE Sensors Journal,* vol. 6, no. 3, pp. 605,612, June 2006.

[36] J. Faiz and H. Ebrahimpour, "Precise derating of three-phase induction motors with unbalanced voltages," in *Industry Applications Conference, 2005. Fourtieth IAS Annual Meeting*, 2-6 Oct. 2005.

[37] "IEEE Guide for AC Motor Protection," *IEEE Std C37.96-2000,* pp. 1-112, Sept. 8 2000.

[38] P. B. Cummings, J. R. Dunki-Jacobs and R. H. Kerr, "Protection of Induction Motors Against Unbalanced Voltage Operation," *IEEE Transactions on Industry Applications,* Vols. IA-21, no. 3, pp. 778,792, May 1985.

[39] D. Mirabbasi, G. Seifossadat and M. Heidari, "Effect of unbalanced voltage on operation of induction motors and its detection," in *ELECO 2009. International Conference on Electrical and Electronics Engineering*, Bursa, 5-8 Nov. 2009.

[40] C.-Y. Lee, B.-K. Chen, W.-J. Lee and Y.-F. Hsu, "Effects of various unbalanced voltages on the operation performance of an induction motor under the same voltage unbalance factor condition," in *Industrial and Commercial Power Systems Technical Conference, 1997*, Philadelphia, PA , May 1997.

[41] A. G. Siraki and P. Pillay, "An In Situ Efficiency Estimation Technique for Induction Machines Working With Unbalanced Supplies," *Energy Conversion, IEEE Transactions on,* vol. 27, no. 1, pp. 85,95, March 2012.

[42] P. Gnacinski, "Derating of an induction machine under voltage unbalance combined with over or undervoltages," *Energy Conversion and Management,* vol. 50, no. 4, pp. 1101,1107, April 2009.

[43] L. Ching-Yin, "Effects of unbalanced voltage on the operation performance of a three-phase induction motor," *IEEE Transactions on Energy Conversion,* vol. 14, no. 2, pp. 202,208, Jun 1999.

[44] "IEEE Recommended Practice for Electric Power Distribution for Industrial Plants," *IEEE Std 141-1993,* pp. 1-768, April 29 1994.

[45] H. R. Reed and R. J. W. Koopman, "Induction Motors on Unbalanced Voltages," *Transactions of the American Institute of Electrical Engineers,* vol. 55, no. 11, pp. 1206,1213, Nov. 1936.

[46] J. E. Williams, "Operation of 3-Phase Induction Motors on Unbalanced Voltages [includes discussion]," *IEEE Trans., Power Apparatus and Syst., Part III.,* vol. 73, no. 1, pp. 125,133, Jan. 1954.

[47] C. C. Mosher, III, Reduced Continuous Rating of The Three-Phase Induction Motor when Operated with Unbalanced Voltages. MS Thesis, Austin, Tex.: The University of Texas, Aug 1955.

[48] J. R. Moser, Derating of Polyphase Induction Motors Due to External Unbalance. M. S. Thesis, Madison, Wis.: University of Wisconsin, 1956.

[49] M. M. Berndt, Theoretical and Experimental Methods of Deratind Polyphase Induction Motors Under Conditions of Fixed Line Voltage Unbalance, M. S. Thesis, Madison, Wis.: University of Wisconsin, 1957.

[50] B. N. Gafford, W. C. Duesterhoeft and C. C. Mosher, III , "Heating of Induction Motors on Unbalanced Voltages," *Transactions of the American Institute of Electrical Engineers. Power Apparatus and Systems, Part III.,* vol. 78, no. 3, pp. 282,286, April 1959.

[51] M. M. Berndt and N. L. Schmitz, "Derating of polyphase induction motors operated with unbalanced line voltages," *Transactions of the American Institute of Electrical Engineers, Power*

Apparatus and Systems, Part III., vol. 81, no. 3, pp. 680,683, April 1962.

[52] W. H. Kersting and W. H. Phillips, "Phase frame analysis of the effects of voltage unbalance on induction machines," *IEEE Transactions on Industry Applications,* vol. 33, no. 2, pp. 415,420, Mar/Apr 1997.

[53] Y.-J. Wang, "Analysis of effects of three-phase voltage unbalance on induction motors with emphasis on the angle of the complex voltage unbalance factor," *IEEE Transactions on Energy Conversion,* vol. 16, no. 3, pp. 270,275, Sep 2001.

[54] J. Faiz, H. Ebrahimpour and P. Pillay, "Influence of unbalanced voltage on the steady-state performance of a three-phase squirrel-cage induction motor," *IEEE Transactions on Energy Conversion,* vol. 19, no. 4, pp. 657,662, Dec 2004.

[55] P. Pillay and M. Marubini, "Loss of Life in Induction Machines Operating With Unbalanced Supplies," *IEEE Transactions on Energy Conversion,* vol. 21, no. 4, pp. 813,822, December 2006.

[56] P. Gnacinski, "Windings Temperature and Loss of Life of an Induction Machine Under Voltage Unbalance Combined With Over- or Undervoltages," *IEEE Transactions on Energy Conversion,* vol. 23, no. 2, pp. 363,371, June 2008.

[57] M. Anwari and A. Hiendro, "New Unbalance Factor for Estimating Performance of a Three-Phase Induction Motor With Under- and Overvoltage Unbalance," *IEEE Transactions on Energy Conversion,* vol. 25, no. 3, pp. 619,625, Sept. 2010.

[58] T. Spooner and J. P. Foltz, "Study of Noises in Electrical Apparatus," *Transactions of the American Institute of Electrical Engineers,* vol. 48, no. 3, pp. 747,751, July 1929.

[59] L. E. Hildebrand, "Quiet Induction Motors," *Transactions of the American Institute of Electrical Engineers,* vol. 49, no. 3, pp. 848,852, July 1930.

[60] W. R. Appleman, "The Cause and Elimination of Noise in Small Motors," *Transactions of the American Institute of Electrical Engineers,* vol. 56, no. 11, pp. 1359,1367, Nov. 1937.

[61] W. J. Morrill, "Harmonics Theory of Noise in Induction Motors," *Transactions of the American Institute of Electrical Engineers,* vol. 59, no. 8, pp. 474,480, Aug. 1940.

[62] G. H. Rawcliffe and A. M. Menon, "A simple new test for harmonic-frequency losses in a.c. machines," *Proceedings of the IEE - Part II: Power Engineering,* vol. 99, no. 68, pp. 145,150, April 1952.

[63] G. C. Jain, "The Effect of Voltage Waveshape on the Performance of a 3-Phase Induction Motor," *IEEE Transactions onPower Apparatus and Systems,* vol. 83, no. 6, pp. 561,566, June 1964.

[64] E. A. Klingshirn and H. E. Jordan, "Polyphase Induction Motor Performance and Losses on

Nonsinusoidal Voltage Sources," *IEEE Transactions on Power Apparatus and Systems,* Vols. PAS-87, no. 3, pp. 624,631, March 1968.

[65] B. J. Chalmers and B. R. Sarkar, "Induction-motor losses due to nonsinusoidal supply waveforms," *Proceedings of the Institution of Electrical Engineers,* vol. 115, no. 12, pp. 1777,1782, December 1968.

[66] G. W. McLean, G. F. Nix and S. R. Alwash, "Performance and design of induction motors with square-wave excitation," *Proceedings of the Institution of Electrical Engineers,* vol. 116, no. 8, pp. 1405,1411, August 1969.

[67] F. G. G. D. Buck, "Losses and Parasitic Torques in Electric Motors Subjected to PWM Waveforms," *IEEE Transactions on Industry Applications,* Vols. IA-15, no. 1, pp. 47,53, Jan. 1979.

[68] K. Venkatesan and J. F. Lindsay, "Comparative Study of the Losses in Voltage and Current Source Inverter Fed Induction Motors," *IEEE Transactions on Industry Applications,,* Vols. IA-18, no. 3, pp. 240,246, May/June 1982.

[69] F. G. G. De Buck, P. Giustelinck and D. De Backer, "A Simple but Reliable Loss Model for Inverter-Supplied Induction Motors," *IEEE Transactions on Industry Applications,* Vols. IA-20, no. 1, pp. 190,202, January/February 1984.

[70] IEEE Task Force, "The Effects of Power System Harmonics on Power System Equipment and Loads," *IEEE Transactions on Power Apparatus and Systems,* Vols. PAS-104, no. 9, pp. 2555,2563, September 1985.

[71] P. G. Cummings, "Estimating Effect of System Harmonics on Losses and Temperature Rise of Squirrel-Cage Motors," *IEEE Transactions on Industry Applications,* Vols. IA-22, no. 6, pp. 1121,1126, November/December 1986.

[72] T. Kataoka, Y. Kandatsu and T. Akasaka, "Measurement of equivalent circuit parameters of inverter fed induction motors," *IEEE Transactions on Magnetics,* vol. 23, no. 5, pp. 3014,3016, Sep. 1987.

[73] T. M. Undeland and N. Mohan, "Overmodulation and Loss Considerations in High-Frequency Modulated Transistorized Induction Motor Drives," *IEEE Transactions on Power Electronics,* vol. 3, no. 4, pp. 447,452, October 1988.

[74] P. K. Sen and H. A. Landa, "Derating of induction motors due to waveform distortion," *IEEE Transactions on Industry Applications,* vol. 26, no. 6, pp. 1102,1107, Nov/Dec 1990.

[75] "IEEE Recommended Practices and Requirements for Harmonic Control in Electrical Power Systems, IEEE Std 519-1992," IEEE, April 9 1993.

[76] P. L. Alger, G. Angst and E. J. Davies, E. John, "Stray-Load Losses in Polyphase Induction Maclines," *Transactions of the American Institute of Electrical Engineers, Power Apparatus and*

Systems, Part III., vol. 78, no. 3, pp. 349,355, April 1959.

[77] IEEE Task Force, "Effects of Harmonics on Equipment," *IEEE Transactions on Power Delivery,* vol. 8, no. 2, pp. 672,680, April 1993.

[78] C.-Y. Lee, W.-J. Lee, Y.-N. Wang and J.-C. Gu, "Effects of voltage harmonics on the electrical and mechanical performance of a three-phase induction motor," in *IEEE Industrial and Commercial Power Systems Technical Conference*, Edmonton, Alta., 3-8 May 1998.

[79] K. Yamazaki, "Loss calculation of induction motors considering harmonic electromagnetic field in stator and rotor," *Electrical Engineering in Japan,* vol. 147, no. 2, pp. 63,73, 2004.

[80] A. Jalilian, V. J. Gosbell, B. S. P. Perera and P. Cooper, "Double Chmber Calorimeter (DCC): a New Approach to Measure Induction Motor Harmonic Losses," *IEEE Transactions on Energy Conversion,* vol. 14, no. 3, pp. 680,685, September 1999.

[81] A. Jalilian, V. J. Gosbell and B. S. P. Perera, "Performance of a 7.5 kW induction motor under harmonically distorted supply conditions," in *Canadian Conference on Electrical and Computer Engineering*, Halifax, NS, 7-10 Mar. 2000.

[82] E. Nicol Hildebrand and H. Roehrdanz, "Losses in three-phase induction machines fed by PWM converter," *IEEE Transactions on Energy Conversion,* vol. 16, no. 3, pp. 228,233, Sep. 2001.

[83] P. W. Wheeler, J. C. Clare, M. Apap and K. J. Bradley, "Harmonic Loss Due to Operation of Induction Machines From Matrix Converters," *IEEE Transactions on Industrial Electronics,* vol. 55, no. 2, pp. 809,816, February 2008.

[84] A. Maamoun, A. M. A. Mahmoud, A. F. Kheireldin, A. F.; S and M. A. Saleh, "The harmonic effects in an induction motor fed from a cycloconverter," in *Fourth International Conference on Power Electronics and Variable-Speed Drives*, London, 17-19 Jul. 1990.

[85] "Testing Data of 128 Induction Motor," Hydro-Québec, Shawinigan, 2012.

[86] N. M. Kaufman, "A 100 Motor Study: Investigating pre-EPAct motors as a subset of the industrial motor population with regards to the economics of motor repair/replace decisions," North Carolina State University, U.S., 2005.

[87] M. Al-Badri and P. Pragasen, "A Novel Technique for Refurbished Induction Motors' Efficiency Estimation Based on," in *CIGRÉ 2014 Conference and Exhibition, Session 45*, Paris, 24-29 August 2014.

[88] M. Al-Badri, P. Pillay and P. Angers, "A Novel Algorithm for Estimating Refurbished Three-Phase Induction Motors Efficiency Using Only No-Load Tests," *Energy Conversion, IEEE Transactions on,* vol. 30, no. 2, pp. 615,625, June 2015.

[89] M. Al-Badri and P. Pragasen, "Evaluation of measurement uncertainty in induction machines efficiency estimation," in *Power and Energy (PECon), 2014 IEEE International Conference on*, Kuching, Malaysia, 1-3 Dec. 2014.

[90] M. Al-Badri, P. Pillay and P. Angers, "A Novel In Situ Efficiency Estimation Algorithm for Three-Phase IM Using GA, IEEE Method F1 Calculations and Pre-Tested Motor Data," *Energy Conversion, IEEE Transactions on. (Early Access Article),* 2015.

[91] Hydro-Québec, "128 Induction Motors Testing Data," Shawinigan, Québec, CANADA, 2012.

[92] G. C. Soukup, "Determination of Motor Quality Through Routine Electrical Tests," *IEEE Transactions on Industry Applications,* vol. 25, no. 5, pp. 873,880, Sep/Oct 1989.

[93] "Testing of Three-phase squirrel cage induction motors during refurbishment," Canadian Standards Association, CAN/CSA C392-11, 2011.

[94] P. C. Sen, "Principles of Electric Machines & Power Electronics", 2nd ed., John Wiley & Sons, 1999.

[95] "International Standard IEC 60034-2-1," Edition.1, 2007-09.

[96] R. S. Colby and D. L. Flora, "Measured efficiency of high efficiency and standard induction motors," in *Industry Applications Society Annual Meeting, 1990*, Seattle, WA, USA, October 1990.

[97] S. G. Rabinovich, Measurement Errors and Uncertainties, Theory and Practice, New York: Springer Science and Media, Inc., 2005.

[98] W. Cao, K. J. Bradley, H. Zhang and I. French, "Experimental Uncertainty in Estimation of the Losses and Efficiency of Induction Motors," in *Industry Applications Conference, 2006. 41st IAS Annual Meeting. Conference Record of the 2006 IEEE*, Tampa, FL , 2006.

[99] B. Lu, W. Cao and T. G. Habetler, "Error Analysis of Motor-Efficiency Estimation and Measurement," in *Power Electronics Specialists Conference, 2007. PESC 2007. IEEE*, Orlando, FL , 2007.

[100] B. Herndler, P. Barendse and M. A. Khan, "Error Analysis of Efficiency Estimation Methods for Induction Motors," in *Electric Machines & Drives Conference (IEMDC), 2011 IEEE International*, Niagara Falls, ON, 2011.

[101] R. Babau, I. Boldea, T. J. E. Miller and N. Muntean, "Complete Parameter Identification of Large Induction Machines From No-Load Acceleration–Deceleration Tests," *IEEE Transactions on Industrial Electronics,,* vol. 54, no. 4, pp. 1962,1972, Aug. 2007.

[102] L. Whei-Min, S. Tzu-Jung and W. Rong-Ching, "Parameter Identification of Induction Machine With a Starting No-Load Low-Voltage Test," *IEEE Transactions on Industrial Electronics,* vol. 59,

no. 1, pp. 352,360, Jan. 2012.

[103] H. A. Toliyat, E. Levi and M. Raina, "A review of RFO induction motor parameter estimation techniques," *IEEE Transactions on Energy Conversion,* vol. 18, no. 2, pp. 271,283, June 2003.

[104] "Test methods, marking requirements, and energy efficiency levels for three-phase induction motors," Canadian Standards Association (CSA), C390-10, 2010.

[105] J. Walkenbach, Excel® 2010 Power Programming with VBA, Indianapolis, Indiana: Wiley Publishing, Inc., 2010.

[106] R. R. Bishop and G. G. Richards, "Identifying induction machine parameters using a genetic optimization algorithm," in *Southeastcon '90. Proceedings., IEEE*, New Orleans, LA, 1-4 April, 1990.

[107] P. Pillay, R. Nolan and T. Haque, "Application of genetic algorithms to motor parameter determination for transient torque calculations," *IEEE Transactions on Industry Applications,* vol. 33, no. 5, pp. 1273,1282, Sep./Oct. 1997.

[108] F. Alonge, F. D'Ippolito, G. Ferrante and F. M. Raimondi, "Parameter identification of induction motor model using genetic algorithms," *Control Theory and Applications, IEE Proceedings,* vol. 145, no. 6, pp. 587,593, Nov 1998.

[109] H. H. Weatherford and C. W. Brice, "Estimation of induction motor parameters by a genetic algorithm," in *Pulp and Paper Industry Technical Conference, 2003. Conference Record of the 2003 Annual*, Charleston, SC, USA , 16-20 June 2003.

[110] Z. Xiaoyao and C. Haozhong, "The induction motor parameter estimation through an adaptive genetic algorithm," in *UPEC 2004. 39th International Universities Power Engineering Conference*, Bristol, UK , 8-8 Sept. 2004.

[111] L. Bin Lu, C. Wenping, I. French, K. J. Bradley and T. G. Habetler, "Non-Intrusive Efficiency Determination of In-Service Induction Motors using Genetic Algorithm and Air-Gap Torque Methods," in *42nd IAS Annual Meeting Industry Applications Conference. Conference Record of the 2007 IEEE*, New Orleans, LA , 23-27 Sept. 2007.

[112] K. Kampisios, P. Zanchetta, C. Gerada and A. Trentin, "Identification of Induction Machine Electrical Parameters Using Genetic Algorithms Optimization," in *IAS '08. IEEE Industry Applications Society Annual Meeting*, Edmonton, Alta., 5-9 Oct. 2008.

[113] R. L. Haupt and S. E. Haupt, Practical Genetic Algorithms, 2nd ed., New Jersey: John Wiley & Sons, Inc., 2004.

[114] D. A. Paice, "Motor Thermal Protection by Continuous Monitoring of Winding Resistance," *IEEE Trans. on Ind. Elect. and Ctrl Instr.,* Vols. IECI-27, no. 3, pp. 137,141, Aug. 1980.

[115] L. Sang-Bin and T. G. Habetler, "An online stator winding resistance estimation technique for temperature monitoring of line-connected induction machines," *IEEE Trans. Ind. Appl.,* vol. 39, no. 3, pp. 685,694, May-June 2003.

[116] M. Ishida and K. Iwata, "A New Slip Frequncy Detector of an Induction Motor Utilizing Rotor Slot Harmonics," *IEEE Transactions on Industry Applications,* Vols. vol.IA-20, no. 3, pp. 575,582, May 1984.

[117] A. Ferrah, K. G. Bradley and G. M. Asher, "Sensorless speed detection of inverter fed induction motors using rotor slot harmonics and fast Fourier transform," in *Power Electronics Specialists Conference, 1992. PESC '92 Record., 23rd Annual IEEE*, Toledo, 29 Jun-3 Jul 1992.

[118] K. D. Hurst and T. G. Habetler, "Sensorless speed measurement using current harmonic spectral estimation in induction machine drives," *IEEE Transactions on Power Electronics,* vol. 11, no. 1, pp. 66,73, Jan 1996.

[119] P. Pillay and Z. Xu, "Labview implementation of speed detection for mains-fed motors using motor current signature analysis," *IEEE Power Engineering Review,* vol. 18, no. 6, pp. 47,48, June 1998.

[120] K. D. Hurst and T. G. Habetler, "A comparison of spectrum estimation techniques for sensorless speed detection in induction machines," *IEEE Transactions on Industry Applications,* vol. 33, no. 4, pp. 898,905, Jul/Aug 1997.

[121] A. K. Zairani, Extraction of Nonstationary Sinusoids, Toronto: Ph.D Thesis, University of Toronto, 2002.

[122] A. Boglietti, A. Cavagnino, M. Lazzari and M. Pastorelli, "International standards for the induction motor efficiency evaluation: a critical analysis of the stray-load loss determination," *IEEE Transactions on Industry Applications,* vol. 40, no. 5, pp. 1294,1301, Sept.-Oct. 2004.

[123] A. Nagornyy, A. K. Wallace and A. V. Jouanne, "Stray load loss efficiency connections," *IEEE Industry Applications Magazine,* vol. 10, no. 3, pp. 62,69, May-Jun 2004.

[124] C. A. Gross, Electric Machines, Boca Raton, FL: CRC Press, 2007.

[125] J. J. Grainger and W. D. Stevenson, J, Power System Analysis, Singapore: McGraw-Hill, 1994.

[126] E. B. Agamloh, "The repeatability of IEEE standard 112B induction motor efficiency tests," in *Electric Machines and Drives Conference, 2009. IEMDC '09. IEEE International*, Miami, FL , 3-6 May 2009.

[127] P. Pillay and M. Manyage, "California Electricity Situation," *IEEE Power Engineering Review,* vol. 21, no. 5, pp. 10,12, May 2001.

[128] Y.-J. Wang, "Analysis of effects of three-phase voltage unbalance on induction motors with

emphasis on the angle of the complex voltage unbalance factor," *IEEE Transactions on Energy Conversion,* vol. 16, no. 3, pp. 270,275, Sep. 2001.

[129] L. Su-Jin, K. Ji-Min, A. Dong-Kyun and H. Jung-Pyo, "Equivalent Circuit Considering the Harmonics of Core Loss in the Squirrel-Cage Induction Motor for Electrical Power Steering Application," *Magnetics, IEEE Transactions on,* vol. 50, no. 11, pp. 1,4, Nov. 2014.

[130] C. Wenping, K. J. Bradley, J. C. Clare and P. W. Wheeler, "Comparison of Stray Load and Inverter-Induced Harmonic Losses in Induction Motors Using Calorimetric and Harmonic Injection Methods," *Industry Applications, IEEE Transactions on,* vol. 46, no. 1, pp. 249,255, Jan.-feb. 2010.

[131] E. B. Agamloh, "Induction Motor Efficiency," *Industry Applications Magazine, IEEE,* vol. 17, no. 6, pp. 20,28, Nov.-Dec. 2011.

[132] S. E. Zocholl, E. O. Schweitzer and A. Aliaga-Zegarra, "Thermal Protection of Induction Motors Enhanced by Interactive Electrical and Thermal Models," *IEEE Trans. Power Apparatus and Syst.,* Vols. PAS-103, no. 7, pp. 1749,1755, July 1984.